

1-1-1973

Rheological and physical properties of poly-1-olefin series.

Jeou-shyong Wang
University of Massachusetts Amherst

Follow this and additional works at: https://scholarworks.umass.edu/dissertations_1

Recommended Citation

Wang, Jeou-shyong, "Rheological and physical properties of poly-1-olefin series." (1973). *Doctoral Dissertations 1896 - February 2014*. 600.
<https://doi.org/10.7275/1cc2-bb93> https://scholarworks.umass.edu/dissertations_1/600

This Open Access Dissertation is brought to you for free and open access by ScholarWorks@UMass Amherst. It has been accepted for inclusion in Doctoral Dissertations 1896 - February 2014 by an authorized administrator of ScholarWorks@UMass Amherst. For more information, please contact scholarworks@library.umass.edu.

UMASS/AMHERST



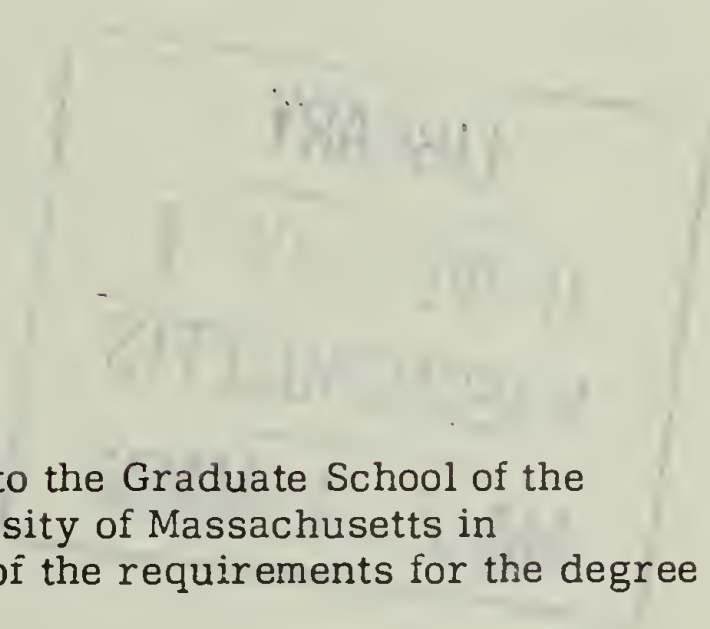
312066 0015 5427 7

RHEOLOGICAL AND PHYSICAL PROPERTIES
OF
POLY-1-OLEFIN SERIES

A Dissertation Presented

By

Jeou-shyong Wang



Submitted to the Graduate School of the
University of Massachusetts in
partial fulfillment of the requirements for the degree of

DOCTOR OF PHILOSOPHY

July 1973

Major Subject: Polymer Science and Engineering

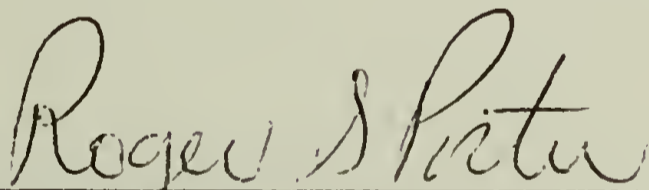
RHEOLOGICAL AND PHYSICAL PROPERTIES
OF
POLY-1-OLEFIN SERIES

A Dissertation

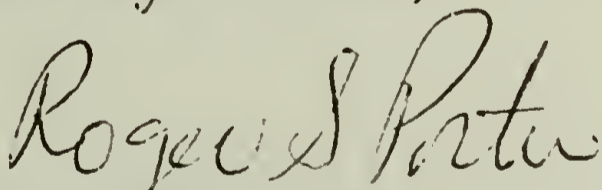
By

Jeou-shyong Wang

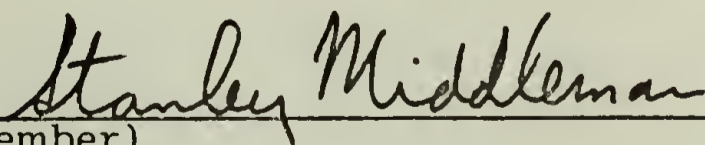
Approved as to style and content by:



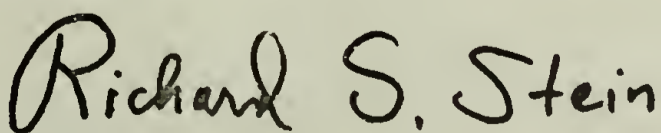
(Chairman of Committee)



(Head of Department)



(Member)



(Member)

July 1973

Dedicated to my parents.

Acknowledgement

The author would like to express his sincere thanks to his thesis director, Professor Roger S. Porter, for his guidance, encouragement and support throughout the course of this work.

Thanks are extended to my thesis committee, Professor Richard S. Stein and Professor Stanley Middleman, for their suggestions and reviewing the thesis.

Acknowledgement is made to Dr. Jack R. Knox for his supplying of samples, Professor Sadao Mori for his GPC characterization of samples and Professor Julian F. Johnson for his discussion of dilution solution experiments.

The author also wishes to express his gratitude to Dr. William M. Prest for his improvement of Weissenberg Rheogoniometer and his enthusiasm.

ABSTRACT

In Chapter I, a series of poly-1-olefins from poly-1-butene up to poly-1-octadecene have been characterized. The melting point was measured by Differential Scanning Calorimetry (DSC-1B) and dilatometry; the specific volume, volume expansion coefficient by dilatometry, and unperturbed chain dimension by intrinsic viscosity at near theta condition.

A trend is confirmed for melting point and revealed for expansion coefficient of first a decrease with increasing side-chain length in the polyolefins, followed by an increase with further increase in length. The minimum is near poly-1-hexene and poly-1-heptene. The specific volume of the poly-1-olefin series exhibits a maximum around this same composition. The minima in melting point and thermal expansion coefficient and the maximum in specific volume are discussed in terms of chain-to-chain packing density. It is suggested that packing density is a minimum in this region.

Two melting points were found for each of several higher poly-1-olefins from poly-1-tridecene up to poly-1-octadecenes.

It is found that the theta temperature of poly-1-olefin series, as measured in two solvents, anisole and cyclohexanone, exhibits a minimum at poly-1-pentene. However, the characteristic ratios and the steric factors increase with increasing side-chain length for the entire series of measured poly-1-olefins.

In Chapter II, the temperature coefficients for the viscosity of poly-1-olefin series, i.e., flow activation energy were calculated from the viscosity measurement by using a Weissenberg Rheogoniometer Model R 17. Eight poly-1-olefins from polypropylene to poly-1-octadecene were measured. All tests were made at over 100°C above the glass transition temperature and above the measured melting point for each of the poly-1-olefins.

The plots of log viscosity versus $1/T^{\circ}\text{K}$ gave entirely linear correlations for all of the polymers in these measurement temperature ranges. The correlations were also independent of shear stress for each of the polymers.

It was found that the flow activation energies of the poly-1-olefin series change markedly and go through a maximum as a function of polyolefin pendant group chain length exhibiting a maximum in the range of the poly-1-hexene to poly-1-octene.

In Chapter III, based on the free volume concept and the equation by Doolittle, a new empirical equation is proposed for the flow activation energy E^* for polymer melts for the range of over 150° above glass transition temperature T_g . The E^* is the temperature coefficient of viscosity for the Newtonian region or at constant shear stress for non-Newtonian flow. Data show that the E^* of linear polymers reaches a constant value for a broad temperature range above $T_g + 150^{\circ}$. The proposed equation for this region predicts the E^* of polymer melts from volume expansion coefficient, α_v in degrees^{-1} above T_g and from the $T_g^{\circ}\text{K}$. The E^* calculated from this equation is found to be in agreement with measurements within experimental precision of about ± 1 Kcal/mole.

Correlation have also been developed between E^* and α_v and between E^* and T_g by simplifying this new equation by use of the Simha-Boyer expression. It is thus shown that a polymer having a lower α_v or higher T_g generally has a higher E^* . However, generally more satisfactory results are obtained by calculating E^* from both α_v and T_g .

The effects of polymer composition, molecular weight, branching and microstructure on E^* are also discussed. It is proposed that these factors influence E^* in the way in which they effect α_v and T_g .

In Chapter IV, the steady state and dynamic melt rheology for the poly-1-olefin series has been investigated. The series includes poly-1-butene, poly-1-hexene, poly-1-heptene, poly-1-octene, poly-1-undecene, poly-1-tridecene, poly-1-hexadecene and poly-1-octadecene. They were investigated by use of a Weissenberg Rheogoniometer. Corresponding tests on poly-1-butene were also made in an Instron Capillary Rheometer.

The empirical relation of Cox and Merz was obeyed for the entire series of poly-1-olefin and at all experimental temperatures.

Graessley's theory was used to calculate the flow curves for the poly-1-olefins using the measured molecular weight distribution. The purpose was to investigate the effect of polymer composition on the shear rate dependence of viscosity. It was found that all experimental flow curves except poly-1-hexene can be fitted with the calculated curves using the individual molecular weight distributions. The conclusion is thus made that flow curves of poly-1-olefin predominately depend on molecular weight distribution and are essentially independent of side-chain length even for poly-1-olefins with pendant groups as long as 16 carbon atoms.

If low shear limit Newtonian viscosity η_0 for all poly-1-olefins can be expressed by the equation, $\eta_0 = K\bar{M}_w^{3.4}$, or by $\eta_0 = K'\bar{P}_w^{3.4}$, where \bar{M}_w is the weight average molecular weight and \bar{P}_w is the weight average degree of polymerization, the K and K' values decrease systematically as the side-chain length increases from poly-1-hexene to poly-1-octadecene. However, K' values decrease more slowly than K values.

The dynamic shear storage modulus, G' , loss modulus, G'' , and the reciprocal of dynamic shear compliance, $1/J'$ versus frequency curves at different

temperatures can be superposed according to time-temperature superposition. The theory of second order fluid was only fitted by the data of poly-1-heptene and poly-1-octene. That is, at low frequency, half normal stress $(\sigma_{11} - \sigma_{22})/2$ can be correspondent to G' , the steady shear modulus G is correspondent to the reciprocal of low frequency limit dynamic compliance $1/J_e^0$ and shear stress τ_{12} is correspondent to G'' .

The steady shear modulus G for members of this poly-1-olefin series was found to be insensitive to molecular weight distribution for these broad distribution samples. The value of G , however, decreases with increasing the length of pendant groups from poly-1-hexene to poly-1-octadecene.

It was found that the steady state and dynamic viscoelastic properties of poly-1-olefin series have the same temperature dependence. The flow activation energy E^* was calculated from η_0 , from η_a at constant shear stress and from $|\eta^*|$ at constant product for $\omega|\eta^*|$. Three ways all give the same E^* which is independent of temperature over the measured range in the melt.

Preface

This thesis consists of four related manuscripts concerning the rheological and physical properties of poly-1-olefin series. The suggestions for future studies are presented in the last chapter.

Chapter I deals with some characterization of physical properties for poly-1-olefin series.

Chapter II shows the temperature-viscosity coefficient for poly-1-olefin melts.

Chapter III develops a method to predict temperature viscosity behavior for polymer melts.

Chapter IV discusses the steady state and dynamic rheological properties of poly-1-olefin melts.

Chapter V contains some suggestions for future studies from this work.

Table of Contents

CHAPTER I

THE PHYSICAL PROPERTIES OF POLY-1-OLEFIN - THERMAL BEHAVIOR AND DILUTE SOLUTION PROPERTIES

Synopsis	1
Introduction	2
Experiments	3
Results and Discussion	6
References	18

CHAPTER II

TEMPERATURE COEFFICIENTS FOR THE VISCOSITY OF POLY-1-OLEFINS

Introduction	38
Experiments	41
Results and Discussion	42
References	45

CHAPTER III

PREDICTION OF VISCOSITY-TEMPERATURE BEHAVIOR FOR POLYMER MELTS

Synopsis	52
Introduction	52
Analysis	55
Discussion	58
Conclusion	65
References	73

CHAPTER IV

STEADY STATE AND DYNAMIC RHEOLOGY OF POLY-1-OLEFIN
MELTS

	84
Synopsis	84
Introduction	85
Experiments	87
Results and Discussion	89
References	101

CHAPTER V

SUGGESTIONS FOR FUTURE STUDIES 120

(1) The Temperature Coefficient of Unperturbed Dimension of Poly-1-Olefin Series	120
(2) Unit Cell and Heat of Fusion Determinations for the Poly-1-Olefin Series	123
(3) Determine the E^* of Completely Linear Polyethylene by Viscosity Studies on Hydrogenated Polybutadiene	125
(4) The Effect of Pressure on Flow Activation Energy	125
(5) The Blend of Poly-1-Olefins	126
(6) Copolymers of Ethylene with other 1-Olefins	127
(7) Correlation Between Normal Stress Coefficient and Viscosity References	127

APPENDIX A

Computer Program to Calculate Viscosity from Instron Capillary Rheometer and Rabinowitsch Correction	131
---	-----

APPENDIX B

The Calculation of Flow Curve from Graessley Theory	135
---	-----

APPENDIX C

The Tabulated Data of Chapter IV

C H A P T E R I

PHYSICAL PROPERTIES OF THE POLY-1-OLEFINS

- THERMAL BEHAVIOR AND DILUTE SOLUTION PROPERTIES -

Synopsis

A series of poly-1-olefins from poly-1-butene up to poly-1-octadecene have been characterized. The melting point was measured by Differential Scanning Calorimetry (DSC-1B) and dilatometry; the specific volume, volume expansion coefficient by dilatometry, and unperturbed chain dimension by intrinsic viscosity at near theta condition.

A trend is confirmed for melting point and revealed for expansion coefficient of first a decrease with increasing side-chain length in the polyolefins, followed by an increase with further increase in length. The minimum is near poly-1-hexene and poly-1-heptene. The specific volume of the poly-1-olefin series exhibits a maximum around this same composition. The minima in melting point and thermal expansion coefficient and the maximum in specific volume are discussed in terms of chain-to-chain packing density. It is suggested that packing density is a minimum in this region.

Two melting points were found for each of several higher poly-1-olefins from poly-1-tridecene up to poly-1-octadecenes.

It is found that the theta temperature of poly-1-olefin series, as measured in two solvents, anisole and cyclohexane, exhibits a minimum at poly-1-pentene. However, the characteristics ratios and the steric factors increase with increasing side-chain length for the entire series of measured poly-1-olefins.

Introduction

The thermal behavior and dilute solution properties for the lower members of the poly-1-olefin series, i.e., polyethylene, polypropylene and poly-1-butene have been studied intensively. However, only a few systematic studies on the properties of the higher members of the series have so far been published.¹⁻¹² The melting and glass transition temperatures of the poly-1-olefin series have been measured by several sets of workers.¹⁻⁴ It has been found that the melting and glass transition temperatures first decrease with increasing side-chain length, go through a minimum and then increase with increasing for the highest members studied. The minimum in the series varies somewhat from report to report.

The crystalline forms of several isotactic poly-1-olefins from poly-1-hexene to poly-1-octadecene have been investigated by X-ray.⁵ Thus Turner-Jones found two crystalline forms in poly-1-tetradecene, poly-1-hexadecene and poly-1-octadecene. For these higher members, two melting points have also been found by several works.^{1,6,7} Takayanagi⁸⁻¹² investigated the viscoelastic properties and crystal transformations of several poly-1-olefins and discussed in detail the effect of chemical structure on these properties.

Flory¹³ has published the unperturbed dimension of poly-1-butene and poly-1-pentene. For higher poly-1-olefins, Shirayama et al.¹⁴ has given the unperturbed dimension of poly-1-octene and poly-1-octadecene. For other higher members, no information on chain dimensions has been reported heretofore.

The purpose of the present work is to examine the absolute values and trends for the melting transitions, specific volumes, volume expansion and molecular conformation characteristics for the poly-1-olefins. The relationships

obtained from this work may thus lead to a better understanding of the effects of polymer structures on physical properties.

The samples studied included poly-1-butene, poly-1-pentene, poly-1-hexene, poly-1-heptene, poly-1-octene, poly-1-nonene, poly-1-decene, poly-1-undecene, poly-1-dodecene, poly-1-tridecene, poly-1-hexadecene and poly-1-octadecene. One sample of each polymer was generally available. Three samples of poly-1-octadecene were used which differed in molecular weight and distribution.

Experimental

Sample Preparation. Most of the polymerizations were carried out in the following manner: A 300 ml. four-necked flask equipped with stirrer, reflux condenser, thermometer, and addition funnel was used. The flask was equipped with heating mantle, cooling bath, or neither depending upon the temperature of polymerization. The flask assembly was dried for at least one hour in an oven at 135°C before use.

The flask was then charged with 100 ml. of heptane followed by the required amount of titanium tetrachloride and aluminum triisobutyl. After an aging period of 10-30 min., the olefin (25-50 grams) was added, usually at the predetermined temperature of polymerization. The time of polymerization varied from 1-24 hours, depending on olefin reactivity.

At the end of the polymerization period, the slurry was cooled or warmed to room temperature and treated with 100 ml. of either isopropanol or 50:50 methanol-isopropanol. The polymer was slurried several times with fresh alcohol and usually treated for 2-3 hours on the steam bath with additional alcohol. The polymer was frequently further purified by solution in hot hexene

followed by reprecipitation with excess alcohol. The resulting polymer, after partial air drying, was dried in a vacuum oven at a temperature dependent upon the melting point of the polymer.

Due to the solubility of these polymers in hydrocarbon solvents, the atactic fractions could not usually be separated by extraction. In order to obtain the maximum degree of stereoregularity in each polymer, two techniques were employed. In some cases, lower polymerization temperatures were employed (-78°C to $+25^{\circ}\text{C}$), and in other cases catalyst systems were used which gave more stereoregular polymer. The stereoregular polymers are believed to be isotactic by this polymerization. These polymers were polymerized by Avison Corporation, Marcus Hook, Pennsylvania.

Determination of Molecular Weight and Distribution. The molecular weights and distributions for the poly-1-olefins were obtained by using a Waters Associates Gel Permeation Chromatograph (GPC Model 200). 1,2,4-trichlorobenzene was used as the elution solvent. To prevent degradation and to simplify the measurement of the corresponding intrinsic viscosities, the operating temperature was chosen to be 80°C . All samples were completely dissolved in this solvent at this temperature. The universal calibration was used to calculate the molecular weights and distributions. The details of this procedure have been described elsewhere.¹⁵ The samples studied along with their molecular weights and distributions are listed in Table 1.

Determination of Melting Point, Specific Volume and Volume Expansion Coefficient. The melting points of the poly-1-olefins were determined by dilatometry and Differential Scanning Calorimetry (Perkin-Elmer DSC-1B). The specific volume at 27°C was determined by a density gradient column. The specific volume at other temperatures was measured by dilatometry. The

volume expansion coefficient was calculated from specific volumes at different temperatures.

The polymers examined by dilatometry were poly-1-butene, poly-1-hexene, poly-1-heptene, poly-1-nonene, poly-1-undecene, poly-1-tridecene, poly-1-octadecene, Sample 1. The other poly-1-olefins were measured exclusively by DSC, due to the small amounts available.

The dilatometer construction was according to Bekkedahl.¹⁶ The dilatometers were made by Pyrex glass and consisted of a bulb sealed to a capillary tube. The capillaries were precision-bore tubing of inside diameter 1 mm. The tubes were calibrated by partial filling with mercury, observing the length and by weighing. Dilatometers, containing 1.5-2.0 grams of polymer, were evacuated for 5-6 hours prior to test. The vacuum reached was $<10^{-3}$ mm Hg. Mercury was then admitted to the evacuated system through a two-way stopcock, until it filled the dilatometer bulb and stood at a suitable height in the capillary with weighing before and after the addition of mercury. The dilatometers were placed in a stirred temperature bath and heated from ambient at a rate of about $0.2^{\circ}\text{C}/\text{min}$.

Norman Weeks, a graduate student at University of Massachusetts, checked this technique with an extremely heating rate. The equilibrium values of temperature and volume were taken to compare the values at heating rate of $0.2^{\circ}\text{C}/\text{min}$, for poly-1-butene. It was found that the equilibrium melting point was 1.5°C lower than the value of heating rate of a $0.2^{\circ}\text{C}/\text{min}$, but the expansion coefficient above the melting point was identical.

The DSC was calibrated by using standard samples of Indium and P-nitrotoluene. The peak of DSC thermogram was taken as the melting point.

The samples in DSC were precooled by liquid nitrogen down to -100°C and then heated at a rate of $5^{\circ}\text{C}/\text{min}$.

Measurements of Intrinsic Viscosity. Cannon-Ubbelohde dilution viscometers were used. Capillary dimensions were chosen so that kinetic energy correlations for efflux times were negligible. Efflux times, reproducible to $\pm 0.05\%$ were obtained for solvent and for each solution. Approximate 0.1% by weight of antioxidant was added to the solutions of poly-1-olefin to inhibit oxidative degradation. The viscosities were measured in an oil bath which was controlled to 0.01°C .

Results and Discussion

The samples, poly-1-hexene, poly-1-heptene, poly-1-octene, poly-1-nonene and poly-1-undecene were amorphous as received. Attempts were made to crystallize these polymers by cooling them from room temperature to 0°C by ice over 12 hours. By this treatment, poly-1-nonene and poly-1-undecene became markedly crystalline and poly-1-heptene modestly so by observing the volume change for melting. The poly-1-hexene and poly-1-octene samples were not crystallizable by these techniques with no melting point features observed by either dilatometry or DSC. The specific volume vs. temperature from dilatometry is plotted in Figures 1-5 for the samples of poly-1-butene, poly-1-hexene, poly-1-heptene, poly-1-nonene and poly-1-undecene. For the higher members, two melting transitions were found. The lower melting points for poly-1-tridecene, poly-1-hexadecene and poly-1-octadecene were 39 , 41 and 42°C respectively, and the higher melting points 55 , 70 and 74°C . These dilatometric melting features are shown in Figures 6 and 7 for poly-1-tridecene and poly-1-octadecene (Sample 1). Figures 8-10 show the corresponding two melting points of poly-1-tridecene, poly-1-hexadecene and poly-1-octadecene (Sample 1) from DSC measurements. The other two poly-1-octadecene samples, see Table 2, also show two melting points. They have the same lower melting point (42°C) as poly-1-octadecene (Sample 1). For the higher melting point, 74°C and 68°C were found respectively for poly-1-octadecene, Samples 2 and 3.

and in our poly-1-hexadecene and the three poly-1-octadecene samples. We concur with the conclusion that poly-1-tridecene is the minimum side-chain length that can involve side-chain crystallization. When the higher members of poly-1-olefin series were cooled from the melt to 0°C at 20°C/min., then the lower melting point disappeared and only the higher melting point remained.

Aubrey and Barnatt⁶ showed that if poly-1-octadecene were extracted with hexene, then the solvent-soluble polymer had only the lower melting point and solvent-insoluble fraction had the higher melting point. The same results were also found previously by Beck, Knox and Price¹ by using pentene as an extracting solvent. They suggested that the two melting phenomena were due to different species, such as atactic and isotactic polymer. The higher melting point is due to the melting of isotactic polymer and the lower melting point is due to the melting of atactic polymer. However, if atactic form can crystallize, the side chain rather than main chain is involved in crystallization.^{1,6}

Two melting peaks exist in our high member poly-1-olefins. The lower melting peak is much smaller than the higher melting peak. This contrasts with results of Aubrey and Barnatt⁶ and with Maron et al.⁷ Their samples show a larger peak for the lower melting form than for the higher. As mentioned under our polymer preparation, the samples had been purified by hexene extraction. However, due to the solubility of these polymers in hydrocarbon solvent, the atactic fractions could not be separated completely from isotactic polymer. It may be inferred that there is a small atactic fraction in our isotactic samples. This small atactic portion may contribute to the small peak of lower melting point. The fact that the lower melting point for poly-1-tridecene and for our higher poly-1-olefins can be eliminated by fast cooling the sample from the melt may indicate a slower crystallization of atactic species.

The specific volumes of poly-1-olefins are compared at the same temperature in Figure 11. The specific volume extrapolated from the melt state to absolute zero is also shown at the bottom of this figure. The values should correspond to trends in chain-to-chain packing. It may be seen that this density becomes less and less until it hits a peak at around poly-1-hexene to poly-1-heptene. The densities then increase slightly with increasing side-chain length leveling off for the higher members of the series.

The volume expansion coefficient above the melting point, α_m , in $\text{ml/g}^\circ\text{C}$ was calculated from the slope of the plot of specific volume vs. temperature. It was found that α_m is essentially a constant for each polymer above the melting point. Also, the α_m of the poly-1-olefins shows a minimum around poly-1-hexene and poly-1-heptene. Takayanagi has pointed out for a side chain of infinite length, the melting point should reach the melting point of high density polyethylene.¹² The melting point of the higher poly-1-olefin, for which melting points increase with the length of side chain, can be plotted vs. $1/(N+2)$, where N is the number of carbons in the side chain. The plot can thus be extrapolated to infinite side-chain length. Our data shown in Figure 12 confirms that the extrapolation of melting point to infinite side-chain length reaches the melting point of high density polyethylene. In this extrapolation, the higher melting point of poly-1-tridecene, poly-1-hexadecene and poly-1-octadecene was used. Accordingly, the α_m is also plotted vs. $1/(N+2)$. Again the extrapolation reach the value of α_m for high density polyethylene as shown in Figure 13. The melting point and α_m data used were obtained from dilatometry in our laboratory.

According to X-ray studies,⁵ the side chains for upper members of poly-1-olefins have almost the same structure as the main chain of polyethylene. This is thus consistent with the fact that the extrapolated melting point and expansion coefficient for infinite side-chain length have the same values as for polyethylene.

The minimum value of melting point, α_m and the maximum in specific volume, which occurs around poly-1-hexene to poly-1-octene, can be explained by the packing state of the molecules and/or the conformation of the molecules. The conformation and packing of the molecules in the crystalline region have been presented for the poly-1-olefin series.⁵ However, Takayanagi¹² has shown that the conformation of molecules and the packing of molecule chains in the amorphous region or in the melt are not completely random but are similar to those in the crystalline region. This is consistent with Plate's studies²⁰ of poly (alkyl acrylates) and poly (alkyl methacrylates). He found that the higher members, i.e., long side chains, show some order by X-ray diffraction well above the highest melting point which he describes as a "polymer liquid crystal".²¹

As mentioned, the specific volumes for the poly-1-olefin series, extrapolated from the melt state to absolute zero, have a maximum around poly-1-hexene or poly-1-heptene. This may indicate the chain-to-chain packing density in the amorphous state is smallest in this region. Takayanagi¹¹ has also shown that the packing state of poly-1-olefin molecules becomes more open as the side-chain length increases from polypropylene to poly-1-octene and that as the side-chain length is made yet longer, the packing of molecules becomes more dense. In our case, the changeover appears to be in the region of poly-1-hexene and poly-1-octene.

Unperturbed Chain Dimension. The above discussions of molecular packing are based on the bulk properties for the poly-1-olefins. It is thus of interest to investigate changes in individual chain dimension with composition from intrinsic viscosities near a theta temperature. At theta conditions, mole-

cules exhibit their unperturbed dimension, i.e., dimension determined by bond distances, bond angles and the potentials for hindered bond rotation.²²

The theta temperature, T_{θ} can be considered the incipient immiscibility temperature for polymer molecules of infinite molecular weight. It has been shown from thermodynamic considerations that for dilute polymer solutions at T_{θ} the second virial coefficient A_2 is zero and higher coefficients are near zero.²² Therefore one must either measure the second virial coefficient A_2 at several temperatures and find T_{θ} by interpolation or extrapolation to $A_2=0$ or determine the T_{θ} by extrapolating the critical miscibility temperature of a polymer-solvent system to infinite molecular weight. Both methods are not available for the poly-1-olefins because of limited sample sizes.

In this method, the precipitation temperature is determined as a function of volume concentration at very low concentration. The reciprocal of the absolute precipitation temperature is plotted versus the log of the volume fraction of polymer. The concentrations employed were generally from 1.0 to 0.001 volume percent, the resulting line was extrapolated to a polymer volume fraction of one and this value taken as the theta temperature. An advantage of this method is the need for only one molecular weight for each polymer. To check the accuracy of the method, poly-1-butene was first tested. The T_{θ} measured in Anisole is compared in Figure 14 with the literature value by Krigbaum.²⁴ At very low concentration, the reciprocal of precipitation temperature as a function of polymer volume fraction is linear. The temperature obtained from extrapolation to pure polymer is $88 \pm 1^{\circ}\text{C}$. This is close to the T_{θ} (89.1°C) for consolute temperatures as a function of isotactic molecular weights given by Krigbaum.²⁴ The method²³ therefore seems to be a convenient way, with a precision of about $1 - 2^{\circ}\text{C}$ for locating T_{θ} . The T_{θ} for the poly-1-olefins was measured in two solvents, anisole and cyclohexanone. The results as a function of composition are shown in Figures 15 and 16. The T_{θ} for two

different solvents show a common minimum at poly-1-pentene. The sequence of three poly-1-octadecene samples have a T_{θ} at 70, 73 and 71°C in anisole and 94, 97 and 92°C in cyclohexane respectively. The temperature coefficient of $[\eta]$ for poly-1-olefins, in the vicinity above T_{θ} , is only +1%/°C from 70-90°C. Therefore, any small error in T_{θ} introduced by the test method is of not importance in the determination of $[\eta]$ at T_{θ} .

The unperturbed mean-square end-to-end distance $\langle R_o^2 \rangle$ is obtained from the measurements of intrinsic viscosity $[\eta]_{\theta}$ at theta condition. $[\eta]_{\theta}$ is related to $\langle R_o^2 \rangle$ by the following equation:

$$[\eta]_{\theta} = \Phi \frac{\langle R_o^2 \rangle^{3/2}}{M} M^{1/2} = KM^{1/2} \quad (1)$$

Where Φ is the universal constant of theoretical value 2.87×10^{21} for $[\eta]$ in dl/g. M is polymer molecular weight. Weight average molecular weight was used here for the calculation. The values of $\langle R_o^2 \rangle^{1/2}/M^{1/2}$ calculated in this way are shown in Table 3. The values found in literature are also listed in the table. The data show a small increase in chain dimensions from poly-1-butene to poly-1-hexene, then a decrease with increasing side-chain length. The apparent decrease in size for the higher members of the series is due in part to a decrease in chain length with increasing side-chain length for comparisons at constant molecular weight. This effect can be eliminated by calculation of the characteristic ratio, $\langle R_o^2 \rangle/n\ell^2$, which is normalized to main chain length n . The bond length ℓ , for all members must be very similar and near 1.54 Å. The calculated values of $\langle R_o^2 \rangle/n\ell^2$ are shown in Table 3 along with available literature data. It is obvious that the characteristic ratio for poly-1-olefin series monotonically increases with increasing side-chain length.

The steric factor, σ , is defined by the equation:

$$\sigma = [\langle R_o^2 \rangle / \langle R_o^2 \rangle_f]^{1/2}$$

Where $\langle R_o^2 \rangle_f$ is the theoretical mean square end-to-end distance for free-rotation. The values of σ of the poly-1-olefins is listed in Table 3. They also systematically increase with increasing side-chain length. Difference between workers cited in Table 3 may be due to 1) the different values of Φ used in calculation; 2) different tacticities in samples; and 3) effects of molecular weight distribution.

The purpose of our work is to compare the chain dimensions for the poly-1-olefins at similar condition in order to know the change in dimension with the composition. Although the samples of poly-1-octadecene have different unperturbed dimensions, the difference, however, does not affect the observed trend with composition.

Acknowledgement

The authors would like to express appreciation to Professor Julian Johnson for helpful discussions of theta temperature experiments.

TABLE 1

Poly-1-olefin

Molecular Weight and Molecular Weight Distribution
by Calibrated Gel Permeation Chromatography

Polymer	M_n	M_w	M_w/M_n
Poly-1-butene	6.30×10^4	8.50×10^5	13.50
Poly-1-hexene	4.00×10^3	1.70×10^4	4.30
Poly-1-heptene	8.70×10^3	5.90×10^4	6.80
Poly-1-octene	1.10×10^4	8.00×10^4	7.30
Poly-1-nonene	6.80×10^4	3.70×10^5	5.40
Poly-1-undecene	3.80×10^5	1.20×10^6	11.00
Poly-1-hexadecene	3.40×10^5	2.50×10^6	7.40
Poly-1-octadecene			
Sample 1	7.30×10^5	3.50×10^6	4.80
Sample 2	2.10×10^5	3.50×10^6	13.00
Sample 3	6.90×10^3	4.30×10^5	6.20

TABLE 2

The Melting Points of Poly-1-Olefins

Poly-1-Olefin	This Work, °C		Literature, °C			
	Dilatometer	DSC	Ref. A	Ref. B	Ref. C	Ref. D
Poly-1-butene	128	126	---	132	120	125
Poly-1-pentene	---	70	---	80	70	73
Poly-1-hexene	---	---	---	---	-55	---
Poly-1-heptene	38	37	---	17	-40	---
Poly-1-octene	---	---	20	---	-38	---
Poly-1-nonene	30	32	29	19	---	---
Poly-1-decene	---	35	32	34	---	29
Poly-1-undecene	40	39	41	---	---	---
Poly-1-dodecene	---	44	47	49	45	46
Poly-1-tridecene	55 39	55 39	55 ---	---	---	52 ---
Poly-1-hexadecene	---	70 41	67 32	67.5 ---	---	63 ---
Poly-1-octadecene Sample 1	75 42	74 42	75 43	---	---	---
Sample 2	---	74	---	---	---	---
Sample 3	---	42	---	---	---	---
	---	68	---	---	---	---
	---	42	---	---	---	---

TABLE 2

(Cont.)

- Ref. A D. L. Beck, J. R. Knox and J. A. Price. Presented before Division of Petroleum Chemistry, National ACS Meeting, March 31 - April 4, 1963.
- Ref. B K. J. Clark, A. Turner-Jones and D. J. H. Sandiford, Chem. and Ind. (London) 2010 (1962).
- Ref. C F. P. Reding, J. Polymer Sci., 21, 547 (1956).
- Ref. D W. Philippoff and E. G. M. Torngvist, J. Polymer Sci., C23, 881 (1968).

TABLE 3

Unperturbed Chain Dimension, $\langle R_0^2 \rangle^{1/2}/M^{1/2}$, Characteristic Ratio, $\langle R_0^2 \rangle/n\ell^2$, and Steric Factor σ for the Poly-1-olefins

Polymer	$\langle R_0^2 \rangle^{1/2}/M^{1/2}$ $\times 10^{11}$	$\langle R_0^2 \rangle/n\ell^2$	σ	Ref.
Poly-1-butene	721 775	6.2	1.73 1.86	* 25
Isotactic	1130		2.70	24
Atactic	1000		2.40	24
Poly-1-pentene	785	9.2	2.10	13
Poly-1-hexene	861	13.0	2.55	*
Poly-1-octene	690-800		2.36-2.74	14
Poly-1-decene	697	14.0	2.64	*
Poly-1-tridecene	638	15.5	2.78	*
Poly-1-octadecene Sample 1	584	18.3	3.0	*
Sample 2	610	19.6	3.12	*

* This work.

REFERENCES

1. D. L. Beck, J. R. Knox and J. A. Price, presented before Division of Petroleum Chemistry, ACS Meeting, March 31 - April 4, 1963.
2. K. J. Clark, A. Turner-Jones and D. J. H. Sandiford, Chem. and Ind. (London) 2010 (1962).
3. F. P. Reding, J. Polymer Sci., 21, 547 (1956).
4. M. S. Dannis, J. Appl. Polymer Sci., 1, 121 (1959).
5. A. Turner-Jones, Makromol. Chem., 71, 1 (1964).
6. D. W. Aubrey and A. Barnatt, J. Polymer Sci., A-2, 6, 241 (1968).
7. C. A. Daniels, S. H. Maron and P. J. Livesey, J. Macromol. Sci.-Phys., B 4, 47 (1970).
8. S. Manabe, M. Takayanagi, Kogyo Kagaku Zasshi, 73, 1572 (1970).
9. S. Manabe, S. Minami, M. Takayanagi, Kogyo Kagaku Zasshi, 73, 1577 (1970).
10. S. Manabe, M. Takayanagi, Kogyo Kagaku Zasshi, 73, 1581 (1970).
11. S. Manabe, S. Nakamura, S. Uemura, and M. Takayanagi, Kogyo Kagaku Zasshi, 73, 1587 (1970).
12. S. Manabe and M. Takayanagi, Kogyo Kagaku Zasshi, 73, 1595 (1970).
13. J. E. Mark and P. J. Flory, J. Am. Chem. Soc., 87, 1423 (1965).
14. K. Shirayama, T. Matsuda and S. I. Kita, Die Makromol. Chem., 147, 157 (1971).
15. J. V. Dawkins and J. W. Maddock, European Polymer J., 7, 1537 (1971).
16. L. A. Wood and N. Bekkedahl, J. Res. Nat. Bur. Stand., 36, 489 (1946).
17. G. Natta, P. Corradini, Makromol. Chemie, 16, 213 (1955).

18. G. Natta, P. Corradini and I. W. Bassi, *Makromol. Chemie*, 21, 240 (1956).
19. J. S. Wang, R. S. Porter and J. R. Knox, *J. Polymer Sci.*, B8, 671 (1970).
20. N. A. Plate', V. P. Shivaev, *Vysokomol. Soedin*, 13, 410 (1971).
21. N. A. Plate', Seminar at University of Massachusetts (1971).
22. P. J. Flory, *Principles of Polymer Chemistry*, Cornell Univ. Press, Ithaca, New York (1953).
23. C. F. Cornet and H. Van Ballegooijen, *Polymer*, 7, 293 (1966).
24. W. R. Krigbaum, J. E. Kurz and P. Smith, *J. Phys. Chem.*, 65, 1984 (1961).
25. M. Kurata and W. H. Stockmayer, *Fortschr. Hochpolymer Forsch.*, 3, 196 (1963).

CAPTIONS FOR FIGURES

1. The specific volume versus temperature for poly-1-butene.
2. The specific volume versus temperature for poly-1-hexene.
3. The specific volume versus temperature for poly-1-heptene.
4. The specific volume versus temperature for poly-1-nonene.
5. The specific volume versus temperature for poly-1-undecene.
6. The specific volume versus temperature for poly-1-tridecene.
7. The specific volume versus temperature for poly-1-octadecene.
8. The DSC thermogram of poly-1-tridecene.
9. The DSC thermogram of poly-1-hexadecene.
10. The DSC thermogram of poly-1-octadecene, Sample 1.
11. The specific volumes of poly-1-olefins.
12. The melting point of poly-1-olefins versus $1/(N+2)$. N is the number of side chain carbon.
13. The expansion coefficient of poly-1-olefins versus $1/(N+2)$.
14. Theta temperature of poly-1-butene from Cornet's method.
15. Theta temperature of poly-1-olefin series in Anisole.
16. Theta temperature of poly-1-olefin series in cyclohexaone.

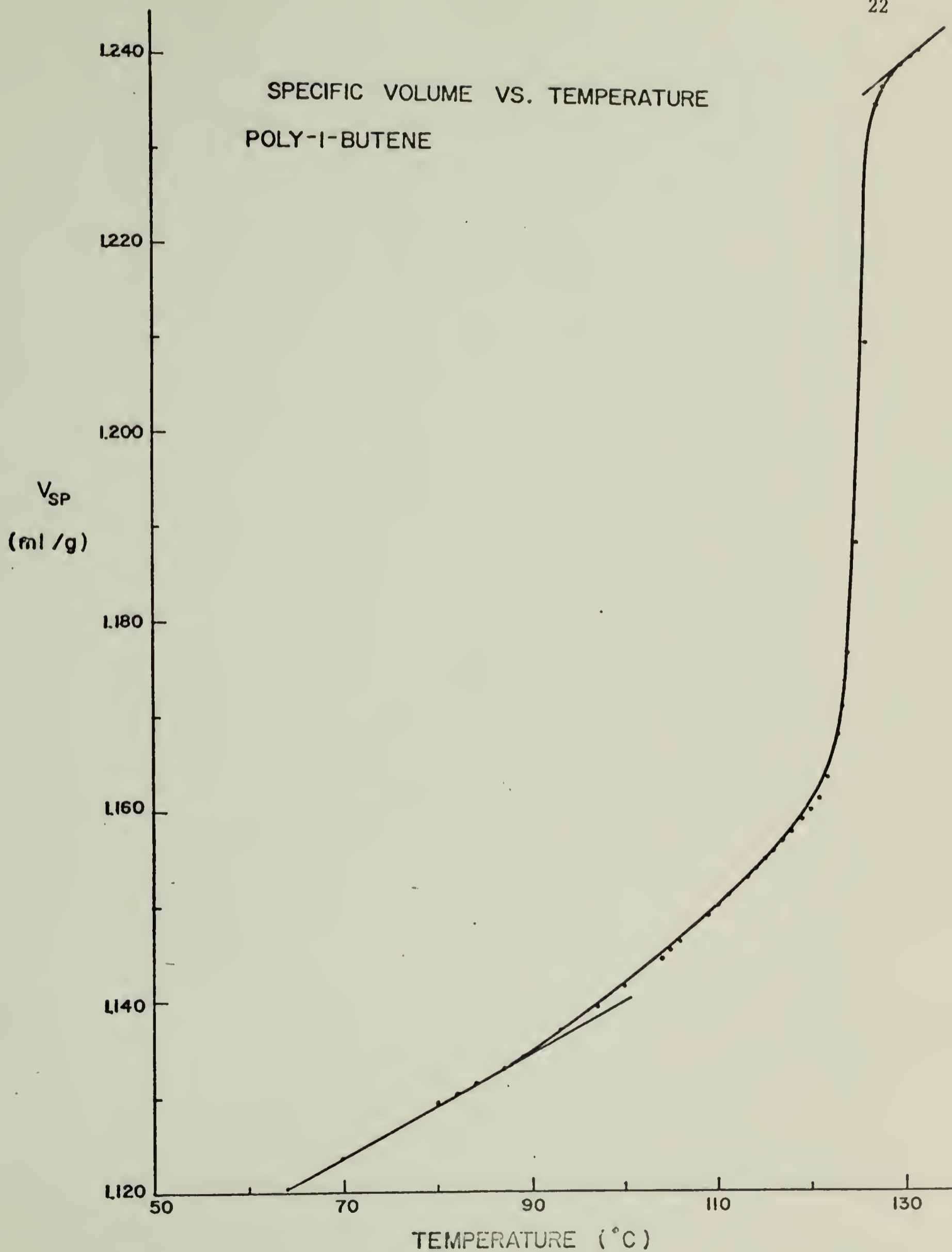


Figure I-1

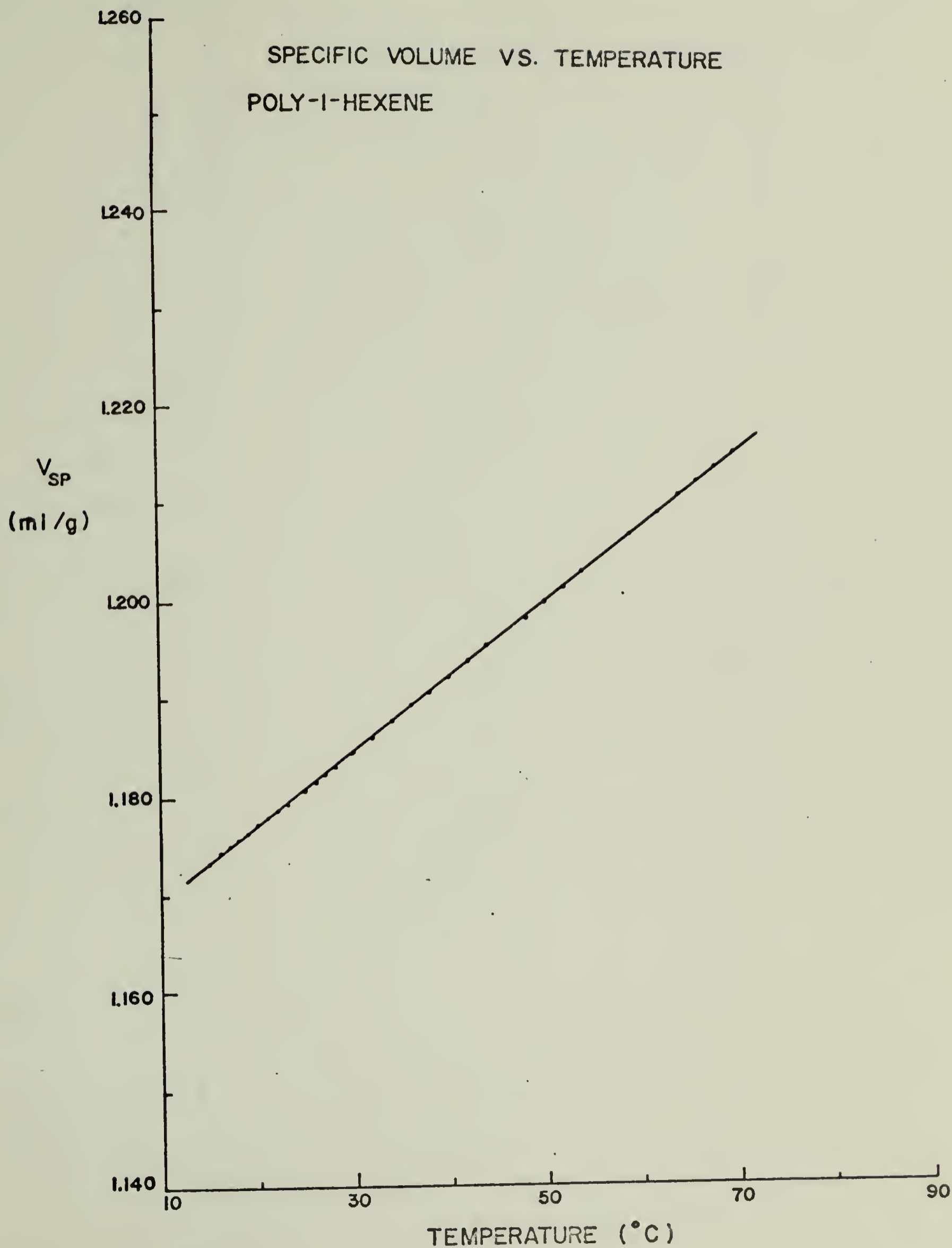


Figure I-2

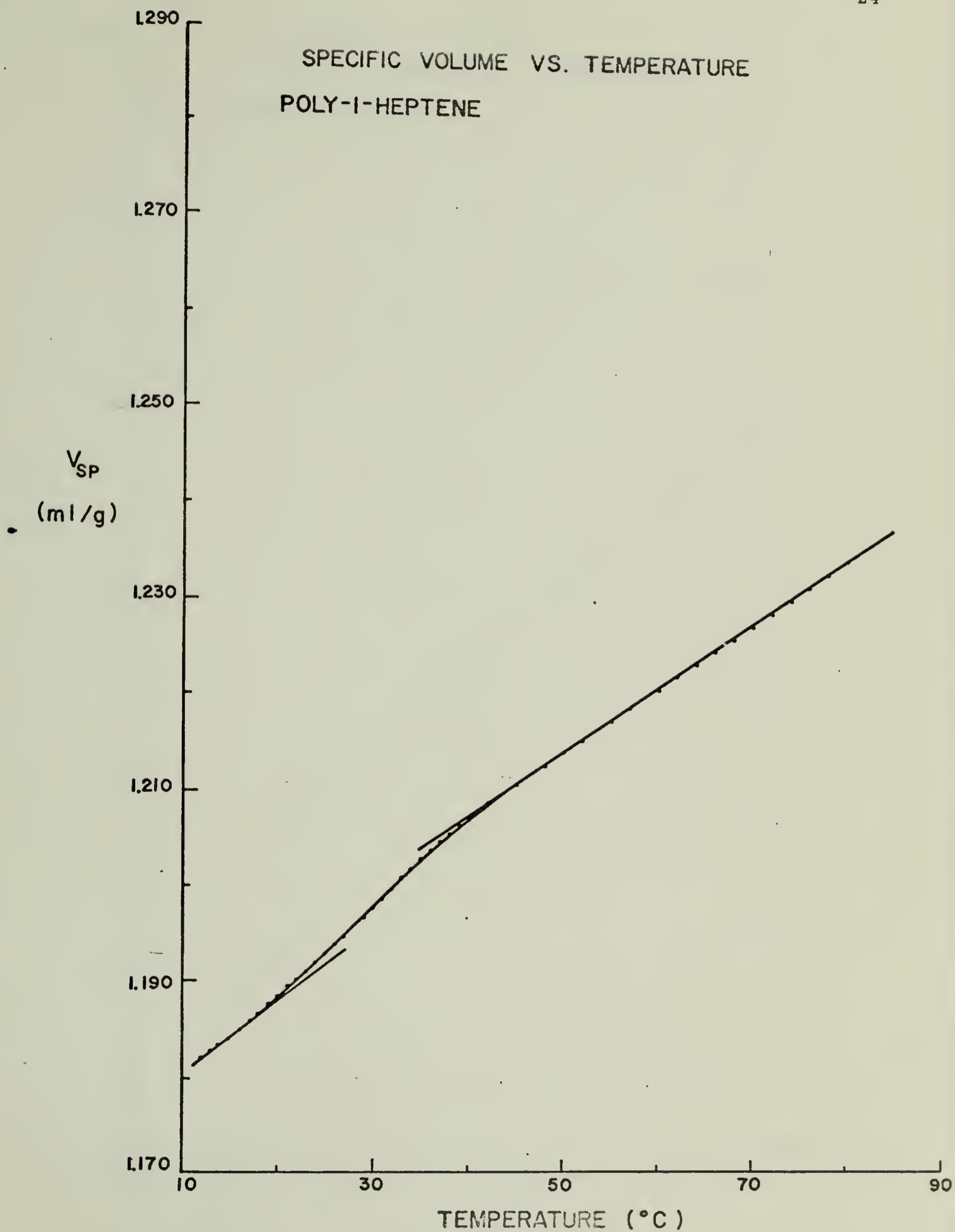


Figure I-3

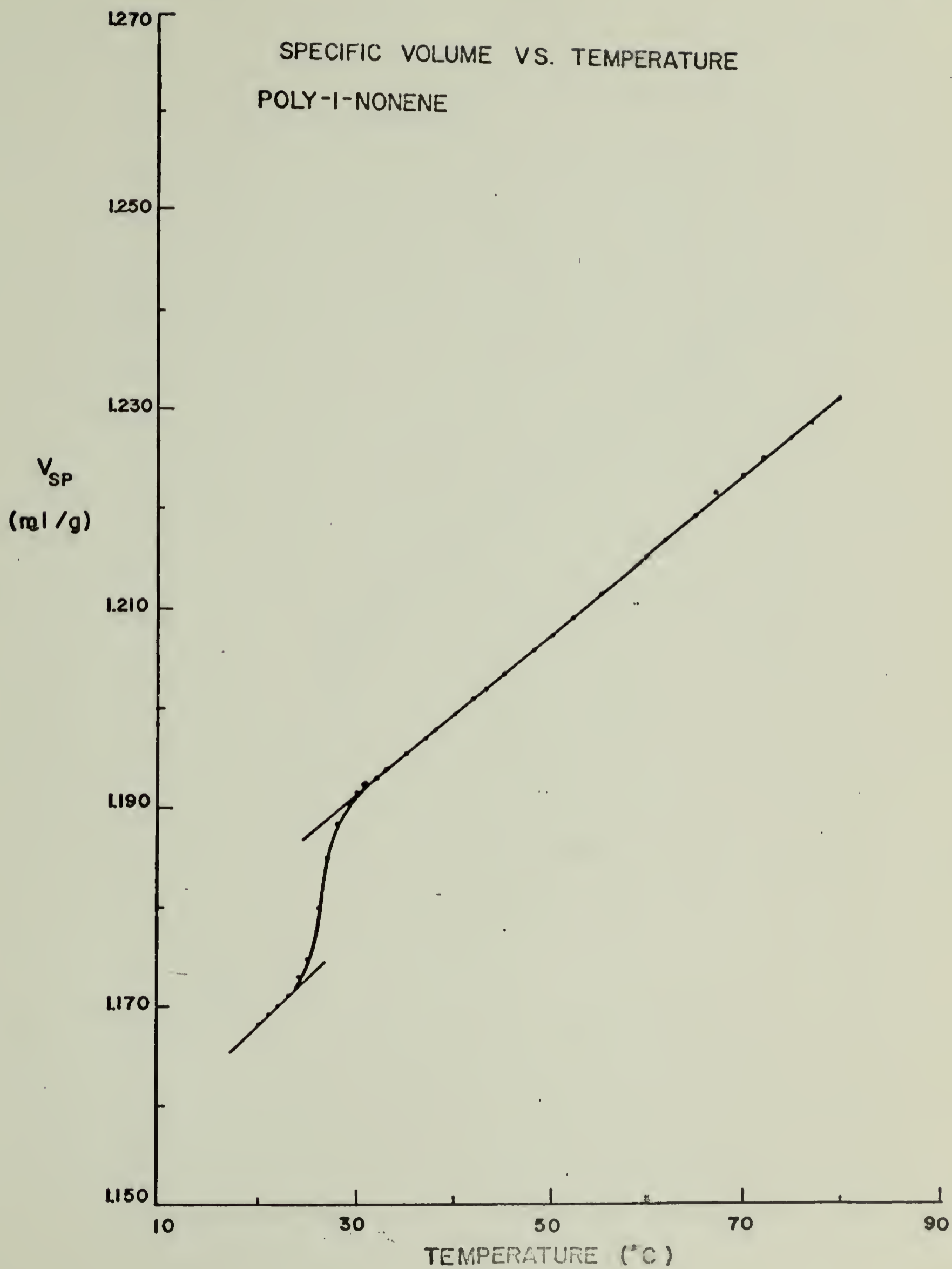


Figure I-4

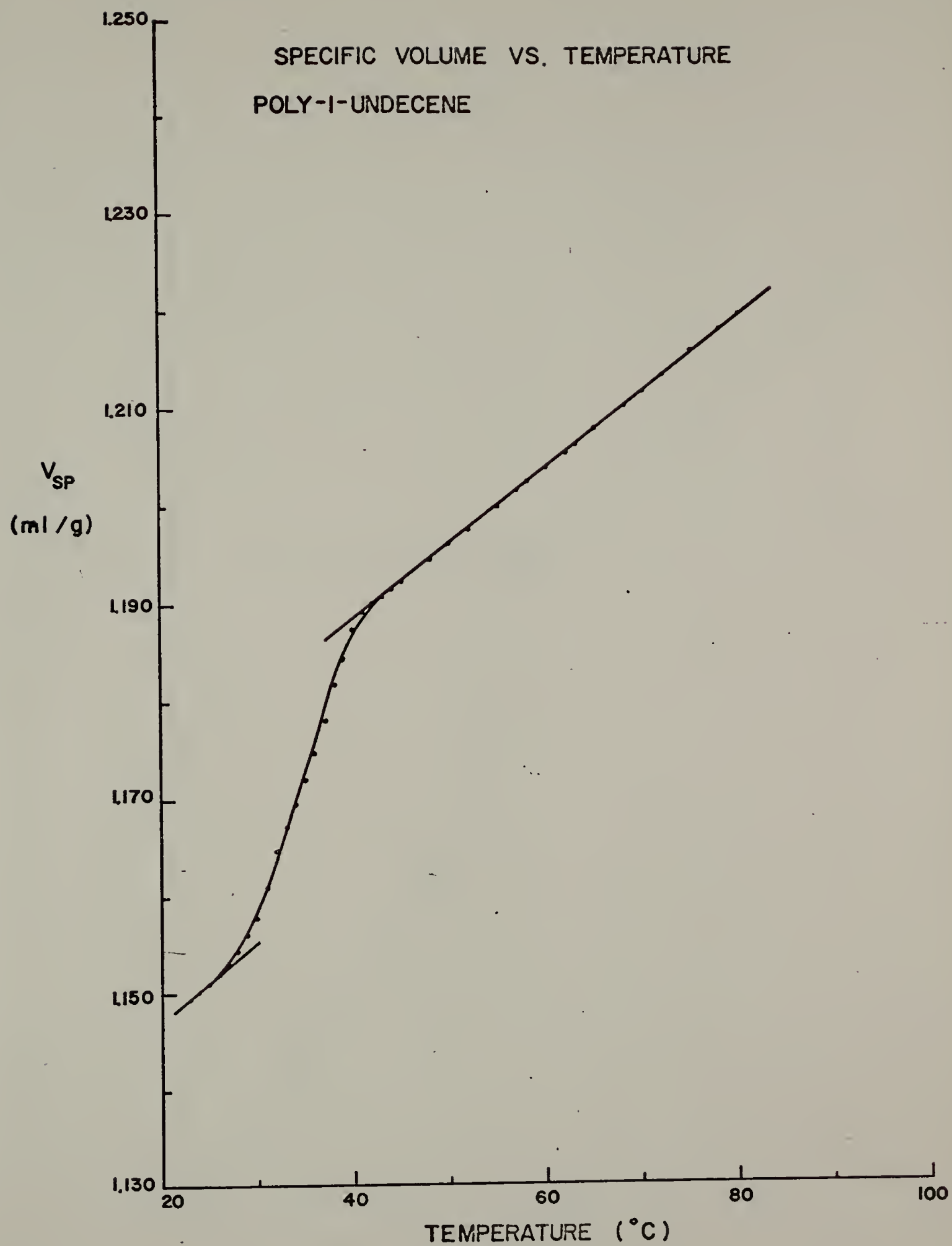


Figure I-5

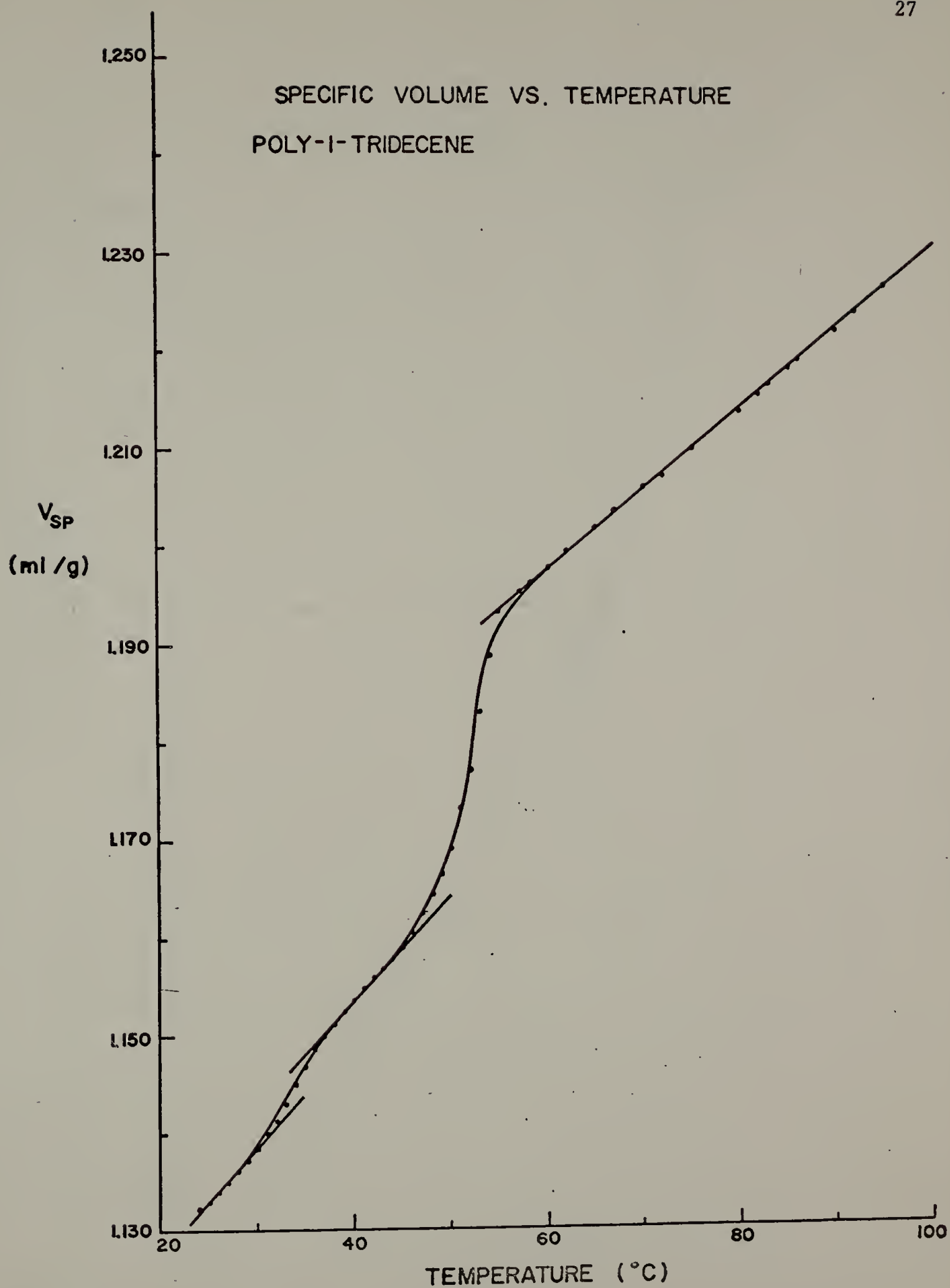


Figure I-6

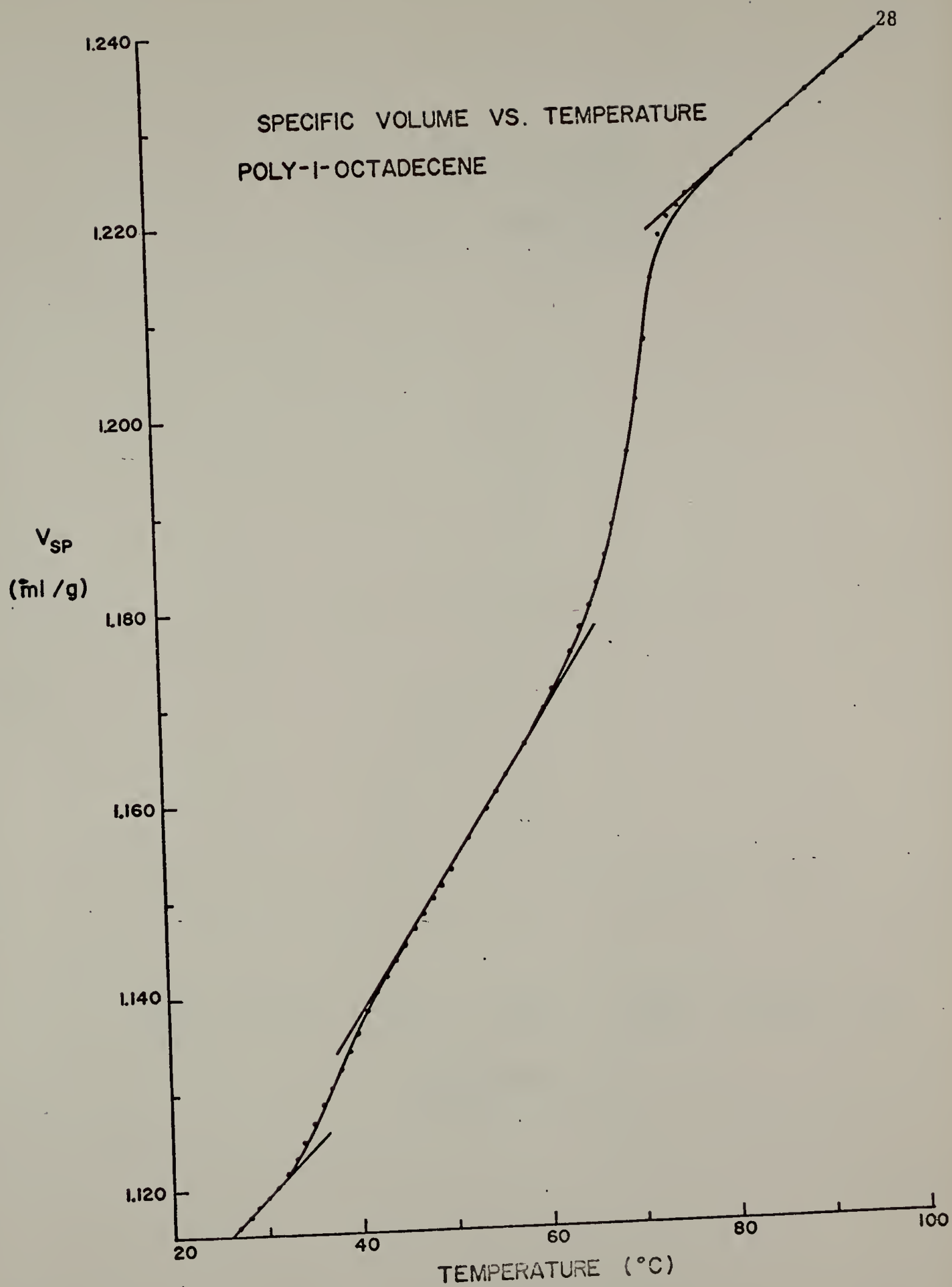


Figure I-7

DSC THERMOGRAM
POLY-1-TRIDECENE

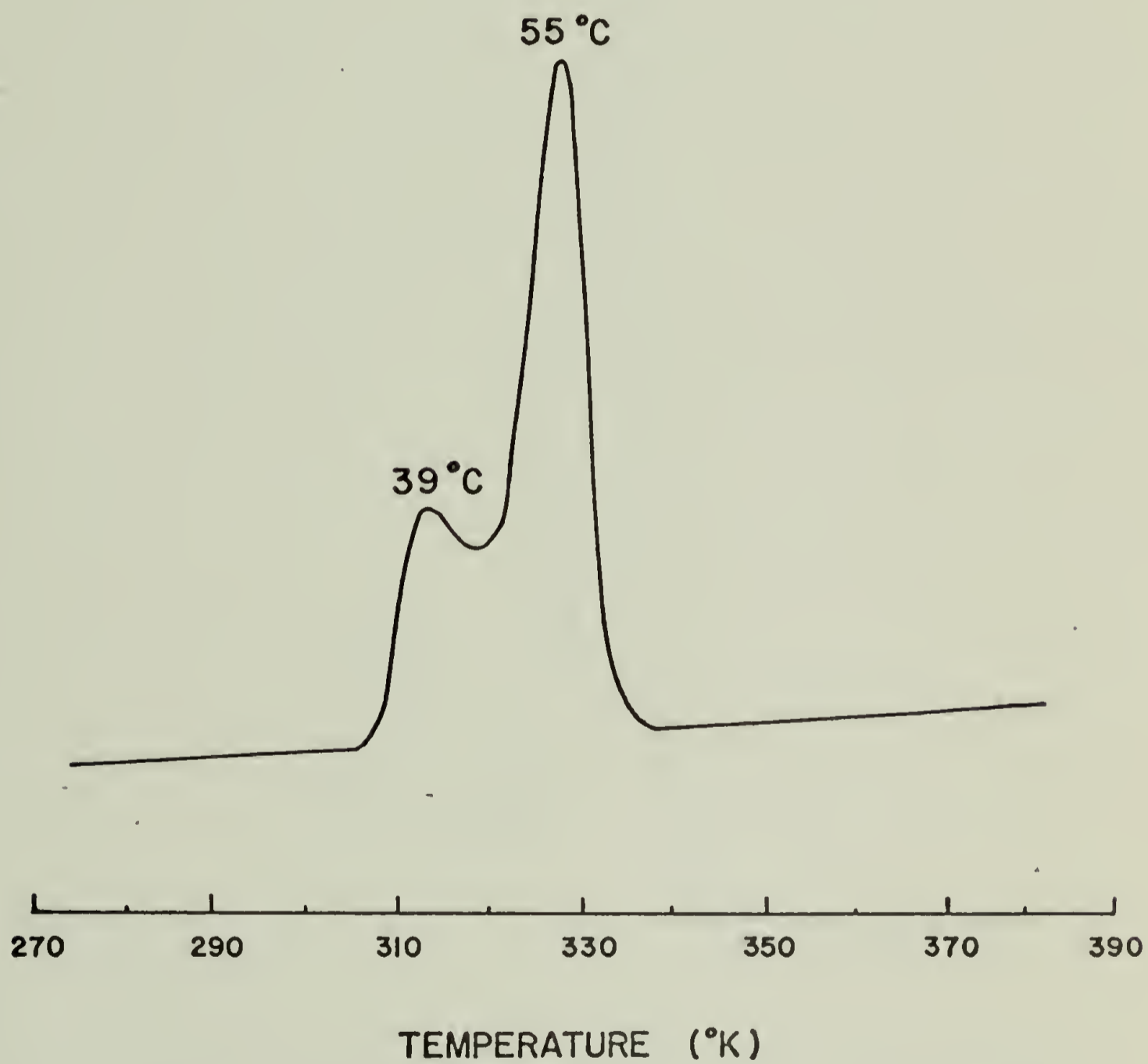


Figure I-8

DSC THERMOGRAM
POLY-1-HEXADECENE

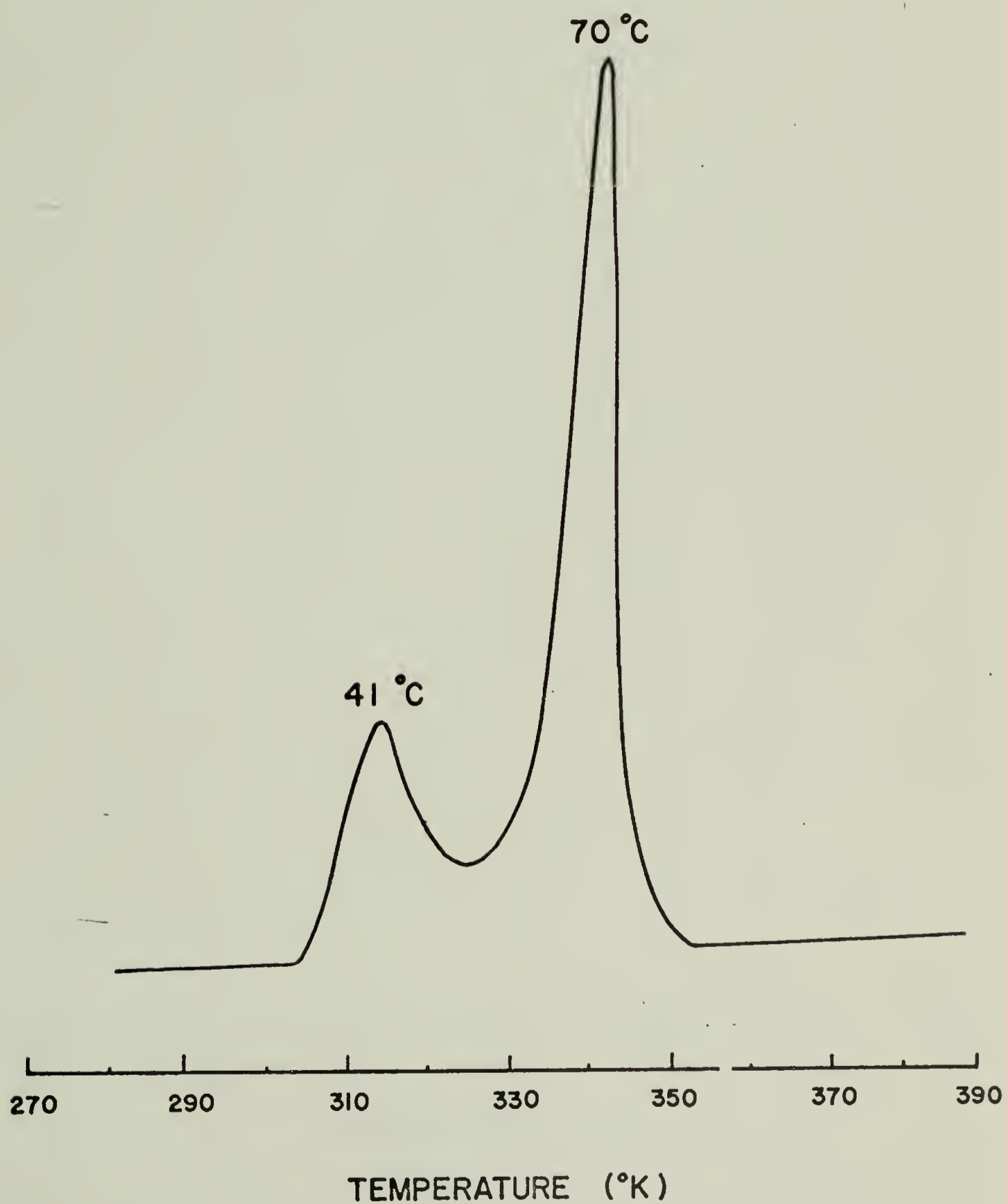


Figure I-9

DSC THERMOGRAM
POLY-1-OCTADECENE
(SAMPLE 1)

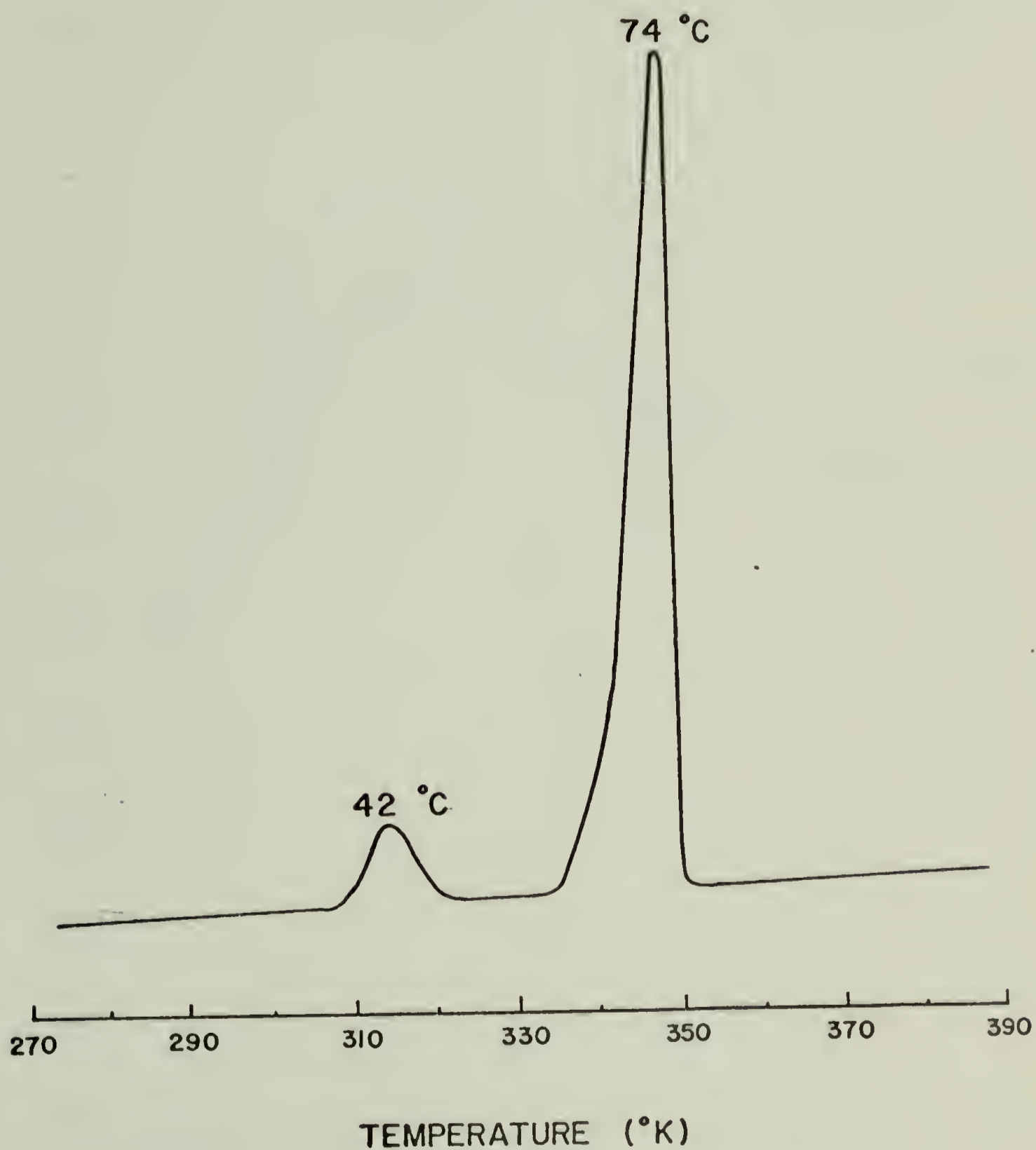


Figure I-10

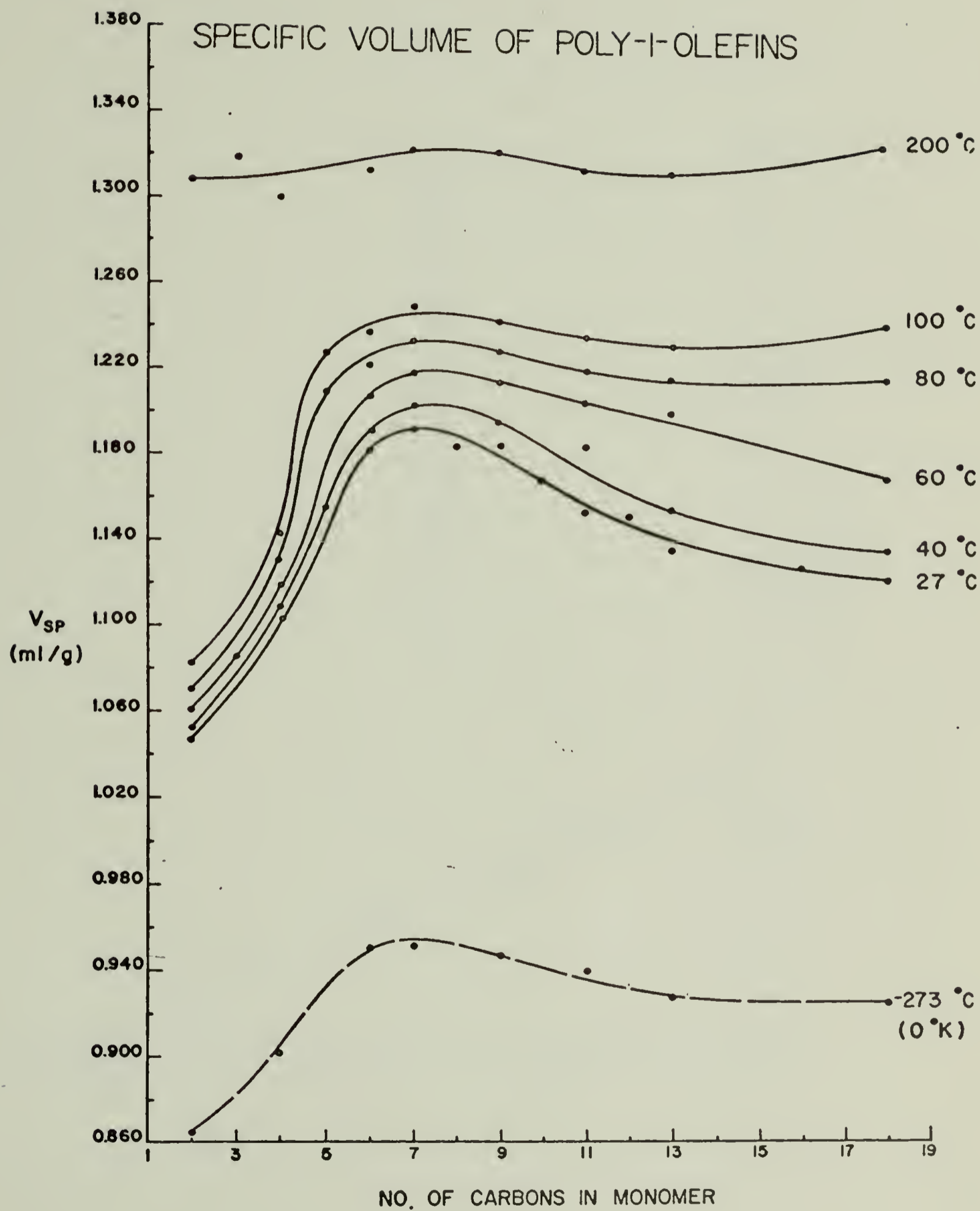


Figure I-11

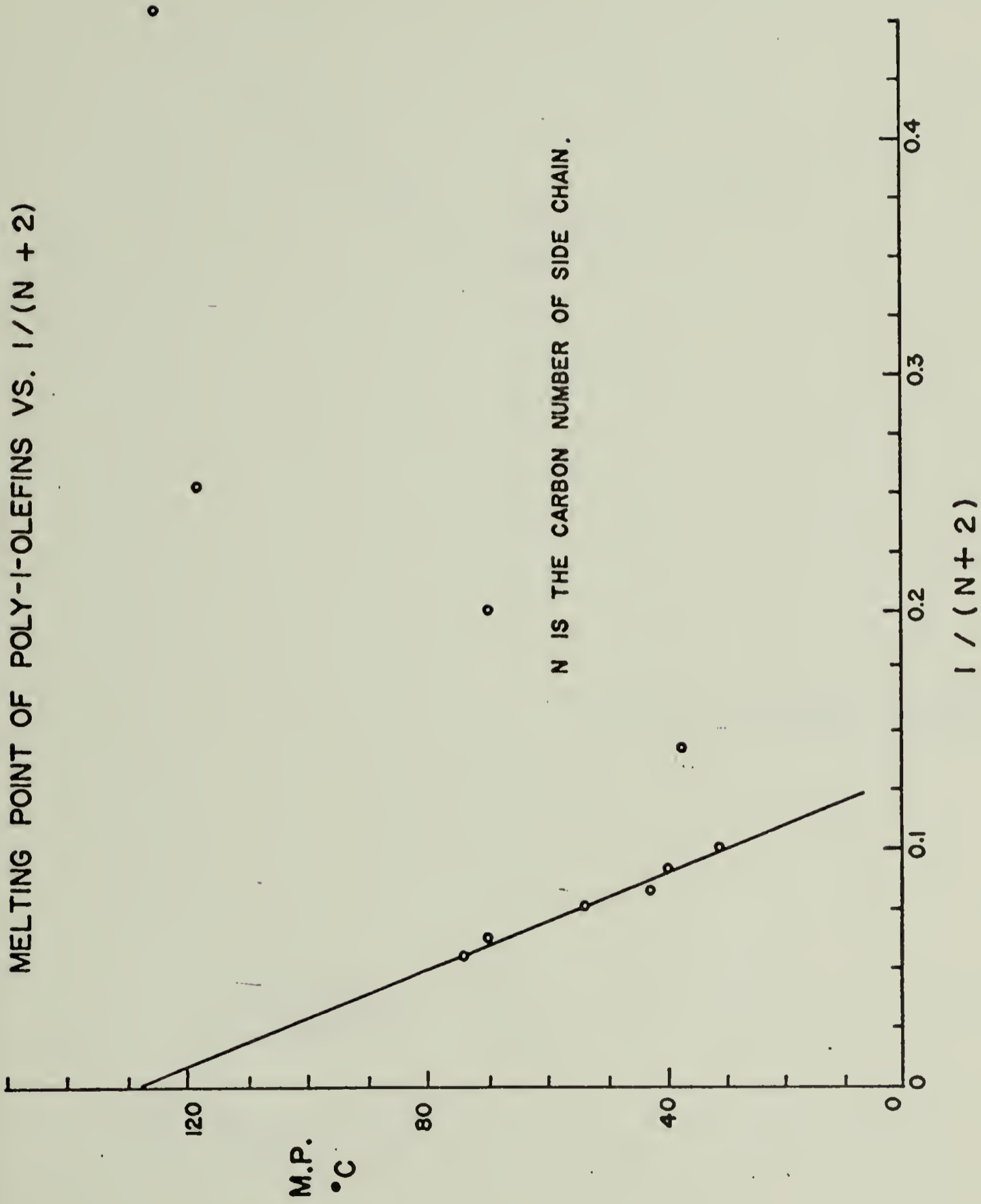


Figure I-12

EXPANSION COEFFICIENT OF POLY-1-OLEFIN MELTS VS. $1/(N+2)$

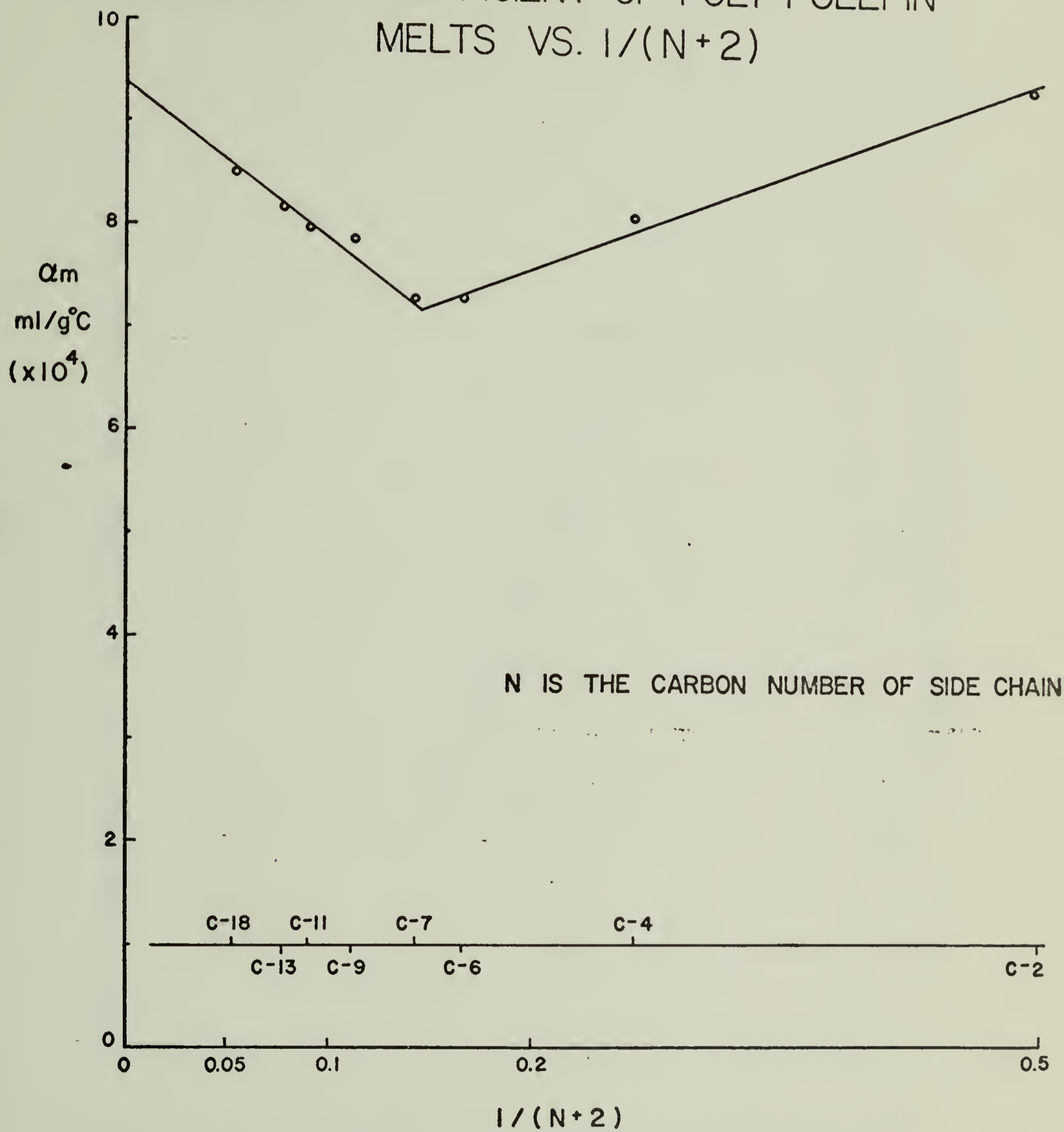


Figure I-13

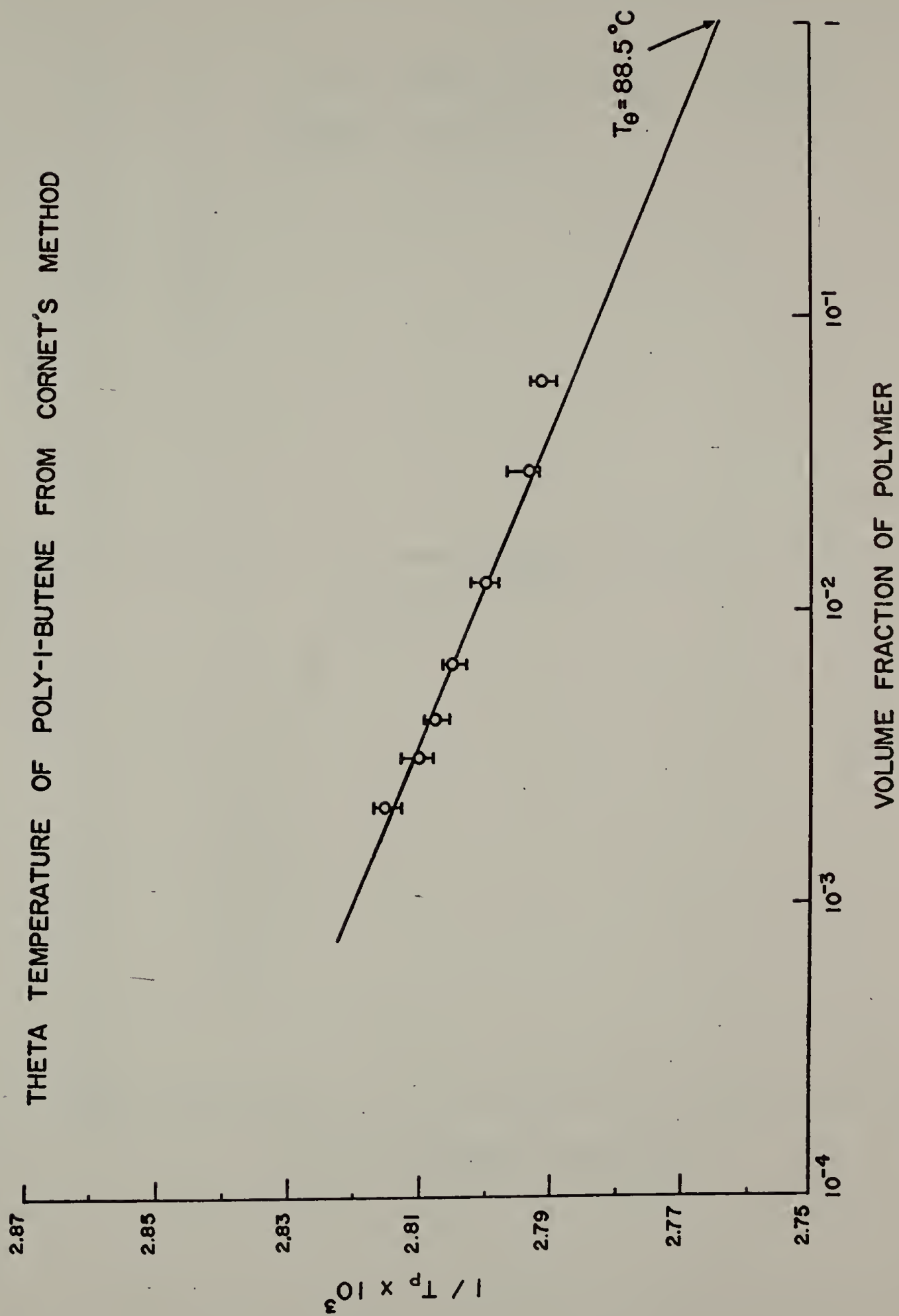


Figure I-14

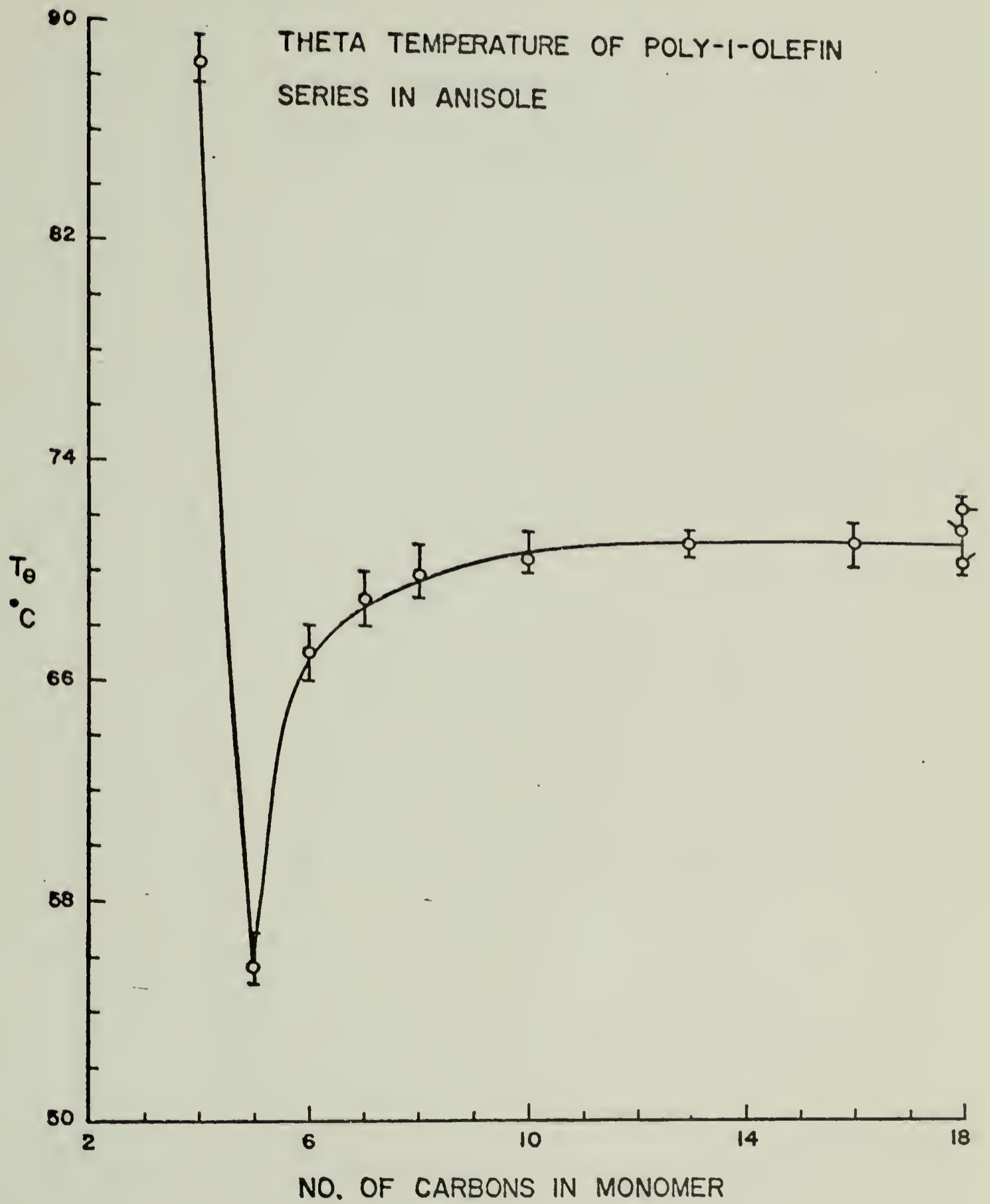


Figure I-15

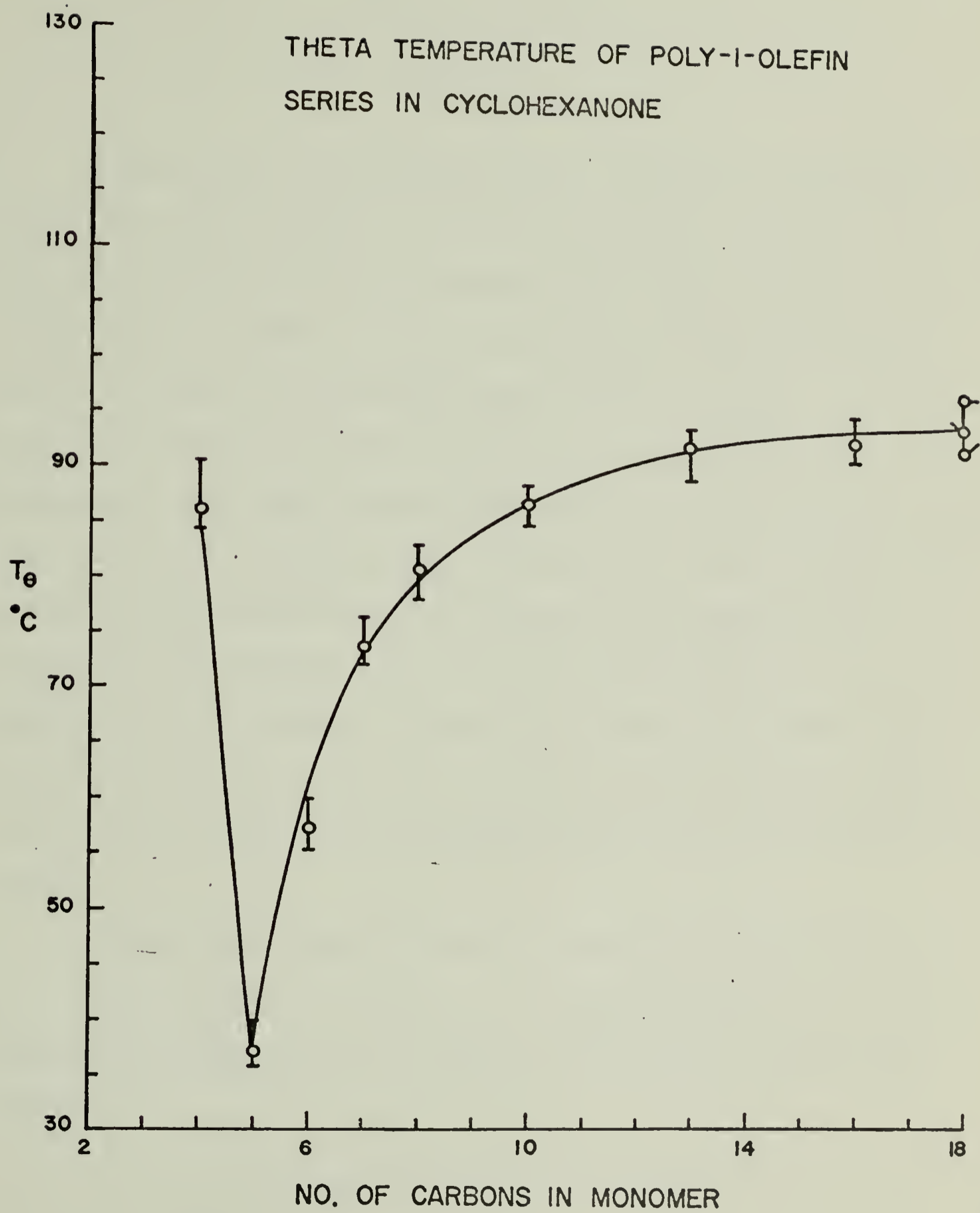


Figure I-16

CHAPTER II

TEMPERATURE COEFFICIENTS FOR THE VISCOSITY OF POLY-1-OLEFINS

Introduction

Because of their commercial importance, hundreds of studies have been reported on the flow properties of the lower polyolefins, principally in low and high density polyethylene and on polypropylene. To the rheologist, the poly-1-olefin series represents a fundamental compositional series for evaluating the effect of chemical composition on flow properties of polymers. Fundamental data of flow properties, however, is rare on the higher members of the poly-1-olefin series. It has been shown for other polymers that an important rheological characteristic, the viscosity change with temperature, can be determined from a single sample of any one polymer, provided certain compositional and test measurement requirements are met.^{1,2,3} From this background, it has been possible in this investigation to evaluate the characteristic viscosity temperature coefficient for the series of poly-1-olefins in terms of activation energy for viscous flow and to relate these characteristic values to compositional parameters.

It is most widely known in the form presented by Eyring, see Equation (1), which expresses a useful and precise viscosity-temperature coefficient in terms of an activation energy for viscous flow E^* , the gas constant R and a constant, C .

$$\eta_T = Ce^{E^*/RT} \quad (1)$$

where η_T is the viscosity at absolute temperature T .

General evaluations of activation energies or viscous flow have previously been reported for a series of linear, amorphous polymers.¹⁻⁴ From these previous studies, the following general conclusions can be drawn for E^* :

- 1) Data covering a relatively narrow temperature range of 50-100°C for measurements far above the glass transition temperature T_g ($T > T_g + 100^\circ\text{C}$) generally yield linear plots $\log \eta$ versus $1/T$.
- 2) The activation energy measured at a series of constant stresses, E_τ^* including the non-Newtonian shear regions, gives activation energies identical with the value for the limiting low shear viscosities.
- 3) Activation energies are independent of polymer molecular weight M and the distribution of molecular weight, so long as the M exceeds a minimum number which is characteristic of the particular polymer. This low limit molecular weight corresponds closely to the appearance of non-Newtonian flow, i.e., to the attainment of critical molecular weight M_c from which the exponent of viscosity-molecular weight relations become 3.4. M_c is generally below 50,000 for linear amorphous polymers, being about 4,000 for polyethylene and 38,000 for polystyrene.

Unlike E_τ^* , which is not changed with shear stress, the activation energy measured at a constant shear rate $E_\dot{\gamma}^*$ for linear, amorphous polymers decreases with increasing shear above the onset of non-Newtonian flow. Bestul and Belcher⁵ have derived the following equation:

$$\begin{aligned} (d\eta/dT)_{\dot{\gamma}} / (d\eta/dT)_\tau &= (d\ln\eta/d\ln\dot{\gamma})_\tau + 1 \\ &= (d\ln\tau/d\ln\dot{\gamma})_T \end{aligned} \quad (2)$$

If the power law equation $\dot{\gamma} = A\tau^n$ holds for the non-Newtonian region, then the temperature derivations in the Bestul-Belcher equation simplify to the corresponding activation energy E_τ^* and $E_\dot{\gamma}^*$, and the relation $E_\tau^*/E_\dot{\gamma}^* = n$ results. If n is independent of temperature, this indicates that $E_\dot{\gamma}^*$ is equal to E_τ^* in the low shear Newtonian region when n is unity.

It is known that E^* can be calculated also from shift factor a_T . Mendelson has pointed out^{6,7} a_T can be obtained from shifting the flow curve (log shear stress τ_w vs. log shear rate $\dot{\gamma}_w$) at various temperatures along the horizontal or log shear rate axis to superimpose the flow curve at reference temperature. i.e.:

$$\begin{aligned} a_T &= \dot{\gamma}_w(\text{ref}) / \dot{\gamma}_w(T) && \text{(constant stress)} \\ &= \eta_a(T) / \eta_a(\text{ref}) && \text{(constant stress)} \end{aligned}$$

The resulting shift factor a_T can be expressed as a function of temperature by an Arrhenius-type equation of the form:

$$a_T = K \exp [E_a^* / RT] \quad (3)$$

where E_a^* is the "shift factor" activation energy. E_a^* is consistent with E_τ^* . This is because a horizontal shift of $\log \tau_w$ versus $\log \dot{\gamma}_w$ is equivalent to a vertical shift of $\log \eta_a$ versus $\log \tau_w$.

For many polyolefins, it has been shown that a correlation can be developed between E_τ^* and the molar volume of pendant groups appended to the chain.¹⁻³ This correlation shows that E_τ^* increases markedly and regularly with the increase of molar volume for short pendant groups.

It has also been shown that E^* has a more general relationship with structure than exhibited by correlations with pendant volume which are limited to hydrocarbon polymers. The more general correlation has been developed using the conformation parameter which is the ratio of the mean-square displacement length for fixed valence angles and free rotation to the unperturbed mean-square displacement length in a theta solvent.¹ A number of different linear amorphous polymers have provided a good correlation between E_t^* and conformation parameters. Polyethers, polyamides, polybutadiene, hevea rubber fit the correlation as well as olefin copolymers. Changes in these parameters, however, appear to markedly affect E_t^* by changing the average potential energy function for chain motions which lead to the viscosity changes with temperature.

The samples studied in this investigation provided the most extensive homologous series yet evaluated to test the concepts developed above.

Experiments

This poly-1-olefin series was polymerized by using Ziegler-Natta catalyst, titanium tetrachloride and aluminum triisobutyl. The polymerization procedures have been described in Chapter I.

All viscosity measurements were made using a Weissenberg Rheogoniometer Model R17. Eight poly-1-olefins from polypropylene to poly-1-octadecene have been measured. To eliminate voids and reduce oxidation, the powdery samples were pre-pressed before insertion in the viscometer. Viscosity measurements were made in the shear rate range from 10^{-3} to 1.0 seconds^{-1} using a 5-centimeter plate and a 2° angle cone. Each polyolefin was measured at four temperatures within the range of 80°C to 225°C . All tests were made

at over 100°C above the glass transition temperature and above the measured melting point for each of the poly-1-olefins.

Results and Discussion

The values for the low shear Newtonian viscosity η_0 were obtained on each of the polymers at the lowest rates of shear. Reversible non-Newtonian effects were also observed for all members of this series which were studied.

Importantly, the plots of log viscosity versus $1/T^{\circ}\text{K}$, in accord with Equation 1 gave entirely linear correlations within experimental error for all of the polymers over the entire ranges of viscosity measurement which generally exceeded 100° greater than the corresponding glass transition temperature. It is also significant that the correlations were also independent of stress for each of the polymers studied with the activation energy at high stress being identical to that in the low shear Newtonian region. Such correlations are illustrated in Figure 1 with data on polypropylene. The value calculated for E^* for polypropylene is 8.2 Kcal/mole, which is within the range of previously reported experimental values for this polymer. The observations on polypropylene do lend credence to the evaluations made on the higher members of the poly-1-olefin series.

Figure 2 illustrates typical viscosity data as a function of shear rate for poly-1-olefin, viz, poly-1-butene. The prominent shear thinning, and the failure to approach a limiting viscosity at high shear rate may all be noted as typical for all members of the series which have been investigated. Viscosity shear data in the form of viscosity as a function of shear stress are given in Figure 3 for an additional poly-1-olefin, poly-1-decene. From a cross plot of such data as a function of absolute temperature, the activation energy plots of the

type given in Figure 4 are obtained. Figure 4 exemplifies with poly-1-tridecene, the constant activation energy as a function of shear stress, even though measurements are made in the prominently non-Newtonian region. The observation of a constant E^* with stress is a broad extension of the previously proposed concept which was based on data on other linear amorphous polymers.

These results for E^* of the poly-1-olefin series are shown in Figure 5 that the flow activation energies change markedly and go through a maximum as a function of polyolefin pendant group chain length exhibiting a maximum in the range of poly-1-hexene to poly-1-octene. Subsequently, there is an unexpected decrease in E^* to a virtually constant value of 7.5 Kcal/mole for the longer pendant group polymer, poly-1-hexadecene and poly-1-octadecene. This limiting value of E^* is remarkably to the values for the lowest member of the series, linear polyethylene. The decrease of E^* for the poly-1-olefin series would not have been expected from the previous results on other polymers that E^* increases markedly and regularly with the increase of molar volume for short pendant groups. This is illustrated in Figure 6 where it is noted that at C4 there is already a difference between the E^* for isobutylene and 1-butene with the difference becoming yet larger at higher monomer molecular weights.

The conformation parameter reported in Chapter I for individual poly-1-olefins does not provide either a general correlation with E^* , since the conformation parameter systematically increases with increasing pendant group length for poly-1-olefin. Therefore, the maximum shown in Figures 5 and 6 for E^* of poly-1-olefins requires more evaluation.

It should be noted that viscosity changes with temperature can also be explained from the concept of free volume. This has been shown by the Doolittle equation:

$$\eta_T = Ae^{B/f} \quad (4)$$

where η_T is the viscosity at temperature T , A and B are constant and f is the relative free volume. The variation of viscosity with temperature is due to change of relative free volume with temperature. Therefore, the coefficient of expansion may provide a more general correlation with E^* . This will be developed in the next chapter.

The studies made here and previously developed correlations for the characteristic activation energy all pertain to linear amorphous polymers. For one case, branched polyethylenes, anomalous behavior of E^* with shear stress is observed, that is, the E^* measured at constant stress decreases measurably with stress.^{8,9} For other cases involving linear amorphous polymers, it is possible to observe a reproducible increase of E^* measured at constant stress with increasing stress. It has been previously shown by these workers this increase can be due to a compressional effect at high shear for viscosities measured near the glass transition temperature of polymers for measurements made in pressure capillary viscometers.^{10,11}

References

1. R. S. Porter and J. F. Johnson, J. Polymer Sci., Part C, 15, 373 (1966).
2. R. S. Porter and J. F. Johnson, J. Polymer Sci., Part C, 15, 365 (1966).
3. H. Schott, J. Appl. Polymer Sci., 6, 529 (1962).
4. G. V. Vinogradov, A. YA, Malkin and V. G. Kulichiklin, J. Polymer Sci., Part A-2, 8, 333 (1970).
5. A. B. Bestul and H. V. Belcher, J. Appl. Phys., 24, 696 (1953).
6. R. A. Mendelson, J. Polymer Sci., Part B, 5, 295 (1967).
7. R. A. Mendelson, Polymer Engin. Sci., 8, 235 (1968).
8. R. S. Porter, J. R. Knox and Julian F. Johnson, Trans. Sci. Rheo., 12:3, 409 (1968).
9. J. Meissner, in Proceedings of the Fourth International Congress on Rheology, Interscience, New York (1965), Part 3, p. 437.
10. R. Penwell and R. S. Porter, J. Appl. Polymer Sci., 13, 2427 (1969).
11. R. Penwell, Ph.D. Dissertation at University of Massachusetts (1970).

POLYPROPYLENE

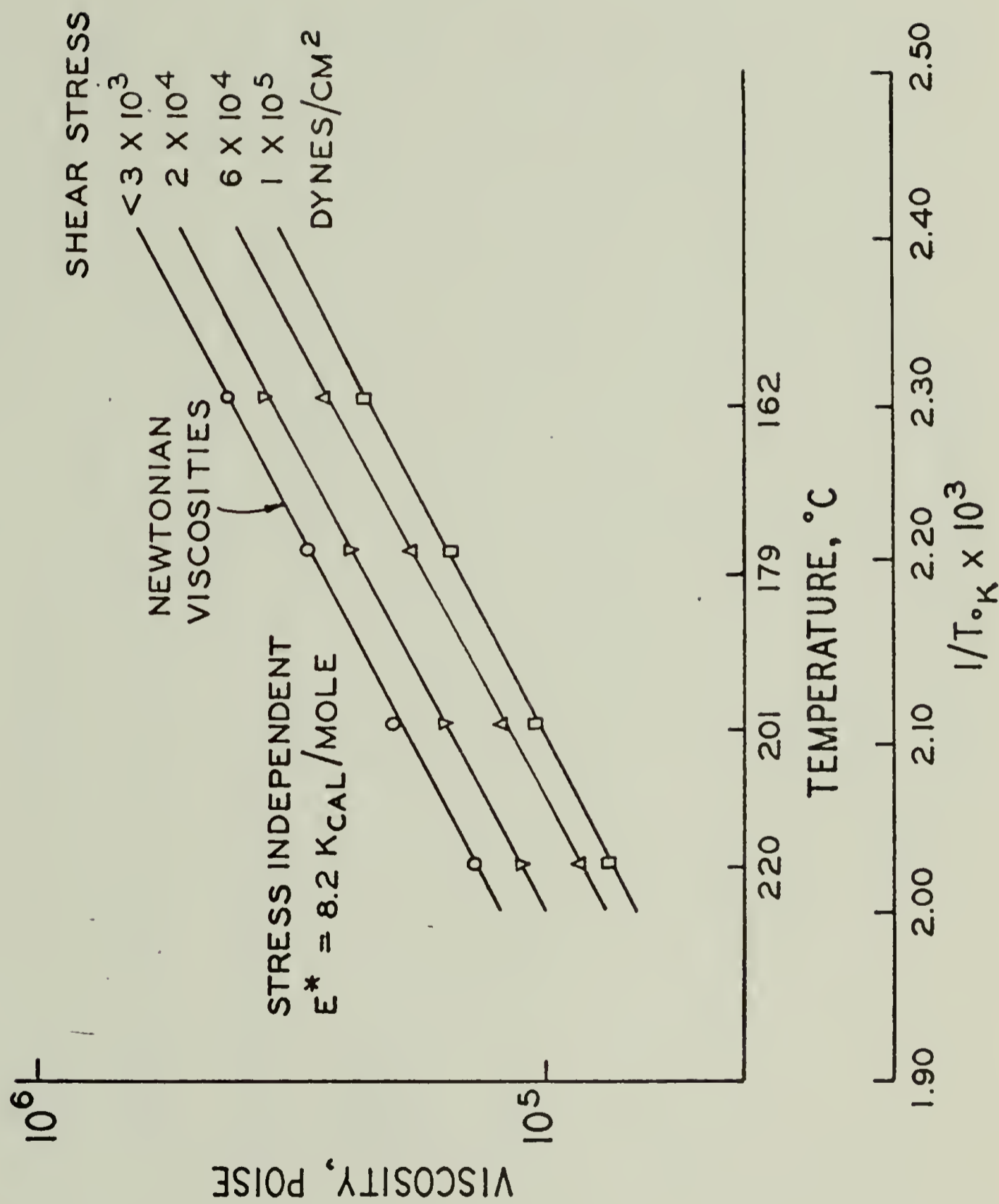


Figure II-1

POLY-1-BUTENE

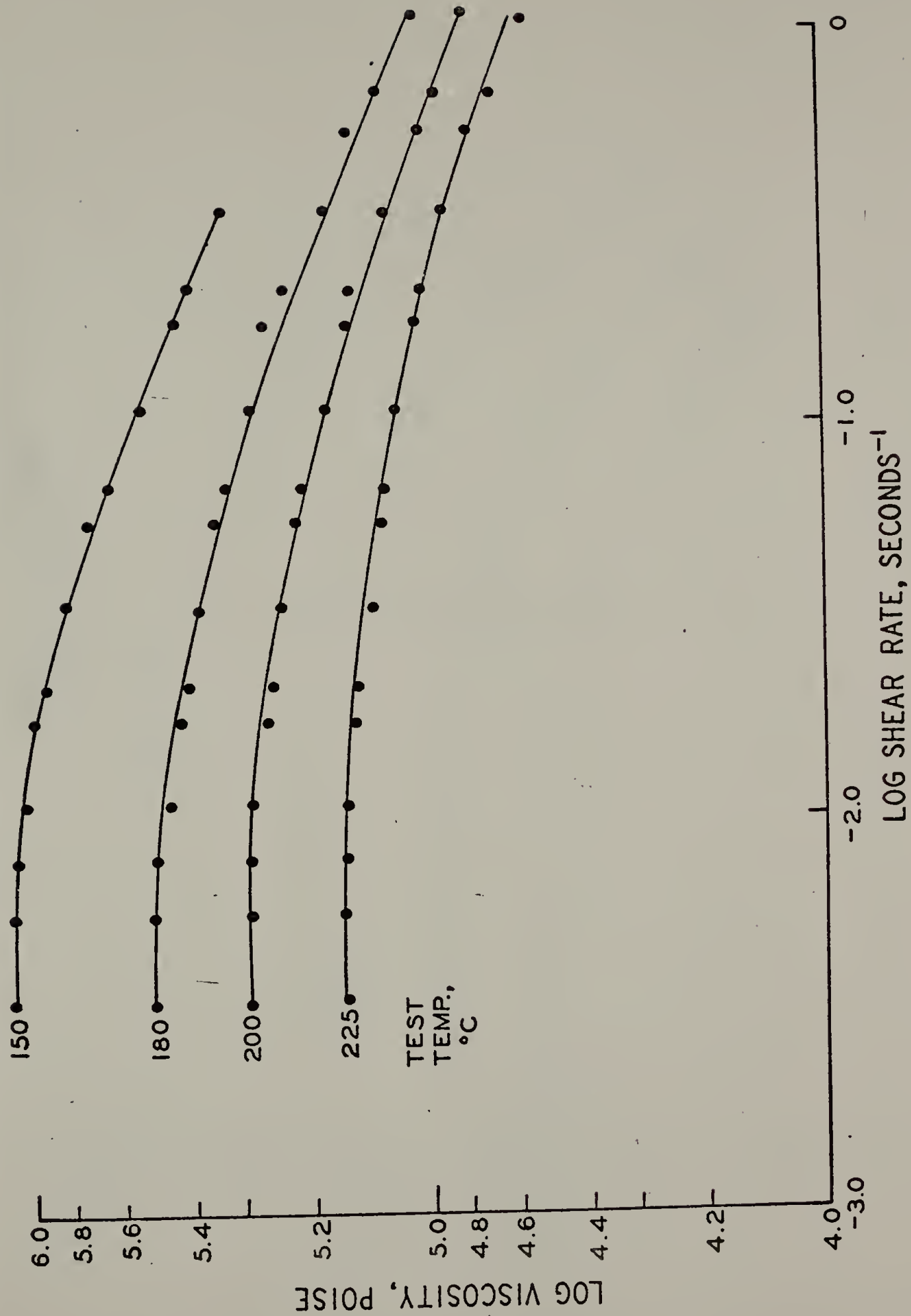


Figure II-2

POLY-1-DECENE

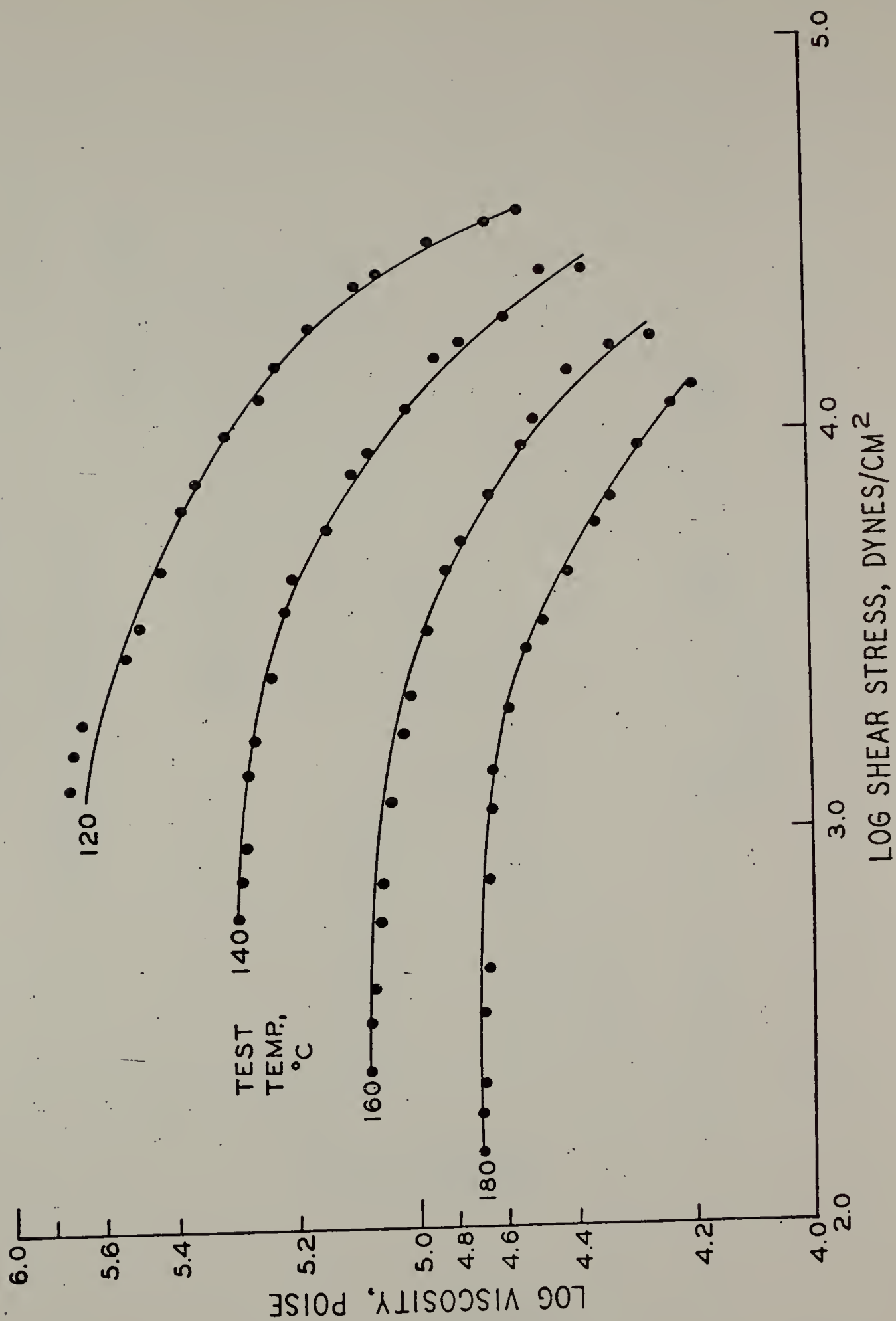


Figure II-3

POLY (1-TRIDECENE)

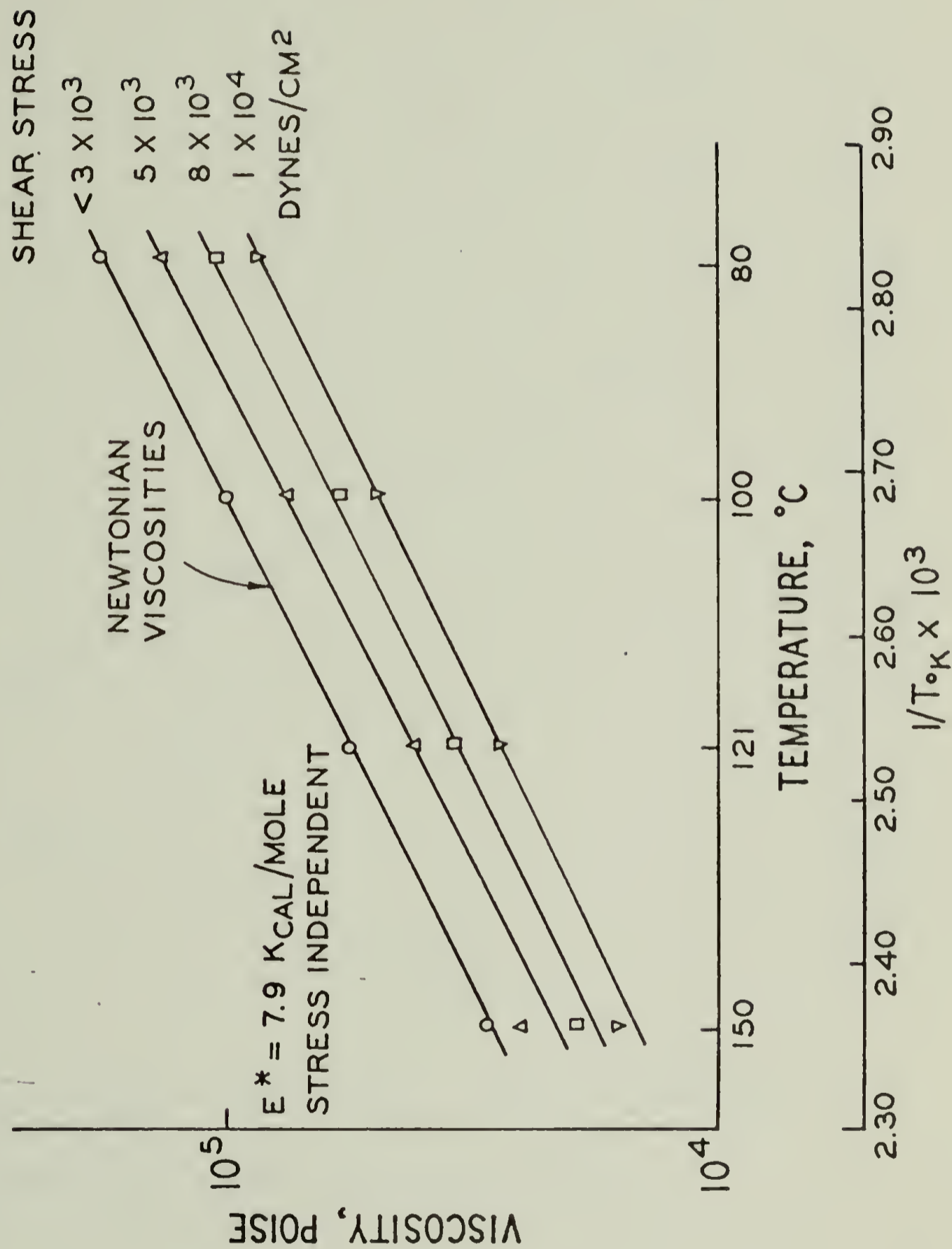


Figure II-4

VISCOSITY TEMPERATURE COEFFICIENTS FOR POLYOLEFINS

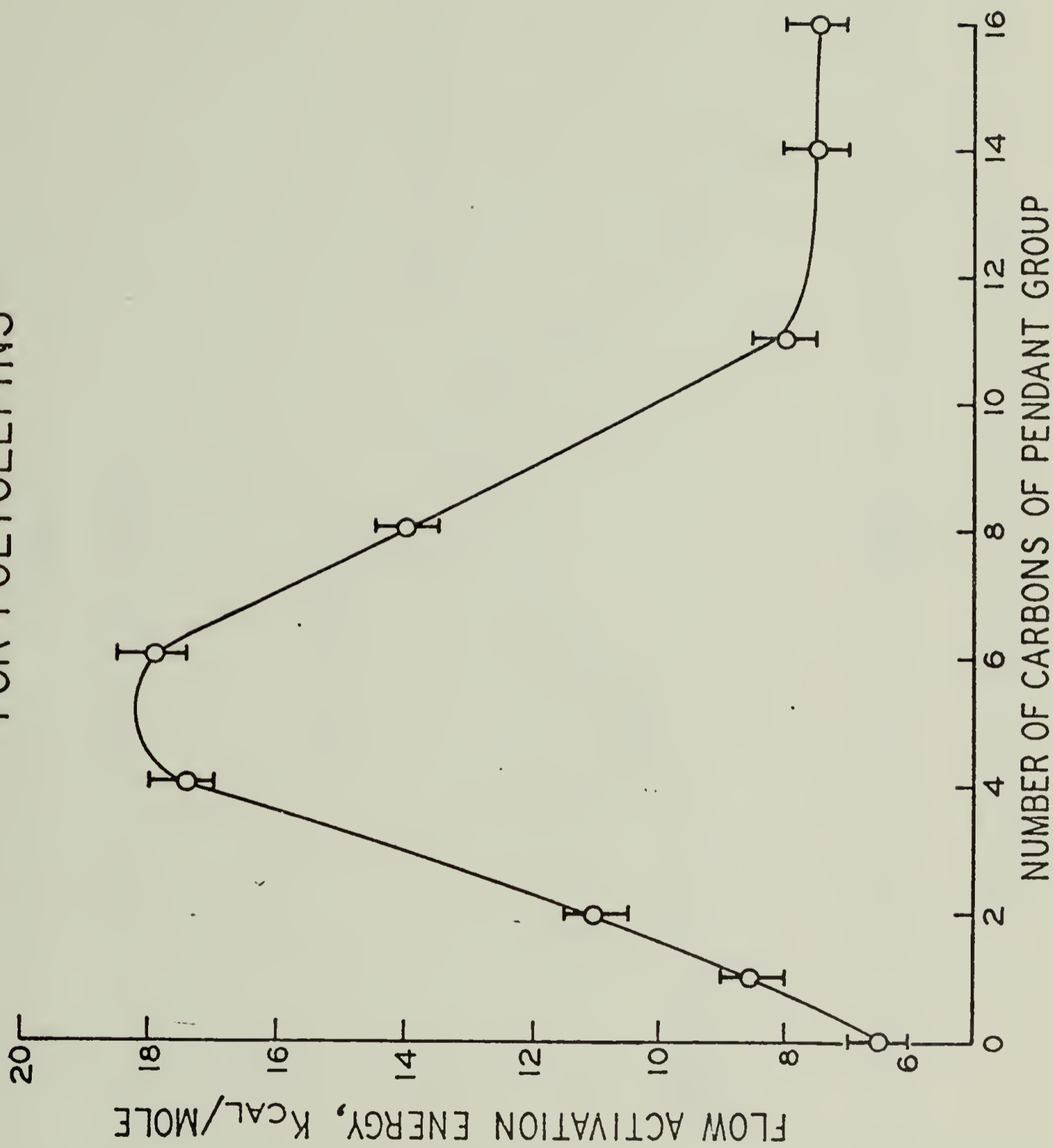


Figure II-5

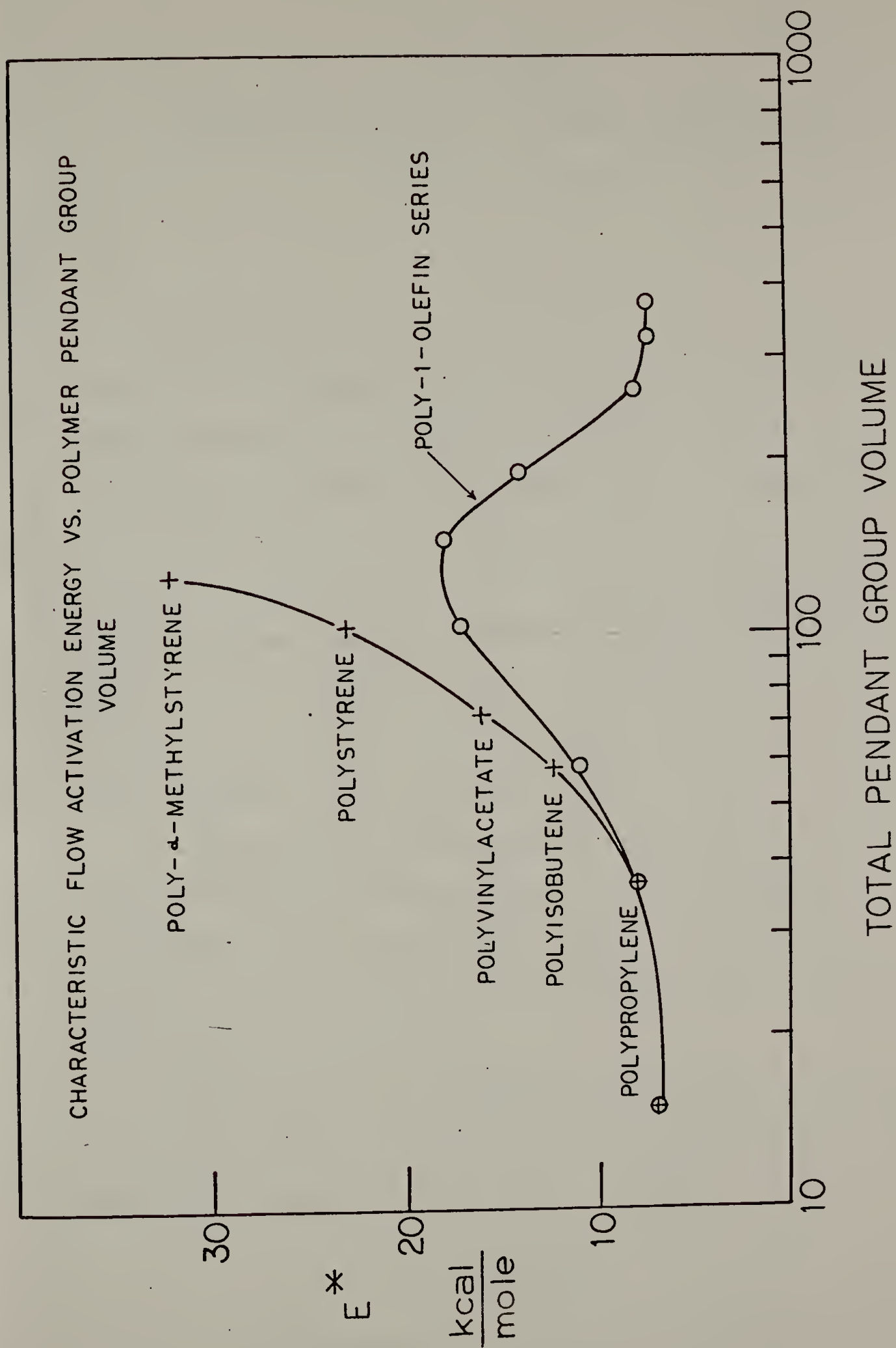


Figure II-6

CHAPTER III

PREDICTION OF VISCOSITY - TEMPERATURE BEHAVIOR FOR POLYMER MELTS

Synopsis

Based on the free volume concept and the equation by Doolittle, a new empirical equation is proposed for the flow activation energy, E^* for polymer melts for the range of over 150° above glass transition temperature T_g . The E^* is the temperature coefficient of viscosity for the Newtonian region or at constant shear stress for non-Newtonian flow. Data show that the E^* of linear polymers reaches a constant value for a broad temperature range above $T_g + 150^\circ$. The proposed equation for this region predicts the E^* of polymer melts from volume expansion coefficient, α_ℓ in degrees⁻¹ above T_g and from the $T_g^\circ K$. The E^* calculated from this equation is found to be in agreement with measurements within experimental precision of about ± 1 Kcal/mole.

Correlation have also been developed between E^* and α_ℓ and between E^* and T_g by simplifying this new equation by use of the Simha-Boyer expression. It is thus shown that a polymer having a lower α_ℓ or higher T_g generally has a higher E^* . However, generally more satisfactory results are obtained by calculating E^* from both α_ℓ and T_g .

The effects of polymer composition, molecular weight, branching and microstructure on E^* are also discussed. It is proposed that these factors influence E^* in the way in which they effect α_ℓ and T_g .

Introduction

Temperature dependence is one of the most important variables in polymer

flow. Two equations are most commonly used to express the viscosity-temperature behavior of polymers. One is an Arrhenius-type equation which has been derived theoretically by Eyring:¹

$$\eta = Ae^{E^*/RT} \quad (1)$$

where η is the absolute viscosity, R is the gas constant, A is the constant, T is the absolute temperature, E^* is called the flow activation energy. This equation is convenient because it contains only two parameters, A and E^* . It has been widely used at elevated temperatures to express the viscosity-temperature behavior for polymer melts. The other equation is the WLF equation² which can be expressed as:

$$\log a_T = -C_1 (T - T_r) / (C_2 + T - T_r) \quad (2)$$

Here C_1 and C_2 are constant, T is absolute temperature. a_T is the shift factor which can be defined as:

$$a_T = \eta T_r \rho_r / \eta_r T \rho \quad (3)$$

where the subscript r refers to reference state; η is absolute viscosity and ρ the density. Because of the relatively small temperature dependence $T_r \rho_r / T \rho$, a_T is very nearly the same as η / η_r .

The WLF equation is now known to have foundation in free volume concepts.² This equation is generally applicable in the temperature range above T_g to about $T_g + 100^\circ\text{C}$. At high temperatures the WLF equation incorrectly

predicts an E^* of 4.1 Kcal/mole for all systems - irrespective of molecular constitution.² Indeed E^* varies widely from polymer to polymer at elevated temperature. Generally, however, E^* is independent of polymer molecular weight and distribution so long as the molecular weight exceeds a minimum value which corresponds closely to the entanglement molecular weight. It has been further shown that E^* measured at a series of constant stresses, including the non-Newtonian region, gives an E^* identical with the value for limiting low shear viscosities.^{3,4}

The E^* changes in a predictable way with chemical composition.^{3,4} For many polyolefins, Schott and independently these authors have shown that a correlation can be developed between E^* and the molar volume of pendant groups appended to the chain.³⁻⁵ This correlation shows that E^* increases markedly and regularly with the increase of molar volume for short pendant groups. Recently, it was found that the E^* of the poly-1-olefin did not always increase with increasing the molar volume of pendant groups.^{6,9} Indeed, the E^* of the poly-1-olefin series shows a maximum in the region of polyhexene-1 and polyoctene-1 and decreases as the molar volume of pendant groups is increased further.⁶

A more general correlation for viscosity-temperature behavior has been developed using the conformational parameter which is the ratio of the measured unperturbed mean-square end-to-end distance in a theta solvent to the calculated mean-square end-to-end distance for fixed valence angles and free internal rotation.³ Using this correlation, the E^* for many different linear amorphous polymers have been successfully correlated. This parameter, however, is available only for the most common polymers and its measurement involves finding an appropriate theta solvent and temperature to obtain the unperturbed

dimensions. Kurata, Stockmayer and Fixman have developed a method for estimating the unperturbed dimensions without the aid of theta-solvent experiments.^{7,8} It is nevertheless necessary to know intrinsic viscosities for several different molecular weights and the procedures are tedious. Shirayama et al.⁴ used the methods of Kurata-Stockmayer and Stockmayer-Fixman. Wang and Porter³⁴ measured the intrinsic viscosity of poly-1-olefins at theta condition. They all found that the conformational parameter of poly-1-olefin increases regularly as the length of the side-chain increases. Thus the decreases of the E^* with the increasing side chain for higher poly-1-olefins cannot be ascribed exclusively to the conformational parameter.

For low molecular weight compounds, extremely tight correlations have been shown between E^* and melting point.¹⁰ These include inert gases, halocarbons, metals and inorganic materials. For the prime hydrocarbon systems, the poly-1-olefins, in contrast, the flow activation energy E^* does not increase with increasing melting point; there is indeed an inverse correlation.

The present work explores the possibility of developing simple and quantitative predictions of viscosity-temperature behavior of polymer melts from related polymer properties, explicitly the thermal expansion coefficient of the melt, α_ℓ , and the glass transition temperature, T_g .

Analysis

The change of viscosity has been widely explained on the basis of free volume. Doolittle¹¹ introduced an empirical equation for viscosity-temperature behavior of simple liquids:

$$\eta = C \exp [B V_0 / (V - V_0)] \quad (4)$$

where C , B are empirical constants, the latter is the order of unity, V is the observed specific volume and V_0 is the specific volume for a zero free-volume state. The equation is also consistent with the theory of Cohen and Turnbull¹² which considers molecular transport occurs in liquids only when local microvoids exceed certain critical volumes.

It is convenient to define a fractional free volume f as $(V-V_0)/V \simeq (V-V_0)/V_0$, which is also a function of temperature. So the Equation (4) becomes:

$$\eta = C \exp (B/f) \quad (5)$$

The difference between certain theories arises from varying definitions of free volume. One by Simha and Boyer defines free volume¹³ f as $\alpha_\ell T$, with α_ℓ , the volume expansion coefficient above T_g and T the absolute temperature. In this definition, Simha and Boyer assume the occupied volume V_0 is the volume derived from the linear extrapolation of the liquid state to absolute zero temperature. The free volume is assumed to vanish at absolute zero. In this definition, they speculate that the free volume at T_g is $f_g = \alpha_\ell T_g = 0.164$. This is much higher than the $f_g = 0.025$ given by the WLF equation.² If the fractional free volume vanishes at a certain temperature, T_2 , rather than at absolute zero, then the fractional free volume can be given as:

$$f = \alpha_\ell (T - T_2) \quad (6)$$

Therefore, the Doolittle Equation (5) can be expressed as:

$$\eta = C \exp [B/\alpha_\ell (T - T_2)] \quad (7)$$

This new form is equivalent to the empirical Vogel equation for the temperature dependence of viscosity:¹⁴

$$\eta = K \exp [D / (T - T_0)] \quad (8)$$

The Vogel equation considers D , K , T_0 as three parameters used to fit experimental data.

An E^* can be expressed in terms of α_ℓ and T_2 by differential equation (7):

$$\begin{aligned} E^* &= R d \ln \eta / d (1/T) \\ &= RB / [\alpha_\ell (1 - T_2/T)^2] \end{aligned} \quad (9)$$

It must be realized that certain assumptions and simplifications will be made in order to obtain E^* from other experimentally obtainable parameters and to predict E^* in a simple way.

Gibbs and DiMarzio¹⁵ have predicted, on the basis of a lattice model of a polymer system, that equilibrium configuration entropy becomes zero at a characteristic temperature. If T_2 corresponds to that temperature, then T_2 can be relative to the experimentally obtainable parameter T_g , the glass transition temperature:

$$T_2 = K' T_g \quad (10)$$

where K' is a constant. T_g can be conveniently defined as the temperature at which the plot of specific volume vs. temperature changes slope. Recent investigations

show that K' lies close to 0.77 and that it is relatively independent of polymer molecular weight, structure and polarity.^{16,17} Therefore the relationship $T_2 = 0.77 T_g$ will be used to derivate the following equation.

A plot of log viscosity versus $1/T$ is generally curved but approaches linearity at high temperature, i.e., the E^* decreases as temperature increases and approaches a constant value above a certain high temperature. At this high temperature, the temperature dependence of polymer viscosity can be simply characterized by a constant flow activation energy E_C^* . If this E_C^* can be found above the certain high temperature $T_g + m$, the ratio T_2/T in Equation (9) can be represented by $0.77 T_g / (T_g + m)$, where $B \approx 1$, Equation (9) is thus rewritten as:

$$E_C^* = (R/\alpha_\ell) (T_g + m)^2 / (0.23 T_g + m)^2 \quad (11)$$

m is the temperature constant above T_g , where E^* approaches temperature independently. Many data show that E^* will become a constant for temperatures about 150° above T_g . Therefore, Equation (12):

$$E_C^* = (R/\alpha_\ell) (T_g + 150)^2 / (0.23 T_g + 150)^2 \quad (12)$$

will be used to calculate E_C^* and be checked against the extensive literature.

Discussion

The above analysis and the value $m = 150$ are more empirical than theoretical. However, the advantage of the Equation (12) is that the E_C^* can be predicted easily from a simple dilatometry experiment in which α_ℓ in degree⁻¹ and $T_g^\circ K$ can be found.

Table 1 gives the characteristic E_C^* values for several polymers studied in this and other laboratories. The temperature range and shear condition for E_C^* experiments are also shown in this table. Table 2 shows the corresponding α_ℓ and Tg of these polymers. The α_ℓ for the melts of the poly-1-olefins were determined dilatometrically in this laboratory. Uniform-bore glass dilatometers of the sealed-off type were used as described elsewhere.¹⁸ α_ℓ was found to be strikingly constant over a 50°C range above the melting points for the individual poly-1-olefins. The α_ℓ of the other polymers shown in Table 2 were found in literature with the references given, using the α_ℓ and Tg values in Table 2, the calculated E_C^* from Equation (12) is shown in the last column of Table 1. The measured values, also in Table 1, are in good agreement with the calculated E_C^* , on consideration of some different experimental conditions and a precision of E^* of about ± 1 Kcal/mole.

The exact temperature at which E^* becomes constant cannot be precisely defined, but in the range of 100°C to 200°C above Tg. Thus the m value may also vary from 100 to 200. The calculations for E_C^* are also tried by using $m = 100$ or $m = 200$ in Equation (11). It was found that E_C^* calculated from $m = 100$ is higher than experimental value, about 20%, and E_C^* calculated from $m = 200$ is lower than experimental value about 15% in average. Therefore, the value $m = 150$ used in calculation is better than $m = 100$ or 200 in general.

Several factors can affect the E^* of polymers:

(1) Temperature. The plot of $\log \eta_0$ vs. $1/T$ is generally curved if temperature below $T_g + 100^\circ\text{C}$. The plot generally approaches linearity at high temperature with the E^* becoming constant. This is shown in Figure 1 where the E^* of poly-1-hexene is plotted vs. $(T - T_g)$. The higher experimental E^* over the calculated value is in essence a temperature effect. In Figure 2, the E^* of poly-

isobutylene is shown to reach a constant value at about $T_g + 150^\circ$. The calculated E_c^* (shown by lower dash line) is in very good agreement with the experimental value for polyisobutylene. For polystyrene, because of instability at high temperature above 250°C , just $T_g + 150$, the experimental E^* of polystyrene shown in Figure 2 never reaches the calculated E_c^* (shown by upper dash line).

(2) Shear. The prior discussion has been exclusively on E^* measured in the low-shear Newtonian region or at a constant and high shear stress, E_τ^* . Viscosity measurements on a variety of linear amorphous polymers indicate a constant E_τ^* from the low shear Newtonian region up to stresses $>16^6$ dynes/in²,²⁻⁴ which is well within the non-Newtonian region. The constant E_τ^* is also found in the new data on a series of poly-1-olefins.⁶ Figure 3 shows viscosities as a function of temperature for poly-1-hexadecene for the Newtonian region and at several constant and high shear stresses. The lines at different constant shear stresses are parallel with the line for Newtonian flow. This means that the E^* does not change with shear stress. Unlike E_τ^* , the activation energy measured at a constant shear rate $E_{\dot{\gamma}}^*$ for linear, amorphous polymers decreases with increasing shear above the onset of the non-Newtonian flow.^{3,4}

(3) Molecular Weight. For a given polymer, E^* increases up to a certain molecular weight and subsequently becomes independent of molecular weight.^{4,23-25} Shirayama⁹ studied the E^* of poly-1-olefin series. No molecular weight dependence of E^* was found in the molecular weight range of 3×10^4 .

According to Equation (12), the factors that can affect T_g and α_ℓ are expected to have an effect on E^* . Molecular weight can affect both T_g and α_ℓ . Experiments on a number of polymers show that as polymer molecular weight is increased, T_g rises, and α_ℓ decreases. If the molecular weight increases to a

certain value, both T_g and α_ℓ becomes independent of molecular weight.²²

The molecular weight dependence of T_g and α_ℓ can be described by the following experimental equation:²²

$$T_g = T_\infty - A'/M \quad (13)$$

$$\alpha_\ell = \alpha_\infty + B'/M \quad (14)$$

where T_∞ and α_∞ are the limiting values at high molecular weight for T_g and α_ℓ ; A' and B' are constant. Therefore, the molecular weight dependence of E^* can also be corrected by the equation:

$$E^* = E_\infty^* - C'/M \quad (15)$$

where E_∞^* is the activation energy E^* at very high molecular weight. C' is a constant. Fox and Flory²³ reported that T_g , viscosity-temperature coefficient and specific volume of polystyrene are changed with increasing molecular weight toward asymptotic limits which are practically reached at the same molecular weight about 30,000. Vinogradov²⁵ found that the E^* and specific volume of polybutadiene both become independent of molecular weight when the molecular weight is higher than critical molecular weight M_c of polybutadiene.

(4) Branching. The E^* of branched polyethylene is up to 18 Kcal/mole or much higher than the 6-7 Kcal/mole for linear polyethylene.¹⁹⁻²⁰ Also, the E^* for branched polyethylenes decrease with shear stress.¹⁹ The E^* for linear polymers are independent of stress even well into the shear region for non-Newtonian flow. Long chain branches are postulated to be responsible for the

anomalous flow behavior and the high activation energy.¹⁹ An E^* for polypropylene of 18-12 Kcal/mole has been reported. This is much higher than the usual value 9 ± 1 Kcal/mole. Vinogradov subsequently found the high E^* values for polypropylene depended on shear stress.²⁷⁻²⁸ Moreover, it was subsequently found that these polypropylenes contained long chain branches.²⁹ In contrast, for polybutadiene with long branches, Kraus and Gruver³⁰ found that E^* is not higher than for the linear polymer and that the E^* is not stress dependent. The length, concentration and distribution of branches may be crucial in generating these differences.

The branches can also affect T_g . Substitution of a branched for a linear molecule of the same molecular weight can increase the free volume and lower T_g .²² However, for the long chain branch, crowding at junction points like cross-links may be expected to raise the T_g .²² Therefore, it is reasonable to expect that branches can either lower or raise the T_g or have no effect. The higher E^* of branched polyethylene and polypropylene are expected to be associated with a lower value of α_l and a higher value of T_g than the corresponding linear polymers. Marker et al.³² showed a lower slope in specific volume-temperature plots for branched polyethylene than that for linear polyethylene above the melting point. However, the exact value of T_g and α_l for branched polyethylene are still not available, the E^* of branched polymers are thus not yet predicted by the Equation (12).

(5) Microstructure. Microstructure is also expected to affect E^* , particularly if it can affect T_g and α_l . Vinogradov et al.²⁵ reported that the E^* of polybutadiene is decreased from 8 Kcal/mole to 4.7 Kcal/mole, if the percentage of cis-1,4 polybutadiene is changed from 40% to 96%. However, their thermomechanically determined T_g also decreases from -83°C to -96°C , if percentage

of cis-1,4 polybutadiene changes from 60% to 90%, but the effect of microstructure on α_ℓ are not reported.

Tacticity effect on E^* have not been found so far although they may be expected from these new correlations. The effect of tacticity on Tg of mono- and di-substituted vinyl polymers $(CH_2CXY)_n$ is expected when $X \neq Y$ and neither X or Y is hydrogen.³³ Therefore, it is not expected that the E^* of poly-1-olefin series will be affected by tacticity. Indeed the different tacticities of poly-1-octadecene show the same E^* .³⁴

Other factors such as crosslinking, diluent concentration and pressure can also effect Tg and α_ℓ . Therefore, it is expected that the E^* can also be affected by these factors.

(6) Chemical Composition. The relation between E^* and chemical composition is also influenced by the structure effects on Tg and α_ℓ .

Simha and Boyer¹³ proposed an empirical equation based on the iso-free volume concept for Tg:

$$\alpha_\ell Tg = K_2 = \text{constant} \quad (16)$$

The average value of K_2 for fourteen polymers is 0.164, the estimated fractional free volume at Tg. If this equation is substituted into Equation (12) first for α_ℓ and alternatively for Tg, the equations can be plotted with E_C^* vs α_ℓ or E_C^* vs Tg as shown in Figure 4 and Figure 5. These two figures show that E_C^* increases with decreasing α_ℓ and increases with increasing Tg with polymers having the higher Tg or the lower α_ℓ generally showing the higher E^* . This is consistent with Eyring's rate process theory.² The flow takes place through the creation of a void within the fluid (volume effect) followed by the jump of

a molecular segment into the hole (molecular structure effect). The E^* is thus related to the chain "stiffness" of the polymer molecules. If the molecular chains are more stiff, the dimension of the flow unit is increased and E^* would be increased. T_g strongly depends on molecular "stiffness". At the glass transition temperature there is sufficient thermal energy to surmount the rotational energy barrier and begin the motion of the major segments of the chain backbone. Therefore, a lower T_g reflects the ease of rotational motion of the chain backbone. This, therefore, also corresponds to a lower E^* . However, the E^* is not exclusively dependent on T_g or on α_ℓ . The α_ℓ and T_g for the poly-1-olefin series show a minimum in the region of poly-1-hexene to poly-1-octene; the E^* of the series show the maximum in this region. This suggests that α_ℓ may be the predominant single correlation for E^* if only one parameter is considered. It should be noted that Figure 4 shows that when $\alpha_\ell < 4.0 \times 10^{-4} \text{ deg}^{-1}$ the E^* increases rapidly. A 10% variation in α_ℓ around $3.5 \times 10^{-4} \text{ deg}^{-1}$ represents >20% changes in E^* . This sensitivity is avoided by the more general Equation (12). In this equation a 10% variation in α_ℓ leads to a 10% change in E^* for the same T_g . This is because the value $\alpha_\ell T_g = 0.164$ proposed by Simha and Boyer¹³ is an average for 14 polymers. Therefore, it is more satisfactory to predict E^* from the Equation (12) involving both T_g and α_ℓ .

It is well known that apparent T_g varies with the rate of measurement and the method. Roughly T_g changes about 3° for a decade change in heating or cooling rate.¹ If T_g is ill-defined by 10°C , the calculated change in E^* based on Equation (12), is less than 1 Kcal/mole. It should be emphasized that E^* is a sensitive measure for viscosity-temperature dependence. A variation of ~ 1 Kcal/mole may be expected for precise viscosity measurements over a broad temperature range.

Figure 5 shows additional data on E^* and T_g found in the literature, but for which α_ℓ is not available. This includes ethylene-acrylic acid copolymers at four different acid concentrations,²¹ hydroxyl and carbosyl terminated polybutadienes, butadiene-acrylonitrile copolymer,³⁵ and a polyester.³⁶ The E^* for the polyester shown in Figure 5 were measured at a shear rate of 24 sec^{-1} rather than at a constant shear stress.³⁶ If it is still in Newtonian region at this shear rate, these E^* of polyester will be the same as those measured at a constant shear stress, otherwise the real value of E^* will be expected to be higher than the value of E^* measured at constant shear rate. The E^* of Biphenol-A polycarbonate in the Newtonian region or at constant shear stress is 26 Kcal/mole.³⁷ At shear rate 24 sec^{-1} , the E^* of Biphenol-A polycarbonate is 21 Kcal/mole³⁶ which is much less than predicted value 27 Kcal/mole.

Recently, Plate et al.⁵⁸ measured the E^* of poly(n-alkyl acrylate) and poly(n-alkyl methacrylate) series. They found that E^* decreases regularly as the side chain length increases. When n-alkyl side chain length gets to 16 carbons, E^* goes to 6-7 Kcal/mole. This low value of E^* for long side chain polymers was also found in our poly-1-olefin series. The T_g of poly(n-alkyl methacrylate) series decreases and α_ℓ increases regularly as the side chain length increases from poly(methyl methacrylate) to poly(n-dodecyl methacrylate).⁵⁹ These results confirm the correlation of E^* with T_g and α_ℓ .

Conclusion

This paper has drawn attention to new correlations that can express the flow activation energy E^* in terms of the melt expansion coefficient α_ℓ and glass transition temperature T_g . Equation (12) can be practically used to predict the

E^* for polymers at temperatures over $T_g + 150^\circ\text{C}$. The equation is found to give a good fit to a wide range of experimental data.

The use of α_ℓ and T_g to estimate the E^* of polymer melts is more convenient and accurate than other methods, since α_ℓ and T_g are easily measured and readily available.

If the Simha-Boyer empirical equation $\alpha_\ell T_g = 0.164$ is used in conjunction with Equation (12), then α_ℓ or T_g each separately provides a correlation with E^* . For polymers with the higher T_g or the lower α_ℓ exhibits, as predicted, the higher E^* .

Based on these equations, it is shown how the molecular weight, branching and microstructure of polymers affect E^* in the way in which they influence α_ℓ and T_g .

TABLE 1
EXPERIMENTAL AND CALCULATED FLOW ACTIVATION
ENERGIES FOR POLYMERS

Polymers	Temperature Range °C	Shear (a) Condition	Experimental E* (Kcal/mole)	Calculated E* (Kcal/mole)	Reference
Linear Polyethylene	150 ~ 300	Constant Stress	6.3		3, 4
	150 ~ 300	Constant Stress	7.1	6.3	3, 4
	150 ~ 220	Constant Stress	5.8-8.2		3, 4
	163 ~ 274	Constant Stress	6.8		3, 4
Polypropylene	195 ~ 260	Constant Stress	9 ± 1		3, 4
	180 ~ 240	Newtonian Viscosity	8.5		6
	175 ~ 260	Shift Factor	10	9.3	31
	195 ~ 260	Shift Factor	9.2		38
	---	Constant Stress	17.8		36, 39
	190 ~ 310	Constant Stress	21 (b)		27
	180 ~ 240	Constant Stress	18 (b)		28
Poly-1-butene	150 ~ 225	Newtonian Viscosity	11		6
	130 ~ 230	Shift Factor	12.1		9
	---	Constant Stress	14.8	10	36, 39
	150 ~ 250	Shift Factor	11.9		31
Poly-1-hexene	40 ~ 80	Newtonian Viscosity	18 (d)		6
	130 ~ 230	Shift Factor	12.1		9
	40 ~ 70	Shift Factor	17 (c), (d)	11	40
	---	Constant Stress	10.6		36, 39
Poly-1-heptene	40 ~ 100	Newtonian Viscosity	17 (d)	11	6

Polymers	Temperature Range °C	Shear Condition (a)	Experimental E* (Kcal/mole)	Calculated E* (Kcal/mole)	Reference
Poly-1-tridecene	80 ~ 140	Newtonian Viscosity	8	9.1	6
Poly-1-octadecene	80 ~ 140	Newtonian Viscosity	7.5		6
	130 ~ 230	Shift Factor	7.4	9.2	9
Polystyrene	at 227	Constant Stress	23 (d)	18	3, 4
	at 217	----	24 (e)		24
Poly (vinyl acetate)	at 200	----	15 (f)	14	41
Polydimethylsiloxane	-21 ~ 140	Shift Factor	3.65	4.3	42
	40 ~ 150	Constant Stress	4.4 ~ 3.6		43
	20 ~ 100	----	3		44
Polybutadiene	at 152	Constant Stress	4.7 (g)		30
	20 ~ 100	Newtonian Viscosity	8 ~ 4.7 (h)	7.8	25
	15 ~ 50	Newtonian Viscosity	8.4		35
Polyisobutene	38 ~ 149	Constant Stress	12.3		3, 4
	20 ~ 150	Constant Stress	13.5		3, 4
	217	Constant Stress	10.3	10.2	24
	200	Constant Stress	10.6		24
	150	Constant Stress	12.0		24
Hevea Rubber	80 ~ 140	----	10.2		45
	---	----	9.9	10.3	46
	---	----	8		47
GRS Rubber X672, 21% Styrene 79% Butadiene	38 ~ 93	Constant Stress	8.1 ~ 9.7	10	3, 4

Polymers	Temperature Range °C	Shear (a) Condition	Experimental E* (Kcal/mole)	Calculated E* (Kcal/mole)	Reference
Poly(4 methyl -1-pentene)	280 ~ 310	Constant Stress	31 ± 4 (k)	17 (e)	3, 4
poly(vinyl chloride)	<165 >165	At shear rate 30 sec ⁻¹	18.4 (j)	18	48
		At shear rate 30 sec	35.5		
Poly(ethylene telephthalate)	250 ~ 325	At shear rate 24 sec ⁻¹	20	20	36

COMMENT ON E^*

- (a) The shear conditions which experimental E^* were measured. The "shift factor" means E^* were measured from the temperature "shift factor" a_T which can be obtained from shifting the flow curve (log shear stress vs. log shear rate) at various temperature along the horizontal or log shear rate axis to superimpose the flow curve at reference temperature.³¹
- (b) Branched polypropylene - Personal communication to R. S. Porter from G. V. Vinogradov.
- (c) Calculated from Reference 40.
- (d) The temperature range is below $T_g + 150^\circ\text{C}$.
- (e) If molecular weight $> 25,000$ E^* is independent of M.W. Also reported $E^* = 30$ Kcal/mole at $T = 200^\circ\text{C}$. $E^* = 38$ Kcal/mole at $T = 175^\circ\text{C}$. See Figure 3.
- (f) Also listed $E^* = 23$ Kcal/mole at $T = 150^\circ\text{C}$. $E^* = 37$ Kcal/mole at $T = 100^\circ\text{C}$.
- (g) E^* changes from about 8 Kcal/mole at 300°K to 4.7 Kcal/mole at 425°K .
- (h) E^* changes from 8 Kcal/mole to 4.7 Kcal/mole if the % of cis-1,4 polybutadiene changes from 40% to 96%.
- (i) Filled siloxane E^* decrease from 4.4 Kcal/mole to 3.6 Kcal/mole when shear stress increases from 0 to 150 p.s.i.
- (j) E^* is unresolved, because PVC may exhibit microgel, crystallinity, chain branching and flow by domain.
- (k) Uncertain data.
- (l) Due to high volume expansion coefficient.

TABLE 2

TABLE OF VOLUME EXPANSION COEFFICIENT α_ℓ
AND GLASS TRANSITION TEMPERATURE T_g OF POLYMERS IN TABLE 1

Polymers	$\alpha_\ell \times 10^4 \text{ (deg}^{-1}\text{)}$	$T_g \text{ (}^\circ\text{K)}$	Reference
Linear Polyethylene	8.3	148	13, 49-51
Polypropylene	8.0	250 ~ 243	49-52, 54
Poly-1-butene	7.5	248 228	49-52 53
Poly-1-hexene	6.2 6.5	223 218	49-52 40
Poly-1-heptene	6.0	213	52
Poly-1-tridecene	7.3	2.5	52
Poly-1-octadecene	7.6	233	52
Polystyrene	5.5	373	13, 49, 50
Poly(vinyl acetate)	5.98	302	13
Polydimethylsiloxane	12	150	13
Polybutadiene	7.8	188	13
Polyisobutylene	6.18	199	13

Polymers	$\alpha_g \times 10^4 \text{ (deg}^{-1}\text{)}$	Tg ($^{\circ}\text{K}$)	Reference
Hevea Rubber	6.16	201	13
GRS Rubber	6.6	213	50
Poly(4 methyl-1-pentene)	7.6	302 398	55 56
Polyvinyl chloride	5.2	355	13
Poly(ethylene terephthalate)	4.5	337	57

References

1. S. Glastone, K. J. Kaidler, H. Eyring. The Theory of Rate Process, McGraw-Hill Book Company, Inc. (1941).
2. J. D. Ferry, Viscoelastic Properties of Polymers, Chapter 11, Second Edition, John Wiley and Sons, Inc. (1970).
3. R. S. Porter and J. F. Johnson, J. Polymer Sci., Part C, 15, 373 (1966).
4. R. S. Porter and J. F. Johnson, J. Polymer Sci., Part C, 15, 365 (1966).
5. H. Schott, J. Appl. Polymer Sci., 6, 529 (1962).
6. J. S. Wang, R. S. Porter and J. R. Knox, J. Polymer Sci., Part B, 8, 671 (1970).
7. M. Kurata and W. H. Stockmayer, Fortchr. Hochpolymer-Forsch., 3, 196 (1963).
8. H. W. Stockmayer and M. Fixman, J. Polymer Sci., C1, 137 (1963).
9. K. Shirayama, T. Matsuda, S. Kita, Die Makromol. Chemie, 147, 155 (1971).
10. J. O'M. Bockris and S. R. Richards, J. Phys. Chem., 69, 671 (1965).
11. (a) A. K. Doolittle, J. Appl. Phys., 22, 1471 (1951).
(b) A. K. Doolittle and D. B. Doolittle, J. Appl. Phys., 28, 901 (1957).
12. (a) M. H. Cohen and D. Turnbull, J. Chem. Phys., 31, 1164 (1959).
(b) D. Turnbull and M. H. Cohen, *ibid*, 34, 120 (1961).
13. R. Simha and R. F. Boyer, J. Chem. Phys., 37, 1003 (1962).
14. H. Vogel, Physik. Z., 22, 645 (1921).
15. (a) E. A. DiMarzio and J. H. Gibbs, J. Polymer Sci., 40, 121 (1959).
(b) E. A. DiMarzio and J. H. Gibbs, J. Polymer Sci., A1, 1417 (1963).
16. G. Adams and J. H. Gibbs, J. Chem. Phys., 43, 139 (1965).

17. R. S. Stearns, I. N. Duling and R. H. Johnson, A. C. S. Preprint, Petrol. Chem. Div., 11, No. 1, 5 (1966).
18. N. Bekkedahl, J. Res. Nat. Bur. Stand., 42, 145 (1949).
19. R. S. Porter, J. P. Knox and Julian F. Johnson, Trans. Soc. Rheology, 12:3, 409 (1968).
20. J. Meissner, in Proceedings of the Fourth International Congress on Rheology, Interscience, New York, (1965), Part 3, P. 437.
21. L. L. Blyler, Jr. and T. W. Haas, Polymer Preprints, 10, No. 1, 72 (1969).
22. M. L. Miller, The Structure of Polymers, Chapter 6, P. 291, 296, Reinhold, New York (1966).
23. T. G. Fox, Jr. and P. J. Flory, J. Appl. Phys., 21, 581 (1950).
24. T. G. Fox, Jr. and P. J. Flory, J. Am. Chem. Soc., 70, 2384 (1948).
25. G. V. Vinogradov, A. Ya. Malkin, and V. G. Kulichiklin, J. Polymer Sci., Part A-2, 8, 333 (1970).
26. R. S. Porter and J. F. Johnson, Chem. Review, 66, 1 (1966).
27. G. V. Vinogradov and N. P. Prozorovskaya, Rheol. Acta, 3, 156 (1964).
28. M. L. Friedman, G. V. Vinogradov, A. Ya. Malkin and O. M. Ponadiv, Vysokomol. Soedin, 12, (10) 2162 (1970).
29. Personal communication to R. S. Porter from G. V. Vinogradov.
30. J. T. Gruver and G. Kraus, J. Polymer Sci., A2, 797 (1964).
31. R. A. Mendelson, Polymer Eng. Sci., 8(3), 235 (1968); J. Polymer Sci., B5, 295 (1967).
32. E. L. Marker and S. L. Aggarwal, J. Polymer Sci., 38, 359 (1959).
33. F. E. Karasz and W. J. MacKnight, Macromolecules, 1, 537 (1968).
34. Unpublished work by authors.

35. E. A. Collins, T. Mass. and W. H. Bauer, Rubber Chem. and Techn., 43, 1109 (1970).
36. R. L. Combs and R. G. Natta, J. Polymer Sci., Part C, 30, 407 (1970).
37. (a) J. M. O'Reilly and W. M. Prest, Jr., General Electric Report.
(b) M. Yamada and R. S. Porter, unpublished data (1972).
38. A. N. Dunlop, H. W. Williams, J. Polymer Sci., 14, 1753 (1970).
39. R. L. Combs, D. F. Slonakin, H. W. Coover, Jr., J. Appl. Polymer Sci., 13, 519 (1969).
40. S. F. Kurath, E. Passaglia and R. Pariser, J. Appl. Physics, 28, 499 (1957).
41. R. J. Kokes and F. A. Long, J. Am. Chem. Soc., 75, 6143 (1953).
42. D. J. Plazek, W. Dannhauser and J. D. Ferry, J. Colloid Sci., 16, 101 (1961).
43. E. L. Warrick, Ind. Eng. Chem., 47, 1816 (1955).
44. W. Weber, Rheological Acta, 1, 63 (1958).
45. I. L. Hopkins, J. Appl. Physics, 25, 1300 (1953).
46. R. S. Spencer, J. Polymer Sci., 5, 591 (1950).
47. G. M. Bartenev, Vysokomolekuliarnyi Soedineniia, 6, 335 (1964).
48. E. A. Collins and A. P. Metzger, Polymer Eng. Sci., 10, 57 (1970).
49. J. Brandrup and E. H. Immergut, Polymer Handbook, Interscience, New York (1966).
50. O. Griffin Lewis, Physical Constants of Linear Homopolymers, Springer-Verlag, New York, Inc. (1968).
51. M. S. Danna, J. Appl. Polymer Sci., 1, 121 (1959).
52. D. L. Beck, J. R. Knox and J. A. Price, Presented before the Division of Petroleum Chemistry; American Chemical Society, Los Angeles Meeting March 31 - April 4, 1963.

53. G. Natta, F. Dausso and G. Moraghio, J. Polymer Sci., 25, 119 (1957).
54. F. P. Reding, J. Polymer Sci., 21, 547 (1956).
55. J. H. Griffith and B. G. Ranby, J. Polymer Sci., 44, 369 (1960).
56. B. G. Ranby, K. S. Chan and H. Brumberger, J. Polymer Sci., 58, 545, (1962).
57. K. H. Hellwege, J. Henning and W. Knappe, Kolloid Z. Z. Polym., 186, 29 (1962).
58. Plate, Personal communication.
59. S. S. Rogers and L. Mandelkern, J. Phys. Chem., 61, 985 (1957).

1. The E^* of poly-1-hexene as a function of $(T-T_g)$, from the shift factor a_T (40).

○ Kurath et al. (40).

△ Wang et al. (6).

□ Shirayama et al. (9).

— Calculated from W.L.F. equation.

----- Calculated from $\alpha_\ell = 6.2 \times 10^{-4} \text{ deg}^{-1}$, $T_g = 223^\circ\text{K}$ by the equation (12).

2. The E^* of polystyrene and polyisobutylene as a function of $(T-T_g)$, (40).

△ polystyrene $T_g = 373^\circ\text{K}$.

□ polyisobutylene $T_g = 200^\circ\text{K}$.

Dashed lines predicted by the equation (12).











3. Viscosities of poly-1-hexadecene as a function of temperature in Newtonian region and from several constant shear stresses.

4. The E^* of polymers as a function of α_ℓ .

The solid line from the equation (12) and the equation (16).

○ polyethylene, ○ polypropylene, ○ polybutene-1,






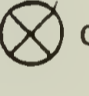




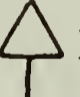



○ polyhexene-1, ○ polyheptene-1, ○ polytridecene-1,

 polyoctadecene-1,  polystyrene,  polyvinylacetate,
 polydimethylsiloxane,  polybutadiene,  polyisobutylene,
 polyvinylchloride,  hevea rubber,  GRS rubber,
 poly(ethylene terephthalate).

5. The E^* of polymers as a function of T_g .

Solid line calculated from equations (12) and (16).

Additional polymers for which E^* and T_g are available but not α_g . These include:

ethylene-acrylic acid copolymer  1.3%,  3.1%,  5.3%,  6.5% acid.
 concentration (21),  hydroxyl terminated polybutadiene,  carboxyl
 terminated polybutadiene,  butadiene acrylonitrile copolymer (35),
 Bisphenol-A polycarbonate (37),  T 18 type a copolyester,  Biphenol-
 A copolyester  poly(CHDM terephthalate),  poly(ϵ -caprolactam),
 poly(decamethylene adipate),  poly(oxydiethylene adipate) (36).

Other symbols as in Figure 4.

FLOW ACTIVATION ENERGY FOR POLY-1-HEXENE

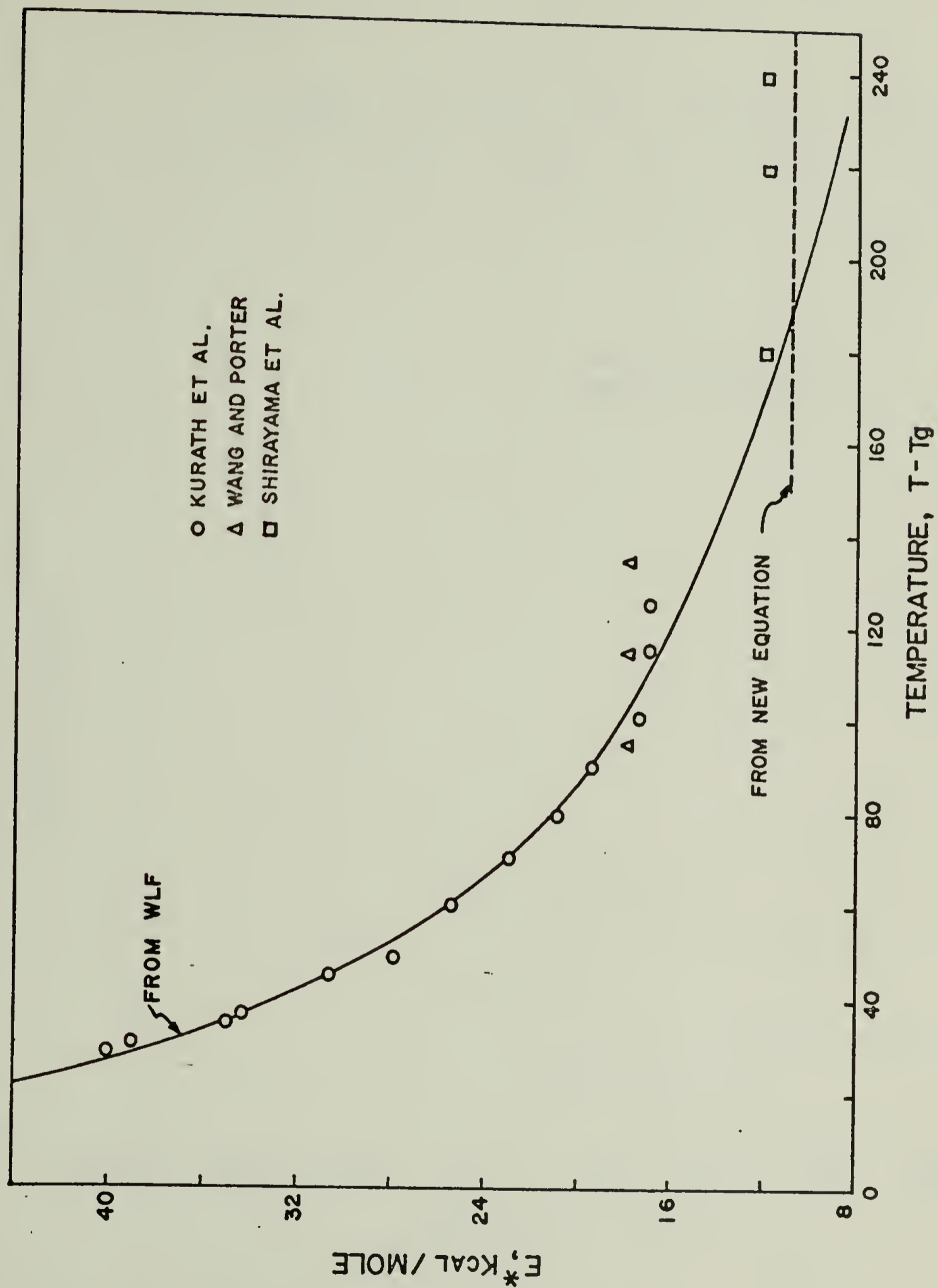


Figure III-1

FLOW ACTIVATION ENERGY FOR POLYSTYRENE AND POLYISOBUTYLENE

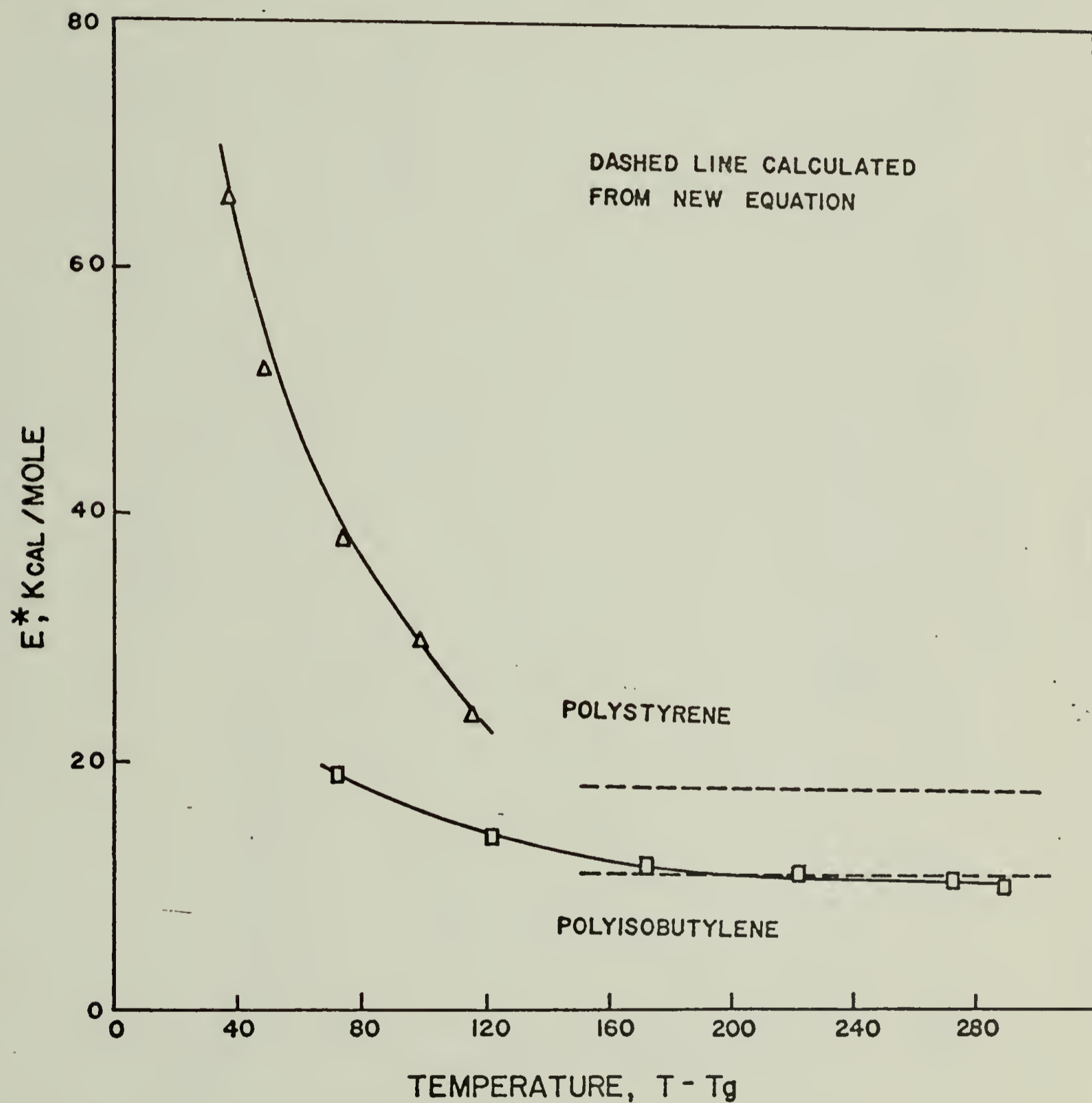


Figure III-2

POLY(1-HEXADECENE)

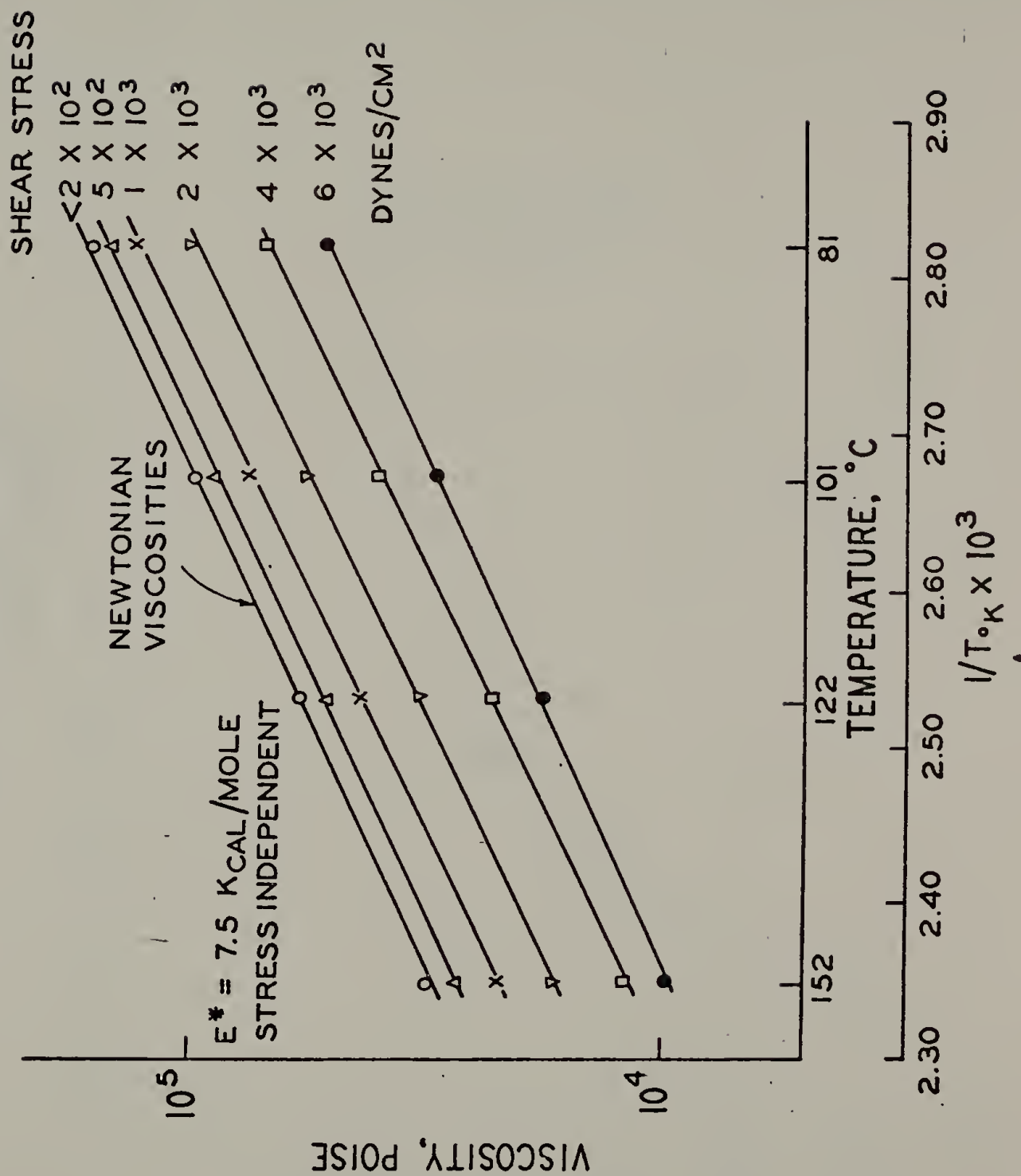


Figure III-3

FLOW ACTIVATION ENERGY AS A
FUNCTION OF VOLUME EXPANSION FOR A
VARIETY OF LINEAR AMORPHOUS POLYMERS

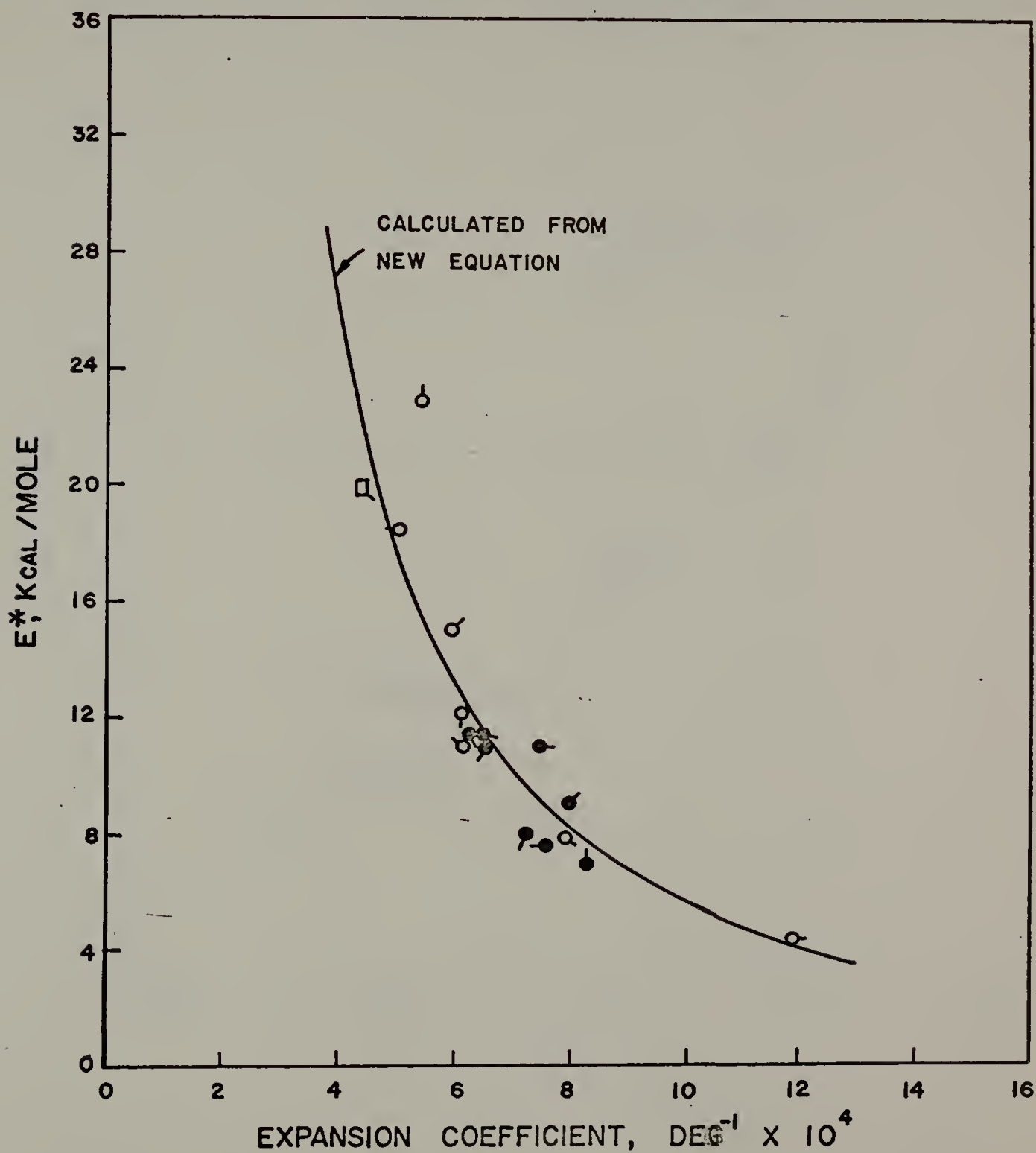


Figure III-4

FLOW ACTIVATION ENERGY AS A FUNCTION
OF GLASS TRANSITION TEMPERATURE FOR A
VARIETY OF LINEAR AMORPHOUS POLYMERS

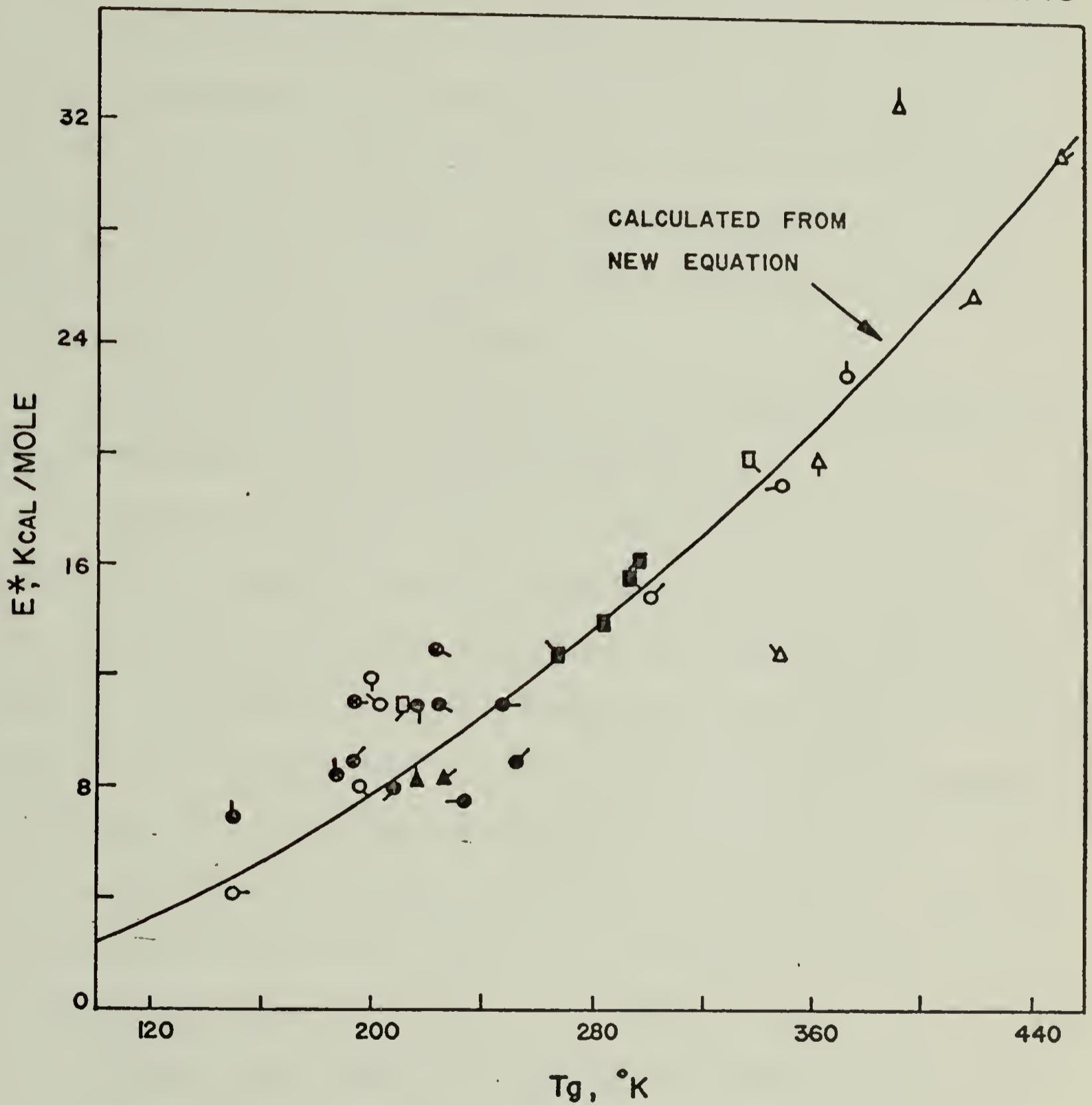


Figure III-5

CHAPTER IV

STEADY STATE AND DYNAMIC RHEOLOGY OF POLY-1-OLEFIN MELTS

Synopsis

The steady state and dynamic melt rheology for the poly-1-olefin series has been investigated. The series includes poly-1-butene, poly-1-hexene, poly-1-heptene, poly-1-octene, poly-1-undecene, poly-1-tridecene, poly-1-hexadecene and poly-1-octadecene. They were investigated by use of a Weissenberg Rheogoniometer. Corresponding tests on poly-1-butene were also made in an Instron Capillary Rheometer.

The empirical relation of Cox and Merz was obeyed for the entire series of poly-1-olefin and at all experimental temperatures.

Graessley's theory was used to calculate the flow curves for the poly-1-olefins using the measured molecular weight distribution. The purpose was to investigate the effect of polymer composition on the shear rate dependence of viscosity. It was found that all experimental flow curves except poly-1-hexene can be fitted with the calculated curves using the individual molecular weight distributions. The conclusion is thus made that flow curves of poly-1-olefin predominately depend on molecular weight distribution and are essentially independent of side-chain length even for poly-1-olefins with pendant groups as long as 16 carbon atoms.

If low shear limit Newtonian viscosity η_0 for all poly-1-olefins can be expressed by the equation, $\eta_0 = K\bar{M}w^{3.4}$, or by $\eta_0 = K'\bar{P}w^{3.4}$, where $\bar{M}w$ is the weight average molecular weight and $\bar{P}w$ is the weight average degree of polymerization, the K and K' values decrease systematically as the side-chain

length increases from poly-1-hexene to poly-1-octadecene. However, K' values decrease more slowly than K values.

The dynamic shear storage modulus, G' , loss modulus, G'' , and the reciprocal of dynamic shear compliance, $1/J'$ versus frequency curves at different temperatures can be superposed according to time-temperature superposition. The theory of second order fluid was only fitted by the data of poly-1-heptene and poly-1-octene. That is, at low frequency, half normal stress $(\sigma_{11} - \sigma_{22})/2$ can be correspondent to G' , the steady shear modulus G is correspondent to the reciprocal of low frequency limit dynamic compliance $1/J_e^0$ and shear stress τ_{12} is correspondent to G'' .

The steady shear modulus G for members of this poly-1-olefin series was found to be insensitive to molecular weight distribution for these broad distribution samples. The value of G , however, decreases with increasing the length of pendant groups from poly-1-hexene to poly-1-octadecene.

It was found that the steady state and dynamic viscoelastic properties of poly-1-olefin series have the same temperature dependence. The flow activation energy E^* was calculated from η_0 , from η_a at constant shear stress and from $|\eta^*|$ at constant product for $\omega|\eta^*|$. Three ways all give the same E^* which is independent of temperature over the measured range in the melt.

Introduction

Polymer melt rheology is influenced by several molecular properties such as molecular weight, molecular weight distribution and branching. However, little effort has been reported in attempts to relate polymer composition to melt rheology. In this regard, the poly-1-olefin series represents the most fundamental compositional series for evaluation of rheological characteristics

for linear amorphous polymers. The lowest members of the series, polyethylenes and polypropylene have been studied extensively. For the higher members, however, rheological studies have been rare. Shirayama et al.¹ reported studies on six different poly-1-olefins by using a rotating-cylinder rheometer. Earlier, Combs et al.² also reported the influence of side-chain length on the melt rheology of five poly-1-olefins using a Melt Indexer. These valuable early results do not, however, provide a clear overall picture. For example, molecular weight distribution is known generally to affect shear thinning characteristics,³ yet the distributions are unspecified in these earlier reports even though they likely differ from sample-to-sample and from study-to-study. It is thus impossible to decide if the side chain length in the poly-1-olefin series has any effect on the shear rate dependence of viscosity.

Graessley has developed a theory based on molecular entanglements⁴ which can be used to calculate flow curves for different breadths of molecular weight distribution. The theory has been successful for a limited number of test cases.⁶ This theory will thus be considered in the light of these new studies on the shear rate dependence of viscosity for the poly-1-olefins. A decision can thus be potentially reached concerning the influence of polymer composition on the shear rate dependence of viscosity.

The rheological properties for the poly-1-olefin were measured in steady state and in dynamic experiments. The measurements were made by using a cone-plate type rheogoniometer (Weissenberg) and a capillary type rheometer (Instron).

Samples

Poly-1-olefin series used here consisted of linear poly-1-butene, poly-1-hexene, poly-1-heptene, poly-1-octene, poly-1-undecene, poly-1-tridecene,

poly-1-hexadecene and poly-1-octadecene. One sample of each polymer was used except for poly-1-octadecene. For this polymer, samples of three different molecular weights and tacticities were tested. All samples were prepared by Avisun Corporation, Marcus Hook, Pennsylvania, and were polymerized by using a Ziegler-Natta catalyst -- titanium tetrachloride and aluminum triisobutyl. The polymerization methods for these samples have been reported previously.⁷ These polymers are believed to be entirely linear. These molecular weights and distributions, as measured by calibrated gel permeation chromatography, are identified in Table 1. The temperature ranges of measurement used in the Weissenberg Rheogoniometer and the Instron Rheometer are also shown in Table 1.

Experiments

The melt rheology was investigated with a Weissenberg Rheogoniometer (Model R17) which was used to measure steady and dynamic viscoelastic properties. A 4° angle, 2.5 cm-diameter cone was chosen to minimize sample size. Various torsion bars were used as appropriate for the viscosity and modulus range. The dynamic properties were measured with an improved version of Birnboim Ultra Low Frequency Phase Meter.⁸ The modified phase meter defines phase angles to less than $\pm 2\%$. The input amplitude was sufficiently small to provide dynamic viscosities and rigidities which were independent of amplitude, i.e., in the region of linear viscoelasticities. In order to eliminate voids and reduce oxidation, the powdery samples were pressed to films before insertion in the Rheogoniometer. The samples were measured over the melt temperature ranges shown in Table 1. The samples were always surrounded with nitrogen gas to decrease degradation. Over the reported temperature ranges, degradation was not present. At yet higher temperature, degradation was observed as a

decrease in steady shear and dynamic viscosity with time. The reproducibility of degradation-free data is better than $\pm 5\%$.

Values of steady shear viscosity and of the first normal stress difference ($\sigma_{11} - \sigma_{22}$) were determined as a function of shear rate. The values of dynamic viscosity η' , the dynamic shear storage modulus G' , and shear loss modulus G'' were obtained from the oscillatory experiments. The absolute value of complex dynamic viscosity $|\eta^*|$ were calculated from G' and G'' by the Equation (1):

$$|\eta^*| = (G'^2 + G''^2)^{1/2} / \omega \quad (1)$$

The shear storage compliance J' has been calculated from G' and G'' by Equation (2):

$$J' = G' / (G'^2 + G''^2) \quad (2)$$

The sample available in large quantity was poly-1-butene. The Instron Rheometer was thus used to measure viscosities at high shear on this sample. The range of shear rates measurable by the Instron is from about 5 to 500 sec^{-1} . In order to avoid measurable entrance effects, a large ratio for capillary length-to-diameter was chosen ($D = 0.060''$, $L = 2.00''$, $L/D = 33.3$). The true shear rate at the capillary wall $\dot{\gamma}_w$ was calculated from the apparent value $\dot{\gamma}_{wa}$, according to the Rabinowitsch equation:⁵

$$\dot{\gamma}_w = \dot{\gamma}_{wa} (3/4 + 1/4 d \log \dot{\gamma}_{wa} / d \log \tau_w) \quad (3)$$

where τ_w is the wall shear stress. The non-Newtonian viscosity η_a is defined as the ratio of shear stress to true shear rate.

The data on molecular weight and molecular weight distribution (MWD) were obtained by using a Waters Associate Gel Permeation Chromatograph (GPC Model 200). In order to avoid degradation and to simplify the corresponding intrinsic viscosity measurements, the GPC operating temperature was 80°C. 1,2,4-trichlorobenzene was the GPC solvent. All polymers dissolved completely in this solvent at this temperature. The universal calibration method was used to calculate the absolute molecular weights and the MWD. The details of the procedure have been described elsewhere.⁹ The intrinsic viscosities were measured in the same solvent and at the same temperature in Cannon-Ubbelohde Dilution Viscometer.

Results and Discussion

Viscosity Change with Shear Rate and Frequency. Figure 1 is the plot of steady state viscosity, η_a , versus shear rate, $\dot{\gamma}$, and of complex dynamic viscosity, $|\eta^*|$ and dynamic viscosity η' versus frequency, ω , for poly-1-butene at three temperatures. The η_a at lower shear rates were measured by the Weissenberg Rheogoniometer. At high shear rates, the Instron Rheometer was used. The excellent agreement between η_a and $|\eta^*|$ was found for each temperature. η' diverges from the $|\eta^*|$ curve in the region where η_a becomes non-Newtonian. At higher frequencies, η' decreases more rapidly than $|\eta^*|$ and η_a for all cases.

The correspondence of linear and nonlinear viscoelastic properties has been tested in numerous studies. Cox and Merz¹⁰ first suggested that for polystyrene melts and for solutions of polyisobutylene in decalin, η_a vs. $\dot{\gamma}$ curves matched $|\eta^*|$ vs. ω curves. This empirical observation has been confirmed by Onogi et al. for polyethylene¹¹ and for polystyrene¹² melts. This coincidence

has also been previously reported for polypropylene melts.¹³ Shroff and Shida¹⁵ have found that the empirical relation of Cox and Merz is good for high-density as well as for low-density polyethylenes with low values for weight-average number of branches per molecule (n_w). The correlation, however, was poor with low-density samples with large values of n_w .

Recently, a dilute solution theory for rigid dumbbells has been published which predicts identity of η_a and $|\eta^*|$ for small values of arguments.¹⁴

For the poly-1-olefins, it should be noted that coincidence between η_a and $|\eta^*|$ was found not only the lower members of the series but also for higher members, e.g., poly-1-hexene to poly-1-octadecene, exhibited agreement between η_a and $|\eta^*|$ over the region of overlapping data. Samples available, however, were inadequate in amount for testing by Instron Rheometer. It is thus a remaining question whether the long pendant groups give results comparable to low density polyethylene.

These η_a vs. $\dot{\gamma}$ and $|\eta^*|$ vs. ω curves at a series of temperature for each polymer have been found to superposed to a single master curve by plotting the ratio of η_a/η_0 and $|\eta^*|/\eta_0$ against $\dot{\gamma}\tau_R$ and $\omega\tau_R$, respectively, as shown in Figures 2-9. Here η_0 is Newtonian viscosity, T is absolute temperature, τ_R is the Rouse relaxation time expressed by:

$$\tau_R = (6/\pi^2) (\eta_0 \bar{M}_w / \rho RT) \quad (4)$$

Here, weight average molecular weight \bar{M}_w was used. Melt density ρ was obtained from dilatometric experiments. R is the gas constant (8.31×10^7 erg deg⁻¹ mole⁻¹). The complex dynamic viscosity $|\eta^*|$ is represented by the filled points in these figure

It is clearly confirmed that $|\eta^*|$ values can be superimposed by plotting with $\omega\tau_R$ and that they overlap with the curves of η_a vs. $\dot{\gamma}\tau_R$.

Graessley's molecular entanglement theories⁴ allow a further calculation of flow curves from molecular weight distribution data obtained here by gel permeation chromatography (GPC). A computer program developed by Graessley¹⁶ was thus used to calculate η/η_0 vs. $\dot{\gamma}\tau_0/2$ for members of the poly-1-olefin series from GPC measures of molecular weight distribution. Here τ_0 is an experimental relaxation time, considered to be an entanglement formation time reduced to $\dot{\gamma} = 0$. In all the figures, the theoretical curve of $\log(\eta_a/\eta_0)$ vs. $\log(\dot{\gamma}\tau_0/2)$ was shifted parallel to the axes to achieve the best fit with experimental data. The experimental relaxation time, τ_0 could thus be calculated from a direct comparison of the $\dot{\gamma}$ axis of the experimental curve with the $\dot{\gamma}\tau_0/2$ of the superimposed theoretical curve. The experimental and calculated Graessley's theoretical flow curve, using the MWD from GPC, are in fairly good agreement for all the poly-1-olefins tested here, except for poly-1-hexene. The curves from GPC were not corrected for band broadening (about 0.2 in \bar{M}_w/\bar{M}_n). This is inconsequential since Graessley's theoretical flow curves do not change sensitively with the ratio of \bar{M}_w/\bar{M}_n for the broad MWD studied here. Actually the shapes of the flow curves are very similar despite the differences in \bar{M}_w/\bar{M}_n for broad MWD.

The experimental flow curve of poly-1-hexene deviates from the theoretical curve even at low shear rates. The reasons for this is as yet unknown. The low molecular weight of poly-1-hexene may be a possible reason. The fit was also not good with data on poly-1-heptene and poly-1-octene in the sensitive high shear region. Measured viscosities for these two polymers were found to decrease more rapidly than the calculated curves. For the other higher poly-

1-olefin, the agreement between experimental and theoretical flow curve is good even for side-chain lengths up to 16 carbon atoms. This means that the flow curves of poly-1-olefin series predominantly depend on molecular weight distribution and are independent of side-chain length in the poly-1-olefins. Therefore, the chemical composition of poly-1-olefin does not significantly affect the flow curve of these polymers with the discrepancies noted above.

The values of experimental relaxation time τ_o for all poly-1-olefins did not equal the Rouse relaxation time τ_R but were of the same order, as shown in Table 2. The ratio of τ_R/τ_o increases with increasing molecular weight regardless of molecular weight distribution and for different poly-1-olefin. The plot of τ_R/τ_o vs. $\bar{M}w$ is virtually a straight line for the poly-1-olefin series as shown in Figure 10. Graessley⁶ has reported that the ratio τ_R/τ_o varies systematically with both concentration, C , and molecular weight, M , and that τ_R/τ_o vs. the product CM yields a single straight line for systems of various concentrations and molecular weights. The results also show that experimental relaxation time obtained by superposition is independent of molecular weight distribution.

Newtonian Viscosity. The low-shear Newtonian viscosities were generally obtained for all the poly-1-olefins except for poly-1-undecene and poly-1-octadecene, Sample 2. Two poly-1-octadecene samples, numbers 1 and 3, which have low-shear Newtonian viscosities η_o show a slope of 3.4 in the plot of $\log \eta_o$ vs. $\log \bar{M}w$.

Poly-1-tridecene, poly-1-hexadecene, and poly-1-octadecene have a similar $\bar{M}w$, however their η_o values at the same temperature decrease systematically with increasing side-chain length. If Newtonian viscosities η_o for each poly-1-olefin are expressed by $\eta_o = K\bar{M}w^{3.4}$ then the value K at the same

temperature decreases systematically from poly-1-hexene to poly-1-octadecene as shown in Table 3. Since the viscosity of polymers seems to be more dependent on the length of the main chain than on molecular weight, η_0 can be expressed by $\eta_0 = K' \bar{P}_w^{3.4}$, here \bar{P}_w is the weight average degree of polymerization. The K' value for the poly-1-olefin series still decreases with increasing side-chain length, but the differences are much less than in K values. This means that the polyolefins having longer side-chain show lower viscosities for the same weight average molecular weight. This is consistent with Shirayama's results.¹ Shirayama et al. studied the molecular weight dependence of viscoelastic properties. At fixed shear rate and temperature, η_a , η' and G' for each polymer sample were expressed by the form $K \bar{M}_n^\alpha$. Here \bar{M}_n is number average molecular weight. They found that the values of α were approximately 3-4 for all the samples and K decreased with increasing side-chain length.

Melt Elasticity. The melt elasticity can be obtained by the measurement of the first normal stress difference, $\sigma_{11} - \sigma_{22}$, in steady shear. This difference can be measured directly with the Weissenberg Rheogoniometer. From the first normal stress difference, the steady shear modulus, G , may be calculated by the following equation:

$$G = 2\tau_{12}^2 / (\sigma_{11} - \sigma_{22}) \quad (5)$$

The dynamic storage modulus G' and loss modulus G'' were also measured from dynamic experiments. The dynamic compliance J' can be calculated from G' and G'' by Equation (2). The G' , G'' and $1/J'$ can also be superimposed on a master curve from measurements made at different temperature. The Figure 11 shows typical data of G' , G'' and $1/J'$ as a function of ωa_T for poly-1-heptene.

The reduced data was superimposed by multiplying the frequency axis by a shift factor a_T . The experimental data do not give a constant limiting value of steady state shear compliance:

$$J_e^0 = \lim_{\omega \rightarrow 0} G' / (G'^2 + G''^2) \quad (6)$$

This result is typical of the response of system with broad molecular weight distribution.

In Figures 12 and 13 the lines represent the master curve of dynamic measurements of G' , G'' and $1/J'$ as a function of ωa_T for poly-1-heptene and poly-1-octene. The data points in these figures give the steady state shear stress τ_{12} , half the primary normal stress difference $(\sigma_{11} - \sigma_{22})/2$ and the shear modulus G , as a function of the reduced shear rate $\dot{\gamma} a_T$. The same shift factor a_T for the steady state and dynamic master curves, indicates that they have the same temperature dependence. The data of poly-1-heptene, poly-1-octene in Figures 12 and 13 show that for these systems G' is equal to $(\sigma_{11} - \sigma_{22})/2$ and τ_{12} is equal to G'' on the low shear region. G is close to $1/J'$ in the low shear region but with less shear rate dependence than the frequency dependence of $1/J'$. G thus becomes smaller than $1/J'$ at the higher shear rates. However, these experimental correlation are only expected to be true at low shear in the Newtonian region, where G''/ω reaches a constant value. For the other poly-1-olefins, the dynamic experiments did not reach a sufficiently low frequency for G''/ω to become constant. Therefore, it was found that $(\sigma_{11} - \sigma_{22})/2$ is larger than G' , τ_{12} is larger than G'' but equal to the complex dynamic shear modulus $|G^*| = (G'^2 + G''^2)^{1/2}$, and G is less than $1/J'$ at the corresponding shear rate and frequency. The equality of τ_{12} and $|G^*|$ corresponds to the empirical relation of Cox and Merz where η_a is equal to $|\eta^*|$.

The steady-shear modulus G versus shear is a test of Hooke's law in shear as described by Baglay.²⁴ These studies apparently show a shear rate and stress independent modulus. The steady-shear modulus G of poly-1-olefins obtained in this study slightly increase with increasing shear rate as shown in Figure 14. This is also a characteristic of the broad MWD for the samples.¹⁸ In Figure 14, G values at the same shear rate for the poly-1-olefin are shown to systematically decrease from poly-1-hexene to poly-1-octadecene as the side-chain length increases. This conclusion is apparently independent of differences in MWD. This is a surprise result since J_e^0 (or $1/G$) is sensitive to molecular weight distribution. The Prest and Porter²⁰ study for blends of polystyrenes showed that the J_e^0 for narrow MWD polystyrenes passes through a high maximum upon addition of low concentrations of a high molecular weight fraction. A similar result was also found for blends of polydimethylsiloxane.¹⁹ However, many studies have shown that J_e^0 does not depend on molecular weight if the molecular weight is higher than critical molecular weight M_c^3 .

Quantitative studies of the MWD dependence of G , especially for broad MWD's have not yet been published. From these studies, the G of the poly-1-olefins is found to be insensitive to MWD for the broad MWD's of samples available.

Temperature Dependence. The temperature dependence of viscoelastic properties can be obtained from either steady state or dynamic experiments and from the shift factors needed for temperature superposition. Figures 12 and 13 show the frequency dependence curve of G' , G'' and $1/J'$ as well as the shear rate dependence of τ_{12} and $(\sigma_{12} - \sigma_{22})$ at various temperatures. They are all satisfactorily superposed by the same shift factor a_T , to give master curves. This indicates that the steady state and dynamic viscoelastic properties for the poly-1-olefins have the same temperature dependence. The activation energy E^* can be calculated from the plot of a_T or η_0 against reciprocal temperature. The two ways give the same E^* .

E^* can also be obtained by the plot of apparent viscosity η_a at constant shear stress vs. $1/T$. E^* is known to be dependent on shear rate but independent of shear stress for linear amorphous polymers.^{21,22} It is shown in addition in this paper that $|\eta^*|$ vs. ω at different temperature can also be used to calculate an E^* . This is shown in Figure 15. In this plot, the $|\eta^*|$ for poly-1-octadecene sample 1 is plotted vs. $1/T$ at different values of the product $\omega|\eta^*|$. η_a are also plotted vs. $1/T$ at different shear stresses, $\dot{\gamma}_a$. The $|\eta^*|$ data are represented by the black points in Figure 15. It is obvious that the lines of $|\eta^*|$ are parallel with the lines of η_a and also parallel with the line of η_0 for the Newtonian region. This means E^* calculated from $|\eta^*|$ at a constant product $\omega|\eta^*|$ is identical with the value calculated from η_a at constant shear stress and with values from the Newtonian viscosity.

The three different molecular weights and tacticities for poly-1-octadecene, samples 1-3, show an E^* at constant shear stress of 7.5, 8.4 and 8.0 Kcal/mole respectively. This confirms that E^* is independent of molecular weight at high molecular weight and independent tacticity within the experimental precision of $E^* \pm 1$ Kcal/mole.

A previous report by these workers²² showed that the E^* for the poly-1-olefin series increases from polyethylene to poly-1-hexene, there is a maxima around poly-1-hexene and poly-1-octene. For the higher member of the series, the E^* decreases with increasing side-chain length. The E^* for the higher members up to poly-1-octadecene are constant and close to the E^* for high-density polyethylene. Later, Shirayama¹ et al. also showed that the E^* of poly-1-olefin reached a maxima at poly-1-hexene, but the E^* for poly-1-hexene was much smaller than reported here.²² This is likely due to the lower temperature of viscosity measurements used here to calculate E^* .²³ The E^* of polymers changes

regularly with chemical composition. It has been shown that volume expansion coefficient α_ℓ above melting point and glass transition temperature T_g of polymers could be used to correlate with E^* for different polymers including poly-1-olefin series.²³

TABLE 1

Poly-1-olefin

Molecular Weight, Molecular Weight Distribution and
Temperature Range for Viscosity Measurements

Polymer	M_n	M_w	M_w/M_n	Viscosity Test Range, °C
poly-1-butene	6.30×10^4	8.50×10^5	13.5	150 - 230
poly-1-hexene	4.00×10^3	1.70×10^4	4.3	40 - 80
poly-1-heptene	8.70×10^3	5.90×10^4	6.8	40 - 80
poly-1-octene	1.10×10^4	8.00×10^4	7.3	40 - 80
poly-1-undecene	3.80×10^5	1.20×10^6	3.2	80 - 140
poly-1-tridecene	2.40×10^5	2.60×10^6	11.0	80 - 120
poly-1-hexadecene	3.40×10^5	2.50×10^6	7.4	80 - 140
poly-1-octadecene				
Sample 1	7.30×10^5	3.50×10^6	4.8	80 - 140
Sample 2	2.10×10^5	2.70×10^6	13.0	100 - 140
Sample 3	6.90×10^3	4.30×10^5	62.0	80 - 140

TABLE 2

Rouse, τ_R , and Experimentent, τ_o , Relaxation Times
 (All at 80°C except poly-1-butene at 170°C)

Polymer	τ_R (sec)	τ_o (sec)	τ_R/τ_o	τ_o
poly-1-butene	5.8	1.3	4.5	5.2×10^5
poly-1-hexene	0.023	0.012	0.2	4.4×10^5
poly-1-heptene	0.082	0.15	0.55	4.5×10^4
poly-1-octene	0.11	0.18	0.62	4.5×10^4
poly-1-tridecene	77	10.3	7.5	8.2×10^5
poly-1-hexadecene	33	5.8	5.6	3.2×10^5
poly-1-octadecene Sample 1	2.8	0.3	9.5	2.6×10^4

TABLE 3

K and K' value of poly-1-olefin at 80°C

Polymer	$K = \eta_o / \bar{M}_w^{3.4}$	$K' = \eta_o / \bar{P}_w^{3.4}$
poly-1-hexene	1.9×10^{-11}	6.6×10^{-5}
poly-1-heptene	8.9×10^{-13}	6.9×10^{-6}
poly-1-octene	7.5×10^{-13}	5.2×10^{-6}
poly-1-tridecene	7.6×10^{-17}	6.2×10^{-9}
poly-1-hexadecene	6.4×10^{-17}	3.7×10^{-9}
poly-1-octadecene		
Sample 1	3.3×10^{-18}	4.7×10^{-10}
Sample 3	3.3×10^{-18}	4.7×10^{-10}

* Low shear Newtonian viscosities of poly-1-undecene and poly-1-octadecene (Sample 2) were not found at 80°C.

References

1. K. Shirayama, T. Matsuda and S. I. Kita, *Makromol. Chem.*, 147, 155 (1971).
2. R. L. Combs, D. F. Slonaker and H. W. Coover, Jr., *J. Appl. Polymer Sci.*, 13, 519 (1969).
3. J. D. Ferry, *Viscoelastic Properties of Polymers*, Second Ed., John Wiley & Sons, Inc., New York, New York (1970).
4. (a) W. W. Graessley, *J. Chem. Phys.*, 47, 1942 (1967).
(b) W. W. Graessley, *J. Chem. Phys.*, 54, 5143 (1971).
5. S. Middleman, *The Flow of High Polymers*, Chapter 2, Interscience Publishers, (1968).
6. (a) W. W. Graessley and L. Segal, *AIChE, J* 16, 261 (1970).
(b) W. W. Graessley and L. Segal, *Macromolecules*, 2, 49 (1969).
7. D. L. Beck, J. R. Knox and J. A. Price; Presented before the A.C.S. Division of Petroleum Chemistry, Los Angeles Meeting, April (1963).
8. M. H. Birnboim, U.S. Pat. 3,286,176 (Nov. 15, 1966).
9. J. V. Dawkins and J. W. Maddock, *European Polymer J.*, 7, 1537 (1971).
10. W. P. Cox and E. H. Merz, *J. Polymer Sci.*, 28, 619 (1958).
11. S. Onogi, T. Fujii, H. Kato and S. Ogihara, *J. Phys. Chem.*, 68, 1598, (1964).
12. S. Onogi, H. Kato, S. Ulki and T. Ibaragi, *J. Polymer Sci.*, 15C, 481 (1966).
13. J. W. C. Adamse, H. Janeschitz-Kriegl, J. L. Den Otter and J. L. S. Wales, *J. Polymer Sci.*, A2, 6, 871 (1968).
14. R. B. Bird, H. B. Warner, Jr., and D. C. Evans, *Adv. Polymer Sci.*, 8, 1 (1971).

15. R. N. Shroff and M. Shida, J. Polymer Sci., A2, 8, 1917 (1970).
16. Private communication with Professor W. Graessley, Northwestern University.
17. R. A. Mendelson, W. A. Bowles and F. L. Finger, J. Polymer Sci., A2, 8, 105 (1970).
18. H. Endo, T. Fujimoto and M. Nagasawa, J. Polymer Sci., A2, 9, 345 (1971).
19. W. M. Prest, Jr., J. Polymer Sci., A2, 8, 1897 (1970).
20. W. M. Prest, Jr. and R. S. Porter, Polymer J., 4, 154 (1973).
21. R. S. Porter and J. F. Johnson, J. Polymer Sci., 15C, 365 373 (1966).
22. J. S. Wang, R. S. Porter and J. R. Knox, J. Polymer Sci., 8B, 671 (1970).
23. J. S. Wang and R. S. Porter, to be submitted.

Captions for Figures

1. The steady state viscosity η_a versus shear rate $\dot{\gamma}$ from Weissenberg Rheogoniometer and Instron Rheometer, complex dynamic viscosity $|\eta^*|$ and dynamic viscosity versus frequency η' for poly-1-butene.
2. The comparison of experimental flow curve of poly-1-butene with Graessley's theoretical flow curve. The solid line was calculated from Graessley's theory.
3. The comparison of experimental flow curve of poly-1-hexene with Graessley's theoretical flow curve.
4. The comparison of experimental flow curve of poly-1-heptene with Graessley's theoretical flow curve.
5. The comparison of experimental flow curve of poly-1-octene with Graessley's theoretical flow curve.
6. The comparison of experimental flow curve of poly-1-undecene with Graessley's theoretical curve.
7. The comparison of experimental flow curve of poly-1-tridecene with Graessley's theoretical flow curve.
8. The comparison of experimental flow curve of poly-1-hexadecene with Graessley's theoretical flow curve.
9. The comparison of experimental flow curve of poly-1-octadecene with Graessley's theoretical flow curve.
10. The ratio of Rouse relaxation time to experimental relaxation time τ_R/τ_0 vs. weight average molecular weight for different poly-1-olefins.
11. The superposition curve of G' , G'' and $1/J'$ of poly-1-heptene reduced to temperature 80°C .

12. Shear rate dependence of $(\sigma_{11} - \sigma_{22})/2$, τ_{12} and G and frequency dependence of G' , G'' and $1/J$ for poly-1-heptene reduced to 80°C .
13. Shear rate dependence of $(\sigma_{11} - \sigma_{22})/2$, τ_{12} and G and frequency dependence of G' , G'' and $1/J'$ for poly-1-octene reduced to 80°C .
14. The shear modulus G of poly-1-olefins vs. shear at 100°C .
15. The change of viscosity of poly-1-octadecene (Sample 1) with temperature from steady shear viscosity η_a (open points) and complex viscosity $|\eta^*|$ (filled points).

APPARENT VISCOSITY η_a , COMPLEX DYNAMIC VISCOSITY $|\eta^*|$ AND DYNAMIC
VISCOSITY η' VERSUS SHEAR RATE $\dot{\gamma}$ AND FREQUENCY ω
FOR POLY-1-BUTENE

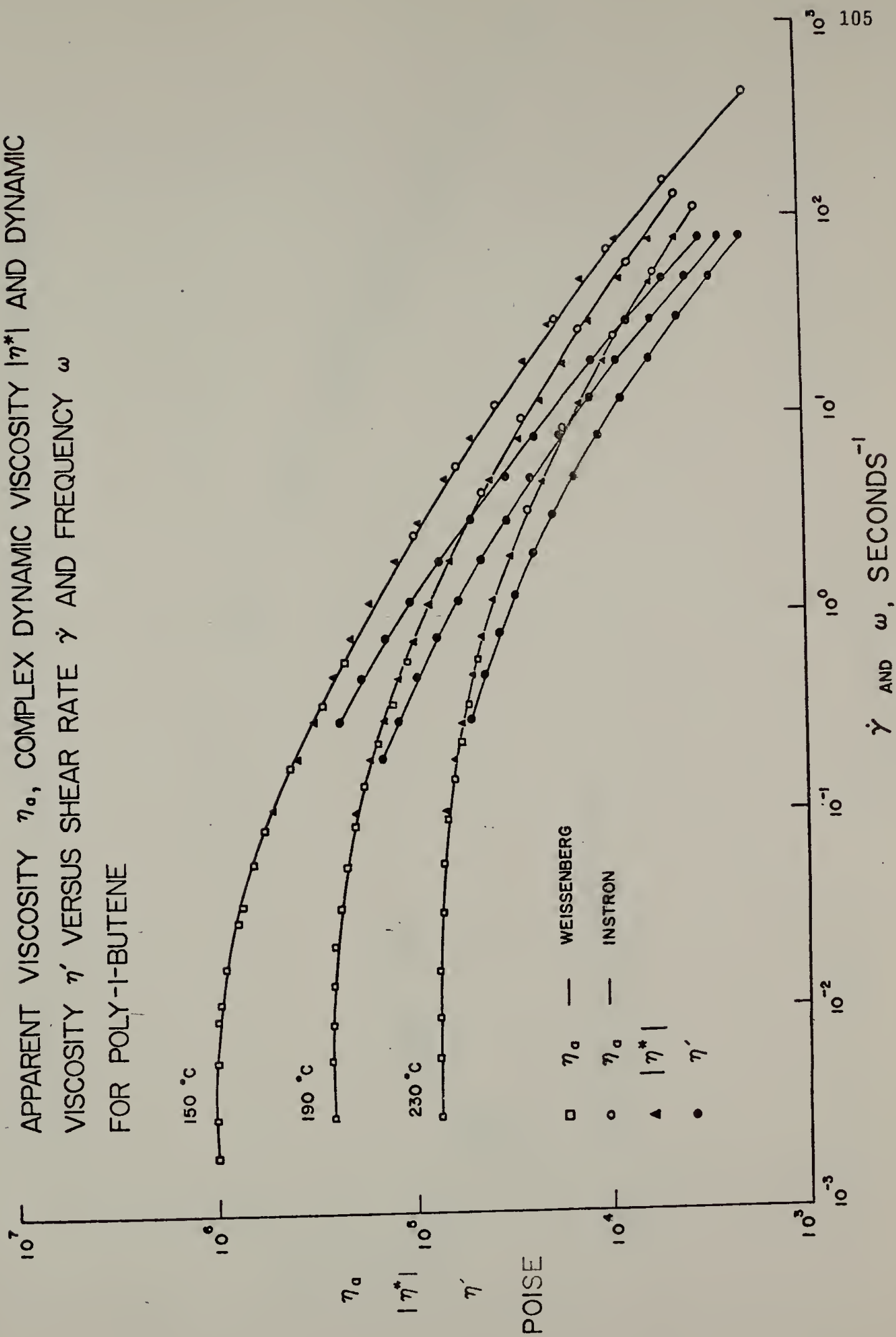


Figure IV-1

THE EXPERIMENTAL AND THEORETICAL FLOW CURVE FOR POLY-1-BUTENE

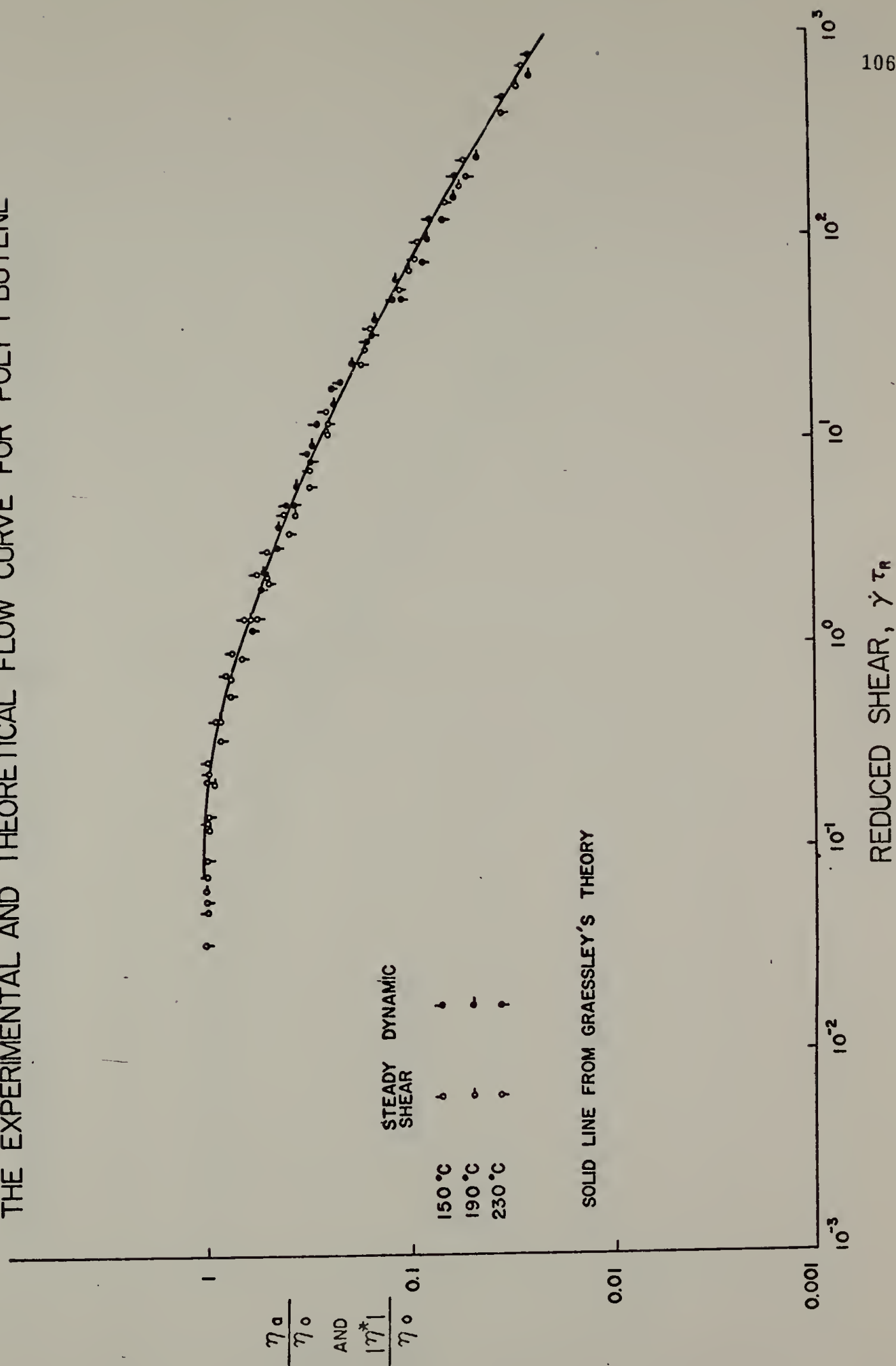


Figure IV-2

THE EXPERIMENTAL AND THEORETICAL FLOW CURVE FOR POLY-1-HEXENE

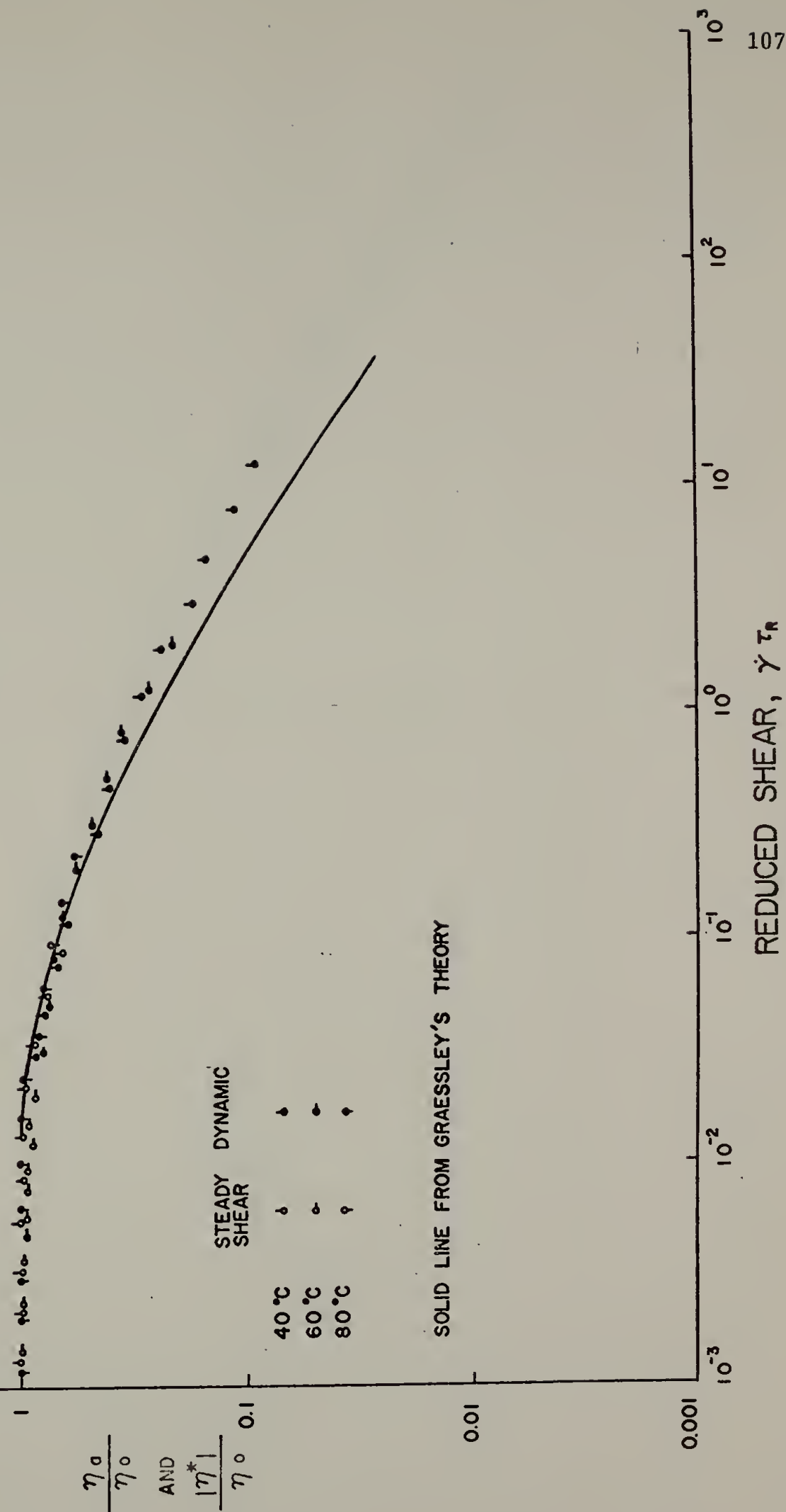


Figure IV-3

THE EXPERIMENTAL AND THEORETICAL FLOW CURVE FOR POLY-1-HEPTENE

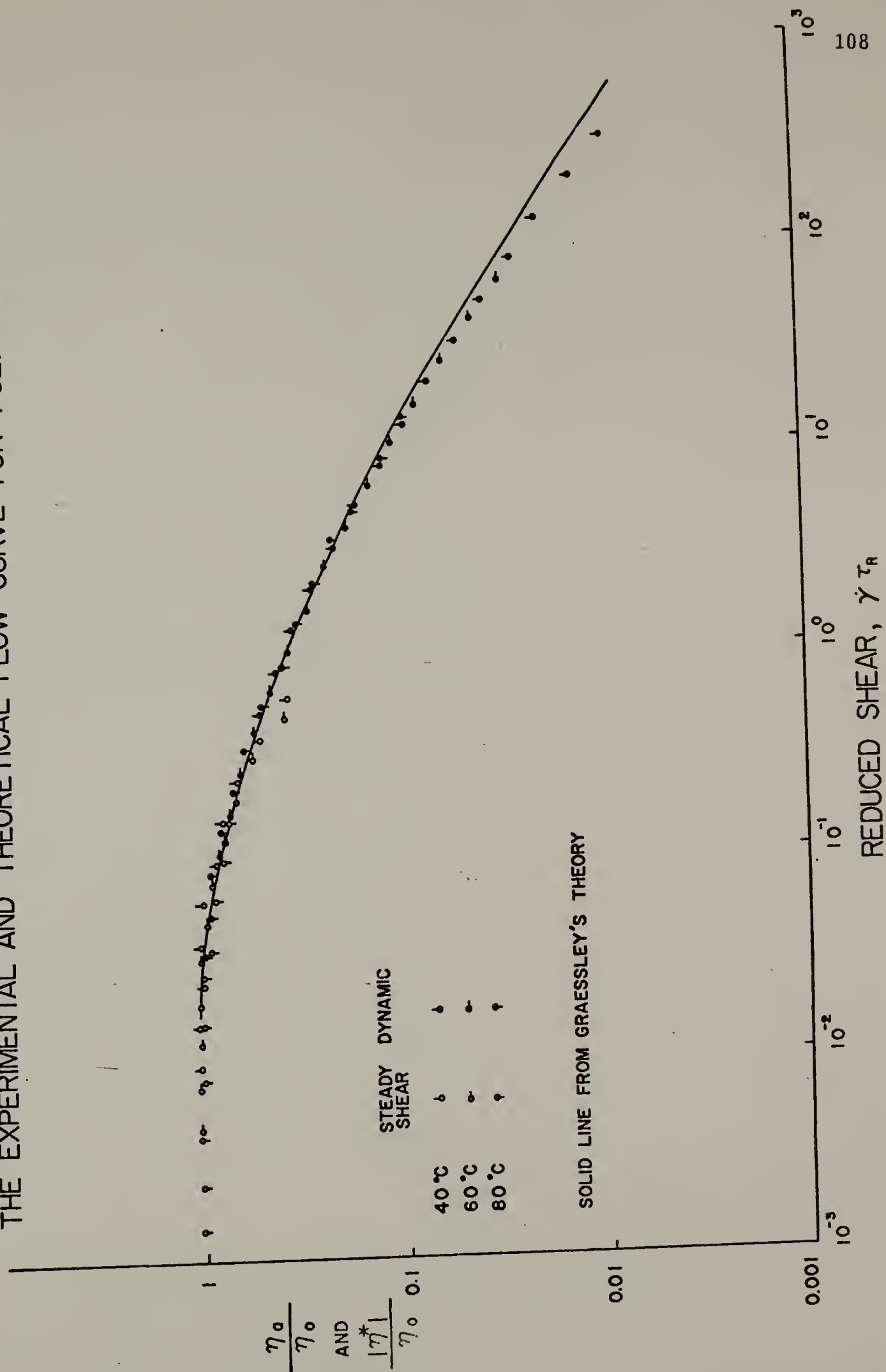


Figure IV-4

THE EXPERIMENTAL AND THEORETICAL FLOW CURVE FOR POLY-1-OCTENE

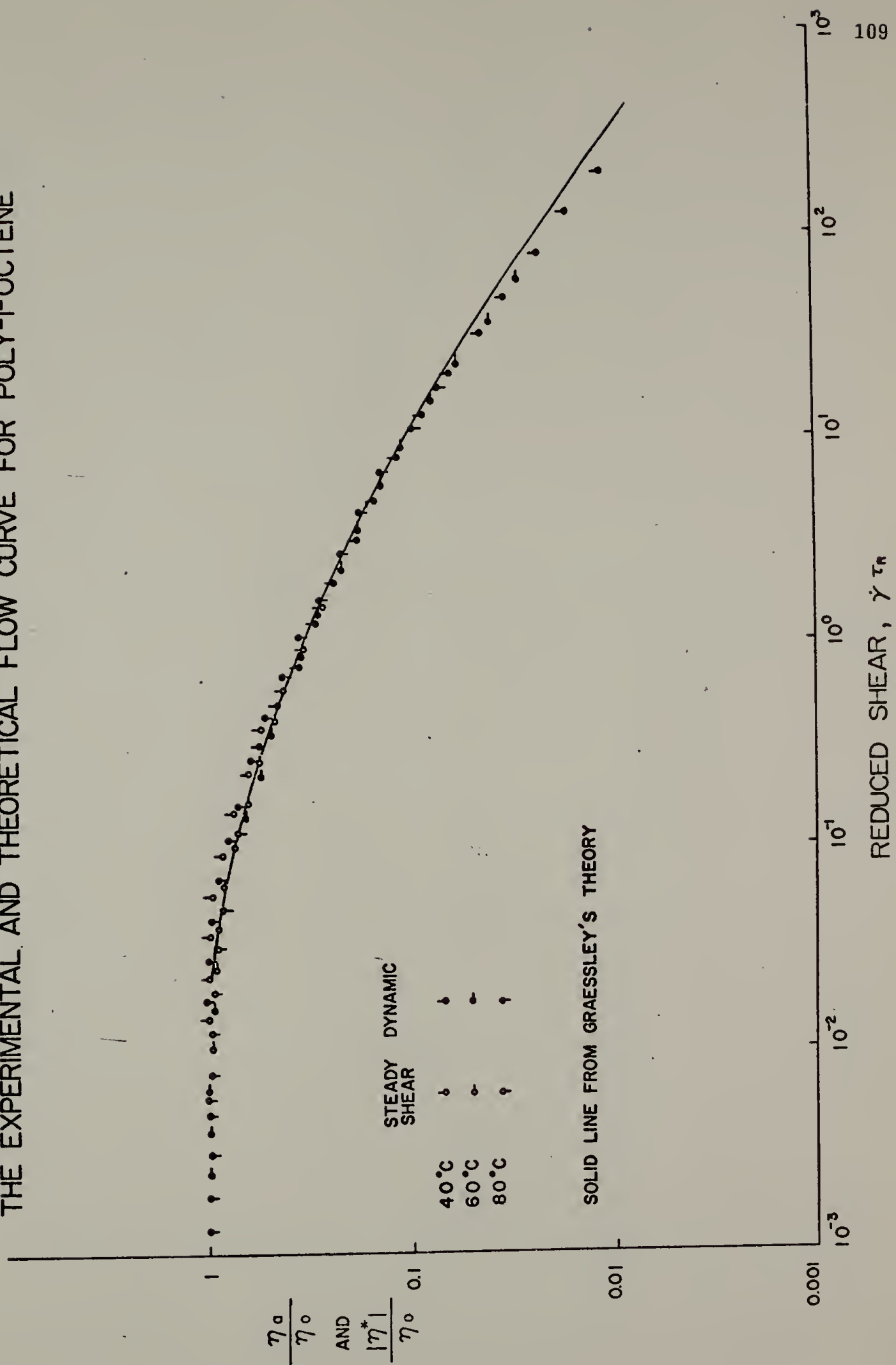


Figure IV-5

THE EXPERIMENTAL AND THEORETICAL FLOW CURVE FOR POLY-1-UNDECENE

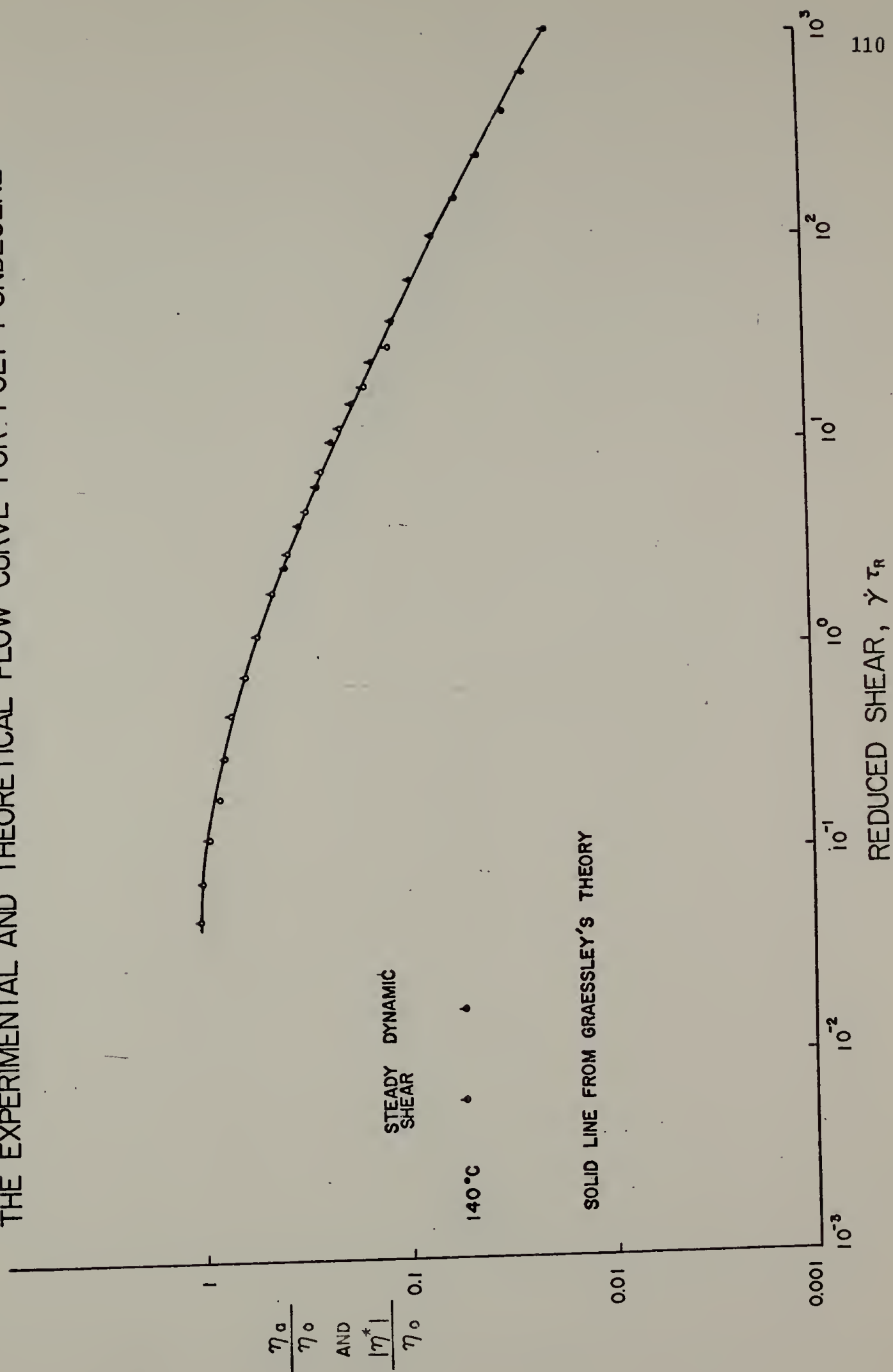


Figure IV-6

THE EXPERIMENTAL AND THEORETICAL FLOW CURVE FOR POLY-1-TRIDECENE

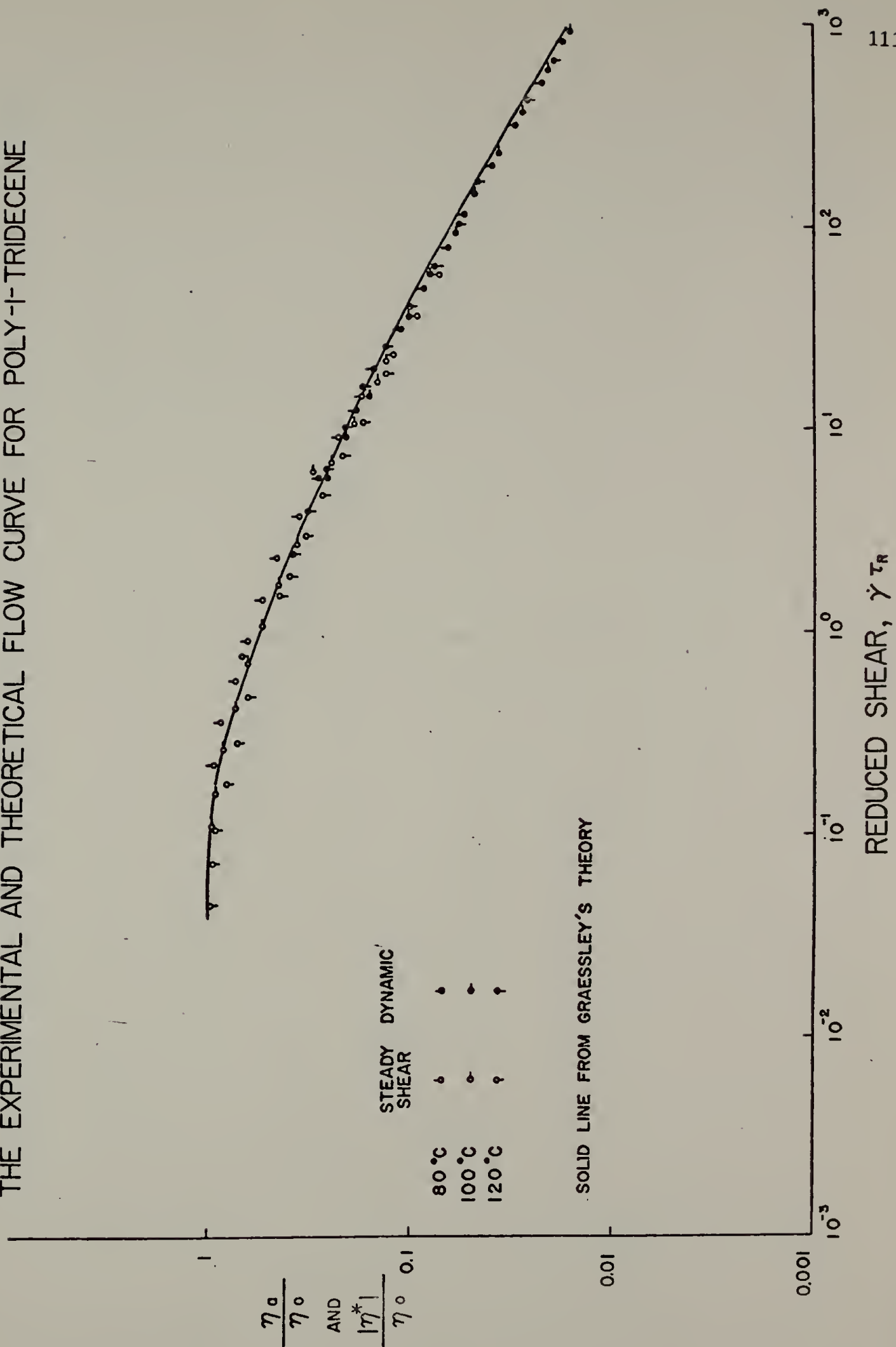


Figure IV-7

THE EXPERIMENTAL AND THEORETICAL FLOW CURVE FOR POLY-1-HEXADECENE

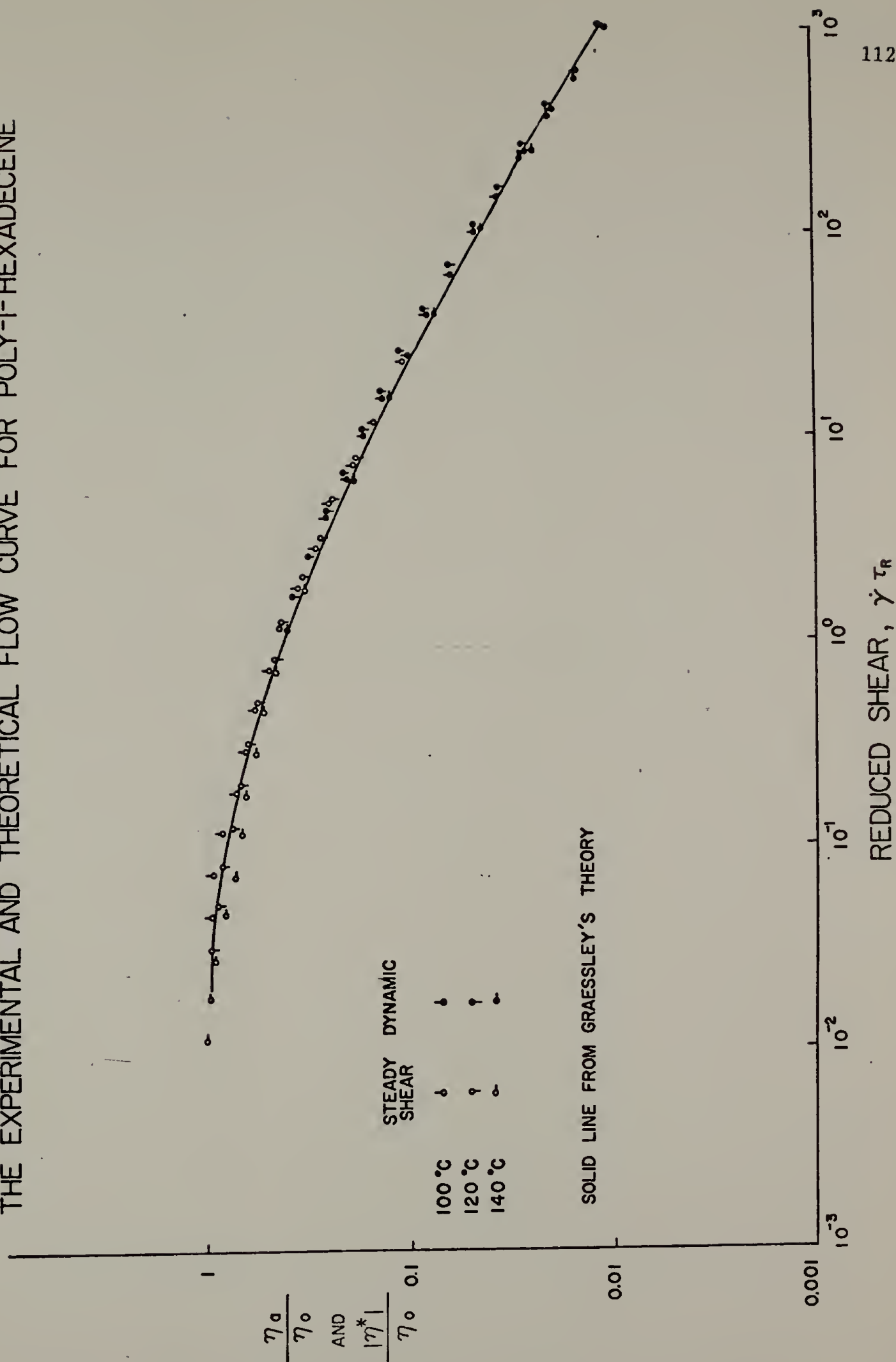


Figure IV-8

THE EXPERIMENTAL AND THEORETICAL FLOW CURVE FOR POLY-1-OCTADECENE

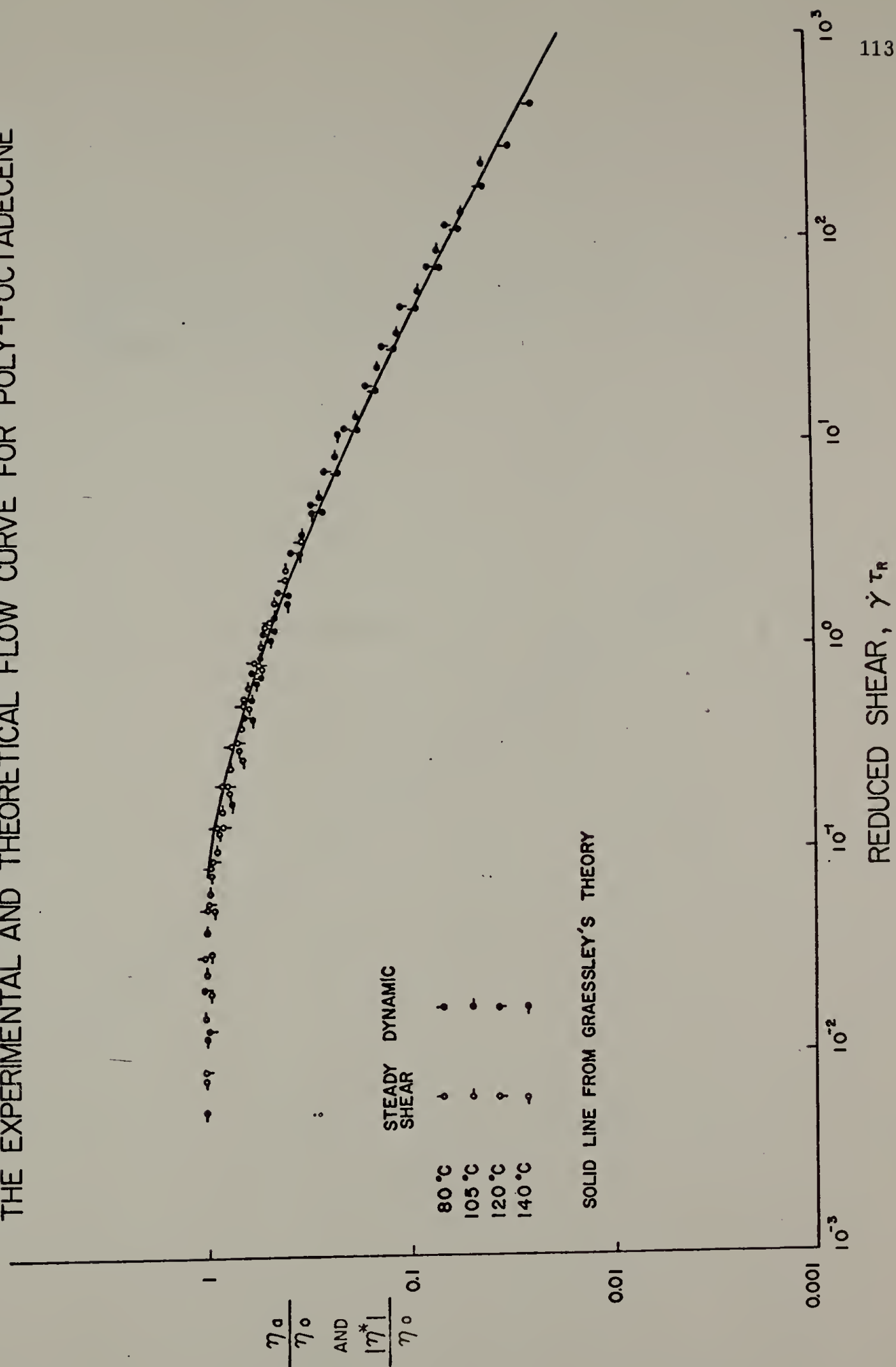


Figure IV-9

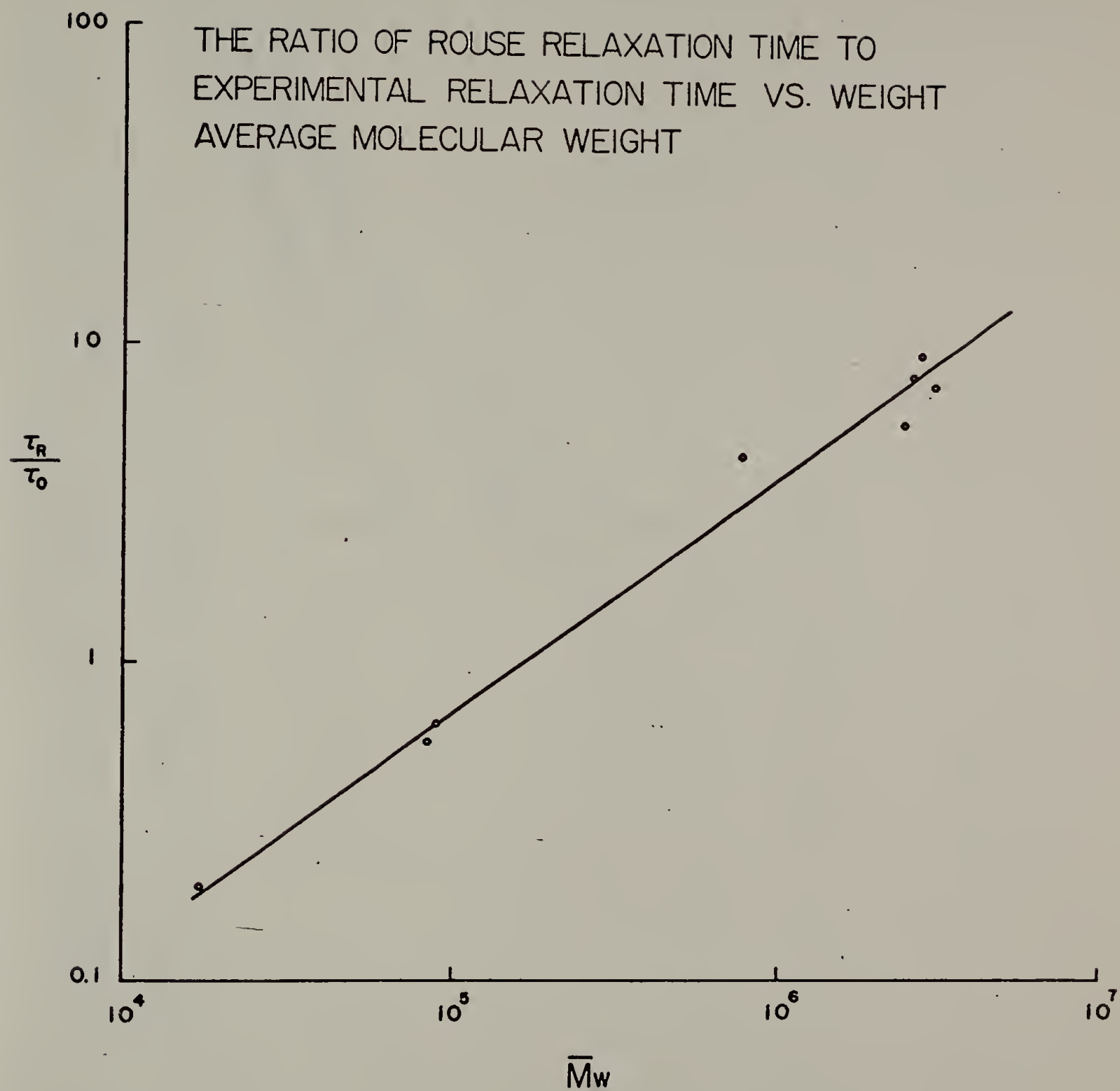


Figure IV-10

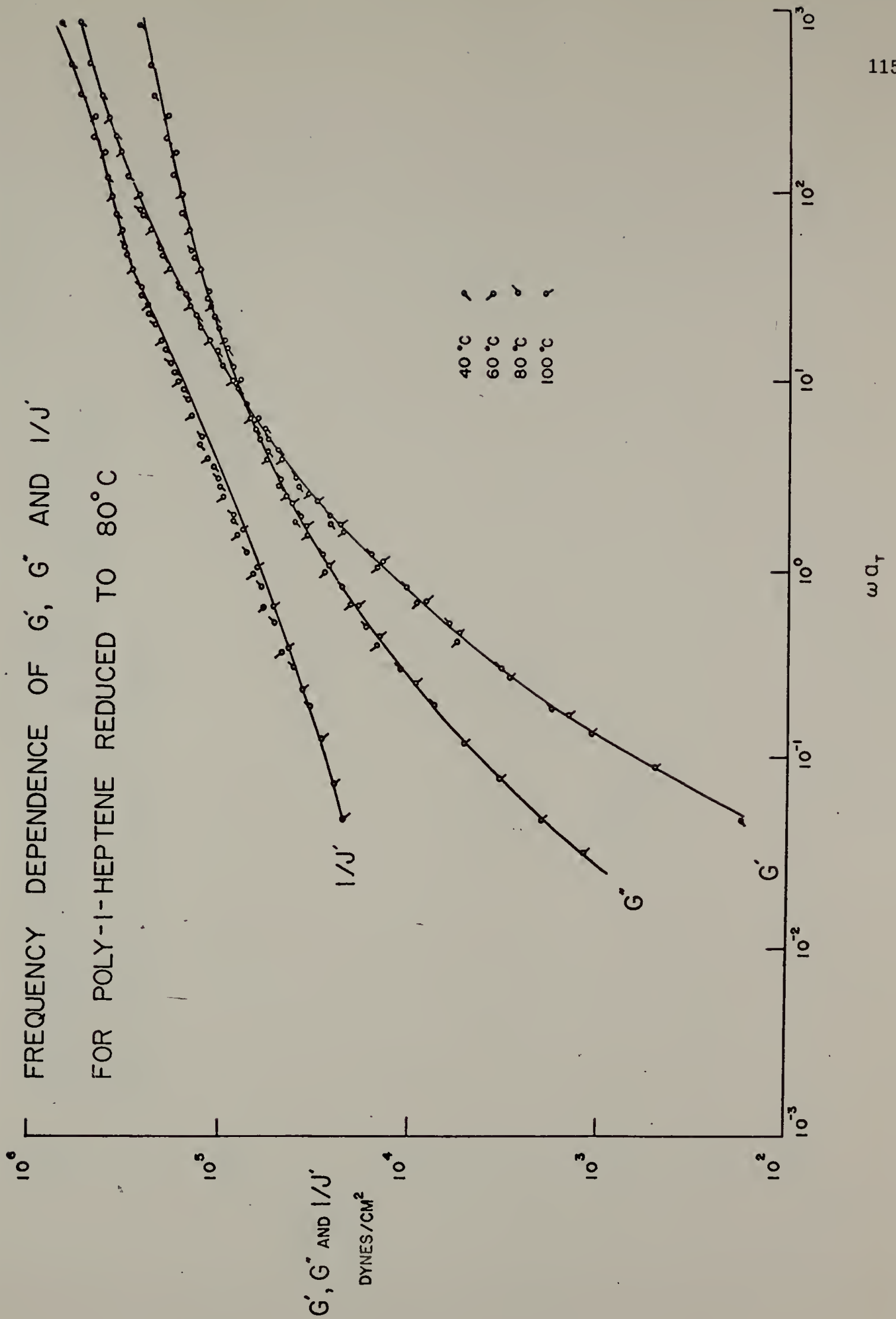


Figure IV-11

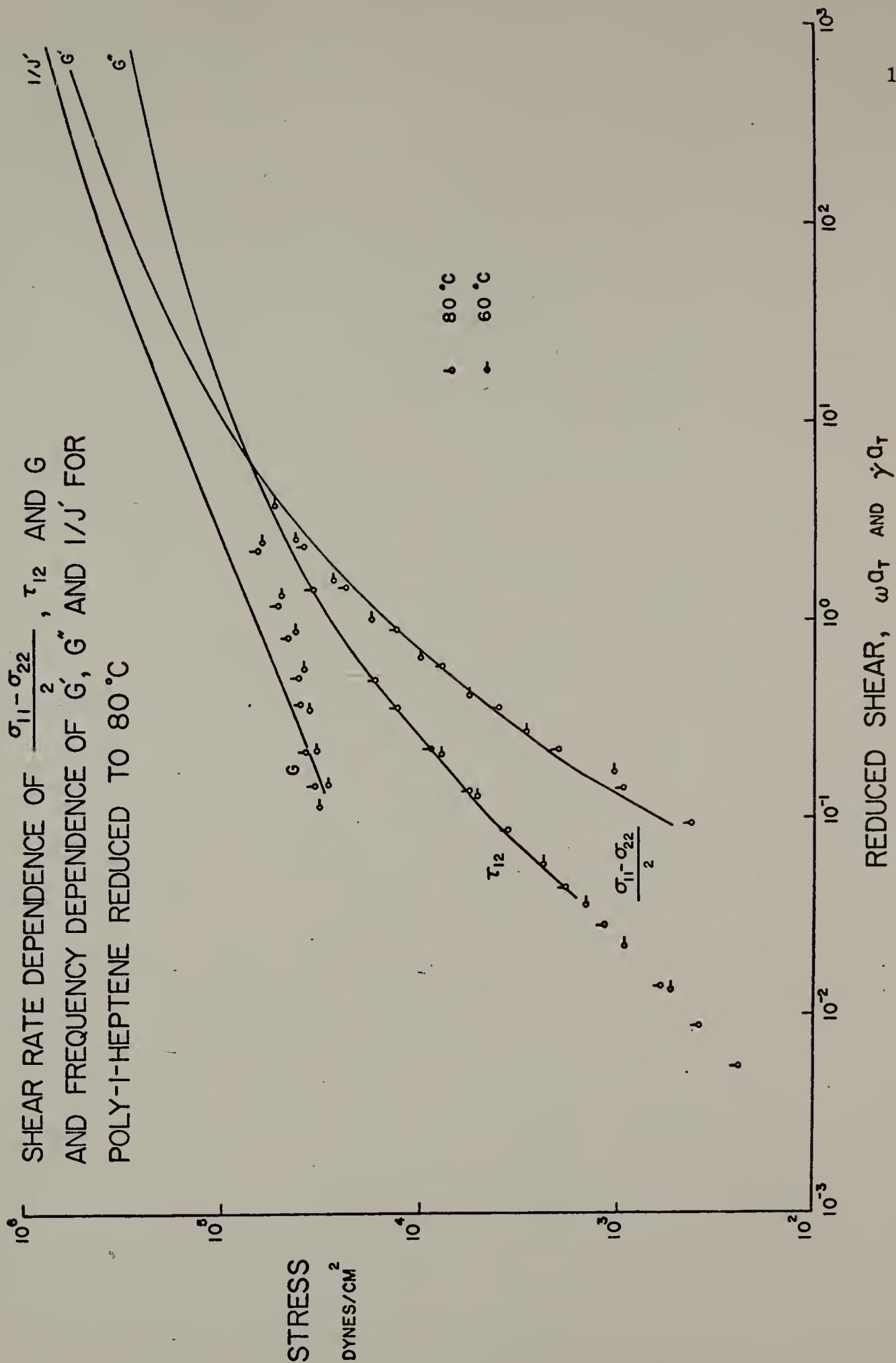


Figure IV-12

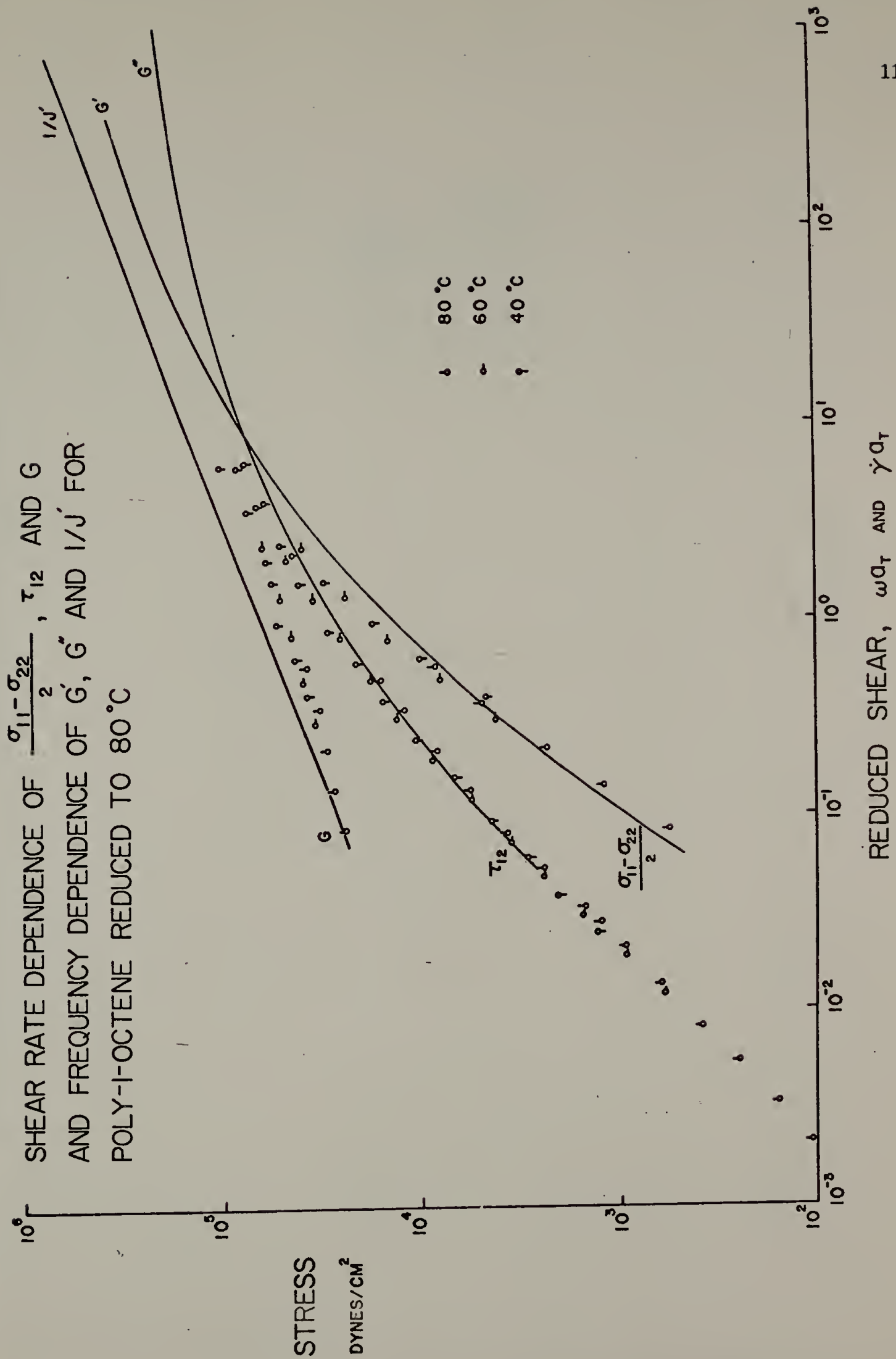


Figure IV-13

THE SHEAR MODULUS G OF POLY-1-OLEFIN VS. SHEAR AT 100 °C

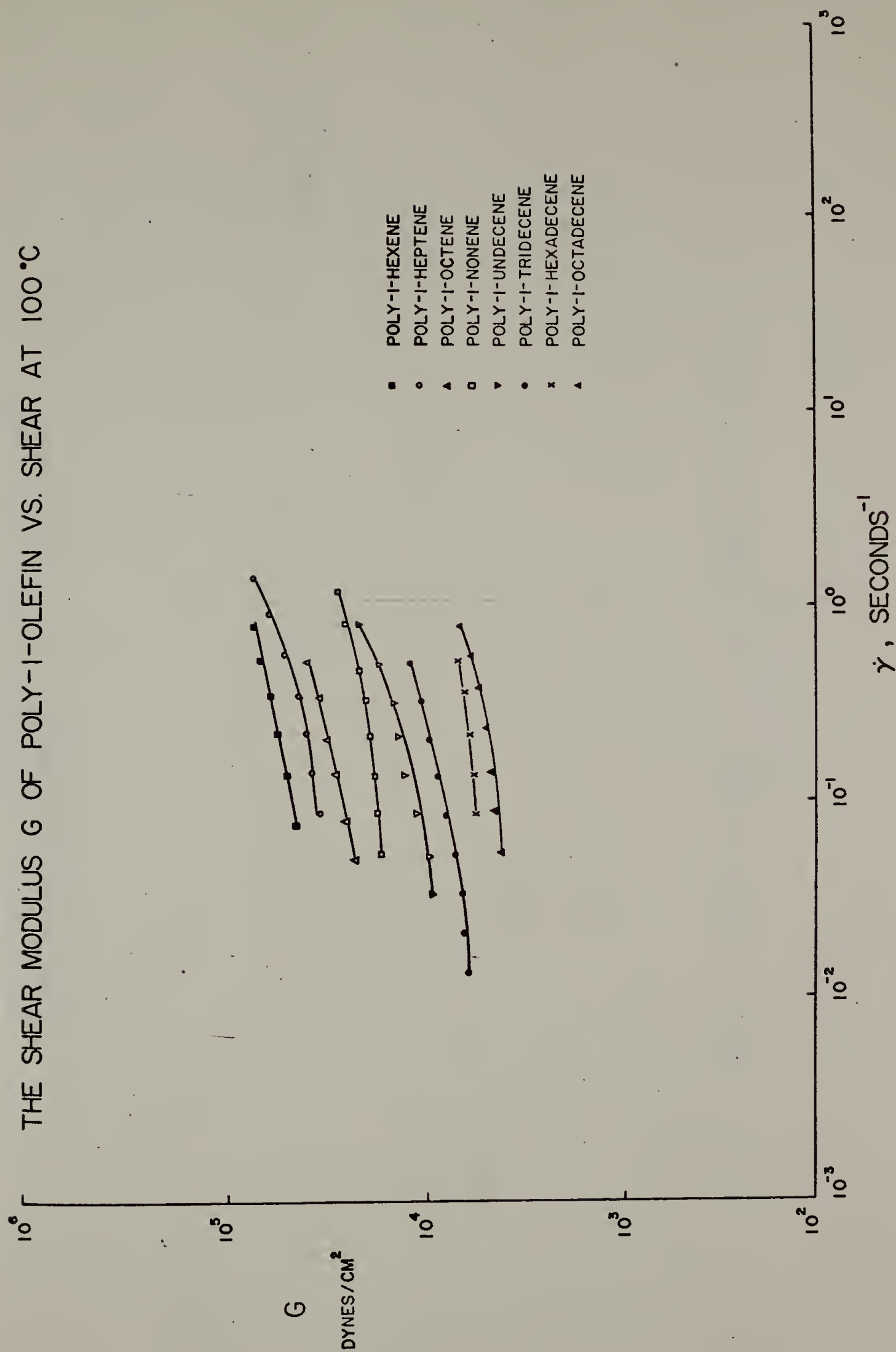


Figure IV-14

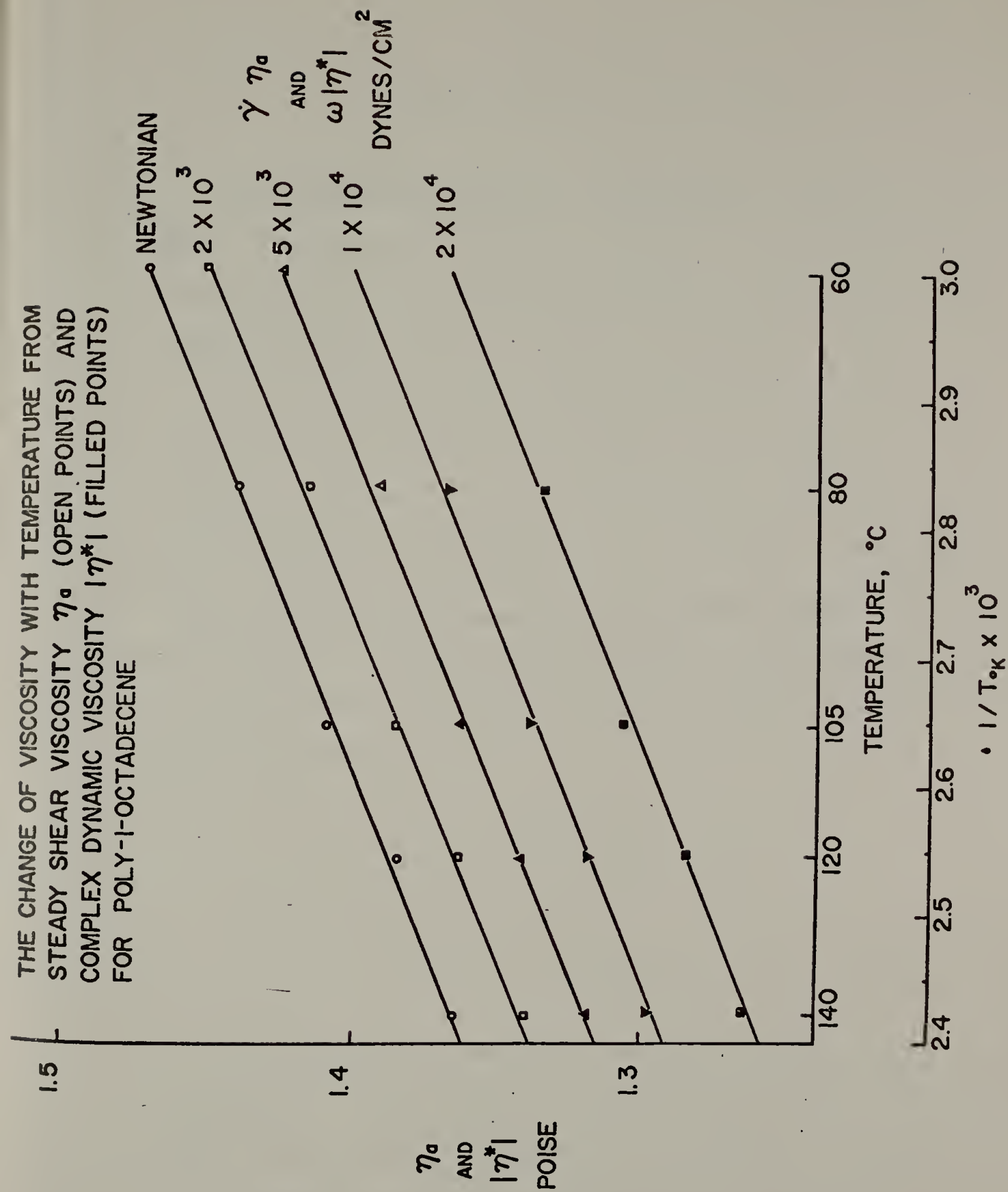


Figure IV-15

CHAPTER V

SUGGESTIONS FOR FUTURE STUDIES

The Temperature Coefficient of Unperturbed Dimension of Poly-1-olefin Series. The temperature coefficient of the mean-square unperturbed end-to-end distance $d \ln \langle r^2 \rangle_0 / dT$ can be determined in several ways: (a) Stress-temperature measurements on elongated amorphous network of the polymer; (b) Intrinsic viscosity-temperature measurements in athermal solvents; (c) Intrinsic viscosity determinations in a series of solvent at their respective theta temperature. Methods (a) and (c), the chains are in their unperturbed configurations and thus it is unnecessary to correct its long-range interactions. However, method (b), the corrections are necessary, and the athermal nature of the solvent facilitates the required correction of chain dimensions to their unperturbed value. The procedures of the correction for the method (b) are shown in the following:

$$[\eta] = \Phi [\langle r^2 \rangle_0 / M]^{3/2} M^{1/2} \alpha^3 = K M^{1/2} \alpha^3 \quad (1)$$

$$\alpha^5 - \alpha^3 = 27 (2\pi)^{-3/2} (V^2 / N_A V_1) [\langle r^2 \rangle_0 / M]^{-3/2} M^{1/2} (1/2 - x_1) \quad (2)$$

α is an expansion factor arising from long-range interactions, V and V_1 are the specific volume of polymer and molar volume of solvent, N_A is the Avogadro number, x_1 is a parameter characterizing the interaction of polymer and solvent.

A change in temperature may affect the intrinsic viscosity through K and α^3 , the change of the latter is likely to be dominated. In a very good solvent, α should decrease with increasing in temperature. In an athermal solvent, it should

be independent of temperature and in poor solvent it should increase with temperature.

Solving Equation (1) for the temperature coefficient of $\langle r_o^2 \rangle$ and using Equation (2) to eliminate the temperature coefficient of α gives:

$$\begin{aligned} d\ln\langle r_o^2 \rangle/dT = (5/3 - 1/\alpha^2) d\ln[\eta]/dT - (1 - 1/\alpha^2) [2\beta_2 - \beta_1 - \\ (1/2 - x_1)^{-1} (dx_1/dT)] \end{aligned} \quad (3)$$

where: $\beta_1 = (1/V_1) (dV_1/dT)$

$\beta_2 = (1/V) (dV/dT)$

are thermal expansion coefficients of solvent and polymer respectively.

If measurement is made in an athermal solvent, α has been equated to zero as a first approximation. So is $\langle r_o^2 \rangle/M$, V , V_1 and β_1 and β_2 are known, the α value can be calculated from Equation (2), then α can be obtained from the intrinsic viscosity measurements at different temperatures by using Equation (3).

The intrinsic viscosities of several poly-1-olefins in anisole solution over the temperature range 70°C to 130°C are shown in Figure 1. Anisole is a poor solvent for poly-1-olefins, it can be expected that the intrinsic viscosity rises rapidly in the vicinity of theta temperature (around 70°C) but at a deaccelerating rate as the temperature departs from theta temperature. It is inappropriate to get $d\ln\langle r_o^2 \rangle/dT$ from these measurements. Since at this poor solvent, x_1 and dx_1/dT cannot be neglected and α also changes with temperature. Therefore, it needs a large correction to get $d\ln\langle r_o^2 \rangle/dT$ from $d\ln[\eta]/dT$ according to Equation (3).

be independent of temperature and in poor solvent it should increase with temperature.

Solving Equation (1) for the temperature coefficient of $\langle r_o^2 \rangle$ and using Equation (2) to eliminate the temperature coefficient of α gives:

$$\begin{aligned} d\ln\langle r_o^2 \rangle/dT = (5/3 - 1/\alpha^2) d\ln[\eta]/dT - (1 - 1/\alpha^2) [2\beta_2 - \beta_1 - \\ (1/2 - x_1)^{-1} (dx_1/dT)] \end{aligned} \quad (3)$$

where: $\beta_1 = (1/V_1) (dV_1/dT)$

$\beta_2 = (1/V) (dV/dT)$

are thermal expansion coefficients of solvent and polymer respectively.

If measurement is made in an athermal solvent, x_1 has been equated to zero as a first approximation. So is $\langle r_o^2 \rangle/M$, V , V_1 and β_1 and β_2 are known, the α value can be calculated from Equation (2), then α can be obtained from the intrinsic viscosity measurements at different temperatures by using Equation (3).

The intrinsic viscosities of several poly-1-olefins in anisole solution over the temperature range 70°C to 130°C are shown in Figure 1. Anisole is a poor solvent for poly-1-olefins, it can be expected that the intrinsic viscosity rises rapidly in the vicinity of theta temperature (around 70°C) but at a deaccelerating rate as the temperature departs from theta temperature. It is inappropriate to get $d\ln\langle r_o^2 \rangle/dT$ from these measurements. Since at this poor solvent, x_1 and dx_1/dT cannot be neglected and α also changes with temperature. Therefore, it needs a large correction to get $d\ln\langle r_o^2 \rangle/dT$ from $d\ln[\eta]/dT$ according to Equation (3).

It is suggested that the intrinsic viscosities of poly-1-olefin series be measured in an athermal solvent, n-hexadecene, at different temperatures. In this solvent, it can be expected that α is independent of temperature and x_1 , dx_1/dT can be neglected. Therefore, $d\ln\langle r_o^2 \rangle/dT$ can be easily to get from $d\ln[\eta]/dT$ by Equations (1), (2) and (3).

The method (c) can be also used to measure $d\ln\langle r_o^2 \rangle/dT$ of poly-1-olefin series. The theta temperature at several different theta solvent needs to be known. We have found that temperature at two theta solvents anisole and cyclohexanone shown in Chapter 1. It is suggested to find other theta solvents and theta temperatures from which one can compare $d\ln\langle r_o^2 \rangle/dT$ of poly-1-olefin series in the same temperature range.

The samples should be fractionated into a narrow molecular weight distribution and be highly tactic polymers. Since several experiments indicate that the isotactic form has larger unperturbed dimension than the corresponding atactic or syndiotactic form.² The experimental difference is about 10-15% and this is consistent with current theories of macromolecular conformations.^{3,4} In the less stereoregular polymers, the temperature coefficient $d\ln\langle r_o^2 \rangle/d\ln T$ may be positive or negative depending upon the chain configuration.⁵ It is the possible reason that the temperature coefficient $d\ln\langle r_o^2 \rangle/d\ln T$ found in literature has different values for the same polymer.

Unit Cell and Heat of Fusion Determinations for the Poly-1-olefin Series.

If a partly crystalline polymer may be regarded as a two-phase mixture of crystalline and amorphous polymer, the computation of the percent crystallinity from density and heat of fusion is straightforward, provided values for the density and the heat of fusion of a 100% crystalline polymer and of 100% amorphous polymer are known.

The density of rapidly quenched sample can potentially provide a value for the density of completely amorphous polymer. When quenching does not entirely prevent crystallization, one can estimate the densities of the completely amorphous polymer by extrapolating densities, measured at a series of temperatures above the melting point, to a temperature below the melting point.

The density of an entirely crystalline polymer can be computed from unit cell dimensions.

The unit cell for lower members of the poly-1-olefin series, e.g., polyethylene, polypropylene and poly-1-butene has been determined by x-ray diffraction. However, for the higher members of the series, the unit cell dimensions have not yet been reported. It is suggested here that x-ray diffraction be used to determine the unit cell dimensions. After the dimension of the unit cell is known, one can calculate the densities of complete crystallines of poly-1-olefins.

The heat of fusion for partially crystalline polymer is a function of percent crystallinity. Therefore, if the percentage is known, the heat of fusion for 100% crystallinity can be obtained from the extrapolation of data on partially crystalline poly-1-olefins. The heat of fusion of partially crystalline poly-1-olefins can be measured from DSC or other available calorimetry.

The heat of fusion per repeating unit of poly-1-olefins can be also estimated from an equation derived by Flory.⁸ The equation relates the depression of the melting point caused by the addition of diluent to the volume fraction of diluent V_ℓ , i.e.:

$$1/T_m - 1/T_m^0 = (R/\Delta H_u) (V_u/V_\ell) (V_\ell - x_1 V_\ell^2)$$

Where ΔH_u is the enthalpy of fusion per repeating unit, V_u/V_ℓ is the ratio of

molar volume of the diluent, and x is an interaction parameter, T_m^0 is the melting point of undiluted polymer.

Once T_m^0 has been determined, the values of ΔH_u and x_1 can be obtained by plotting the quantity $(1/T_m - 1/T_m^0)/V_\ell$ against V_ℓ . According to the equations the intercepts should equal $(R/\Delta H_u)(V_u/V_\ell)$ and x_1 may be computed from the slope.

Determine the E^* of Completely Linear Polyethylene by Viscosity Studies on Hydrogenated Polybutadiene. High density polyethylene produced from the polymerization of ethylene at extremely high pressure or from the polymerization of ethylene with Ziegler-Natta catalysts or with supported metal oxide catalysts reportedly still contains few branches, about one side chain per 200 carbon atoms in the main chain. It is known that the flow activation energy E^* of branched polyethylene is much higher than that of linear one. The E^* of branched polyethylene is as high as 18Kcal/mole comparing to 6-7Kcal/mole for "linear" polyethylene. The E^* of 5.5Kcal/mole is the lowest value which have ever been found for high density polyethylene.⁹

For the completely linear polyethylene without any short or long side-chain, it is possible that the E^* of this linear polyethylene may be lower than 5.5Kcal/mole. The required completely linear polyethylene is possibly obtained from hydrogenating linear polybutadiene. They are available from Phillips Petroleum Company and they are also narrow MW distribution. It is suggested that the E^* of this hydrogenated polybutadiene is measured and compared with the E^* of usual high density polyethylene.

The Effect of Pressure on Flow Activation Energy. According to Equation (12) discussed in Chapter 3, the factors effect on glass transition temperature T_g and volume expansion coefficient above glass transition temperature α_ℓ will also

affect flow activation energy. The pressure can affect T_g and α_ℓ , therefore it is suggested here that the pressure can also affect E^* .

Penwell's Ph.D. thesis at University of Massachusetts shows that T_g of polystyrene changes from 100 to 130°C when the pressure is increased from 300 to 1400 bars. Also, α_ℓ of polystyrene decreases from 4.48 deg⁻¹ to 2.84 deg⁻¹ if the pressure increases from 300 bars to 1400 bars. The data above was used to calculate E^* from Equation (12) in Chapter III. The E^* of polystyrene will increase from 22Kcal/mole to 36Kcal/mole if pressure increases from 300 bars to 1400 bars. However no data has been found to show this prediction.

For branched polyethylenes, it was found that the E^* measured at constant stress decreases with stress and pressure,^{10,11} but the E^* of linear polyethylene is independent of shear stress and pressure. Since the exact value of T_g and α_ℓ are still not available, the E^* of branched polyethylene are thus not yet predicted by the Equation (12) in Chapter III.

It is suggested that viscosities at different temperatures are measured at high pressure. The E^* may be calculated from this high pressure experiments and may be compared with the prediction.

The Blend of Poly-1-olefins. The rheological and physical properties all show marked changes with composition for the poly-1-olefin series. The maximum and minimum value of properties occur in the middle range of composition, i.e., near poly-1-hexene and poly-1-octene. This variation with composition is similar to the mixture of two incompatible component systems with different concentration of components. Therefore, it is interesting to blend two intermediate side-chain length poly-1-olefin, for example, poly-1-butene with poly-1-decene by a 50:50 ratio. We may check whether the blend of C4 polymer (poly-1-butene) with C10 polymer (poly-1-decene) will have the properties of C7 polymer (poly-1-heptene).

Copolymers of Ethylene with other 1-olefins. In general, the copolymer of ethylene with other 1-olefins can be used to study the rheological and physical properties in relation to the side-chain length and structure. The early studies of the effect of side-chain on the properties of branched polymer molecules are mostly based on low density polyethylene, but few systematic studies of the effect of varying the branch length and frequency on the properties of branched polymers have so far been published.

Since the side chain structure of low-density polyethylene is much more complicated, the investigation on various ethylene/-olefin copolymer is believed to be very useful. They may be regarded as "model-polymer" having the definite length of side chain.

Correlation Between Normal Stress Coefficient and Viscosity. The normal stress coefficient is defined as

$$\psi_{12} = (\sigma_{11} - \sigma_{22}) / \dot{\gamma}^2$$

where $(\sigma_{11} - \sigma_{22})$ is normal stress, $\dot{\gamma}$ is shear rate. Many fluids exhibit a quadratic dependence of normal stress on shear rate in the limit of low shear rate. For such fluids ψ_{12} would approach a constant value ψ_{12}^0 characteristic of the fluid.

In accordance with a number of constitutive equations, both continuum and molecular, the normal stress coefficient ψ_{12} should decrease with increasing shear rate. Furthermore, the rate of decrease of ψ_{12} should be about twice as great as the rate of decrease of η with shear rate,¹² i.e., ψ_{12}/ψ_{12}^0 is proportional to $(\eta/\eta_0)^2$.

Our normal stress data from the Weissenberg Rheogoniometer cannot reach a constant value ψ_{12}^0 . Most theoretical analyses agree that the zero shear normal stress coefficient ψ_{12}^0 should be given by $C_2 \eta_0 \lambda$, where λ is the dominant relaxation time of the fluid and C_2 is a constant of order of unity.

Few data are available from which ψ_{12}/ψ_{12}^0 may be calculated as a function of shear rate, and few tests of the above prediction have been found.

It is suggested that more normal stress data are collected and tested with the above prediction. If the relationship $\psi_{12}/\psi_{12}^0 \sim (\eta/\eta_0)^2$ are supported, one can easily predict normal stress coefficient from viscosity measurements.

References

1. P. J. Flory, A Ciferri and R. Chiang, J. Am. Chem. Soc., 83, 1023 (1961).
2. S. Bywater, J. Polymer Sci., Part C, 30, 135 (1970).
3. Birshtein and Ptitsyn, Conformations of Macromolecules, Wiley, New York (1966).
4. Flory: Statistical Mechanics of Chain Molecules, Interscience Publishers, New York (1969).
5. A. Abe, Polymer J., 1, 232 (1970).
6. G. Natta, P. Corradini, Makromol. Chemie, 16, 313 (1955).
7. G. Natta, P. Corradini and I. W. Bassi, Makromol. Chemie, 21, 240 (1956).
8. Flory: Principles of Polymer Chemistry, Cornell University Press (1953).
9. L. Boghetich and R. F. Kratz, presented Soc. Rheology, November 1964.
10. R. S. Porter, J. R. Knox and Julian F. Johnson, Trans. Sci. Rheo., 12:3, 409 (1968).
11. J. Meissner, in Proceedings of the Fourth International Congress on Rheology, Interscience, New York (1965) Part 3, P. 437.
12. S. Middleman, The Flow of High Polymers, Chapter 5, P. 186, Interscience Publishers (1968).

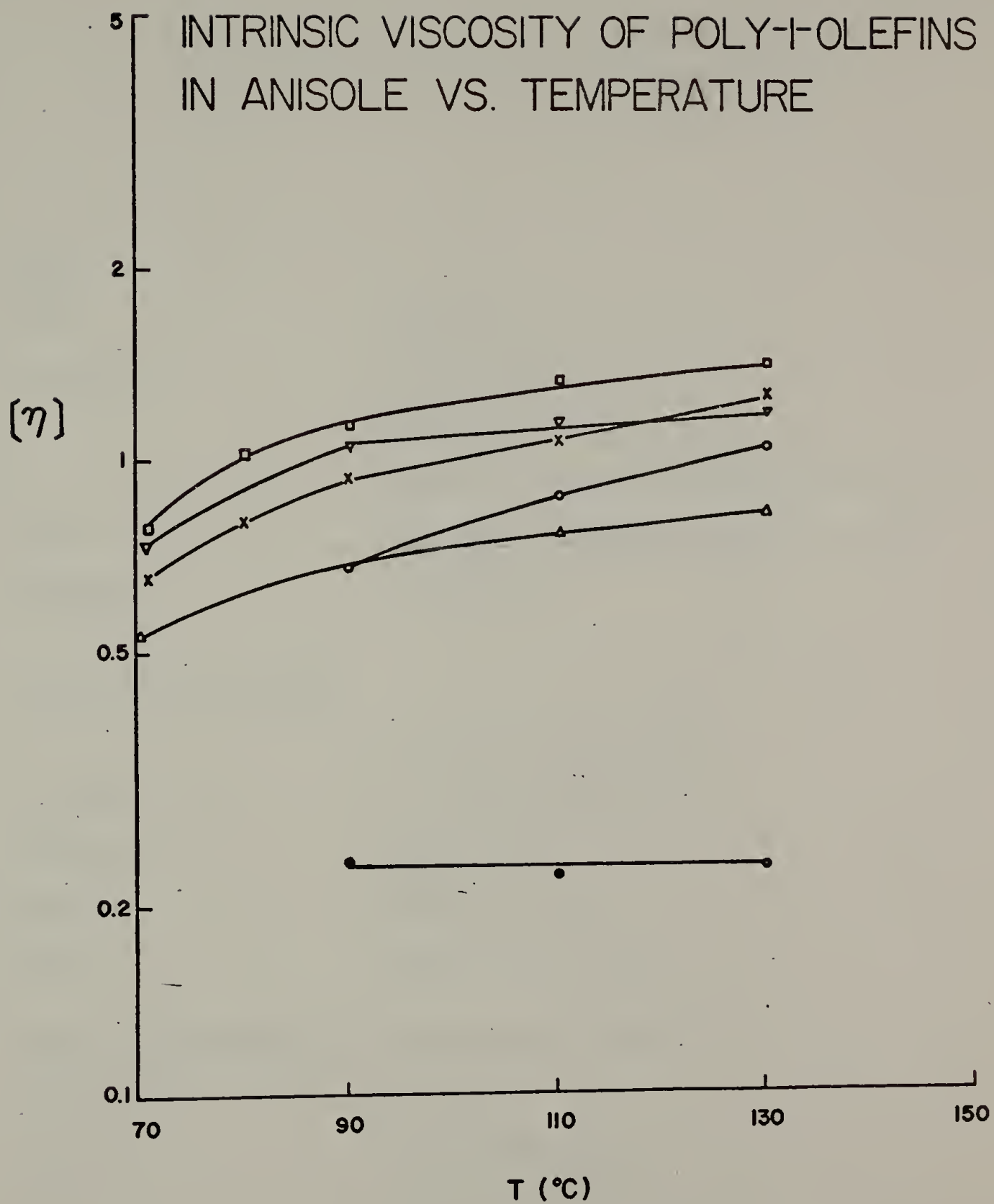


Figure V-1

APPENDIX A

Computer Program to Calculate Viscosity from Instron
Capillary Rheometer and Rabinowitsch Correction

READ

DIAM	Capillary diameter by inches
CLENGTH	Capillary length by inches
T	Measurement temperature
M	Numbers of measurement points for each capillary
FORCE	The force in grams read in Instron recorder
SHERATE	The shear rate

PRINT IN MAIN PROGRAM

T	Measurement temperature
STRESSV	Shear stress (Dynes/cm ²)
SHEARATE	Shear rate (Sec ⁻¹)
ETAV	Viscosity (Poises)
PRESS	Pressure drop (Bars)

PRINT IN SUBPROGRAM (Rabinowitsch Correction)

STRESS	Shear stress
CORATE	Corrected shear rate
VISCO	Corrected viscosity
SLPO	The slop of shear stress vs. shear rate curve.

LIST INSTRON

```

001 PROGRAM ANTONIO
010*THIS PROGRAM CALCULATES THE SHEAR SRESS,VISCOSITY AND
011*PRESSURE IN CAPILLARY FLOW
012*M=NO. OF CAPILLARIES
013*=NO. OF POINTS FOR EACH CAPILLARY
014*T=TEMPERATURE OF MEASUREMENT
020 DIMENSION FORCE(20),SHERATE(20)
021CSTRESSV(20)
040 READ,DIAM,CLENGTH
041 READ,T
042 READ,M
060 DO 130 I=1,M
100 READ,FORCE(I),SHERATE(I)
130 CONTINUE
145 AREA=.713
150 PRINT 160,T
160 FORMAT(* THE FOLLOWING ARE CALCULATED FOR PN AT T=*,F5.1//)
161 PRINT 162,DIAM,CLENGTH
162 FORMAT(* CAPILLARY DIAM. =*,F6.3,* AND THE LENGTH =*
163CF6.3,/)
164 PRINT 166
166 FORMAT(1X,17HSTRESS(DYNES/CM2),2X,10HSHEAR RATE,2X,17HVIS
167CCOSITY(POISES),2X,14HPRESSURE(BARS))
170 DO 310 I=1,M
230 STRESSV(I)=DIAM*981.*FORCE(I)/(4.*AREA*CLENGTH)
240 ETAV=STRESSV(I)/SHERATE(I)
250 PRESS=FORCE(I)/700.
260 PRINT 270,STRESSV(I),SHERATE(I),ETAV,PRESS
270 FORMAT(3X,E12.6,4X,E12.6,3X,E12.6,6X,E12.6)
310 CONTINUE
311 PRINT 312
312 FORMAT(*      *,//)
315 CALL CORRECT(M,STRESSV,SHERATE)
320 END

```

LIST CORRECT

```

010 SUBROUTINE CORRECT(M,STRESS,SHERATE)
020 DIMENSION STRESS(20),SHERATE(20),X(20),Y(20),T(20)
21 DIMENSION CORATE(20),VISCO(20)
070 SY=0.
080 SXY=0.
090 SX2Y=0.
100 SX=0.
110 SX2=0.
120 SX3=0.
130 SX4=0.
135 DO 160 I=1,M
140 Y(I)=0.43429*LOG(STRESS(I))
150 X(I)=0.43429*LOG(SHERATE(I))
160 CONTINUE
170 DO 250 I=1,M
180 SY=SY+Y(I)
190 SXY=SXY+X(I)*Y(I)
200 SX2Y=SX2Y+X(I)**2*Y(I)
210 SX=SX+X(I)
220 SX2=SX2+X(I)**2
230 SX3=SX3+X(I)**3
240 SX4=SX4+X(I)**4
250 CONTINUE
260 B11=M
270 B12=SX
280 B13=SX2
290 B14=SY
300 A12=B12/B11
310 A13=B13/B11
320 A14=B14/B11
330 B22=SX2-B12*A12
340 B23=SX3-B13*A12
350 B24=SXY-B14*A12
360 A23=B23/B22
370 A24=B24/B22
380 B33=SX4-B13*A13-B23*A23
390 B34=SX2Y-B14*A13-B24*A23
400 C2=B34/B33
410 C1=A24-C2*A23
420 C0=A14-C2*A13-C1*A12
422 PRINT 423
423 FORMAT(3X,*SHEAR STRESS*,2X,*RATE(CORRECTED)*,2X,*TRUE
424CAPPR. VISCO*,5X,*SLOP*)
425 DO 470 I=1,M
426 T(I)=C1+2.0*0.43429*C2*LOG(SHERATE(I))
430 CORATE(I)=SHERATE(I)*((3*T(I)+1)/(4*T(I)))
440 VISCO(I)=STRESS(I)/CORATE(I)
450 PRINT 460,STRESS(I),CORATE(I),VISCO(I),T(I)
460 FORMAT(3X,E12.6,4X,E12.6,3X,E12.6,6X,E12.6)
470 CONTINUE
475 RETURN
480 END
490 ENDPROG

```

LIST DATA

010 0.0604 2.00
 020 220.
 030 7
 040 14000. 1.675
 041 20500. 3.35
 042 27500. 6.70
 043 45500. 16.75
 044 67000. 33.501
 045 81000. 67.002
 046 111000. 167.505

RUN INSTRON

8K

THE FOLLOWING ARE CALCULATED FOR PN AT T=220.0

CAPILLARY DIAM. = .060 AND THE LENGTH = 2.000

STRESS(DYNES/CM2)	SHEAR RATE	VISCOSITY(POISES)	PRESSURE(BARS)
.145430E+06	.167500E+01	.868240E+05	.200000E+02
.212951E+06	.335000E+01	.635676E+05	.292857E+02
.285666E+06	.670000E+01	.426368E+05	.392857E+02
.472648E+06	.167500E+02	.282178E+05	.650000E+02
.695987E+06	.335010E+02	.207751E+05	.957143E+02
.841417E+06	.670020E+02	.125581E+05	.115714E+03
.115305E+07	.167505E+03	.688370E+04	.158571E+03

SHEAR STRESS	RATE(CORRECTED)	TRUE APPR. VISCO	SLOP
.145430E+06	.196411E+01	.740438E+05	.591572E+00
.212951E+06	.403149E+01	.528219E+05	.551352E+00
.285666E+06	.830204E+01	.344092E+05	.511132E+00
.472648E+06	.217062E+02	.217747E+05	.457963E+00
.695987E+06	.451747E+02	.154066E+05	.417741E+00
.841417E+06	.946213E+02	.889248E+04	.377521E+00
.115305E+07	.254736E+03	.452646E+04	.324352E+00

TIME: 0.667 SEC.

APPENDIX B

The Calculation of Flow Curve from Graessley Theory

A quantitative theory of non-Newtonian behavior based on entanglement of polymer molecules has been presented by Graessley. According to the theory, there is a dynamic steady state in the formation and disappearance of entanglements in the flow of polymer, and the decrease in viscosity with shear rate is simply a consequence of the net decrease in entangle density induced by flow. With the equations from this theory, a viscosity-shear rate master curve can be calculated for any specific distribution of molecular weights. The calculation of a set of values of η/η_0 vs. $\dot{\gamma}\tau_0/2$ is based on the following equations:

$$\eta/\eta_0 = (A/B) * (C/D) * (E/F) \quad (1)$$

where:

$$A = \int_0^{\infty} n^2 h(\theta) \cdot P(n) dn$$

$$B = \int_0^{\infty} n^2 \cdot P(n) dn$$

$$C = \int_0^{\infty} n P(n) dn$$

$$D = \int_0^{\infty} n g(\theta) P(\eta) dn$$

$$E = \int_0^{\infty} n^{7/2} \cdot g^{5/2}(\theta) P(\eta) dn$$

$$F = \int_0^{\infty} n^{7/2} \cdot p(n) dn$$

Here n is the length of a polymer chain, $P(n)$ is the fraction of chains in the

range n and $n+dn$. The functions $h(\theta)$ and $g(\theta)$ in Equation (1) are given as:

$$g(\theta) = (2/\pi) (\cot^{-1} \theta + \theta / (1 + \theta^2))$$

$$h(\theta) = (2/\pi) (\cot^{-1} \theta + \theta (1 - \theta^2) / (1 + \theta^2))$$

The variable θ is defined by:

$$\theta = (\dot{\gamma} \tau_0 / 2) (\eta / \eta_0) (n / n_w)^2 h(\theta) F(\dot{\gamma})$$

$$\text{where } F(\dot{\gamma}) = \int_0^\infty n^2 h(\theta) P(n) dn / \int_0^\infty n^2 p(n) dn$$

The parameter τ_0 is a characteristic relaxation time, related to the time to form entanglement couples in the undisturbed system, n_w is the weight average number of repeating units per chain.

The flow curves calculated from different molecular weight are illustrated in the Fig. A-1.

Curve 1 is the flow curve of monodisperse system ($\bar{M}_w / \bar{M}_n = 1$) and Curve 2 is the flow curve of most probable distribution of molecular weights ($\bar{M}_w / \bar{M}_n = 2$) with the Schulz-Zimm model distribution. Curve 3, 4, 5 and 6 are calculated directly from GPC molecular weight distribution.

The calculations show that broadening the distribution causes deviations from the zero shear viscosity at lower shear rates and results in a smaller slope over a large portion of the high shear region. Furthermore, calculations have shown that the higher molecular weight averages such as \bar{M}_w and \bar{M}_z are much more important than \bar{M}_n in controlling the shape of the master curve.

The computer program supplied by Professor Graessley is listed below.

COMMENTS ON COMPUTER PROGRAM ETA WWG

READ 1. Reads in the GPC calibration of count number vs. M.

- I: The first count in the calibration.
- J: The last count in the calibration.
- CQ(K): Molecular weight of the polymer emerging as count K.

READ 2. Reads in GPC data obtained on a sample of polymer.

- SAM: Sample identification number.
- M: The first count at which a non-zero reading is obtained for the sample.
- N: The last count at which a non-zero reading is obtained.
- DQ(K): The height of the chromatogram at count K.

PRINT 34.

- SAM Identity of sample.
- PN: Number-average molecular weight according to the GPC.
- PWM: Weight-average molecular weight.
- RR: $\bar{M}_z \bar{M}_{z+1} / \bar{M}_w$ for the sample.

ITEM 1: This instruction is the value of $(\eta/\eta_0) (\dot{\gamma} \tau_0 / 2)$ for the first point on the viscosity curve. The value $A = 0.01$ is small enough for narrow distributions ($M_w/M_n \approx 2$ and smaller) but needs to be smaller for broader distributions ($A = 0.0001$ sufficed to give the curves for some broader molecular weight distributions).

ITEM 2: This instruction controls the spacing of successive points on the viscosity shear-rate curve. For a higher density of points take $A = A*1.3$ or $A = A*1.1$ for example.

ITEM 3: This instruction controls the stopping of calculation. As written the calculation stops when the last value of η/η_0 is less than 0.001. Appropriate alteration as desired should be obvious.

```

PROGRAM FTA WVG
DIMENSION CO(100),C(100),EO(100),R(100),F(500),P(500),GW(100),
1 DW(500),VIS(200),GNUM(200)
1 FORMAT(2I3/(F6.1,10F7.1))
2 FORMAT(F4.1,2I3,14F5.1/16F5.1)
4 FORMAT(1Y,7F17.3)
5 FORMAT(8X,*SHEAR STRESS*,7X,*SHEAR RATE*,8X,*VISCOSITY*,5X,
1 *ENT. DENSITY*,8X,*DIE SWELL*,4X,*CONST. J SWELL*)
6 FORMAT(1H1,10Y,*INTEGRATE*)
34 FORMAT(1H1,40X,F4.1,/,20X,3F20.3,///)
DO 45 IJK=1,5
READ 1,I,J,(CO(K),K=I,J)
36 READ 2,SAM,M,N,(DO(K),K=M,N)
IF (EOF,60) 30,40
40 S=0.0
T=0.0
U=0.0
V=0.0
W=0.0
JJ=40
DO 10 K=M,N
A=CO(K)
P=DO(K)
S=S+B/A
T=T+B
U=U+P*A
V=V+P*A*A
W=W+P*A*A*A
10 CONTINUE
PWM=1/T
PN=T/S
DR=W*T*T/11**3
DO 11 K=M,N
C(K)=CO(K)/PWM
D(K)=DO(K)/T
11 CONTINUE
PRINT 34, SAM,PN,PWM,RP
PRINT 5
CALL VISC(C,D,M,N,F,P,DW,GW)
A=.0001
20 S1=0 & S2=0 & S3=0 & L=1
S4=0.
C6=0. & C6=0.
DO 13 I=1,JJ
X=A*I/JJ
DO 6 K=L,500
IF (X,LE,DW(K)) GO TO 7
6 CONTINUE
PRINT 9
STOP
7 IF (K,EO,1) GO TO 8
RA=(X-DW(K-1))/(DW(K)-DW(K-1))
VEF(K-1)+DAX (F(K)-F(K-1))
G=CW(K-1)+DAX*(GW(K)-GW(K-1))
GO TO 14
8 RA=X/DW(K)
V=1.+(F(K)-1.)*DAX
G=1.+(GW(K)-1.)*DAX
14 VIS(I)=V
GNUM(I)=G

```

Item 1

12 L=V

DO 12 I=1,JJ

S5=S5+Y**5/VIS(I)

S6=S6+Y**2/VIS(I)

DO 12 J=1,I

X=A*I/JJ & Y=A*J/JJ

W=X*Y/VIS(I) & Z=W*Y*Y

S1=S1+W*GNUM(J)

S2=S2+Z*GNUM(I)

S3=S3+W & S4=S4+Z

12 CONTINUE

FS=S2/S1 & FSD=S4/S3 & EST=S5/S6/2.

V=VIS(JJ) & G=GNUM(JJ)

SD=A/V

RD=SD*2.5*3.3000./DPM

R=FS*RD.

RDP=SWFLL(R)

R=FSD*RP

RDP=SWFLL(R)

R=EST*RP

RDT=SWFLL(R)

PRINT 4 ,A,SR,V,G,RP,RDP,RDT

Item 2 A=A*I.5

Item 3 IF (V.GT..001) 20,36

45 CONTINUE

30 STOP

END

SUBROUTINE VISCOS(C,D,M,N,F,R,PW,GW)

DIMENSION C(100),D(100),DG(100),S(100),F(500),R(500),GW(500),

1 PW(500)

G(X)=(ATAN(1./X)+X/(1.+X*X))/1.5707926

H(X)=(ATAN(1./X)+X*(1.-X*X)/(1.+X*X)**2)/1.5707226

GP=.01

DO 13 K=1,500

FA=.0

FR=.0

FC=.0

FD=.0

FE=.0

FF=.0

FG=.0 & FH=.0.

DO 12 I=M,N

A=C(I)

B=D(I)

Z=GP*A*A

T=THETA(Z)

FA=FA+(G(T)*A)**2.5*P

FR=FR+A**2.5*R

FC=FC+G(T)*B

FD=FD+B

FE=FE+H(T)*A*B

FF=FF+A*B

FG=FG+B*G(T)/A

FH=FH+B/A

12 CONTINUE

E(K)=FA*FF*FD/FR/FE/FC

D(K)=GP/F(K)*FF/FF

GW(K)=FC/FH

DW(K)=F(K)*G(K)

GR=GR*1.025

13 CONTINUE

RETURN

END

FUNCTION THETA(Z)

141

H(X)=(ATAN(1./X)+X*(1.-X*X)/(1.+X*X)**2)/1.5707926

DH(X)=8.*X**2/(1.+X*X)**3/1.5707926

IF (Z.LT..1) GO TO 20

IF (Z.GT.1000.) GO TO 21

IF (Z.LT.3.) GO TO 22

T=(Z*16./(3.*3.1415926))**.25

GO TO 33

32 T=.1*(Z/.1)**.8

33 DO 25 J=1,30

TN=T-(T-Z*H(T))/(1.+Z*DH(T))

IF (ABS(T/TN-1.)-.00001) 7,7,8

8 T=TN

25 CONTINUE

STOP

7 T=TN

GO TO 30

20 T=Z

GO TO 30

21 T=(Z*16./(3.*3.1415926))**.25

30 THETA=T

RETURN

END

FUNCTION SWELL(X)

3 FORMAT(1H1,10X,*SWELL*)

IF (X.LT.1.) GO TO 21

T=X**.5

GO TO 22

21 T=1.1

22 DO 24 T=1.25

F=T*T+2./T-3.-X

FD=2.*(T-1./T/T)

TN=T-F/FP

IF (ABS(TN/T-1.).LT..00001) GO TO 23

T=TN

24 CONTINUE

PRINT 3

STOP

23 SWELL=TN**.5

RETURN

END

SCOPF

@L-AD

@RUN,10,1000

1 16

8.50E4 7.00E4 5.65E4 4.50E4 3.60E4 2.77E4 2.13E4 1.57E4 1.13E4 7.50E3 4

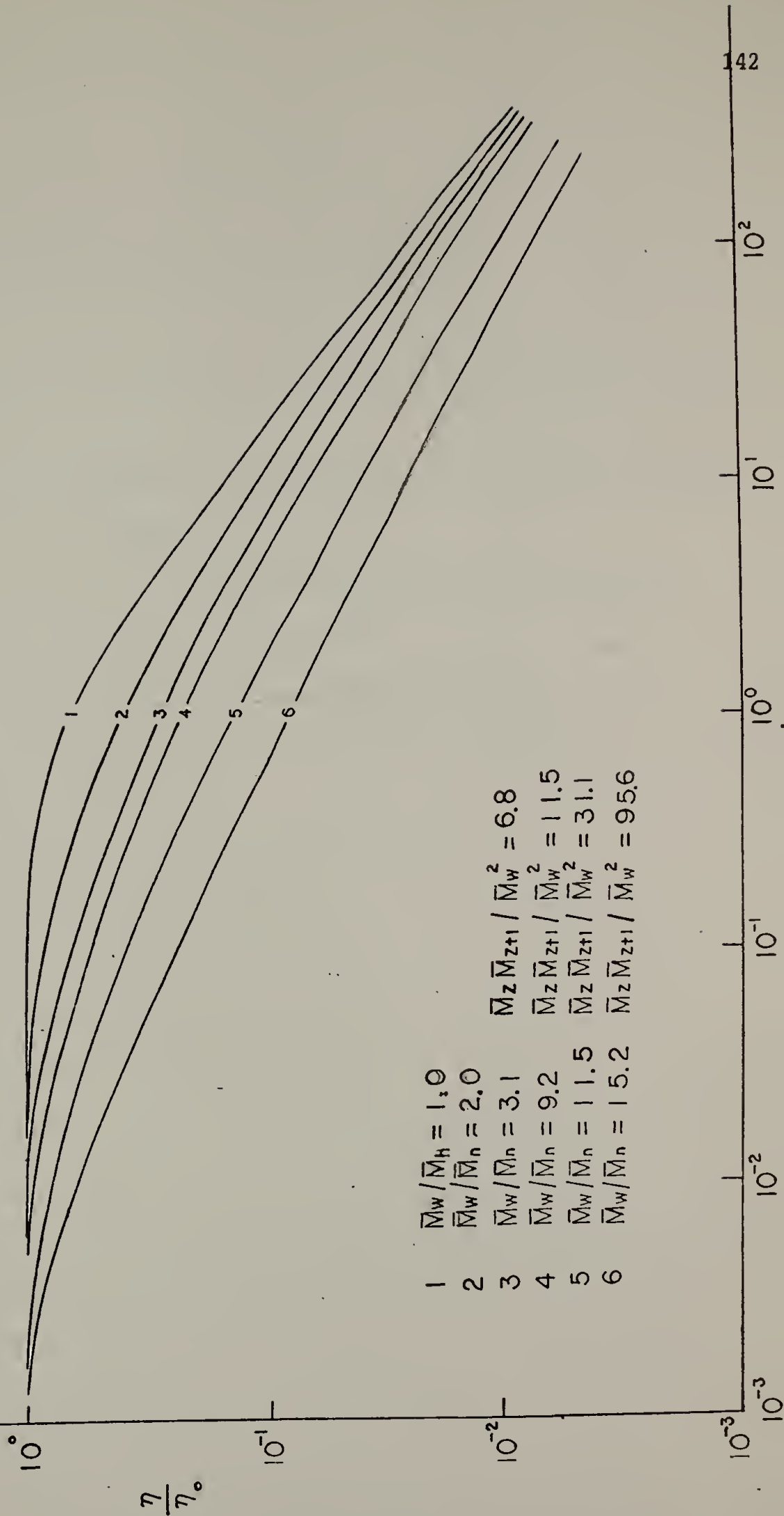
2.95E3 1.70E3 9.20E2 4.90E2 2.43E2

6.00 1 16 5.00 16.0 28.0 41.0 55.0 68.0 77.0 79.0 80.0 78.0 72.0 62.0

32.0 22.0

@@

GRAESSLEY'S FLOW CURVE WITH DIFFERENT MOLECULAR WEIGHT DISTRIBUTION



APPENDIX C

The Tabulated Data of Chapter IV

This Appendix includes the raw data used to plot the figures in Chapter IV.

These data are obtained from the measurements of Weissenbergh Rheogoniometer as described in Chapter IV.

The computer program used was shown in William M. Prest's Ph.D. Thesis (1972) at the University of Massachusetts.

The symbols in this Appendix are described as follows:

EASTAR: Complex dynamic viscosity or steady viscosity.

ETAP: Dynamic viscosity.

GP: Storage modulus or normal stress.

G2P: Loss modulus or shear stress.

SHEAR RATE: Frequency or shear rate

JP: Storage compliance or $(\sigma_{11} - \sigma_{22}) / 2\tau_{12}^2$.

1/JP: Reciprocal of JP or $2\tau_{12}^2 / (\sigma_{11} - \sigma_{22})$.

AMP, PHI 1, PHI 2, THETA, FILT are the data of phase meter used to measure dynamic experiments.

The data of steady state experiments are listed below the data of dynamic experiments. The steady state data start from the row where the column of ETAP becomes blank.

THE WEISSENBERG RHEOGONIOMETER TEST RESULTS

ETASTAR	ETAP	GP	G2P	SHEAR RATE	JP	1/JP	AMP	PHI 1	PHI 2	THETA	FILTER
POLYBUTYLENE T-170 C 12/4/M/											
2.594+005	2.224+005	2.514+004	4.201+004	0.184 0	1.050+005	9.527+004	0.0299	55.41	57.60*	59.07	-0
2.195+005	1.615+005	3.697+004	5.417+004	0.299 0	8.596+006	1.163+005	0.0398	51.54	53.81*	55.69	-0
2.171+005	1.793+005	3.656+004	5.355+004	0.299 0	8.697+006	1.150+005	0.0393	51.50	53.81*	55.67	-0
1.837+005	1.465+005	5.259+004	6.926+004	0.475 0	6.954+006	1.438+005	0.0522	47.84	50.42*	52.80	-0
1.825+005	1.461+005	5.180+004	6.916+004	0.475 0	6.938+006	1.441+005	0.0519	48.05	50.80*	53.18	-0
1.523+005	1.112+005	7.790+004	8.366+004	0.750 0	5.962+006	1.677+005	0.0676	44.21*	46.36 R	47.05	-0
1.513+005	1.112+005	7.697+004	8.343+004	0.750 0	5.973+006	1.674+005	0.0672	44.49*	46.56 R	47.32	-0
1.249+005	8.713+004	1.064+005	1.036+005	1.189 0	4.824+006	2.073+005	0.0865	40.80*	42.47 R	44.25	-0
1.235+005	8.657+004	1.051+005	1.027+005	1.189 0	4.865+006	2.055+005	0.0855	40.93*	42.54 R	44.35	-0
1.014+005	6.646+004	1.444+005	1.253+005	1.885 0	3.951+006	2.531+005	0.1080	36.87*	38.11 R	40.95	-0
1.009+005	6.646+004	1.444+005	1.252+005	1.885 0	3.959+006	2.527+005	0.1081	37.10*	38.13 R	41.18	-0
7.989+004	4.910+004	1.883+005	1.467+005	2.987 0	3.305+006	3.025+005	0.1322	33.26*	33.50 R	37.92	-0
7.917+004	4.613+004	1.871+005	1.447+005	2.987 0	3.345+006	2.990+005	0.1311	33.32*	33.29 R	37.72	-0
6.279+004	3.610+004	2.431+005	1.712+005	4.735 0	2.750+006	3.036+005	0.1597	29.89*	30.29 R	35.16	-0
7.088+004	4.147+004	2.722+005	1.963+005	4.735 0	2.417+006	4.138+005	0.1773	29.86*	30.34 R	35.81	-0
5.325+004	3.160+004	2.027+005	1.499+005	4.735 0	3.189+006	3.136+005	0.1586	31.77*	32.67 R	36.49	-0
5.257+004	3.132+004	1.992+005	1.484+005	4.735 0	3.225+006	3.101+005	0.1370	31.93*	33.07 R	36.62	-0
4.040+004	2.272+004	2.507+005	1.705+005	7.504 0	2.727+006	3.657+005	0.1623	28.99*	29.12 R	34.23	-0
3.013+004	1.593+004	3.032+005	1.895+005	11.893 0	2.368+006	4.222+005	0.1865	26.26*	26.54 R	31.92	-0
3.005+004	1.590+004	3.034+005	1.889+005	11.893 0	2.376+006	4.210+005	0.1860	26.26*	26.54 R	31.91	-0
2.938+004	1.523+004	3.014+005	1.883+005	11.893 0	2.386+006	4.190+005	0.1852	26.37*	26.54 R	32.00	-0
2.981+004	1.577+004	3.009+005	1.876+005	11.893 0	2.393+006	4.178+005	0.1848	26.33*	26.54 R	31.94	-0
2.169+004	1.174+004	3.552+005	2.005+005	18.850 0	2.125+006	4.707+005	0.2075	23.79*	23.78 R	29.69	-0
2.150+004	1.054+004	3.521+005	2.005+005	18.850 0	2.144+006	4.663+005	0.2060	23.81*	23.79 R	29.67	-0
1.580+004	7.423+003	4.167+005	2.248+005	29.875 0	1.870+006	5.347+005	0.2532	21.73*	21.84 R	28.03	-0
1.102+004	5.059+003	4.650+005	2.395+005	47.348 0	1.702+006	5.875+005	0.2546	20.60*	24.35 R	27.32	-0
2.684+004	1.310+004	1.755+006	2.873+005	75.042 0	4.328+007	2.310+006	0.5904	4.17	12.54*	29.36	-0
4.740+004	3.050+004	1.714+005	1.449+005	4.735 0	3.403+006	2.939+005	0.1255	31.44	35.56*	40.21	-0
5.453+004	3.032+004	2.145+005	1.437+005	4.735 0	3.218+006	3.108+005	0.1410	29.32*	29.57 R	33.82	-0
5.268+004	2.891+004	2.085+005	1.369+005	4.735 0	3.352+006	2.984+005	0.1367	28.98*	30.22 R	33.29	-0
6.580+004	3.387+004	1.586+005	1.162+005	2.987 0	4.104+006	2.437+005	0.1108	32.48*	33.85 R	36.23	-0
8.690+004	5.489+004	1.270+005	1.035+005	1.885 0	4.733+006	2.113+005	0.0941	35.77*	37.95 R	39.18	-0
5.108+005	1.000+006	2.319+006	0.000	6.291+014	1.589+013	0.0000	0.0000			35.80	-0
4.907+005	1.000+006	5.403+006	0.011	1.713+014	5.839+013	0.0000	0.0000			72.66	0.656
4.657+005	1.000+006	8.128+006	0.017	7.567+015	1.321+014	0.0000	0.0000			72.43	0.639
4.317+005	1.000+006	1.504+006	0.035	2.212+015	4.521+014	0.0000	0.0000			72.43	0.639
3.831+005	1.000+006	2.114+006	0.052	1.148+015	8.941+014	0.0000	0.0000			72.75	0.643
3.072+005	1.000+006	3.383+006	0.110	4.369+016	2.289+015	0.0000	0.0000			72.45	0.681
2.504+005	1.000+006	4.320+006	0.175	2.619+016	3.819+015	0.0000	0.0000			72.31	0.660
1.821+005	1.000+006	6.343+006	0.348	1.243+016	8.047+015	0.0000	0.0000			72.27	0.664
1.362+005	1.000+006	7.518+006	0.552	8.847+017	1.130+016	0.0000	0.0000			72.25	0.691
2.968+004	1.000+006	1.034+005	3.482	4.679+017	2.137+016	0.0000	0.0000			72.05	0.700
3.930	2.530	1.000	5.320	0.670	47.610	1922.00	1350.00	-0.000		72.24	0.760

THE WEISSENBERG RHEOGONIOMETER TEST RESULTS

ETASTAR	ETAP	GP	G2P	SHEAR RATE	JP	1/JP	AMP	PHI 1	PHI 2	THETA	FILTER
POLYBUTENE T=190° K=1.922+10+3 2/3/71											
1,611+005	1,413+005	1,458+004	2,664+004	0,188 0	1,580+005	6,327+004	0,0187	58,05	60+39*	61,33	-0
1,395+005	1,178+005	2,229+004	3,521+004	0,299 0	1,284+005	7,790+004	0,0255	54,26	56,44*	57,67	-0
1,178+005	9,579+004	3,246+004	4,536+004	0,473 0	1,043+005	9,584+004	0,0339	50,97	52,84*	54,42	-0
9,768+004	7,392+004	4,791+004	5,547+004	0,750 0	8,918+006	1,121+005	0,0442	47,26*	49,34 B	49,19	-0
7,952+004	5,709+004	6,583+004	6,790+004	1,189 0	7,360+006	1,359+005	0,0564	43,58*	45,79 B	45,89	-0
6,448+004	4,393+004	8,895+004	8,281+004	1,885 0	6,022+006	1,661+005	0,0714	40,17*	41,59 B	42,96	-0
6,472+004	4,402+004	8,945+004	8,297+004	1,885 0	6,009+006	1,664+005	0,0717	40,06*	40,06 B	42,86	-0
5,199+004	3,364+004	1,184+005	1,005+005	2,987 0	4,909+006	2,037+005	0,0897	37,00*	37,30 B	40,32	-0
3,994+004	2,408+004	1,509+005	1,140+005	4,735 0	4,218+006	2,371+005	0,1071	33,39*	34,70 B	37,09	-0
4,074+004	2,569+004	1,497+005	1,216+005	4,735 0	4,024+006	2,485+005	0,1093	35,15*	33,90 B	39,10	-0
4,011+004	2,452+004	1,503+005	1,161+005	4,735 0	4,167+006	2,400+005	0,1076	33,92*	35,44 B	37,70	-0
4,031+004	2,459+004	1,512+005	1,164+005	4,735 0	4,152+006	2,409+005	0,1081	33,83*	35,22 B	37,61	-0
3,665+004	2,257+004	1,367+005	1,069+005	4,735 0	4,541+006	2,202+005	0,0991	34,52*	36,70 B	38,02	-0
3,661+004	2,421+004	1,300+005	1,146+005	4,735 0	4,327+006	2,311+005	0,0994	37,65*	35,46 B	41,41	-0
2,696+004	1,627+004	1,613+005	1,221+005	7,504 0	3,942+006	2,537+005	0,1139	33,18*	34,15 B	37,43	-0
2,028+004	1,164+004	1,975+005	1,384+005	11,893 0	3,395+006	2,945+005	0,1332	30,64*	30,63 B	35,02	-0
1,543+004	8,394+003	2,441+005	1,582+005	18,850 0	2,885+006	3,466+005	0,1568	28,07*	28,43 B	32,96	-0
1,118+004	5,743+003	2,864+005	1,716+005	29,875 0	2,570+006	3,892+005	0,1767	25,72*	27,21 B	30,93	-0
7,880+003	3,857+003	3,254+005	1,826+005	47,348 0	2,337+006	4,279+005	0,1959	23,81*	26,39 B	29,31	-0
5,600+003	2,396+003	3,798+005	1,798+005	75,042 0	2,151+006	4,649+005	0,2214	19,90*	20,51 B*	25,34	-0
2,724+005		1,000+006	1,504+003	0,009	2,212+013	4,521+012	0,0000			76,49	65,59
2,685+005		1,000+006	2,349+003	0,009	9,059+014	1,104+013	0,0000				
2,576+005		1,000+006	3,571+003	0,014	3,921+014	2,550+013	0,0000				
2,566+005		1,000+006	5,638+003	0,022	1,573+014	6,358+013	0,0000				
2,429+005		1,000+006	8,457+003	0,032	6,990+015	1,431+014	0,0000				
2,213+005		1,000+006	1,222+004	0,055	3,350+015	2,985+014	0,0000				
1,987+005		1,000+006	1,738+004	0,087	1,654+015	6,045+014	0,0000				
1,762+005		1,000+006	2,443+004	0,139	8,376+016	1,194+015	0,0000				
1,497+005		1,000+006	3,289+004	0,220	4,622+016	2,163+015	0,0000				
1,255+005		1,000+006	4,370+004	0,348	2,619+016	3,819+015	0,0000				
1,003+005		1,000+006	5,544+004	0,552	1,627+016	6,148+015	0,0000				
7,896+004		1,000+006	6,907+004	0,872	1,048+016	9,541+015	0,0000				
3,930	2,500	1,000	5,320	0,400	47,610	1922,00	1330,00	-0,000			

EIASTIC FTAI GP GPP SHEAR RATE JP 1/JP AMP PHI 1 PHI 2 JHEA FILTER

POLYHEXENE T=40 C (AFTER 60 C) K=207.5 6090MI

1.113+005	1.096+005	4.600+003	2.048+004	0.188	0	1.044-005	9.575+004	0.1168	70.81	70.81	77.35	-0	42.23	68.65	0.112	0.658
1.029+005	9.909+004	8.273+003	2.960+004	0.299	0	8.758-006	1.142+005	0.1665	65.17	65.17	74.40	-0	40.33	68.79	0.1751	0.657
9.347+004	8.847+004	1.428+004	4.189+004	0.473	0	7.293-006	1.371+005	0.2295	58.64	58.64	71.18	-0	82.84	68.52	0.1662	0.660
9.365+004	8.862+004	1.433+004	4.196+004	0.473	0	7.289-006	1.372+005	0.2299	58.59	58.59	71.16	-0	85.30	68.79	0.1615	0.657
9.349+004	8.846+004	1.443+004	4.188+004	0.473	0	7.283-006	1.379+005	0.2274	58.76	58.76	71.31	-0	82.81	68.52	0.1729	0.660
8.245+004	7.629+004	2.424+004	5.725+004	0.750	0	6.271-006	1.595+005	0.3014	50.95	50.95	67.07	-0	109.26	68.82	0.1774	0.657
17.404+004	6.597+004	4.021+004	7.834+004	1.189	0	5.186-006	1.928+005	0.3862	42.74	42.74	62.84	-0	138.67	68.17	0.1699	0.663
6.231+004	5.326+004	6.093+004	1.004+005	1.885	0	4.417-006	2.264+005	0.4599	35.61	35.61	58.76	-0	166.51	68.74	0.1681	0.657
5.376+004	4.385+004	9.289+004	1.310+005	2.987	0	3.602-006	2.777+005	0.5405	28.51	28.51	54.67	-0	194.72	68.39	0.1697	0.661
4.586+004	3.510+004	1.398+005	1.662+005	4.735	0	2.964-006	3.374+005	0.6123	22.00	22.00	49.95	-0	218.64	67.86	0.1690	0.666
4.823+004	3.629+004	1.505+005	1.718+005	4.735	0	2.885-006	3.466+005	0.6227	20.86	20.86	48.79	-0	222.00	67.68	0.1680	0.668
3.976+004	2.789+004	2.127+005	2.093+005	7.504	0	2.389-006	4.187+005	0.6800	16.06	16.17	44.55	-0	241.83	67.51	0.1702	0.669
3.161+004	2.091+004	2.831+005	2.475+005	11.893	0	2.002-006	4.994+005	0.7264	12.61	12.61	41.17	-0	256.06	66.93	0.1759	0.675
2.283+004	1.658+004	2.964+005	3.119+005	18.850	0	1.601-006	5.246+005	0.7691	12.58	12.58	46.47	-0	268.10	66.18	0.1847	0.683
2.052+004	1.201+004	4.970+005	3.589+005	29.875	0	1.323-006	7.561+005	0.8197	7.16	7.16	35.84	-0	280.14	64.88	0.1810	0.697
1.525+004	0.243+003	6.076+005	3.903+005	47.348	0	1.165-006	8.583+005	0.8593	5.05	5.05	32.72	-0	308.49	68.16	0.1736	0.663
1.251+004	6.362+003	7.912+005	4.774+005	75.042	0	9.266-007	1.079+006	0.9298	2.40	2.40	31.11	-0	328.25	67.02	0.1692	0.674
1.040+004	6.459+003	6.119+005	4.847+005	75.042	0	1.004-006	9.958+005	0.9236	3.39	3.39	38.39	-0	326.07	67.02	0.1745	0.674
4.270+003	4.093+003	9.132+004	3.072+005	75.042	0	8.892-007	1.125+006	0.9106	12.66	12.66	73.46	-0	322.93	67.35	0.1842	0.671
2.493+003	2.493+003	7.080+003	1.870+005	75.042	0	2.022-007	4.945+006	0.9064	22.92	22.92	87.85	-0	319.85	66.99	0.1924	0.675
1.974+004	1.191+004	4.514+005	3.559+005	29.875	0	1.366-006	7.321+005	0.8134	8.02	8.02	38.26	-0	277.78	64.83	0.1817	0.697
1.967+004	1.135+004	4.799+005	3.445+005	29.875	0	1.375-006	7.272+005	0.8137	7.35	7.35	35.68	-0	278.06	64.87	0.1741	0.697
2.489+004	1.544+004	3.679+005	2.911+005	18.850	0	1.672-006	5.982+005	0.7692	9.85	9.85	38.36	-0	267.43	66.00	0.1727	0.685
2.443+004	1.493+004	3.622+005	2.814+005	18.850	0	1.722-006	5.808+005	0.7641	9.89	9.89	37.85	-0	266.02	66.10	0.1775	0.684
5.663+004	5.498+004	1.708+005	6.539+005	11.893	0	3.740-007	2.674+006	0.9157	13.00	13.00	75.37	-0	322.35	66.85	0.1704	0.676
1.293+005		1.001+006	2.841+002	0.002		6.196-012	1.614+011	0.0000								
1.282+005		1.000+006	4.464+002	0.003		2.509-012	3.965+011	0.0000								
1.268+005		1.000+006	7.000+002	0.006		1.020-012	9.800+011	0.0000								
1.334+005		1.000+006	1.167+003	0.009		3.673-013	2.722+012	0.0000								
1.317+005		1.000+006	1.826+003	0.014		1.499-013	6.669+012	0.0000								
1.339+005		1.000+006	2.942+003	0.022		5.776-014	1.731+013	0.0000								
1.355+005		1.000+006	4.717+003	0.035		2.247-014	4.451+013	0.0000								
1.333+005		1.000+006	7.355+003	0.055		9.242-015	1.082+014	0.0000								
1.334+005		4.769+003	1.167+004	0.087		1.752-005	5.709+004	0.2044								
1.299+005		1.246+004	1.801+004	0.139		1.922-005	5.204+004	0.3461								
1.131+005		1.571+004	2.486+004	0.220		1.272-005	7.863+004	0.3161								
1.020+005		2.439+004	3.551+004	0.348		9.670-006	1.034+005	0.3434								
9.007+004		4.064+004	4.971+004	0.552		8.223-006	1.216+005	0.4088								

3.930 2.500 1.000 5.320 0.400 16.290 207.50 1330.00 -0.000

ETASTAR ETAP GP GZP SHEAR RATE JP 1/JF AMP PHI 1 PHI 2 JHEFA FILTER

POLYMERENE f=60 C K=207.5 6/9/71

2.167+004	2.164+004	2.068+002	4.079+003	0.188 0	1.240-005	8.067+004	0.0234	85.77*	85.77	87.11	-0	8.46	68.48	0.1729	0.660
2.149+004	2.144+004	2.875+002	4.041+003	0.188 0	1.752-005	5.708+004	0.0232	84.62*	84.62	85.95	-0	8.34	68.13	0.1592	0.663
2.167+004	2.163+004	2.613+002	4.077+003	0.188 0	1.565-005	6.389+004	0.0234	85.01*	85.01	86.35	-0	8.46	68.47	0.1642	0.660
2.060+004	2.053+004	5.083+002	6.133+003	0.299 0	1.342-005	7.450+004	0.0353	83.26*	83.26	85.28	-0	12.75	68.66	0.1760	0.658
2.084+004	2.075+004	5.714+002	6.194+003	0.299 0	1.475-005	6.780+004	0.0356	82.71*	82.71	84.75	-0	12.84	68.37	0.1704	0.661
2.007+004	1.992+004	1.141+003	9.432+003	0.473 0	1.264-005	7.911+004	0.0542	80.03*	80.03	83.12	-0	19.53	68.43	0.1695	0.660
1.974+004	1.951+004	2.275+003	1.464+004	0.750 0	1.037-005	9.646+004	0.0838	76.43*	76.43	81.18	-0	30.15	68.51	0.1645	0.662
1.867+004	1.823+004	4.822+003	2.166+004	1.189 0	9.776-006	1.023+005	0.1234	70.56*	70.56	77.48	-0	44.62	68.67	0.1758	0.658
1.758+004	1.691+004	9.004+003	3.188+004	1.885 0	8.203-006	1.219+005	0.1785	64.35*	64.35	74.24	-0	64.37	68.48	0.1704	0.660
1.647+004	1.555+004	1.614+004	4.646+004	2.987 0	6.668-006	1.500+005	0.2516	57.11*	57.11	70.86	-0	90.48	68.27	0.1791	0.662
1.531+004	1.403+004	2.847+004	6.666+004	4.735 0	5.420-006	1.845+005	0.3407	48.62*	47.81	66.88	-0	121.14	67.50	0.1750	0.669
1.524+004	1.403+004	2.812+004	6.644+004	4.735 0	5.403-006	1.851+005	0.3398	48.84*	48.84	67.07	-0	120.36	67.25	0.1754	0.672
1.330+004	1.196+004	4.516+004	8.898+004	7.504 0	4.535-006	2.205+005	0.4235	40.91*	40.91	63.10	-0	150.40	67.41	0.1723	0.670
1.104+004	9.992+003	7.091+004	1.188+005	11.893 0	3.703-006	2.701+005	0.5124	33.08*	33.08	59.19	-0	180.33	66.61	0.1754	0.676
9.8-6+003	7.984+003	1.076+005	1.505+005	18.850 0	3.144-006	3.180+005	0.5891	25.80*	25.80	54.43	-0	205.65	66.27	0.1732	0.682
8.365+003	6.456+003	1.582+005	1.929+005	29.875 0	2.544-006	3.930+005	0.6719	19.29*	19.29	50.53	-0	229.41	64.82	0.1740	0.697
6.549+003	4.749+003	2.132+005	2.258+005	47.348 0	2.211-006	4.524+005	0.7457	13.82*	13.82	46.66	-0	267.30	68.05	0.1727	0.664
4.999+003	3.588+003	2.603+005	2.700+005	75.042 0	1.851-006	5.404+005	0.8627	7.66*	7.66	46.06	-0	305.45	67.13	0.1744	0.673
1.518+004	1.399+004	2.784+004	6.625+004	4.735 0	5.391-006	1.855+005	0.3389	49.01*	49.01	67.22	-0	120.80	67.66	0.1752	0.668
2.481+004		1.000-006	1.370+002	0.006	2.666-011	3.752+010	0.0000								
2.378+004		1.000-006	2.060+002	0.009	1.156-011	8.651+010	0.0000								
2.305+004		1.000-006	3.176+002	0.014	4.896-012	2.043+011	0.0000								
2.262+004		1.000-006	4.971+002	0.022	2.023-012	4.942+011	0.0000								
2.258+004		1.000-006	7.862+002	0.035	8.088-013	1.236+012	0.0000								
2.298+004		1.000-006	1.268+003	0.055	3.109-013	3.216+012	0.0000								
2.262+004		1.000-006	1.978+003	0.087	1.278-013	7.827+012	0.0000								
2.232+004		1.000-006	3.094+003	0.139	5.222-014	1.915+013	0.0000								
2.193+004		1.000-006	4.819+003	0.220	2.153-014	4.644+013	0.0000								
2.185+004		1.000-006	7.609+003	0.348	8.636-015	1.158+014	0.0000								
2.114+004		1.000-006	1.167+004	0.552	3.673-015	2.722+014	0.0000								
1.485+004	1.364+004	2.772+004	6.460+004	4.735 0	5.609-006	1.783+005	0.3326	48.99*	48.99	66.79	-0	119.15	68.02	0.1762	0.664

3.930 2.500 1.000 5.320 0.400 16.290 207.50 1330.00 -0.000

4.530+003	4.200+003	5.067+002	1.255+003	0.299 0	2.767-004	3.614+003	0.0078	67.61*	67.61	* 68.02	-0	2.75	67.18	0.942	-0.073
4.493+003	4.428+003	3.591+002	2.097+003	0.473 0	7.936-005	1.260+004	0.0122	79.61*	79.61	80.30	-0	4.32	67.16	0.837	0.673
4.453+003	4.449+003	1.381+002	2.106+003	0.473 0	3.098-005	3.228+004	0.0121	85.57*	85.57	* 86.27	-0	4.28	67.05	0.789	0.674
4.493+003	4.402+003	1.743+002	3.371+003	0.750 0	1.530-005	6.538+004	0.0194	85.95*	85.95	87.06	-0	6.86	67.23	0.660	0.672
4.700+003	4.641+003	8.824+002	5.520+003	1.189 0	2.824-005	3.541+004	0.0320	79.12*	79.12	* 80.93	-0	11.33	67.32	0.655	0.671
4.588+003	4.566+003	5.385+002	5.430+003	1.189 0	1.809-005	5.529+004	0.0313	82.57*	82.57	84.35	-0	11.13	67.60	0.612	0.668
4.630+003	4.604+003	9.149+002	8.679+003	1.885 0	1.201-005	8.324+004	0.0499	81.16*	81.16	84.00	-0	17.55	66.81	0.774	0.676
4.485+003	4.447+003	1.747+003	1.329+004	2.987 0	9.727-006	1.028+005	0.0761	78.20*	78.20	82.53	-0	26.78	66.79	0.726	0.677
4.447+003	4.359+003	4.166+003	2.064+004	4.735 0	9.396-006	1.064+005	0.1177	71.98*	71.98	78.60	-0	41.21	66.49	0.749	0.680
4.354+003	4.322+003	1.002+003	8.146+003	1.885 0	1.487-005	6.725+004	0.0469	80.34*	80.34	83.01	-0	16.56	67.04	0.620	0.674
4.265+003	4.219+003	1.868+003	1.260+004	2.987 0	1.151-005	8.690+004	0.0723	77.48*	77.48	81.58	-0	25.57	67.09	0.700	0.674
4.153+003	4.100+003	3.128+003	1.941+004	4.735 0	8.091-006	1.236+005	0.1106	74.59*	74.59	80.86	-0	38.83	66.64	0.700	0.678
3.856+003	3.769+003	6.082+003	2.829+004	7.504 0	7.266-006	1.376+005	0.1596	68.90*	68.90	77.88	-0	55.96	66.57	0.693	0.679
3.597+003	3.453+003	1.196+004	4.107+004	11.893 0	6.538-006	1.530+005	0.2274	61.16*	61.16	73.77	-0	79.06	65.99	0.687	0.685
3.340+003	3.140+003	2.148+004	5.918+004	18.850 0	5.420-006	1.845+005	0.3171	52.72*	52.72	70.06	-0	108.76	65.11	0.835	0.694
3.083+003	2.841+003	3.580+004	8.487+004	29.875 0	4.220-006	2.370+005	0.4333	43.61*	43.61	67.14	-0	145.34	63.68	0.748	0.710
2.585+003	2.301+003	5.576+004	1.089+005	47.348 0	3.724-006	2.685+005	0.5533	33.39*	33.39	62.90	-0	195.64	67.12	0.695	0.673
1.244+003	7.476+002	7.460+004	5.610+004	75.042 0	8.563-006	1.168+005	0.5661	17.06*	17.06	8 36.95	-0	196.79	65.99	0.678	0.685
4.024+003	3.967+003	3.205+003	1.878+004	4.735 0	8.828-006	1.133+005	0.1072	74.27*	74.27	80.33	-0	37.68	66.73	0.722	0.677
4.595+003		1.000-006	2.536+001	0.006	7.773-010	1.287+009	0.0000								
5.219+003		1.000-006	4.565+001	0.009	2.399-010	4.168+009	0.0000								
4.756+003		1.000-006	6.594+001	0.014	1.150-010	8.697+009	0.0000								
4.617+003		1.000-006	1.015+002	0.022	4.858-011	2.058+010	0.0000								
4.515+003		1.000-006	1.572+002	0.035	2.022-011	4.946+010	0.0000								
4.411+003		1.000-006	2.435+002	0.055	8.434-012	1.186+011	0.0000								
4.349+003		1.000-006	3.804+002	0.087	3.455-012	2.895+011	0.0000								
4.208+003		1.000-006	5.833+002	0.139	1.469-012	6.806+011	0.0000								
4.271+003		1.000-006	9.384+002	0.220	5.678-013	1.761+012	0.0000								
4.224+003		1.000-006	1.471+003	0.348	2.311-013	4.328+012	0.0000								
4.228+003		1.000-006	2.333+003	0.552	9.183-014	1.089+013	0.0000								
4.233+003		1.000-006	3.703+003	0.875	3.646-014	2.742+013	0.0000								
3.879+003	3.819+003	3.203+003	1.808+004	4.735 0	9.496-006	1.053+005	0.1034	74.13*	74.13	79.97	-0	36.25	66.58	0.750	0.679
3.930	2.500	1.000	5.320	0.400	16.290	207.50	1330.00	-0.000							

THE WEISSENBERG RHEOGONIOMETER TEST RESULTS

ETASTAR	ETAP	GP	G2P	SHFAR RATE	JP	1/JP	AMP	PHI 1	PHI 2	THETA	FILTER
POI THEPTFN T=100 K=207.5 2/17/71											
9,370+003	9,353+003	1,051+002	1,763+003	0,188 0	3,370-005	2,967+004	0,0101	85,89	86,02*	86,60	-0
9,847+003	9,826+003	1,955+002	2,935+003	0,299 0	2,258-005	4,428+004	0,0169	84,38	85,24*	86,21	-0
9,541+003	9,507+003	2,387+002	2,840+003	0,299 0	2,938-005	3,404+004	0,0164	84,20	84,28*	85,21	-0
9,796+003	9,730+003	5,373+002	4,607+003	0,473 0	2,498-005	4,003+004	0,0266	81,40	81,85*	83,36	-0
9,627+003	9,500+003	1,169+003	7,129+003	0,750 0	2,241-005	4,463+004	0,0412	76,80	78,37*	80,70	-0
9,334+003	9,109+003	2,425+003	1,083+004	1,189 0	1,968-005	5,083+004	0,0628	71,72	73,88*	77,40	-0
9,115+003	8,756+003	4,776+003	1,650+004	1,882 0	1,618-005	6,181+004	0,0958	66,31	68,60*	73,88	-0
8,901+003	8,329+003	9,380+003	2,488+004	2,987 0	1,327-005	7,538+004	0,1439	59,27	61,62*	69,36	-0
8,391+003	7,572+003	1,709+004	3,587+004	4,732 0	1,083-005	9,235+004	0,2048	51,90	53,88*	64,53	-0
6,513+003	6,051+003	1,140+004	2,865+004	4,735 0	1,199-005	8,339+004	0,1648	58,32	59,51*	68,31	-0
6,286+003	5,866+003	1,069+004	2,777+004	4,732 0	1,207-005	8,285+004	0,1597	58,50	60,39*	68,96	-0
5,564+003	5,047+003	1,758+004	3,788+004	7,504 0	1,008-005	9,920+004	0,2149	52,18	53,88*	65,12	-0
4,801+003	4,240+003	2,678+004	5,043+004	11,865 0	1,215-006	1,217+005	0,2790	45,58	47,78*	62,04	-0
3,955+003	3,279+003	4,170+004	6,180+004	18,850 0	7,502-006	1,333+005	0,3410	39,58*	41,26	56,00	-0
3,359+003	2,613+003	6,300+004	7,806+004	29,872 0	6,261-006	1,597+005	0,4261	31,74*	34,35	51,10	-0
2,748+003	2,141+003	8,155+004	1,014+005	47,348 0	4,818-006	2,075+005	0,5406	26,28*	29,57	51,19	-0
2,459+003	1,892+003	1,184+005	4,414+005	75,042 0	3,480-006	2,874+005	0,7559	14,64*	16,58	50,07	-0
5,615+003	5,291+003	8,894+003	2,505+005	4,732 0	1,258-005	7,946+004	0,1443	60,64	62,65*	70,47	-0
6,424+003	6,270+003	2,639+003	1,182+004	1,882 0	1,800-005	5,556+004	0,0684	71,14	73,59*	77,43	-0
6,784+003	6,734+003	6,141+002	5,053+003	0,750 0	2,370-005	4,220+004	0,0292	80,36	81,43*	83,09	-0
6,913+003	6,893+003	1,548+002	2,059+003	0,299 0	3,629-005	2,756+004	0,0119	85,03	85,04*	85,72	-0
5,251+003	4,990+003	7,734+003	2,363+004	4,732 0	1,251-005	7,992+004	0,1360	61,98	64,46*	71,89	-0
5,514+003		1,000+006	3,044+001	0,006	5,398+010	1,853+009	0,0000				
6,909+003		1,000+006	7,609+001	0,011	8,636+011	1,158+010	0,0000				
6,975+003		1,000+006	1,217+002	0,017	3,374+011	2,964+010	0,0000				
6,846+003		1,000+006	2,384+002	0,032	8,797+012	1,137+011	0,0000				
6,893+003		1,000+006	3,804+002	0,052	3,455+012	2,895+011	0,0000				
6,785+003		1,000+006	5,935+002	0,087	1,420+012	7,045+011	0,0000				
6,679+003		1,000+006	7,355+002	0,110	9,242+013	1,082+012	0,0000				
6,685+003		1,000+006	1,167+003	0,172	3,673+013	2,722+012	0,0000				
6,510+003		1,000+006	1,801+003	0,277	1,542+013	6,486+012	0,0000				
6,409+003		1,000+006	2,232+003	0,348	1,004+013	9,963+012	0,0000				
6,433+003		7,045+002	3,551+003	0,552	2,794+005	3,580+004	0,0992				
6,118+003		1,463+003	5,352+003	0,872	2,554+005	3,915+004	0,1367				
5,988+003		2,168+003	6,594+003	1,101	2,492+005	4,012+004	0,1643				
5,813+003		4,335+003	1,015+004	1,745	2,106+005	4,748+004	0,2137				
5,501+003		8,399+003	1,522+004	2,766	1,813+005	5,514+004	0,2760				
5,098+003		1,192+004	1,775+004	3,482	1,891+005	5,288+004	0,3357				
3,676+003		1,951+004	2,029+004	5,519	2,369+005	4,221+004	0,4807				
3,930	2,500	1,000	5,320	0,400	16,290	207,50	1330,00	-0,000			

4.172+004	4.055+004	1.847+003	7.644+003	0.188	0	2.987-005	3.348+004	0.0447	70.63	73.94*	76.43	-0	15.81	67.18	0.717	0.673
3.933+004	3.762+004	3.403+003	1.125+004	0.299	0	2.464-005	4.058+004	0.0661	66.31	69.55*	73.18	-0	23.36	67.07	0.646	0.674
3.729+004	3.503+004	6.053+003	1.658+004	0.473	0	1.942-005	5.149+004	0.0977	60.94	64.70*	69.96	-0	34.72	67.48	0.654	0.670
3.364+004	3.072+004	1.023+004	2.302+004	0.750	0	1.605-005	6.230+004	0.1360	55.01	58.97*	66.11	-0	48.20	67.39	0.700	0.671
2.974+004	2.634+004	1.643+004	3.132+004	1.189	0	1.313-005	7.616+004	0.1834	48.95	52.99*	62.34	-0	65.26	67.57	0.695	0.669
2.602+004	2.109+004	2.874+004	3.975+004	1.882	0	1.195-005	8.371+004	0.2376	43.04	46.35*	54.14	-0	84.37	67.43	0.644	0.670
2.240+004	1.740+004	4.256+004	5.200+004	2.987	0	9.426-006	1.061+005	0.3020	37.20*	39.10*	50.71	-0	106.90	67.21	0.635	0.672
1.907+004	1.400+004	6.134+004	6.620+004	4.735	0	7.521-006	1.330+005	0.3700	31.47*	33.51*	47.22	-0	130.38	66.90	0.696	0.676
1.748+004	1.311+004	5.472+004	6.206+004	4.735	0	7.793-006	1.251+005	0.3493	33.40*	35.61*	48.61	-0	122.95	66.74	0.739	0.677
1.458+004	1.030+004	7.696+004	7.774+004	7.504	0	6.431-006	1.553+005	0.4179	28.82*	28.32*	45.30	-0	146.03	66.34	0.579	0.681
1.175+004	7.520+003	1.074+005	8.944+004	11.893	0	5.499-006	1.819+005	0.4771	22.01*	23.48*	39.78	-0	165.12	65.70	0.587	0.688
9.371+003	2.569+003	1.362+005	1.124+005	18.850	0	4.367-006	2.290+005	0.5445	19.26*	18.93*	39.54	-0	186.19	64.91	0.609	0.690
7.174+003	4.229+003	1.733+005	1.263+005	29.875	0	3.769-006	2.654+005	0.6031	15.29*	15.32*	36.10	-0	202.62	63.79	0.670	0.705
5.272+003	2.662+003	2.155+005	1.260+005	47.344	0	3.458-006	2.892+005	0.6673	10.44*	13.16*	30.33	-0	235.46	66.98	0.721	0.675
4.052+003	1.504+003	2.823+005	1.129+005	75.042	0	3.054-006	3.275+005	0.8003	4.51*	9.30*	21.80	-0	278.20	65.99	0.816	0.685
1.665+004	1.252+004	5.206+004	5.941+004	4.735	0	8.344-006	1.198+005	0.3386	34.03*	36.91*	48.78	-0	119.10	66.79	0.762	0.677
4.411+004	1.000-006	1.000-006	2.435+002	0.006		8.434-012	1.186+011	0.0000								
4.465+004	1.000-006	1.000-006	3.906+002	0.009		3.277-012	3.051+011	0.0000								
4.391+004	1.000-006	1.000-006	6.087+002	0.014		1.349-012	7.411+011	0.0000								
4.401+004	1.000-006	1.000-006	1.217+003	0.028		3.374-013	2.964+012	0.0000								
4.281+004	1.000-006	1.877+003	0.044			1.419-013	7.045+012	0.0000								
4.233+004	0.128+002	3.703+003	0.087			2.964-005	3.374+004	0.1098								
4.098+004	1.734+003	5.681+003	0.139			2.550-005	3.723+004	0.1526								
3.925+004	3.793+003	8.623+003	0.220			3.921+004	0.2199									
3.642+004	7.586+003	1.268+004	0.348			2.359-005	4.240+004	0.2991								
3.492+004	1.463+004	1.928+004	0.552			1.769-005	5.079+004	0.3795								
3.189+004	2.655+004	2.790+004	0.875			1.706-005	5.863+004	0.4759								
2.564+004	4.606+004	3.555+004	11.380			1.022-005	15.409+004	0.0478								
3.930	2.500	1.000	5.320	0.400	15.290	207.50	1330.00	-0.000								

THE WISCONSIN RHEOGONIOMETER TEST RESULTS

ETASTAR	ETAP	GP	G2P	SHEAR RATE	JP	1/JP	AMP	PHI 1	PHI 2	THETA	FILTER
POLYHEPTENE T=60°C K=1922 3/3/71											
1,611+005	1,498+005	7,047+003	1,782+004	0,119 0	1,920+005	5,209+004	0,0118	66,33	67,80*	68,43	-0
1,444+005	1,320+005	1,103+004	2,408+004	0,188 0	1,490+005	6,712+004	0,0168	65,21*	64,49	66,09	-0
1,253+005	1,104+005	1,770+004	3,297+004	0,299 0	1,264+005	7,912+004	0,0230	58,48	60,62*	61,78	-0
1,069+005	9,097+004	2,659+004	4,307+004	0,473 0	1,038+005	9,637+004	0,0309	54,45	56,82*	58,32	-0
8,946+004	7,261+004	3,921+004	5,449+004	0,750 0	8,702+006	1,149+005	0,0407	50,54	52,38*	54,27	-0
7,280+004	5,621+004	5,494+004	6,692+004	1,189 0	7,329+006	1,365+005	0,0519	46,46	48,33*	50,63	-0
5,897+004	4,343+004	7,506+004	8,197+004	1,885 0	6,076+006	1,646+005	0,0659	42,63	44,75*	47,53	-0
4,683+004	3,281+004	9,984+004	9,802+004	2,987 0	5,100+006	1,961+005	0,0817	38,54	41,20*	44,48	-0
3,661+004	2,400+004	1,309+005	1,137+005	4,735 0	4,356+006	2,296+005	0,0993	35,20	37,25*	40,98	-0
3,621+004	2,389+004	1,289+005	1,131+005	4,735 0	4,384+006	2,281+005	0,0984	35,40	37,56*	41,28	-0
2,787+004	1,731+004	1,639+005	1,299+005	7,504 0	3,748+006	2,668+005	0,1175	31,99	34,22*	38,41	-0
2,045+004	1,191+004	1,972+005	1,424+005	11,893 0	3,333+006	3,000+005	0,1343	29,22	31,33*	35,84	-0
1,535+004	7,897+003	2,848+005	1,469+005	18,850 0	2,964+006	3,374+005	0,1537	26,37*	28,43*	30,97	-0
1,122+004	5,911+003	2,848+005	1,768+005	29,875 0	2,535+006	3,945+005	0,1775	24,19	26,46*	31,83	-0
7,886+003	3,872+003	3,253+005	1,833+005	47,348 0	2,333+006	4,286+005	0,1960	22,07	23,89*	29,41	-0
5,815+003	2,421+003	3,967+005	1,817+005	75,042 0	2,084+006	4,799+005	0,2278	19,13	19,17*	24,61	-0
1,836+005	1,467+005	5,241+005	6,935+005	4,732 0	6,935+007	1,442+009	0,3873	34,93*	36,96*	52,93	-0
1,822+005	1,546+005	4,764+005	7,177+005	6,431 0	6,431+007	1,555+009	0,3905	35,59	37,36*	56,32	-0
2,128+005		1,000+006	1,175+003	0,000	3,624+013	2,760+012	0,0000				
2,149+005		1,000+006	1,879+003	0,009	1,416+013	7,064+012	0,0000				
2,169+005		1,000+006	3,067+003	0,014	5,529+014	1,808+013	0,0000				
2,138+005		1,000+006	4,699+003	0,022	2,265+014	4,415+013	0,0000				
2,064+005		1,897+003	7,189+003	0,035	1,835+005	5,450+004	0,1319				
1,830+005		5,419+003	1,010+004	0,052	2,655+005	3,766+004	0,2682				
1,746+005		1,002+004	1,527+004	0,087	2,150+005	4,652+004	0,3283				
1,508+005		1,870+004	2,091+004	0,139	2,138+005	4,677+004	0,4471				
1,325+005		3,251+004	2,913+004	0,220	1,916+005	5,220+004	0,5581				
1,079+005		5,148+004	3,759+004	0,348	1,622+005	5,489+004	0,6843				
7,662+004		7,695+004	4,229+004	0,552	2,152+005	4,648+004	0,9098				
5,371+004		1,046+005	4,699+004	0,875	2,369+005	4,222+004	1,1129				
3,930	2,500	1,000	5,320	0,400	47,610	1922,00	1330,00	-0,000			

4.980+005	4.160+005	3.256+004	4.948+004	0.119	0	9.281-006	1.077+005	0.0360	54.93	54.94*	56.66	-0	12.57	66.27	0.771	0.819
4.065+005	3.275+005	4.605+004	6.172+004	0.188	0	7.765-006	1.288+005	0.0464	48.41	51.15*	53.29	-0	16.23	66.35	0.698	0.818
3.311+005	2.525+005	6.397+004	7.545+004	0.299	0	6.538-006	1.530+005	0.0590	44.37	47.14*	49.71	-0	20.61	66.34	0.732	0.818
2.638+005	1.916+005	8.587+004	9.070+004	0.473	0	5.505-006	1.817+005	0.0735	41.15	43.51*	46.57	-0	25.65	66.26	0.758	0.819
2.074+005	1.423+005	1.132+005	1.068+005	0.750	0	4.673-006	2.140+005	0.0901	37.38	39.79*	43.33	-0	31.44	66.25	0.832	0.819
1.571+005	1.006+005	1.435+005	1.197+005	1.189	0	4.111-006	2.433+005	0.1062	34.16	35.93*	39.83	-0	37.42	66.87	0.903	0.812
1.193+005	7.215+004	1.790+005	1.360+005	1.885	0	3.542-006	2.823+005	0.1252	30.95	32.89*	37.23	-0	43.85	66.49	0.910	0.816
8.930+004	5.109+004	2.188+005	1.526+005	2.987	0	3.074-006	3.253+005	0.1453	28.00	30.14*	34.91	-0	50.50	65.99	0.898	0.822
4.575+004	3.518+004	2.630+005	1.666+005	4.735	0	2.714-006	3.685+005	0.1655	25.20	27.27*	32.35	-0	57.21	65.63	0.912	0.827
2.757+004	3.658+004	2.690+005	1.732+005	4.735	0	2.628-006	3.805+005	0.1695	24.90	27.52*	32.78	-0	58.83	65.90	0.887	0.824
4.887+004	2.427+004	3.183+005	1.821+005	7.504	0	2.367-006	4.225+005	0.1893	22.65	24.38*	29.78	-0	65.40	65.57	0.923	0.828
3.522+004	1.681+004	3.681+005	1.999+005	11.893	0	2.098-006	4.767+005	0.2108	20.63	22.74*	28.52	-0	72.28	65.08	0.940	0.834

STAR NEGATIVE

2.253+004	2.253+004	2.686+000	4.246+005	18.850	0	1.490-011	6.711+010	-0.2273	203.50	226.40*	237.44	-0	-76.82	64.16	-0.984	0.846
1.806+004	7.904+003	4.853+005	2.361+005	29.875	0	1.666-006	6.002+005	0.2578	17.07	19.47*	25.95	-0	85.50	62.97	0.936	0.862
1.247+004	4.747+003	5.461+005	2.248+005	47.348	0	1.566-006	6.386+005	0.2774	16.31*	18.87*	22.38	-0	96.52	66.06	0.941	0.822
8.790+003	3.812+003	5.943+005	2.860+005	75.042	0	1.366-006	7.320+005	0.3106	15.46	17.96*	25.70	-0	106.04	64.61	0.950	0.837
6.584+004	3.546+004	2.626+005	1.679+005	4.735	0	2.703-006	3.700+005	0.1657	25.19	27.47*	32.60	-0	57.50	65.86	0.908	0.824
1.069+006		1.000-006	2.349+003	0.002		9.059-014	1.104+013	0.0000								
1.147+006		1.000-006	3.994+003	0.003		3.135-014	3.190+013	0.0000								
9.620+005		1.000-006	5.309+003	0.006		1.774-014	5.638+013	0.0000								
9.829+005		1.000-006	8.598+003	0.009		6.763-015	1.479+014	0.0000								
9.489+005		1.000-006	1.316+004	0.014		2.889-015	3.462+014	0.0000								
8.019+005		1.000-006	1.762+004	0.022		1.611-015	6.209+014	0.0000								
8.019+005		9.754+003	1.762+004	0.022		1.571-005	6.366+004	0.2768								
7.421+005		1.707+004	2.584+004	0.035		1.278-005	7.825+004	0.3303								
4.214+005		3.414+004	3.430+004	0.055		1.451-005	6.892+004	0.4977								
4.834+005		6.936+004	4.229+004	0.087		1.939-005	5.156+004	0.8201								
3.559+005		9.483+004	4.933+004	0.139		1.948-005	5.133+004	0.9611								
2.459+005		1.463+005	5.403+004	0.220		2.506-005	3.991+004	1.3539								

3.930 2.500 1.000 5.320 0.400 47.610 1922.00 1330.00 -0.000

THE WEISSENBERG RHEOGONIOMETER TEST RESULTS

ETASTAR	ETAP	GP	G2P	SHEAR RATE	JP	1/JP	AMP	PH 1	PHI 2	THETA	FILTER
			POLYOCETENE	1540 C	K=1922	5/31/71					
2.579+005	2.210+005	1.583+004	2.628+004	0.119 0	1.682-005	5.947+004	0.0189	58.3	58.03	58.96	-0
2.138+005	1.760+005	2.286+004	3.318+004	0.188 0	1.408-005	7.103+004	0.0247	54.9	54.29	55.45	-0
1.659+005	1.323+005	2.991+004	3.953+004	0.299 0	1.217-005	8.216+004	0.0302	51.2	51.52	52.90	-0
1.678+005	1.321+005	3.064+004	3.969+004	0.299 0	1.219-005	8.205+004	0.0305	50.6	50.96	52.34	-0
1.749+005	1.385+005	3.191+004	4.136+004	0.299 0	1.169-005	8.552+004	0.0318	50.2	50.92	52.36	-0
1.349+005	1.021+005	4.174+004	4.834+004	0.473 0	1.023-005	9.773+004	0.0386	47.2	47.52	49.20	-0
1.075+005	7.687+004	5.644+004	5.769+004	0.750 0	8.666-006	1.154+005	0.0484	43.5	43.65	45.63	-0
8.301+004	5.603+004	7.278+004	6.671+004	1.189 0	7.467-006	1.339+005	0.0586	40.5	40.25	42.51	-0
6.577+004	4.141+004	9.631+004	7.805+004	1.885 0	6.267-006	1.596+005	0.0725	36.1	36.41	39.03	-0
5.201+004	3.064+004	1.256+005	9.154+004	2.987 0	5.200-006	1.923+005	0.0894	33.9	33.09	36.10	-0
3.924+004	2.134+004	1.559+005	1.010+005	4.735 0	4.517-006	2.214+005	0.1050	29.7	29.67	32.94	-0
3.866+004	2.110+004	1.534+005	9.992+004	4.735 0	4.578-006	2.185+005	0.1036	29.5	29.85	33.09	-0
2.880+004	1.459+004	1.864+005	1.095+005	7.504 0	3.990-006	2.507+005	0.1201	26.5	26.95	30.43	-0
2.106+004	9.923+003	2.209+005	1.180+005	11.893 0	3.522-006	2.839+005	0.1366	24.3	24.43	28.12	-0
1.648+004	7.456+003	2.770+005	1.406+005	18.850 0	2.871-006	3.484+005	0.1646	22.4	22.64	26.91	-0
1.084+004	4.723+003	2.916+005	1.411+005	29.875 0	2.779-006	3.599+005	0.1712	21.5	21.55	25.83	-0
8.073+003	3.272+003	3.495+005	1.549+005	47.348 0	2.392-006	4.181+005	0.1984	19.0	19.30	23.91	-0
5.304+003	2.237+003	3.609+005	1.678+005	75.042 0	2.278-006	4.390+005	0.2119	19.2	19.82	24.94	-0
3.862+004	2.098+004	1.535+005	9.936+004	4.735 0	4.591-006	2.178+005	0.1035	29.0	29.70	32.92	-0
5.560+005		1.000-006	1.222+003	0.002	3.350-013	2.985+012	0.0000				
5.397+005		1.000-006	1.879+003	0.003	1.416-013	7.064+012	0.0000				
4.767+005		1.000-006	2.631+003	0.006	7.222-014	1.385+013	0.0000				
4.727+005		1.000-006	4.135+003	0.009	2.925-014	3.419+013	0.0000				
4.609+005		1.000-006	6.390+003	0.014	1.225-014	8.166+013	0.0000				
4.384+005		1.000-006	9.632+003	0.022	5.389-015	1.856+014	0.0000				
3.913+005		8.339+003	1.363+004	0.035	2.262-005	4.421+004	0.3082				
3.405+005		1.788+004	1.879+004	0.055	2.531-005	3.951+004	0.4757				
3.008+005		2.980+004	2.631+004	0.087	2.152-005	4.646+004	0.5664				
2.542+005		5.148+004	3.524+004	0.139	2.073-005	4.824+004	0.7304				
2.031+005		1.000-006	4.464+004	0.220	2.510-016	3.985+015	0.0000				
2.031+005		8.128+004	4.464+004	0.220	2.040-005	4.902+004	0.9105				
1.619+005		1.246+005	5.638+004	0.348	1.960-005	5.101+004	1.1053				
1.192+005		1.626+005	6.578+004	0.552	1.679-005	5.323+004	1.2357				
3.930	2.500	1.000	5.320	0.400	47.610	1922.00	1330.00	-0.000			

THE WEISSENBERG RHEOGONIOMETER TEST RESULTS

ETASTAR	ETAP	GP	G2P	SHEAR RATE	JP	1/JP	AMP	PH 1	PH 2	THETA	FILTER
POLYOCTENE T=60 C K=207.5 5/31/71											
9.292+004	8.457+004	7.258+003	1.594+004	0.188 0	2.366-005	4.227+004	0.0963	60.50	60.50	65.53	-0
9.328+004	8.487+004	7.297+003	1.600+004	0.188 0	2.360-005	4.237+004	0.0966	60.45	60.45	65.49	-0
8.139+004	7.197+004	1.136+004	2.150+004	0.299 0	1.921-005	5.206+004	0.1304	55.55	55.55	62.17	-0
8.172+004	7.186+004	1.162+004	2.147+004	0.299 0	1.949-005	5.132+004	0.1307	55.00	55.00	61.60	-0
7.007+004	5.965+004	1.741+004	2.824+004	0.473 0	1.582-005	6.322+004	0.1715	49.66	49.96	58.36	-0
6.941+004	5.906+004	1.724+004	2.797+004	0.473 0	1.597-005	6.263+004	0.1701	50.44	50.04	58.36	-0
6.677+004	5.563+004	2.772+004	4.174+004	0.750 0	1.104-005	9.059+004	0.2433	44.39	44.73	56.43	-0
4.783+004	3.746+004	5.534+004	4.458+004	1.189 0	1.092-005	9.157+004	0.2659	39.86	39.58	51.60	-0
3.884+004	2.817+004	5.039+004	5.310+004	1.885 0	9.402-006	1.064+005	0.3177	33.96	33.19	46.51	-0
3.150+004	2.151+004	6.877+004	6.425+004	2.987 0	7.764-006	1.288+005	0.3751	28.28	28.22	43.06	-0
2.455+004	1.569+004	8.944+004	7.427+004	4.735 0	6.618-006	1.511+005	0.4254	23.44	23.94	39.71	-0
2.491+004	1.585+004	9.101+004	7.504+004	4.735 0	6.541-006	1.529+005	0.4289	23.86	23.68	39.51	-0
1.930+004	1.136+004	1.171+005	8.522+004	7.504 0	5.583-006	1.791+005	0.4790	19.86	19.68	36.05	-0
1.478+004	8.373+003	1.448+005	9.958+004	11.893 0	4.688-006	2.133+005	0.5299	17.56	17.05	34.52	-0
1.075+004	5.534+003	1.737+005	1.043+005	18.850 0	4.231-006	2.363+005	0.5671	14.26	14.02	30.99	-0
6.033+003	4.079+003	2.067+005	1.219+005	29.875 0	3.590-006	2.786+005	0.6223	12.06	12.10	29.52	-0
5.631+003	2.751+003	2.326+005	1.303+005	47.348 0	3.273-006	3.056+005	0.6808	9.26	9.82	27.26	-0
3.895+003	1.815+003	2.586+005	1.362+005	75.042 0	3.027-006	3.303+005	0.7999	5.96	5.89	27.78	-0
2.458+004	1.555+004	9.016+004	7.361+004	4.735 0	6.656-006	1.503+005	0.4251	23.44	23.64	39.12	-0
1.501+005		1.000-006	3.297+002	0.002	4.599-012	2.174+011	0.0000				
1.427+005		1.000-006	4.971+002	0.003	2.023-012	4.942+011	0.0000				
1.406+005		1.000-006	7.761+002	0.006	8.301-013	1.205+012	0.0000				
1.421+005		1.000-006	1.243+003	0.009	3.237-013	3.089+012	0.0000				
1.390+005		1.000-006	1.928+003	0.014	1.346-013	7.431+012	0.0000				
1.339+005		1.000-006	2.942+003	0.022	5.776-014	1.731+013	0.0000				
1.282+005		1.000-006	4.464+003	0.035	2.509-014	3.985+013	0.0000				
1.268+005		1.000-006	7.000+003	0.055	1.020-014	9.800+013	0.0000				
1.177+005		1.000-006	1.030+004	0.087	4.715-015	2.121+014	0.0000				
1.177+005		6.774+003	1.030+004	0.087	3.194-005	3.131+004	0.3289				
1.061+005		1.355+004	1.471+004	0.139	3.130-005	3.195+004	0.4605				
9.234+004		2.276+004	2.029+004	0.220	2.764-005	3.618+004	0.5608				
8.011+004		3.793+004	2.790+004	0.348	2.437-005	4.104+004	0.6798				
6.617+004		5.961+004	3.652+004	0.552	2.234-005	4.476+004	0.8160				
2.057+004	1.317+004	7.483+004	6.234+004	4.735 0	7.889-006	1.268+005	0.3803	25.26	25.72	39.80	-0
3.930	2.500	1.000	5.320	0.400	16.290	207.50	1330.00	-0.000			

15

THE WEISSENBERG RHEOGONIOMETER TEST-RESULTS

ETASTAR	ETAP	GP	G2P	SHEAR RATE	JP	1/JP	AMP	PHI 1	PHI 2	THETA	FILTER
POLYOCTENE T=80 C K=207.5 5/24/71											
4.586+004	4.515+004	6.042+002	3.388+003	0.075 0	5.101+005	1.960+004	0.0197	78.79	78.79	79.90	=0
4.567+004	4.472+004	1.102+003	5.319+003	0.119 0	3.736+005	2.676+004	0.0310	76.56	76.56	78.31	=0
4.477+004	4.386+004	1.069+003	5.216+003	0.119 0	3.772+005	2.651+004	0.0304	76.72	76.72	78.43	=0
4.264+004	4.121+004	2.066+003	7.767+003	0.188 0	3.198+005	3.127+004	0.0456	72.59	72.59	75.12	=0
4.348+004	4.222+004	1.954+003	7.959+003	0.188 0	2.909+005	3.438+004	0.0465	73.63	73.63	76.22	=0
3.601+004	3.341+004	6.362+003	1.582+004	0.473 0	2.189+005	4.568+004	0.0942	63.09	63.09	68.10	=0
3.964+004	3.765+004	3.711+003	1.125+004	0.299 0	2.646+005	3.779+004	0.0665	68.13	68.13	71.75	=0
3.641+004	3.391+004	6.280+003	1.605+004	0.473 0	2.113+005	4.732+004	0.0953	63.56	63.55	68.65	=0
3.208+004	2.907+004	1.020+004	2.181+004	0.750 0	1.759+005	5.685+004	0.1299	58.20	58.20	64.96	=0
2.811+004	2.467+004	1.603+004	2.934+004	1.189 0	1.434+005	6.973+004	0.1739	52.58	52.58	61.36	=0
2.398+004	2.029+004	2.406+004	3.825+004	1.885 0	1.178+005	8.488+004	0.2242	46.90	46.90	57.84	=0
2.016+004	1.630+004	3.543+004	4.870+004	2.987 0	9.768+006	1.024+005	0.2804	40.87	40.87	49.32	=0
1.671+004	1.267+004	5.159+004	6.000+004	4.735 0	8.239+006	1.214+005	0.3396	34.40	34.40	49.32	=0
1.610+004	1.249+004	4.810+004	5.915+004	4.735 0	7.085+006	1.412+005	0.3892	29.99	29.99	46.34	=0
1.299+004	9.395+003	6.730+004	7.050+004	7.504 0	5.949+006	1.681+005	0.4453	25.88	25.88	43.84	=0
1.020+004	7.041+003	8.748+004	8.398+004	11.893 0	5.987+006	1.670+005	0.4493	24.38	24.38	41.80	=0
1.047+004	6.976+003	9.284+004	8.299+004	11.893 0	4.991+006	2.004+005	0.5097	20.44	20.44	39.26	=0
8.232+003	5.209+003	1.202+005	9.818+004	18.850 0	4.240+006	2.358+005	0.5761	15.24	15.24	34.06	=0
6.540+003	3.663+003	1.619+005	1.094+005	29.875 0	3.840+006	2.604+005	0.6357	14.22	14.22	36.36	=0
4.430+003	2.626+003	1.689+005	1.243+005	47.348 0	3.624+006	2.760+005	0.7677	7.49	7.49	30.20	=0
3.178+003	1.599+003	2.061+005	1.200+005	75.042 0	8.591+006	1.164+005	0.3231	36.42	36.42	50.95	=0
1.549+004	1.203+004	4.622+004	5.695+004	4.735 0	1.150+010	8.697+009	0.0000				
4.756+004		1.000+006	6.594+001	0.001	4.858+011	2.058+010	0.0000				
4.617+004		1.000+006	1.015+002	0.002	1.898+011	5.270+010	0.0000				
4.661+004		1.000+006	1.623+002	0.003	7.773+012	1.287+011	0.0000				
4.595+004		1.000+006	2.536+002	0.006	8.434+012	1.186+011	0.0000				
4.411+004		1.000+006	2.435+002	0.006	3.194+012	3.131+011	0.0000				
4.523+004		1.000+006	3.957+002	0.009	1.284+012	7.786+011	0.0000				
4.500+004		1.000+006	6.239+002	0.014	5.383+013	1.858+012	0.0000				
4.386+004		1.000+006	9.638+002	0.022	3.109+013	3.216+012	0.0000				
4.584+004		1.000+006	1.268+003	0.028	2.159+013	4.632+012	0.0000				
4.370+004		1.000+006	1.522+003	0.035	8.797+014	1.137+013	0.0000				
4.320+004		1.000+006	2.384+003	0.055	4.062+005	2.462+004	0.1484				
4.175+004		1.084+003	3.652+003	0.087	3.481+005	2.873+004	0.1942				
4.025+004		2.168+003	5.580+003	0.139	3.410+005	2.932+004	0.2803				
3.740+004		4.606+003	8.218+003	0.220	3.071+005	3.256+004	0.3739				
3.496+004		9.104+003	1.217+004	0.348	2.665+005	3.753+004	0.4731				
3.217+004		1.680+004	1.775+004	0.552	8.926+006	1.120+005	0.3111	37.55	37.55	51.67	=0
1.468+004	1.153+004	4.311+004	5.451+004	4.735 0							
3.930	2.500	1.000	5.320	0.400	16.290	207.50	1330.00	-0.000			

THE WEISSENBERG RHEOGONIOMETER TEST RESULTS

ETASTAR	ETAP	GP	G2P	SHEAR RATE	JP	1/JP	AMP	PHI 1	PHI 2	THETA	FILTER
POLYOCTENE T=100°C (AFTER 80) 5/24/71											
1.114+004	1.107+004	2.483+002	2.086+003	0.188 0	5.626+005	1.777+004	0.0121	82.54*	82.54	83.23	-0
1.083+004	1.078+004	2.012+002	2.032+003	0.188 0	4.825+005	2.073+004	0.0117	83.69*	83.69	84.36	-0
1.101+004	1.083+004	9.409+002	5.129+003	0.473 0	3.460+005	2.890+004	0.0298	77.94*	77.94	79.62	-0
1.085+004	1.067+004	9.159+002	5.053+003	0.473 0	3.472+005	2.880+004	0.0294	78.09*	73.20	79.74	-0
1.103+004	1.093+004	4.414+002	3.265+003	0.299 0	4.067+005	2.459+004	0.0189	81.24*	81.24	82.32	-0
1.079+004	1.048+004	1.945+003	7.863+003	0.750 0	2.965+005	3.373+004	0.0460	73.56*	73.56	76.12	-0
1.021+004	9.752+003	3.590+003	1.160+004	1.189 0	2.435+005	4.107+004	0.0683	69.08*	69.08	72.82	-0
9.632+003	9.046+003	6.235+003	1.705+004	1.885 0	1.891+005	5.287+004	0.1004	64.52*	64.52	69.93	-0
8.800+003	7.984+003	1.105+004	2.385+004	2.987 0	1.599+005	6.253+004	0.1411	57.80*	57.80	65.15	-0
8.029+003	7.070+003	1.802+004	3.347+004	4.735 0	1.247+005	8.021+004	0.1955	51.81*	51.81	61.72	-0
6.800+003	6.127+003	1.396+004	2.901+004	4.735 0	1.347+005	7.423+004	0.1697	55.51*	55.51	64.31	-0
5.682+003	4.905+003	2.153+004	3.681+004	7.504 0	4.184+005	8.144+004	0.2454	48.97*	48.97	59.88	-0
4.777+003	3.983+003	4.137+004	4.737+004	11.893 0	9.717+006	1.029+005	0.2726	43.36*	43.36	56.50	-0
4.024+003	3.193+003	4.485+004	6.018+004	18.850 0	8.025+006	1.246+005	0.3409	36.82*	36.82	52.51	-0
3.313+003	2.502+003	6.485+004	7.475+004	29.875 0	6.622+006	1.510+005	0.4191	30.61*	30.61	49.07	-0
2.545+003	1.874+003	8.153+004	8.872+004	47.348 0	5.616+006	1.781+005	0.5115	25.30*	25.30	47.43	-0
1.083+003	5.035+002	7.197+004	3.778+004	75.042 0	1.089+005	9.180+004	0.5177	13.78*	13.78	27.70	-0
6.467+003	5.856+003	1.300+004	2.773+004	4.735 0	1.386+005	7.214+004	0.1624	56.44*	56.44	64.90	-0
6.396+003	5.734+003	1.342+004	2.715+004	4.735 0	1.463+005	6.836+004	0.1603	55.45*	55.45	63.71	-0
1.103+004		1.000+006	6.087+001	0.006	1.349+010	7.411+009	0.0000				
1.044+004		1.000+006	9.131+001	0.009	5.997+011	1.667+010	0.0000				
1.061+004		1.000+006	1.471+002	0.014	2.311+011	4.328+010	0.0000				
1.016+004		1.000+006	2.232+002	0.022	1.004+011	9.963+010	0.0000				
1.049+004		1.000+006	3.652+002	0.035	3.748+012	2.668+011	0.0000				
1.011+004		1.000+006	5.580+002	0.055	1.606+012	6.227+011	0.0000				
1.003+004		1.000+006	8.776+002	0.087	6.493+013	1.540+012	0.0000				
9.879+003		1.000+006	1.370+003	0.139	2.666+013	3.752+012	0.0000				
9.696+003		1.000+006	2.130+003	0.220	1.102+013	9.078+012	0.0000				
9.614+003		1.000+006	3.348+003	0.348	4.461+014	2.242+013	0.0000				
9.191+003		1.000+006	5.073+003	0.552	1.943+014	5.146+013	0.0000				
8.988+003		1.000+006	7.862+003	0.875	8.088+015	1.236+014	0.0000				
8.415+003		1.000+006	1.167+004	1.386	3.673+015	2.722+014	0.0000				

5.930 2.500 1.000 5.320 0.400 16.290 207.50 1330.00 -0.000

ETASTAR ETAP GP G2P SHEAR RATE JP 1/JP AMP PHI 1 PHI 2 THETA FILTER

POLYCNONE

T=82°C

K=82°C

3/5/71

1.916+005	1.532+005	2.170+004	2.888+004	0.188	0	1.663-005	6.013+004	0.0221	52.07*	43.65	53.09	-0	7.86	67.43	0.769	0.805
1.511+005	1.007+005	3.366+004	3.010+004	0.249	0	1.651-005	6.057+004	0.0274	38.40	40.76*	41.81	-0	9.72	67.24	0.800	0.807
1.150+005	7.243+004	4.227+004	3.430+004	0.473	0	1.427-005	7.009+004	0.0329	35.77	37.87*	39.06	-0	11.70	67.49	0.828	0.804
1.752+004	5.222+004	5.270+004	3.919+004	0.750	0	1.222-005	8.184+004	0.0395	33.18	35.29*	36.64	-0	13.98	67.27	0.882	0.807
6.537+004	3.707+004	6.403+004	4.409+004	1.189	0	1.059-005	9.439+004	0.0464	30.90	33.05*	34.55	-0	16.43	67.24	0.919	0.807
4.838+004	2.618+004	7.669+004	4.935+004	1.885	0	9.221-006	1.084+005	0.0540	29.01	31.09*	32.77	-0	19.11	67.19	0.888	0.808
3.551+004	1.809+004	9.130+004	5.404+004	2.987	0	8.111-006	1.233+005	0.0623	26.76	28.81*	30.63	-0	22.04	67.18	0.907	0.808
2.608+004	1.271+004	1.078+005	6.020+004	4.735	0	7.071-006	1.414+005	0.0718	24.91	27.18*	29.19	-0	25.23	66.72	0.900	0.813
2.611+004	1.208+004	1.076+005	6.097+004	4.735	0	7.036-006	1.421+005	0.0719	25.07	27.52*	29.55	-0	25.32	66.83	0.897	0.812
1.890+004	8.559+003	1.264+005	6.422+004	7.504	0	6.287-006	1.591+005	0.0816	23.26	24.82*	26.93	-0	28.63	66.61	0.949	0.815
1.335+004	5.975+003	1.419+005	7.106+004	11.893	0	5.633-006	1.775+005	0.0906	21.74	24.27*	26.60	-0	31.55	66.10	0.953	0.821
9.470+003	3.651+003	1.647+005	6.882+004	18.850	0	5.169-006	1.935+005	0.1008	20.45*	22.03*	22.68	-0	34.73	65.40	0.916	0.830
6.768+003	2.784+003	1.843+005	8.318+004	29.875	0	4.508-006	2.218+005	0.1135	19.25	21.62*	24.30	-0	38.25	63.96	0.945	0.848
4.513+003	1.630+003	1.992+005	7.716+004	47.348	0	4.364-006	2.291+005	0.1206	17.92	18.68*	21.17	-0	42.70	67.21	0.948	0.807
3.343+003	1.055+003	2.381+005	7.918+004	75.042	0	3.782-006	2.644+005	0.1434	15.81*	12.79*	18.40	-0	48.67	64.43	0.963	0.980
2.640+004	1.313+004	1.065+005	6.215+004	4.735	0	6.940-006	1.441+005	0.0727	24.81	27.75*	29.82	-0	25.42	66.40	0.893	0.817
1.017+006		1.000-006	1.410+003	0.001		2.517-013	3.974+012	0.0000								
8.553+005		1.000-006	1.879+003	0.002		1.416-013	7.064+012	0.0000								
8.770+005		1.000-006	3.054+003	0.003		5.361-014	1.865+013	0.0000								
7.662+005		1.000-006	4.229+003	0.006		2.796-014	3.576+013	0.0000								
7.144+005		1.000-006	6.249+003	0.009		1.280-014	7.810+013	0.0000								
6.270+005		1.000-006	8.692+003	0.014		6.618-015	1.511+014	0.0000								
5.346+005		1.273+004	1.175+004	0.022		4.615-005	2.167+004	0.5421								
4.452+005		2.330+004	1.551+004	0.035		4.846-005	2.064+004	0.7514								
3.490+005	P ₁₁ P ₂₂	3.522+004	1.926+004	0.055		4.746-005	2.107+004	0.9142								
2.686+005		5.148+004	2.349+004	0.087		4.664-005	2.144+004	1.0956								
1.881+005		7.045+004	2.608+004	0.139		5.180-005	1.931+004	1.3507								
1.390+005		9.483+004	3.054+004	0.220		5.084-005	1.967+004	1.5525								
9.444+004		1.246+005	3.289+004	0.348		5.761-005	1.736+004	1.8947								

3.930 2.500 1.000 5.320 0.400 47.610 1922.00 1330.00 -0.000

1.390+005	1.054+005	1.713+004	1.983+004	0.180	0	2.494+005	4.009+004	0.1364	40.82	43.27*	49.19	-0	48.51	67.50	0.799	0.669
1.113+005	1.682+004	2.404+004	2.290+004	0.299	0	2.176+005	4.596+004	0.1668	37.08*	39.17 R	43.69	-0	59.24	67.44	0.765	0.670
8.763+004	5.737+004	3.136+004	2.717+004	0.473	0	1.821+005	5.490+004	0.2004	33.38*	34.97 R	40.92	-0	71.45	67.70	0.760	0.668
6.770+004	4.230+004	3.963+004	3.170+004	0.750	0	1.536+005	6.512+004	0.2353	30.27*	30.98 R	38.74	-0	84.15	67.90	0.717	0.666
5.192+004	3.054+004	4.994+004	3.633+004	1.169	0	1.310+005	7.636+004	0.2723	26.82*	27.25 R	36.04	-0	97.14	67.73	0.699	0.667
3.935+004	2.201+004	6.149+004	4.148+004	1.865	0	1.118+005	8.947+004	0.3104	24.01*	23.92 R	34.01	-0	110.40	67.53	0.615	0.669
2.804+004	1.524+004	7.316+004	4.552+004	2.947	0	9.853+006	1.015+005	0.3432	21.45*	21.91 R	31.90	-0	121.24	67.07	0.641	0.674
2.191+004	1.089+004	9.001+004	5.156+004	4.735	0	8.365+006	1.195+005	0.3862	18.74*	18.66 R	29.81	-0	135.91	66.81	0.668	0.670
2.239+004	1.114+004	9.194+004	5.276+004	4.735	0	8.183+006	1.222+005	0.3916	18.61*	18.70 R	29.85	-0	138.64	67.22	0.655	0.672
1.623+004	7.583+003	1.077+005	5.691+004	7.504	0	7.260+006	1.377+005	0.4252	16.40*	16.98 R	27.87	-0	149.76	66.86	0.647	0.670
1.176+004	5.249+003	1.252+005	6.242+004	11.893	0	6.398+006	1.563+005	0.4612	14.63*	15.08 R	26.51	-0	160.42	66.03	0.706	0.689
8.611+003	3.621+003	1.473+005	6.825+004	18.850	0	5.590+006	1.789+005	0.5031	12.66*	12.83 R	24.87	-0	172.88	65.24	0.785	0.693
5.544+003	3.635+003	1.251+005	1.086+005	29.879	0	4.559+006	2.193+005	0.5444	11.38	20.06*	24.07	-0	183.76	64.08	0.924	0.702
4.290+003	1.539+003	1.896+005	7.280+004	47.348	0	4.596+006	2.176+005	0.6075	8.44*	11.07 R	21.03	-0	215.91	67.48	0.786	0.670
3.092+003	1.072+003	2.176+005	9.069+004	75.042	0	4.040+006	2.475+005	0.7516	5.20*	14.69 R	20.35	-0	262.22	66.23	0.866	0.682
3.002+003	1.014+003	2.121+005	7.607+004	75.042	0	4.178+006	2.394+005	0.7454	5.46*	5.85 R	19.73	-0	260.06	66.23	0.853	0.682
2.251+004	1.102+004	9.286+004	5.231+004	4.735	0	8.174+006	1.223+005	0.5926	18.29*	18.79 R	29.40	-0	138.55	67.01	0.655	0.674
5.079+005		1.000+006	1.116+003	0.002		4.015+013	2.491+012	0.0000								
4.734+005		1.000+006	1.649+003	0.003		1.840+013	5.436+012	0.0000								
4.411+005		1.000+006	2.435+003	0.006		8.434+014	1.186+013	0.0000								
4.050+005		1.000+006	3.551+003	0.009		3.966+014	2.522+013	0.0000								
3.659+005		1.000+006	5.073+003	0.014		1.943+014	5.146+013	0.0000								
3.347+005		1.000+006	7.355+003	0.022		9.242+015	1.082+014	0.0000								
2.840+005		1.000+006	9.892+003	0.032		5.110+015	1.957+014	0.0000								
2.840+005		9.399+003	9.892+003	0.032		4.292+005	2.370+004	0.4246								
2.461+005		6.409+004	1.370+004	0.052		3.756+005	2.663+004	0.5144								
2.001+005		2.338+004	1.750+004	0.087		3.804+005	2.629+004	0.6657								
1.610+005		3.570+004	2.232+004	0.139		3.590+005	2.786+004	0.8012								
1.270+005		5.419+004	2.790+004	0.220		3.481+005	2.873+004	0.9712								
9.322+004		7.695+004	3.240+004	0.348		3.650+005	2.739+004	1.1851								
5.974+004		9.754+004	3.297+004	0.552		4.486+005	2.229+004	1.4791								
3.930	2.500	1.000	5.320	0.400	16.290	207.50	1330.00	-0.000								

FDI MOVEMENT -1=120 C K=207,5 3/10/71

7.924+004	6.647+004	4.1337+003	1.253+004	0.148	0	3.644-005	2.743+004	0.0819	50.70	53.07*	57.01	-0	24.93	67.09	0.672	0.674
6.764+004	5.243+004	1.270+004	1.566+004	0.299	0	3.127-005	3.198+004	0.1079	46.00*	47.96 R	50.79	-0	38.11	67.05	0.596	0.679
5.544+004	4.252+004	1.686+004	2.013+004	0.473	0	2.445-005	4.091+004	0.1369	41.83	44.05*	50.07	-0	48.28	66.97	0.803	0.675
4.405+004	3.342+004	2.375+004	2.510+004	0.750	0	1.989-005	5.028+004	0.1734	37.66	39.35*	46.59	-0	60.90	66.67	0.815	0.678
3.761+004	2.414+004	3.337+004	2.872+004	1.189	0	1.722-005	5.808+004	0.2104	32.83*	35.14 R	40.72	-0	74.06	66.84	0.892	0.676
2.917+004	1.790+004	4.333+004	3.385+004	1.882	0	1.433-005	6.977+004	0.2501	29.15*	29.77 R	38.01	-0	87.84	66.68	0.687	0.682
2.275+004	1.312+004	5.545+004	3.929+004	2.987	0	1.201-005	8.329+004	0.2922	25.60*	26.02 R	35.33	-0	102.27	66.45	0.664	0.682
1.707+004	9.295+003	6.738+004	4.403+004	4.732	0	1.037-005	9.639+004	0.3295	22.67*	23.50 R	33.00	-0	114.55	66.00	0.793	0.689
1.564+004	9.000+003	6.033+004	4.261+004	4.732	0	1.106-005	9.043+004	0.3107	24.42*	25.96 R	35.24	-0	108.83	66.50	0.834	0.680
1.131+004	7.106+003	6.602+004	5.332+004	7.504	0	9.167-006	1.091+005	0.3465	22.76	26.36*	38.94	-0	120.77	66.17	0.938	0.683
8.299+003	4.976+003	7.899+004	5.918+004	11.893	0	8.108-006	1.233+005	0.3834	19.50	23.56*	36.85	-0	132.94	65.84	0.928	0.686
6.655+003	3.723+003	9.032+004	7.019+004	18.850	0	6.903-006	1.449+005	0.4273	17.24	22.66*	37.86	-0	146.24	64.98	0.929	0.695
4.312+003	2.821+003	9.742+004	8.427+004	29.872	0	5.871-006	1.703+005	0.4770	15.08	22.68*	40.87	-0	160.28	63.79	0.942	0.708
3.334+003	1.370+003	1.446+005	6.486+004	47.348	0	5.772-006	1.732+005	0.5482	11.24*	14.74 R	24.25	-0	192.88	66.79	0.783	0.677
2.371+003	9.186+002	1.640+005	6.895+004	75.042	0	5.182-006	1.930+005	0.7009	7.05*	7.74 R	22.81	-0	243.98	66.13	0.696	0.689
2.078+005		1.006-006	4.565+002	0.062		2.399-012	4.168+011	0.0000								
1.894+005		1.006-006	6.594+002	0.003		1.150-012	8.697+011	0.0000								
1.700+005		1.006-006	9.324+002	0.006		5.678-013	1.761+012	0.0000								
1.566+005		1.006-006	1.370+003	0.009		2.666-013	3.752+012	0.0000								
1.500+005		1.006-006	2.080+003	0.019		1.156-013	8.651+012	0.0000								
1.454+005		1.006-006	3.195+003	0.022		4.896-014	2.043+013	0.0000								
1.311+005		1.006-006	4.565+003	0.032		2.399-014	4.168+013	0.0000								
1.149+005		6.503+003	6.341+003	0.052		8.087-005	1.237+004	0.5128								
9.155+004		1.084+004	8.623+003	0.087		7.287-005	1.372+004	0.6284								
8.415+004		1.680+004	1.167+004	0.139		6.171-005	1.621+004	0.7199								
6.926+004		2.547+004	1.522+004	0.220		5.499-005	1.819+004	0.8368								
5.681+004		3.793+004	1.973+004	0.348		4.846-005	2.064+004	0.9587								
4.595+004		5.419+004	2.536+004	0.552		4.212-005	2.374+004	1.0683								
3.479+004		7.586+004	3.044+004	0.875		4.095-005	2.442+004	1.2463								
2.561+004		9.754+004	3.551+004	1.386		3.868-005	2.585+004	1.3732								
3.930	2.500	1.000	5.320	0.400	16.790	267.50	1330.00	-0.000								

1.532+005	9.665+004	2.240+004	1.822+004	0.188 0	2.687-005	3.722+004	0.0177	37.57	38.49*	39.13	-0	6.32	67.89	0.860	0.799
1.162+005	7.639+004	2.704+004	2.103+004	0.299 0	2.292-005	4.363+004	0.0212	34.75	36.56*	37.29	-0	7.60	68.10	0.851	0.797
8.651+004	5.699+004	3.309+004	2.414+004	0.473 0	1.972-005	5.070+004	0.0249	32.61	35.28*	36.12	-0	8.90	67.85	0.863	0.800
6.489+004	3.712+004	3.993+004	2.786+004	0.750 0	1.684-005	5.937+004	0.0295	27.08	33.94*	34.91	-0	10.54	67.89	0.857	0.799
4.814+004	2.644+004	4.783+004	3.144+004	1.189 0	1.460-005	6.851+004	0.0345	29.68	32.23*	33.31	-0	12.33	67.85	0.874	0.800
3.556+004	1.853+004	5.720+004	3.493+004	1.865 0	1.273-005	7.853+004	0.0402	28.11	30.21*	31.41	-0	14.27	67.45	0.887	0.805
2.583+004	1.283+004	6.698+004	3.832+004	2.987 0	1.125-005	8.891+004	0.0460	26.31	28.47*	29.78	-0	16.29	67.28	0.887	0.807
1.889+004	9.689+003	7.841+004	4.303+004	4.735 0	9.801-005	1.020+005	0.0529	25.09	27.30*	28.76	-0	18.58	66.63	0.914	0.814
1.896+004	8.555+003	7.915+004	4.240+004	4.735 0	9.817-006	1.019+005	0.0531	24.90	26.74*	28.18	-0	18.81	67.23	0.903	0.807
1.376+004	6.160+003	9.229+004	4.622+004	7.504 0	8.662-006	1.154+005	0.0606	23.65	25.05*	26.61	-0	21.26	66.59	0.914	0.815
9.835+003	4.234+003	1.056+005	5.036+004	11.893 0	7.716-006	1.296+005	0.0682	22.40	23.82*	25.51	-0	23.83	66.32	0.921	0.818
7.077+003	2.591+003	1.209+005	5.038+004	18.850 0	6.794-006	1.472+005	0.0773	21.04	23.13*	25.00	-0	26.57	65.28	0.914	0.831
5.060+003	2.644+003	1.385+005	6.105+004	29.045 0	6.051-006	1.653+005	0.0812	19.71	21.81*	23.82	-0	29.33	63.89	0.927	0.849
3.457+003	1.334+003	1.510+005	6.317+004	47.348 0	5.636-006	1.774+005	0.0950	19.93	20.60*	22.71	-0	33.33	66.61	0.970	0.815
2.458+003	8.143+002	1.740+005	6.111+004	75.092 0	5.115-006	1.955+005	0.1095	17.27*	18.05 8	19.35	-0	38.20	66.24	0.890	0.819
1.910+004	9.188+003	7.931+004	4.350+004	4.735 0	9.693-006	1.032+005	0.0535	25.11	27.28*	28.75	-0	18.97	67.30	0.895	0.806
2.169+006			1.000-006	3.007+003	0.001	5.529-014	1.808+013	0.0000							
1.775+006			1.000-006	3.900+003	0.002	3.288-014	3.042+013	0.0000							
1.417+006			1.000-006	4.933+003	0.003	2.054-014	4.868+013	0.0000							
1.149+006			1.000-006	6.343+003	0.006	1.243-014	8.047+013	0.0000							
9.668+005	9.759+003	8.457+003	0.009	6.818-005	1.467+004	0.5767									
7.117+005	1.246+004	9.867+003	0.014	6.401-005	1.562+004	0.6316									
5.774+005	1.436+004	1.269+004	0.022	4.461-005	2.241+004	0.5660									
4.722+005	1.000-006	1.644+004	0.035	1.849-015	5.409+014	0.0000									
3.703+005	1.000-006	2.044+004	0.055	1.197-015	8.355+014	0.0000									
2.847+005	1.000-006	2.490+004	0.087	8.063-016	1.240+015	0.0000									
2.203+005	1.000-006	3.054+004	0.139	5.361-016	1.865+015	0.0000									
1.668+005	1.000-006	3.665+004	0.220	3.723-016	2.688+015	0.0000									
1.174+005	1.000-006	4.088+004	0.348	2.992-016	3.342+015	0.0000									
8.513+004	1.000-006	4.699+004	0.552	2.265-016	4.415+015	0.0000									
3.930	2.500	1.000	5.320	0.400	47.610	1922.00	1330.00	-0.000							

1.289+005	9.731+004	1.004+004	1.158+004	0.119	0	4.274-005	2.340+004	0.0095	48.68	48.68*	49.09	-0	3.26	65.50	0.922	0.829
1.260+005	9.345+004	1.004+004	1.111+004	0.119	0	4.476-005	2.234+004	0.0092	47.25	47.51*	47.91	-0	3.19	65.50	0.896	0.829
1.011+005	7.598+004	1.257+004	1.432+004	0.188	0	3.462-005	2.889+004	0.0117	48.22*	48.22	48.73	-0	4.07	65.77	0.953	0.825
1.011+005	7.192+004	1.340+004	1.356+004	0.188	0	3.688-005	2.711+004	0.0117	43.19	44.86*	45.33	-0	4.07	65.83	0.889	0.824
4.158+004	5.044+004	1.700+004	1.746+004	0.299	0	2.863-005	3.449+004	0.0150	42.62	45.15*	45.77	-0	5.15	65.32	0.880	0.831
4.403+004	4.344+004	2.429+004	2.058+004	0.473	0	2.422-005	4.128+004	0.0186	38.74	42.03*	42.75	-0	6.37	65.20	0.852	0.832
5.067+004	3.285+004	2.897+004	2.465+004	0.750	0	2.002-005	4.995+004	0.0232	36.69	39.55*	40.41	-0	7.76	63.55	0.875	0.854
3.070+004	2.281+004	3.420+004	2.713+004	1.189	0	1.795-005	5.572+004	0.0265	34.51	37.49*	38.43	-0	9.19	65.78	0.865	0.825
2.768+004	1.645+004	4.197+004	3.101+004	1.885	0	1.541-005	6.489+004	0.0316	32.41	35.40*	36.47	-0	10.93	65.75	0.851	0.825
2.082+004	1.163+004	5.190+004	3.475+004	2.987	0	1.333-005	7.500+004	0.0374	32.77*	32.77	33.97	-0	12.87	65.34	0.811	0.831
2.091+004	1.178+004	5.190+004	3.519+004	2.987	0	1.323-005	7.500+004	0.0376	30.96	33.08*	34.30	-0	12.95	65.46	0.875	0.829
1.548+004	8.378+003	6.150+004	3.967+004	4.735	0	1.148-005	8.709+004	0.0438	28.92	31.47*	32.83	-0	15.02	65.18	0.904	0.833
1.534+004	8.397+003	6.077+004	3.976+004	4.735	0	1.152-005	8.678+004	0.0434	29.96	31.84*	33.20	-0	14.87	65.00	0.913	0.835
1.132+004	6.057+003	7.179+004	4.545+004	7.504	0	9.944-006	1.006+005	0.0505	28.22	30.80*	32.34	-0	17.20	64.67	0.877	0.839
4.328+003	4.199+003	8.554+004	4.994+004	11.893	0	8.719-006	1.147+005	0.0584	26.54	28.59*	30.28	-0	19.74	64.14	0.906	0.846
6.079+003	2.749+003	1.022+005	5.182+004	18.830	0	7.783-006	1.285+005	0.0671	25.15*	26.87	26.89	-0	22.37	63.28	0.869	0.858
4.440+003	2.033+003	1.179+005	6.073+004	29.875	0	6.702-006	1.492+005	0.0774	23.47	25.22*	27.25	-0	25.20	61.82	0.901	0.878
3.173+003	1.482+003	1.328+005	7.016+004	47.348	0	5.886-006	1.699+005	0.0881	25.49*	28.59	27.85	-0	30.11	64.89	0.801	0.836
2.270+003	9.563+002	1.545+005	7.176+004	75.042	0	5.324-006	1.878+005	0.1023	22.45*	22.71	24.92	-0	34.26	63.60	0.793	0.853
1.580+004	8.778+003	6.221+004	4.156+004	4.735	0	1.111-005	8.978+004	0.0447	32.29	32.33*	33.75	-0	14.79	62.80	0.918	0.864
4.722+005		1.000-006	1.644+003	0.003		1.849-013	5.409+012	0.0000								
4.256+005		1.000-006	2.349+003	0.006		9.059-014	1.104+013	0.0000								
3.652+005		1.000-006	3.195+003	0.009		4.898-014	2.042+013	0.0000								
3.220+005		1.000-006	4.464+003	0.014		2.510-014	3.985+013	0.0000								
3.220+005		2.980+003	4.464+003	0.014		7.479-005	1.337+004	0.3339								
2.737+005		1.057+004	6.014+003	0.022		1.461-004	6.849+003	0.8785								
2.159+005		1.788+004	7.518+003	0.035		1.582-004	6.321+003	1.1894								
2.159+005		9.724+003	7.518+003	0.035		8.630-005	1.159+004	0.6467								
1.788+005		2.059+004	9.867+003	0.035		1.058-004	9.455+003	1.0435								
1.450+005		3.251+004	1.269+004	0.087		1.010-004	9.900+003	1.2815								
1.118+005		5.148+004	1.551+004	0.139		1.071-004	9.340+003	1.6601								
8.553+004		6.236+004	1.879+004	0.248		8.821-005	1.134+004	1.6579								
4.476+004		7.316+004	2.255+004	0.348		7.191-005	1.391+004	1.6218								
4.937+004		8.670+004	2.725+004	0.552		5.837-005	1.713+004	1.5908								
3.760+004		9.483+004	3.289+004	0.875		4.383-005	2.281+004	1.4416								
3.930	2.500	1.000	5.420	0.400	47.610	1922.00	1330.00	-0.000								

FIASIAK	EIAP	GP	GP	SHEAR RATE	JP	I/JP	AMP	PHI 1	PHI 2	THETA	FILTER					
A	0			PLYUNDEGENE	F=140	K=207.5	3/31/71									
8.510+004	7.338+004	3.233+003	5.507+003	0.075	0	7.929-005	1.291+004	0.0360	56.52	57.81*	59.59	-0	12.83	67.62	0.755	0.803
7.012+004	5.754+004	4.767+003	6.844+003	0.119	0	-6.853-005	-1.459+004	-0.0466	52.96*	52.96	55.15	-0	16.61	67.64	0.742	0.802
5.864+004	4.071+004	6.982+003	8.804+003	0.188	0	5.470-005	1.828+004	0.0611	49.75	50.02*	52.81	-0	21.77	67.63	0.693	0.802
4.837+004	3.714+004	9.458+003	1.109+004	0.299	0	-4.434-005	-2.255+004	-0.0787	43.17	46.70*	50.17	-0	28.00	67.57	0.694	0.804
3.895+004	2.902+004	1.430+004	1.374+004	0.473	0	3.617-005	2.705+004	0.0988	40.84	43.95*	48.17	-0	35.20	67.67	0.854	0.802
3.125+004	2.424+004	-1.647+004	1.669+004	0.750	0	-2.995-005	3.339+004	0.1227	37.84	40.38*	45.39	-0	43.55	67.39	0.830	0.805
2.462+004	1.590+004	2.438+004	1.891+004	1.189	0	2.607-005	3.839+004	0.1485	34.73*	36.87*	40.24	-0	52.69	67.35	0.792	0.806
1.911+004	1.441+004	2.739+004	2.338+004	1.885	0	-2.112-005	4.735+004	0.1777	31.96	33.87*	40.50	-0	62.67	66.94	0.867	0.811
1.473+004	9.143+003	3.452+004	2.731+004	2.987	0	1.782-005	5.613+004	0.2095	30.89*	30.89*	38.36	-0	73.63	66.72	0.858	0.813
1.482+004	9.138+003	3.489+004	2.730+004	2.987	0	1.778-005	5.024+004	0.2104	28.83	30.62*	38.07	-0	73.76	66.54	0.898	0.816
1.127+004	6.974+003	4.499+004	3.160+004	4.735	0	1.510-005	6.622+004	0.2438	25.83	28.02*	36.33	-0	85.22	66.37	0.912	0.818
1.086+004	6.519+003	4.152+004	3.086+004	4.735	0	1.555-005	6.430+004	0.2371	28.48	28.70*	36.88	-0	84.29	67.44	0.923	0.804
2.244+003	4.931+003	5.118+004	3.475+004	7.504	0	1.337-005	7.474+004	0.2727	23.61	25.37*	34.18	-0	96.00	66.13	0.946	0.812
4.201+003	3.132+003	8.392+004	3.725+004	11.893	0	1.170-005	8.545+004	0.3096	21.35*	22.78*	30.35	-0	108.12	66.23	0.840	0.819
4.518+003	2.179+003	7.490+004	4.107+004	18.850	0	1.029-005	9.721+004	0.3461	19.23*	20.88*	28.84	-0	119.01	65.29	0.914	0.831
4.481+003	2.297+003	7.252+004	4.329+004	18.850	0	1.017-005	9.839+004	0.3456	19.04	20.64*	30.84	-0	119.07	65.42	0.951	0.830
3.378+003	1.981+003	8.752+004	5.022+004	29.875	0	8.596-006	1.193+005	0.4009	15.99	18.34*	29.85	-0	135.05	63.95	0.958	0.849
2.427+003	9.306+002	1.091+005	4.406+004	47.348	0	8.038-006	1.244+005	0.4656	12.27*	18.19*	22.55	-0	165.12	67.33	0.823	0.806
1.082+004	6.447+003	4.117+004	3.053+004	4.735	0	1.567-005	6.380+004	0.2393	26.07	28.47*	36.57	-0	85.60	68.77	0.908	0.789
2.195+005		1.000-006	3.044+002	0.001		5.398-012	1.853+011	0.0000								
2.147+005		1.000-006	4.717+002	0.002		2.247-012	4.451+011	0.0000								
1.937+005		1.000-006	6.747+002	0.003		1.099-012	9.103+011	0.0000								
1.774+005		1.000-006	9.790+002	0.006		5.217-013	1.917+012	0.0000								
1.653+005		1.000-006	1.446+003	0.009		2.392-013	4.180+012	0.0000								
1.537+005		1.000-006	2.130+003	0.014		1.102-013	9.078+012	0.0000								
1.281+005		1.897+003	2.815+003	0.022		1.196-004	8.358+003	0.3398								
1.136+005		5.311+003	3.957+003	0.035		1.696-004	5.899+003	0.6711								
9.650+004		9.754+003	5.326+003	0.055		1.719-004	5.817+003	0.9157								
8.002+004		1.928+004	7.000+003	0.087		1.659-004	6.029+003	1.1612								
6.586+004		2.493+004	9.131+003	0.139		1.495-004	6.689+003	1.3650								
5.541+004		3.414+004	1.217+004	0.220		1.152-004	8.683+003	1.4021								
4.297+004		4.335+004	1.496+004	0.348		9.680-005	1.033+004	1.4485								
3.309+004		5.419+004	1.820+004	0.552		8.125-005	1.231+004	1.4837								
2.494+004		6.772+004	2.181+004	0.875		7.119-005	1.405+004	1.5527								
2.262+004		6.232+004	1.978+004	0.875		7.961-005	1.259+004	1.5750								
3.930	2.500	1.000	5.320	0.400	16.290	207.50	1330.00	-0.000								

FTASTAR ELAP GP G2P SHEAR RATE JP 1/JP AMP PHI 1 PHI 2 THETA FILTER
POLYTRILENE T=80 C K=207.5 3/10/71

1.559+005	1.115+005	8.1/4+003	8.368+003	0.075	0	5.973-005	1.674+004	0.0642	43.05*	43.05	45.68	-0	22.78	67.41	0.745	0.805
1.258+005	8.414+004	1.112+004	1.001+004	0.119	0	4.969-005	2.012+004	0.0807	38.90*	38.90	41.99	-0	28.58	67.21	0.594	0.807
1.249+005	8.005+004	1.017+004	1.023+004	0.119	0	4.879-005	2.049+004	0.0803	40.31	40.37*	43.54	-0	28.32	66.95	0.802	0.811
9.508+004	6.459+004	1.349+004	1.180+004	0.188	0	4.200-005	2.381+004	0.0954	34.75	37.58*	41.18	-0	33.82	67.28	0.804	0.807
7.258+004	4.578+004	1.682+004	1.368+004	0.299	0	3.579-005	2.794+004	0.1134	32.53	35.02*	39.12	-0	40.11	67.17	0.843	0.808
7.269+004	4.588+004	1.688+004	1.371+004	0.299	0	3.572-005	2.800+004	0.1135	35.04*	35.04	39.15	-0	40.11	67.07	0.865	0.809
7.297+004	4.624+004	1.688+004	1.382+004	0.299	0	3.548-005	2.818+004	0.1140	35.19*	35.19	39.33	-0	40.27	67.08	0.886	0.809
5.519+004	3.318+004	2.088+004	1.571+004	0.473	0	3.058-005	3.270+004	0.1337	30.23	32.36*	36.97	-0	47.27	67.12	0.883	0.809
4.153+004	2.494+004	2.391+004	1.804+004	0.750	0	2.618-005	3.842+004	0.1557	28.04	30.21*	35.39	-0	54.90	66.94	0.899	0.811
3.097+004	1.716+004	3.087+004	2.041+004	1.189	0	2.260-005	4.425+004	0.1792	25.60	27.95*	33.65	-0	63.32	67.09	0.894	0.809
2.315+004	1.129+004	3.811+004	2.128+004	1.885	0	2.001-005	4.999+004	0.2049	23.45*	24.56	29.18	-0	72.33	67.03	0.835	0.810
1.703+004	8.040+003	4.405+004	2.402+004	2.907	0	1.733-005	5.772+004	0.2313	21.90*	22.69	28.17	-0	81.04	66.51	0.838	0.816
1.540+004	7.340+003	6.407+004	3.475+004	4.735	0	1.206-005	8.292+004	0.3035	20.16*	21.08	28.48	-0	105.39	65.92	0.862	0.823
1.246+004	5.844+003	5.259+004	2.672+004	4.735	0	1.511-005	6.617+004	0.2590	20.20*	20.85	26.94	-0	91.25	66.88	0.852	0.811
8.889+003	4.228+003	5.871+004	3.166+004	7.504	0	1.320-005	7.579+004	0.2852	18.52	20.56*	28.35	-0	100.12	66.64	0.937	0.814
6.374+003	2.896+003	6.754+004	3.444+004	11.893	0	1.175-005	8.510+004	0.3138	18.83*	19.03	27.03	-0	109.12	66.02	0.923	0.822
6.411+003	2.857+003	6.828+004	3.398+004	11.893	0	1.174-005	8.518+004	0.3148	18.41*	18.56	26.47	-0	109.75	66.19	0.885	0.820
6.346+003	3.049+003	6.593+004	3.673+004	11.893	0	1.157-005	8.640+004	0.3140	16.56	20.34*	29.13	-0	109.38	66.12	0.957	0.821
4.526+003	2.017+003	7.643+004	3.791+004	18.850	0	1.050-005	9.524+004	0.3449	15.38	17.57*	26.39	-0	118.46	65.21	0.955	0.832
3.321+003	1.376+003	9.030+004	4.110+004	29.875	0	9.174-006	1.090+005	0.3925	15.12*	14.91	24.47	-0	132.10	63.90	0.956	0.849
1.754+003	9.329+002	7.094+004	4.417+004	47.348	0	1.020-005	9.808+004	0.3923	19.63	20.09*	32.13	-0	139.04	67.28	0.969	0.807
9.083+002	5.241+002	6.571+004	1.811+004	75.042	0	1.414-005	7.070+004	0.4628	8.35*	8.56	19.41	-0	151.16	66.10	0.828	0.821
1.242+004	5.671+003	5.234+004	2.885+004	4.735	0	1.513-005	6.611+004	0.2586	20.38*	20.82	27.16	-0	91.20	66.96	0.853	0.810
7.867+005		1.000-006	1.091+003	0.001		4.204-013	2.379+012	0.0000								
7.157+005		1.000-006	1.572+003	0.002		2.022-013	4.946+012	0.0000								
6.118+005		1.000-006	2.130+003	0.003		1.102-013	9.078+012	0.0000								
5.331+005		1.000-006	2.942+003	0.006		5.776-014	1.731+013	0.0000								
4.523+005		2.188+003	3.957+003	0.009		6.923-005	1.444+004	0.2739								
3.842+005		3.322+003	5.326+003	0.014		6.208-005	1.611+004	0.3307								
2.955+005		9.483+003	6.493+003	0.022		1.125-004	8.891+003	0.7303								
2.403+005		1.571+004	8.370+003	0.035		1.122-004	8.916+003	0.9388								
1.884+005		2.222+004	1.040+004	0.055		1.027-004	9.734+003	1.0683								
1.421+005		3.251+004	1.243+004	0.087		1.053-004	9.501+003	1.3081								
1.043+005		4.335+004	1.446+004	0.139		1.037-004	9.642+003	1.4993								
7.849+004		5.690+004	1.725+004	0.220		9.564-005	1.046+004	1.6495								
5.826+004		6.774+004	2.029+004	0.348		8.226-005	1.216+004	1.6692								

3.930 2.500 1.000 5.320 0.400 16.290 207.50 1330.00 -0.000

THE WEISSBERG RHEOGONIOMETER TEST RESULTS

ETASAR	ETAR	UP	G2P	SHEAR RATE	JP	1/JP	AMP	PHI 1	PHI 2	THETA	FILTER				
POLYTRIDECENE T=100-C K=207.5 3/11/71															
1,083+005	8,343+004	5,130+003	6,265+003	0,075	0	7,839-005	1,276+004	0,0454	5,22	48,42*	50,42 -0	16,15	67,59	0,841	0,803
8,711+004	6,437+004	6,980+003	7,656+003	0,119	0	6,503-005	1,538+004	0,0572	44,90	45,23*	47,65 -0	20,37	67,58	0,834	0,803
6,909+004	4,897+004	9,183+003	9,232+003	0,188	0	5,416-005	1,846+004	0,0710	39,76	42,27*	45,16 -0	25,27	67,54	0,769	0,803
5,707+004	3,717+004	1,274+004	1,110+004	0,299	0	4,451-005	2,247+004	0,0911	37,25*	37,51*	40,65 -0	32,39	67,52	0,419	0,804
5,406+004	3,561+004	1,246+004	1,065+004	0,299	0	4,639-005	2,156+004	0,0878	37,25*	38,81*	40,52 -0	31,13	67,32	0,729	0,805
5,461+004	3,690+004	1,201+004	1,104+004	0,299	0	4,513-005	2,216+004	0,0876	38,11	39,20*	42,60 -0	31,14	67,50	0,873	0,804
4,137+004	2,674+004	1,494+004	1,266+004	0,473	0	3,895-005	2,567+004	0,1035	34,64	36,45*	40,28 -0	36,77	67,47	0,865	0,804
3,187+004	1,940+004	1,871+004	1,490+004	0,750	0	3,270-005	3,058+004	0,1238	33,39	34,12*	38,54 -0	44,06	67,57	0,880	0,803
2,415+004	1,448+004	2,298+004	1,723+004	1,189	0	2,786-005	3,590+004	0,1453	29,25	31,86*	36,86 -0	51,74	67,58	0,876	0,803
1,812+004	1,010+004	2,928+004	1,915+004	1,885	0	2,424-005	4,125+004	0,1682	27,46	28,70*	34,11 -0	59,49	67,15	0,913	0,808
1,348+004	0,654+003	3,467+004	2,048+004	2,987	0	2,138-005	4,677+004	0,1922	24,96*	26,95*	30,57 -0	67,97	67,13	0,888	0,808
9,963+003	4,826+003	4,128+004	2,284+004	4,733	0	1,855-005	5,392+004	0,2184	22,89*	24,87*	28,96 -0	76,72	66,70	0,885	0,819
9,818+003	5,102+003	3,971+004	2,417+004	4,733	0	1,838-005	5,442+004	0,2166	24,87*	24,97*	31,34 -0	76,76	67,29	0,885	0,807
7,260+003	3,388+003	4,818+004	2,543+004	7,504	0	1,623-005	6,160+004	0,2447	21,27*	24,05*	27,83 -0	86,30	66,93	0,901	0,811
5,237+003	2,513+003	5,465+004	2,908+004	11,893	0	1,409-005	7,099+004	0,2730	19,51	21,15*	28,67 -0	95,20	66,22	0,954	0,820
3,820+003	1,644+003	6,500+004	3,099+004	18,850	0	1,254-005	7,977+004	0,3063	17,02*	19,90*	25,49 -0	105,52	65,40	0,889	0,830
2,788+003	1,099+003	7,655+004	3,283+004	29,875	0	1,103-005	9,063+004	0,3500	15,29*	16,63*	23,22 -0	118,26	64,14	0,920	0,840
1,997+003	9,232+002	4,381+004	4,373+004	47,348	0	9,379-006	1,066+005	0,4205	16,34*	16,67*	27,56 -0	148,92	67,24	0,913	0,807
9,879+003	4,832+003	4,079+004	2,289+004	4,733	0	1,864-005	5,364+004	0,2170	23,21*	25,18*	29,31 -0	76,72	67,13	0,885	0,808
4,349+005		1,030+006	3,904+002	0,001		3,455+012	2,895+011	0,0000							
3,827+005		1,000+006	3,348+002	0,001		4,461+012	2,242+011	0,0000							
4,025+005		1,000+006	5,580+002	0,001		1,606+012	6,227+011	0,0000							
3,476+005		1,000+006	4,819+002	0,001		2,153+012	4,644+011	0,0000							
3,578+005		1,000+006	7,862+002	0,002		8,088+013	1,236+012	0,0000							
3,232+005		1,000+006	7,102+002	0,002		9,914+013	1,009+012	0,0000							
3,350+005		1,000+006	1,167+003	0,003		3,673+013	2,722+012	0,0000							
3,059+005		1,000+006	1,065+003	0,003		4,406+013	2,269+012	0,0000							
2,895+005		1,000+006	1,598+003	0,006		1,958+013	5,106+012	0,0000							
2,494+005		1,000+006	2,181+003	0,009		1,051+013	9,515+012	0,0000							
2,195+005		3,143+003	3,044+003	0,014		1,696+004	5,895+003	0,5163							
1,801+005		5,175+003	3,957+003	0,022		1,653+004	6,050+003	0,6540							
1,529+005		6,670+003	5,326+003	0,035		1,528+004	6,544+003	0,8139							
1,222+005		1,355+004	6,747+003	0,055		1,488+004	6,720+003	1,0040							
9,858+004		1,842+004	8,623+003	0,087		1,239+004	8,072+003	1,0685							
7,867+004		2,655+004	1,091+004	0,139		1,116+004	8,959+003	1,2173							
6,002+004		3,793+004	1,319+004	0,220		1,090+004	9,171+003	1,4381							
4,224+004		4,877+004	1,471+004	0,348		1,127+004	8,874+003	1,6577							
2,941+004		6,123+004	1,623+004	0,552		1,162+004	8,606+003	1,8862							
2,665+004		6,232+004	1,471+004	0,552		1,440+004	6,945+003	2,1181							
3,930	2,500	1,000	5,320	0,400	16,290	207,50	1330,00	-0,000							

THE WEISSENBERG RHEOGNOMICMETER TEST RESULTS

ETASTAR	ETAP	GP	G2P	SHEAR RATE	JP	I/JP	AMP	PHI 1	PHI 2	THETA	FILTER					
POLYTRIDECENE T=120 K=207.5 3/12/71																
7.053+004	5.846+004	2.961+003	4.397+003	0.075	0	1.057-004	9.461+003	0.0299	54.57*	54.57	55.99	-0	10.56	67.02	0.918	0.810
7.019+004	5.846+004	2.937+003	4.372+003	0.075	0	1.059-004	9.445+003	0.0298	54.70*	54.70	56.12	-0	10.53	67.17	0.858	0.803
5.919+004	4.732+004	4.228+003	5.628+003	0.119	0	8.532-005	1.172+004	0.0395	51.21	51.29*	53.10	-0	13.92	66.93	0.814	0.811
4.818+004	3.681+004	5.659+003	6.938+003	0.188	0	7.105-005	1.407+004	0.0505	47.26	47.62*	49.83	-0	17.76	66.80	0.765	0.812
3.899+004	2.889+004	7.422+003	8.540+003	0.279	0	5.838-005	1.713+004	0.0640	41.91	44.47*	47.16	-0	22.49	66.72	0.755	0.813
3.128+004	2.179+004	1.553+004	1.036+004	0.473	0	4.323-005	2.073+004	0.0801	38.91	41.20*	44.42	-0	28.11	66.58	0.808	0.815
2.426+004	1.634+004	1.336+004	1.226+004	0.750	0	4.060-005	2.463+004	0.0969	35.90	38.61*	42.35	-0	33.97	66.53	0.885	0.816
1.872+004	1.159+004	1.713+004	1.474+004	1.189	0	3.470-005	2.882+004	0.1162	32.93	35.21*	39.44	-0	40.68	66.48	0.889	0.816
1.429+004	8.155+003	2.133+004	1.845+004	1.885	0	2.940-005	3.402+004	0.1375	30.16	32.82*	37.64	-0	47.98	66.24	0.870	0.819
1.090+004	6.278+003	2.042+004	1.873+004	2.987	0	2.524-005	3.962+004	0.1605	27.73	30.16*	35.51	-0	55.77	65.75	0.885	0.823
9.362+003	4.443+003	2.000+001	3.959+004	4.735	0	1.598-010	6.258+009	0.1858	27.73	27.92	34.45	-0	64.08	65.48	0.942	0.829
7.856+003	4.443+003	3.058+004	2.104+004	4.735	0	2.217-005	4.510+004	0.1812	28.25	28.57*	34.45	-0	62.99	66.01	0.959	0.822
5.791+003	3.101+003	3.631+004	2.337+004	7.504	0	1.923-005	5.201+004	0.2063	24.30	26.82*	33.33	-0	71.46	65.77	0.905	0.825
4.270+003	2.278+003	4.323+004	2.662+004	11.893	0	1.617-005	5.903+004	0.2346	22.21	24.55*	31.62	-0	80.71	65.12	0.936	0.831
3.140+003	1.574+003	5.163+004	2.892+004	18.850	0	1.474-005	6.784+004	0.2671	21.75*	21.87	29.25	-0	90.66	64.43	0.909	0.842
3.116+003	1.773+003	5.193+004	2.796+004	18.850	0	1.497-005	6.678+004	0.2652	20.51	21.18*	28.43	-0	89.96	64.39	0.945	0.843
2.244+003	9.777+002	6.017+004	2.981+004	29.875	0	1.335-005	7.493+004	0.3034	18.62*	18.62	26.36	-0	101.30	63.39	0.896	0.856
2.300+003	9.774+002	6.179+004	2.962+004	29.875	0	1.313-005	7.614+004	0.3080	17.91*	17.91	25.54	-0	102.53	63.21	0.915	0.859
2.301+003	1.073+003	6.171+004	3.026+004	29.875	0	1.306-005	7.655+004	0.3084	18.33*	18.33	26.13	-0	102.60	63.17	0.947	0.859
1.630+003	7.077+002	6.821+004	3.606+004	47.348	0	1.146-005	8.728+004	0.3708	17.89*	18.08	27.87	-0	129.24	66.17	0.841	0.820
7.644+003	4.344+003	2.991+004	2.038+004	4.735	0	2.283-005	4.380+004	0.1770	28.35	28.56*	34.27	-0	63.59	68.21	0.949	0.796
1.740+005		1.000+006	1.522+002	0.001		2.159-011	4.632+010	0.0000								
1.720+005		1.000+006	2.384+002	0.001		8.797-012	1.137+011	0.0000								
1.685+005		1.000+006	3.703+002	0.002		3.646-012	2.742+011	0.0000								
1.602+005		1.000+006	5.580+002	0.003		1.606-012	6.227+011	0.0000								
1.425+005		1.000+006	7.862+002	0.006		8.088-013	1.239+012	0.0000								
1.276+005		1.000+006	1.116+003	0.009		4.015-013	2.491+012	0.0000								
1.134+005		1.000+006	1.572+003	0.014		2.022-013	4.945+012	0.0000								
1.224+005		2.601+003	2.688+003	0.022		1.799-004	5.558+003	0.4837								
8.099+004		4.817+003	3.551+003	0.044		1.934-004	5.170+003	0.6867								
7.352+004		0.122+003	4.058+003	0.025		1.859-004	5.379+003	0.7545								
6.089+004		7.212+003	5.326+003	0.087		1.624-004	6.155+003	0.8648								
5.013+004		1.353+004	6.949+003	0.139		1.403-004	7.130+003	0.9747								
3.994+004		1.751+004	8.776+003	0.220		1.267-004	7.895+003	1.1115								
3.132+004		2.709+004	1.091+004	0.348		1.139-004	8.780+003	1.2422								
2.481+004		3.739+004	1.370+004	0.552		9.967-005	1.003+004	1.3650								
7.172+003	4.279+003	2.749+004	1.997+004	4.735	0	2.381-005	4.199+004	0.1681	29.93	30.36*	36.04	-0	60.16	67.95	0.903	0.799
3.930	2.500	1.600	5.320	0.400	16.290	207.50	1330.00	-0.000								

THE WEISSENBERG RHEOGONIOMETER TEST RESULTS

ETA STAR	FIAT	GP	G2P	SHEAR RATE	JP	1/Jp	AMP	PHI 1	PHI 2	IMETA	FILTER
POLYHEXADECENE I=100°C K=207.5 5/21/71											
4.241+004	3.315+004	3.145+003	3.943+003	0.119 0	1.236-004	8.089+003	0.0285	50.16*	50.16	51.43	-0
3.453+004	2.615+004	4.250+003	4.929+003	0.188 0	1.003-004	9.967+003	0.0365	47.63*	47.65	49.24	-0
2.798+004	2.054+004	5.6/5+003	6.137+003	0.299 0	8.122-005	1.231+004	0.0465	45.29*	45.29	47.25	-0
2.230+004	1.567+004	7.515+003	7.420+003	0.473 0	6.738-005	1.484+004	0.0582	42.30*	42.30	44.64	-0
1.745+004	1.121+004	9.641+003	8.859+003	0.750 0	5.624-005	1.778+004	0.0712	39.82*	39.82	42.59	-0
1.361+004	8.922+003	1.222+004	1.061+004	1.189 0	4.665-005	2.143+004	0.0868	37.71*	37.71	40.98	-0
1.361+004	8.860+003	1.260+004	1.054+004	1.189 0	4.670-005	2.141+004	0.0879	36.68*	36.68	39.92	-0
1.027+004	6.357+003	1.519+004	1.200+004	1.885 0	4.053-005	2.467+004	0.1022	34.69*	34.69	38.32	-0
1.034+004	6.414+003	1.529+004	1.209+004	1.805 0	4.024-005	2.485+004	0.1028	34.69*	34.69	38.34	-0
7.888+003	4.541+003	1.918+004	1.369+004	2.987 0	3.455-005	2.895+004	0.1218	31.46*	31.46	35.51	-0
6.073+003	3.355+003	2.397+004	1.589+004	4.735 0	2.899-005	3.450+004	0.1451	28.94*	28.94	33.54	-0
5.892+003	3.370+003	2.305+004	1.572+004	4.735 0	2.962-005	3.377+004	0.1414	29.73*	29.73	34.30	-0
4.450+003	2.410+003	2.807+004	1.808+004	7.504 0	2.517-005	3.972+004	0.1654	27.65*	27.65	32.79	-0
3.221+003	1.742+003	3.223+004	2.072+004	11.895 0	2.196-005	4.554+004	0.1870	26.94*	26.94	32.74	-0
2.440+003	1.324+003	3.864+004	2.495+004	18.850 0	1.826-005	5.476+004	0.2210	25.97*	25.97	32.86	-0
1.762+003	8.445+002	4.620+004	2.523+004	29.875 0	1.667-005	5.998+004	0.2545	21.64*	21.64	28.64	-0
1.274+003	5.935+002	5.359+004	2.810+004	47.348 0	1.467-005	6.818+004	0.3140	19.36*	19.36	27.76	-0
9.612+002	4.131+002	6.513+004	3.100+004	75.042 0	1.252-005	7.988+004	0.4846	13.44*	13.44	25.46	-0
5.034+003	3.261+003	2.291+004	1.544+004	4.735 0	3.002-005	5.332+004	0.1402	29.50*	29.50	33.99	-0
1.537+005		1.000-006	2.130+002	0.001	1.102-011	9.078+010	0.0000				
1.477+005		1.000-006	3.246+002	0.002	4.744-012	2.108+011	0.0000				
1.355+005		1.000-006	4.717+002	0.003	2.247-012	4.451+011	0.0000				
1.176+005		1.000-006	6.493+002	0.006	1.186-012	8.432+011	0.0000				
1.061+005		1.000-006	9.203+002	0.009	5.802-013	1.723+012	0.0000				
9.513+004		1.000-006	1.319+003	0.014	2.875-013	3.479+012	0.0000				
8.542+004		1.000-006	1.877+003	0.022	1.419-013	7.045+012	0.0000				
7.283+004		1.000-006	2.536+003	0.035	7.773-014	1.287+013	0.0000				
6.250+004		1.000-006	3.449+003	0.055	4.202-014	2.380+013	0.0000				
5.219+004		7.857+003	4.565+003	0.087	1.885-004	5.305+003	0.8606				
4.929+004		7.586+003	4.312+003	0.087	2.040-004	4.901+003	0.8798				
4.098+004		1.192+004	5.681+003	0.139	1.847-004	5.415+003	1.0492				
3.185+004		1.734+004	7.000+003	0.220	1.769-004	5.652+003	1.2386				
2.520+004		2.493+004	8.776+003	0.348	1.618-004	6.179+003	1.4202				
1.930+004		3.360+004	1.065+004	0.552	1.480-004	6.755+003	1.5770				
5.684+003	3.289+003	2.195+004	1.557+004	4.735 0	3.031-005	3.300+004	0.1372	30.81*	30.81	35.36	-0
5.930	2.500	1.000	5.320	0.400	16.290	207.50	1330.00	-0.000			

THE TA-THI-ER

2.703+004	2.268+004	1.749+003	2.697+003	0.119	0	1.693-004	5.908+003	0.0183	56.17*	56.17	57.05	-0	6.50	67.44	0.69/	0.670
2.285+004	1.875+004	2.462+003	3.534+003	0.188	0	1.327-004	7.535+003	0.0244	54.00*	54.00	55.14	-0	8.64	67.22	0.669	0.672
1.923+004	1.516+004	3.536+003	4.528+003	0.299	0	1.071-004	9.335+003	0.0324	50.56*	50.56	52.02	-0	11.39	66.81	0.694	0.676
1.577+004	1.202+004	4.833+003	5.689+003	0.475	0	8.673-005	1.153+004	0.0417	47.84*	40.42	49.66	-0	14.72	66.90	0.670	0.675
1.271+004	9.278+003	6.520+003	6.962+003	0.750	0	7.166-005	1.396+004	0.0528	44.68*	44.68	46.89	-0	18.68	67.14	0.672	0.673
1.021+004	7.133+003	8.686+003	8.483+003	1.189	0	5.892-005	1.697+004	0.0664	41.67*	41.67	44.33	-0	23.34	66.70	0.678	0.678
8.008+003	5.463+003	1.104+004	1.030+004	1.685	0	4.844-005	2.064+004	0.0815	39.84*	39.84	43.03	-0	28.63	66.69	0.650	0.678
8.036+003	5.435+003	1.115+004	1.025+004	1.885	0	4.880-005	2.058+004	0.0817	39.44*	39.44	42.61	-0	28.59	66.40	0.665	0.681
6.198+003	4.046+003	1.403+004	1.209+004	2.987	0	4.092-005	2.444+004	0.0984	37.07*	37.07	40.76	-0	34.48	66.54	0.672	0.679
7.757+003	2.975+003	1.758+004	1.409+004	4.735	0	3.464-005	2.887+004	0.1175	34.50*	34.50	38.72	-0	40.93	66.11	0.626	0.684
4.571+003	2.875+003	1.682+004	1.361+004	4.735	0	3.592-005	2.784+004	0.1134	34.90*	34.90	38.99	-0	39.64	66.30	0.653	0.681
3.468+003	2.105+003	2.069+004	1.579+004	7.504	0	3.054-005	3.274+004	0.1339	32.70*	32.70	37.36	-0	46.62	66.09	0.651	0.684
2.635+003	1.520+003	2.560+004	1.607+004	11.893	0	2.607-005	3.836+004	0.1583	29.99*	29.99	35.23	-0	54.72	65.64	0.681	0.688
2.000+003	1.124+003	3.118+004	2.118+004	18.850	0	2.195-005	4.557+004	0.1882	28.12*	28.12	34.19	-0	64.17	64.75	0.646	0.698
1.507+003	8.205+002	3.775+004	2.451+004	29.875	0	1.863-005	5.367+004	0.2269	25.91*	25.91	33.01	-0	75.87	63.47	0.796	0.712
3.461+002	1.418+002	1.425+004	5.716+003	47.348	0	5.566-005	1.796+004	0.1079	21.66*	21.66	24.20	-0	96.29	169.35	0.705	0.267
8.333+002	3.827+002	5.555+004	2.872+004	75.042	0	1.421-005	7.040+004	0.4499	15.42*	15.42	27.34	-0	155.84	65.76	0.698	0.687
4.514+003	2.828+003	1.666+004	1.339+004	4.735	0	3.647-005	2.742+004	0.1121	34.78*	34.78	36.80	-0	39.35	66.65	0.659	0.678
6.220+004		1.000-006	8.623+001	0.001		6.724-011	1.487+010	0.0000								
6.695+004		1.000-006	1.471+002	0.002		2.311-011	4.328+010	0.0000								
6.118+004		1.000-006	2.130+002	0.003		1.102-011	9.078+010	0.0000								
5.790+004		1.000-006	3.196+002	0.006		4.896-012	2.043+011	0.0000								
5.219+004		1.000-006	4.565+002	0.009		2.399-012	4.168+011	0.0000								
4.939+004		1.000-006	8.848+002	0.014		1.066-012	9.379+011	0.0000								
4.617+004		1.000-006	1.015+003	0.022		4.858-013	2.058+012	0.0000								
4.079+004		1.000-006	1.420+003	0.035		2.479-013	4.035+012	0.0000								
3.584+004		1.897+003	1.978+003	0.055		2.423-004	4.127+003	0.4794								
3.131+004		3.902+003	2.739+003	0.087		2.600-004	3.846+003	0.7122								
2.561+004		5.961+003	3.551+003	0.139		2.364-004	4.230+003	0.8394								
2.147+004		9.217+003	4.717+003	0.220		2.070-004	4.832+003	0.9764								
1.748+004		1.355+004	6.087+003	0.348		1.828-004	5.470+003	1.1128								
1.379+004		1.951+004	7.609+003	0.382		1.685-004	5.935+003	1.2819								
4.519+003	2.915+003	1.635+004	1.380+004	4.735	0	3.571-005	2.800+004	0.1124	36.03*	36.03	40.18	-0	37.83	65.92	0.694	0.707
3.930	2.500	1.000	5.320	0.400	16.290	207.50	1330.00	-0.000								

THE WEISSENBERG RHEOGONIOMETER TEST RESULTS

POLYHEXADECENE T=140°C (AFTER 120°C) 5/21/71

TASTAR	ETAP	GP	G2P	SHEAR RATE	JP	I/JP	AMP	PHI 1	PHI 2	INETA	FILTER				
POLYHEXADECENE T=140°C (AFTER 120°C) 5/21/71															
1.108+004	1.208+004	1.976+003	1.543+003	0.119 0	3.143-004	5.182+003	0.0143	37.50*	37.47	38.00	-0	3.94	52.43	0.859	0.862
1.155+004	9.770+003	1.842+003	2.919+003	0.279 0	1.546-004	6.467+003	0.0196	56.81*	56.81	57.76	-0	7.01	67.82	0.679	0.666
1.173+004	9.890+003	1.885+003	2.955+003	0.299 0	1.534-004	6.517+003	0.0199	56.52*	55.59	57.48	-0	7.11	67.71	0.764	0.667
1.068+003	6.366+003	3.645+003	4.777+003	0.750 0	1.009-004	9.906+003	0.0338	51.13*	51.13	52.67	-0	12.06	67.68	0.701	0.665
1.312+003	3.970+003	6.757+003	7.388+003	1.885 0	6.741-005	1.484+004	0.0554	45.22*	45.22	47.56	-0	19.83	67.97	0.685	0.665
1.364+003	2.301+003	1.162+004	1.089+004	4.735 0	4.580-005	2.183+004	0.0859	39.79*	39.79	43.16	-0	30.34	67.09	0.748	0.674
1.015+003	1.295+003	1.836+004	1.540+004	11.893 0	3.197-005	5.127+004	0.1257	35.36*	35.38	40.00	-0	43.77	66.08	0.777	0.664
1.182+003	7.111+002	2.823+004	2.121+004	27.875 0	2.264-005	4.417+004	0.1873	30.47*	30.47	36.93	-0	63.00	63.86	0.719	0.708
1.376+002	4.587+002	3.318+004	2.172+004	47.348 0	2.110-005	4.740+004	0.2316	25.93*	25.93	33.21	-0	82.23	67.42	0.661	0.670
1.323+003	2.312+003	1.130+004	1.095+004	4.735 0	4.566-005	2.190+004	0.0850	40.70*	40.70	44.09	-0	29.94	66.91	0.758	0.675
1.239+003	2.250+003	1.103+004	1.065+004	4.735 0	4.690-005	2.132+004	0.0829	40.71*	40.71	44.02	-0	29.92	66.89	0.777	0.676
1.142+003	2.159+003	1.077+004	1.027+004	4.735 0	4.864-005	2.056+004	0.0806	40.46*	40.46	43.65	-0	28.35	66.80	0.801	0.677
1.903+003	2.801+003	8.121+003	8.368+003	2.987 0	5.973-005	1.674+004	0.0640	43.23*	43.23	45.86	-0	22.72	67.35	0.747	0.671
1.054+003	4.670+003	4.567+003	5.566+003	1.189 0	8.811-005	1.135+004	0.0403	48.55*	48.85	50.64	-0	14.31	67.40	0.792	0.670
1.266+003	5.816+003	3.267+003	4.364+003	0.750 0	1.099-004	9.096+003	0.0308	51.77*	51.77	53.18	-0	10.93	67.43	0.774	0.670
1.756+003	7.241+003	2.331+003	3.428+003	0.473 0	1.356-004	7.373+003	0.0235	54.68*	54.68	55.80	-0	8.37	67.56	0.813	0.669
1.352+003	1.558+003	1.322+004	1.169+004	7.504 0	4.245-005	2.356+004	0.0946	37.90*	37.90	41.49	-0	33.07	66.38	0.822	0.681
1.385+003	8.216+002	2.101+004	1.549+004	18.850 0	3.084-005	3.243+004	0.1376	31.72*	31.72	36.40	-0	47.23	65.03	0.717	0.695
1.091+003	6.638+002	2.587+004	1.983+004	29.875 0	2.435-005	4.107+004	0.1752	31.36*	31.36	37.48	-0	58.91	63.84	0.769	0.708
1.303+002	3.258+002	4.050+004	2.443+004	75.042 0	1.810-005	5.524+004	0.3833	19.69*	19.69	31.11	-0	133.68	66.21	0.679	0.683
1.065+003	2.145+003	1.037+004	1.015+004	4.735 0	4.923-005	2.031+004	0.0788	41.25*	41.25	44.41	-0	27.67	66.67	0.820	0.678
1.208+004		1.000-006	5.833+001	0.001	1.469-010	6.806+009	0.0000								
1.040+004		1.000-006	8.877+001	0.002	6.345-011	1.576+010	0.0000								
1.714+004		1.000-006	1.294+002	0.003	2.988-011	3.346+010	0.0000								
1.401+004		1.000-006	1.877+002	0.006	1.419-011	7.045+010	0.0000								
1.307+004		1.000-006	1.826+002	0.006	1.499-011	6.669+010	0.0000								
1.015+004		1.000-006	2.638+002	0.009	7.186-012	1.392+011	0.0000								
1.854+004		1.000-006	3.957+002	0.014	3.194-012	3.131+011	0.0000								
1.724+004		1.000-006	5.986+002	0.022	1.396-012	7.166+011	0.0000								
1.447+004		1.000-006	8.522+002	0.035	6.885-013	1.452+012	0.0000								
1.206+004		1.000-006	1.217+003	0.055	3.374-013	2.964+012	0.0000								
1.972+004		1.000-006	1.725+003	0.087	1.681-013	5.949+012	0.0000								
1.720+004		1.000-006	2.384+003	0.139	8.797-014	1.137+013	0.0000								
1.454+004		1.000-006	3.196+003	0.220	4.896-014	2.043+013	0.0000								
1.165+004		1.000-006	4.058+003	0.348	3.036-014	5.294+013	0.0000								
3.930	2.500	1.000	5.320	0.400	16.290	207.50	1330.00	-0.000							

ETASTAR ETAP GP G2P SHEAR RATE JP 1/JP AMP PHI 1 PHI 2 THETA FILTER

POLYOTADFCENE T=60 C (AFTER 80 C) CRYSTALLIZATION HAPPENED 5/16

2.289+004	1.939+004	1.444+003	2.306+003	0.119 0	1.951+004	5.125+003	0.0155	57.19*	57.19	57.94	-0	5.60	68.58'	0.692	0.659
1.890+004	1.570+004	1.933+003	2.959+003	0.183 0	1.563+004	6.399+003	0.0202	55.22*	55.22	56.18	-0	7.30	68.47	0.845	0.660
1.581+004	1.311+004	1.657+003	2.477+003	0.183 0	1.866+004	5.359+003	0.0170	55.42*	55.42	56.23	-0	6.11	68.40	0.889	0.661
1.885+004	1.550+004	2.006+003	2.932+003	0.183 0	1.589+004	6.292+003	0.0202	54.67*	54.67	55.63	-0	7.29	68.56	0.622	0.659
1.551+004	1.243+004	2.748+003	3.729+003	0.299 0	1.281+004	7.807+003	0.0262	52.41*	52.41	53.63	-0	9.44	68.39	0.895	0.661
1.556+004	1.253+004	2.737+003	3.759+003	0.299 0	1.266+004	7.899+003	0.0263	52.73*	52.73	53.95	-0	9.49	68.49	0.792	0.660
1.280+004	1.001+004	3.771+003	4.742+003	0.473 0	1.027+004	9.733+003	0.0341	49.99*	49.99	51.52	-0	12.32	68.61	0.787	0.659
1.041+004	7.892+003	5.095+003	5.925+003	0.750 0	8.344+005	1.198+004	0.0436	47.42*	47.42	49.31	-0	15.76	68.59	0.719	0.659
8.393+003	6.102+003	6.854+003	7.257+003	1.189 0	6.879+005	1.454+004	0.0552	44.85*	44.35	46.65	-0	19.91	68.51	0.682	0.660
6.673+003	4.652+003	9.011+003	8.775+003	1.882 0	5.696+005	1.756+004	0.0687	41.50*	41.50	44.25	-0	24.77	68.46	0.685	0.660
7.044+003	4.859+003	9.615+003	9.158+003	1.882 0	4.424+005	1.834+004	0.0723	40.76*	40.76	43.62	-0	25.86	67.93	0.657	0.662
5.621+003	3.763+003	1.247+004	1.124+004	2.987 0	3.646+005	2.260+004	0.0900	38.58*	38.58	42.03	-0	32.17	67.87	0.706	0.666
4.375+003	2.868+003	1.564+004	1.358+004	4.732 0	3.103+005	3.223+004	0.1092	36.86*	36.86	40.97	-0	38.96	67.73	0.873	0.667
3.331+003	2.103+003	1.939+004	1.578+004	7.504 0	2.524+005	3.962+004	0.1295	34.45*	34.45	39.14	-0	45.95	67.36	0.843	0.671
2.607+003	1.623+003	2.427+004	1.930+004	11.893 0	2.111+005	4.738+004	0.1576	32.88*	32.88	38.51	-0	55.45	66.81	0.890	0.676
2.005+003	1.209+003	3.019+004	2.278+004	18.950 0	1.815+005	5.509+004	0.1895	30.49*	30.49	37.05	-0	65.82	65.92	0.860	0.685
1.520+003	8.606+002	3.743+004	2.571+004	29.872 0	1.561+005	6.405+004	0.2291	27.04*	27.04	34.49	-0	78.28	64.87	0.868	0.697
1.136+003	6.169+002	4.515+004	2.921+004	47.348 0	1.296+005	7.714+004	0.2920	23.78*	23.78	32.91	-0	104.90	68.21	0.866	0.662
8.799+002	4.550+002	5.652+004	3.414+004	75.042 0	3.418+005	2.925+004	0.4678	17.14*	17.14	31.14	-0	165.62	67.75	0.821	0.672
4.677+003	3.056+003	1.677+004	1.447+004	4.735 0	1.990+004	0.1160	36.45*	36.45	40.80	41.41	-0	29.00	68.37	0.585	0.661
7.917+003	5.230+003	1.119+004	9.870+003	1.882 0	1.342+004	0.0805	38.36*	38.36	42.59	45.05	-0	19.67	68.54	0.576	0.659
1.517+004	8.909+003	7.274+003	6.686+003	0.750 0	1.161+004	0.0545	40.48*	40.48	45.67	-0	16.18	68.06	0.599	0.664	
1.713+004	1.222+004	5.670+003	5.801+003	0.473 0	9.822+003	0.0388	43.48*	43.48	45.05	-0	13.96	68.35	0.605	0.661	
2.323+004	1.644+004	4.903+003	4.911+003	0.299 0											
3.930	2.500	1.000	5.320	0.400	16.290	207.50	1330.00	70.000							

ETASTAR ETAP GP G2P SHEAR RATE JP 1/JP AMP PHI 1 PHI 2 THETA FILTER
POI YNOCTAGENE T=80 C K=207.5 5/15/71

1.338+004	1.197+004	7.086+002	1.426+003	0.119	0	2.796+004	3.576+003	0.0091	63.11	63.11	63.58	-0	3.30	68.74	0.747	0.657
1.146+004	9.993+003	1.060+003	1.833+003	0.188	0	2.270+004	4.406+003	0.0123	60.03	60.03	60.64	-0	4.46	68.64	0.757	0.658
9.904+003	8.378+003	1.578+003	2.503+003	0.299	0	1.802+004	5.548+003	0.0169	56.97	56.97	57.79	-0	6.06	68.27	0.748	0.662
8.219+003	8.043+003	8.009+002	3.808+003	0.473	0	5.289+005	1.891+004	0.0223	76.89	76.89	78.14	-0	8.02	68.38	0.890	0.661
6.880+003	5.520+003	3.031+003	4.143+003	0.780	0	1.156+004	8.651+003	0.0292	52.03	52.03	53.37	-0	10.49	68.30	0.862	0.662
5.750+003	4.477+003	4.291+003	5.325+003	1.189	0	9.176+005	1.090+004	0.0384	49.43	49.43	51.14	-0	13.83	68.43	0.820	0.660
4.617+003	3.502+003	3.670+003	6.602+003	1.885	0	7.487+005	1.336+004	0.0484	47.25	47.25	49.35	-0	17.42	68.28	0.780	0.662
3.718+003	2.713+003	7.588+003	8.112+003	2.987	0	6.150+005	1.626+004	0.0612	44.36	44.36	46.92	-0	21.90	67.95	0.775	0.662
3.017+003	2.123+003	1.015+003	1.006+003	4.733	0	4.971+005	2.012+004	0.0777	41.62	41.62	44.75	-0	27.68	67.67	0.820	0.668
2.945+003	2.087+003	9.826+003	9.891+003	4.733	0	5.055+005	1.978+004	0.0759	42.11	42.11	45.20	-0	27.13	67.85	0.837	0.665
2.321+003	1.577+003	1.276+003	1.185+003	7.504	0	4.207+005	2.377+004	0.0936	39.25	39.25	42.90	-0	33.35	67.68	0.815	0.668
1.794+003	1.172+003	1.616+003	1.394+003	11.893	0	3.540+005	2.819+004	0.1134	36.54	36.54	40.79	-0	40.09	67.14	0.848	0.673
1.373+003	8.807+002	1.985+003	1.660+003	18.350	0	2.964+005	3.373+004	0.1372	34.86	34.86	39.91	-0	47.83	66.18	0.873	0.680
1.058+003	6.620+002	2.464+003	1.979+003	29.879	0	2.467+005	4.054+004	0.1710	32.63	32.63	38.78	-0	58.62	65.07	0.927	0.696
7.978+002	4.594+002	3.088+003	2.175+003	47.348	0	2.164+005	4.620+004	0.2235	27.77	27.77	35.17	-0	80.35	66.25	0.845	0.662
6.283+002	3.482+002	3.923+003	2.615+003	75.042	0	1.765+005	5.667+004	0.3849	21.57	21.57	33.70	-0	136.27	67.21	0.798	0.672
2.937+003	2.054+003	9.938+003	9.725+003	4.733	0	5.140+005	1.945+004	0.0757	41.35	41.35	44.39	-0	27.04	67.83	0.840	0.669
2.573+004		1.000+006	1.420+002	0.006		2.479+011	4.035+010	0.0000								
2.609+004		1.000+006	2.283+002	0.009		9.596+012	1.042+011	0.0000								
2.415+004		1.000+006	3.348+002	0.014		4.461+012	2.242+011	0.0000								
2.285+004		1.000+006	5.022+002	0.022		1.983+012	5.044+011	0.0000								
2.083+004		1.000+006	7.254+002	0.035		9.503+013	1.052+012	0.0000								
1.930+004		1.000+006	1.065+003	0.055		4.406+013	2.269+012	0.0000								
1.682+004		1.000+006	1.471+003	0.087		2.311+013	4.328+012	0.0000								
1.427+004		1.000+006	1.978+003	0.139		1.278+013	7.827+012	0.0000								
1.270+004		1.000+006	2.790+003	0.220		6.424+014	1.557+013	0.0000								
1.049+004		1.000+006	3.652+003	0.348		3.748+014	2.668+013	0.0000								
8.639+003		1.000+006	4.768+003	0.552		2.199+014	4.547+013	0.0000								
2.948+003	2.073+003	9.900+003	9.341+003	4.733	0	5.081+005	1.968+004	0.0760	41.77	41.77	44.84	-0	27.22	68.02	0.834	0.669
3.930	2.500	1.000	5.320	0.400	16.290	207.50	1330.00	0.0000								

FTASTAP	ITAP	GP	G2P	SHEAR RATE	JP	1/JP	AMP	PHT 1	PHT 2	THETA	FILTER
POLYOTTADECENE T=105°C K=207.3 S/1471											
7.734+003	6.971+003	6.313+002	1.314+003	0.198 0	2.971-004	3.360+003	0.0084	63.92*	63.92	64.35	-0 2.89 65.65 0.942 0.689
7.772+003	7.010+003	6.467+002	1.319+003	0.188 0	2.966-004	3.371+003	0.0084	63.92*	63.82	64.25	-0 2.90 65.54 0.851 0.690
7.200+003	6.275+003	1.054+003	1.875+003	0.299 0	2.279-004	4.388+003	0.0123	60.05*	60.05	60.66	-0 4.07 62.86 0.952 0.719
7.115+003	6.310+003	0.822+002	1.835+003	0.299 0	2.174-004	4.600+003	0.0122	61.52	61.87*	62.49	-0 4.03 62.92 0.840 0.718
6.196+003	5.346+003	1.461+003	2.532+003	0.473 0	1.721-004	5.810+003	0.0167	58.79	58.86*	59.68	-0 5.56 63.11 0.815 0.716
5.249+003	4.440+003	2.105+003	3.347+003	0.750 0	1.347-004	7.426+003	0.0225	53.60	56.75*	57.84	-0 7.49 63.32 0.725 0.714
4.299+003	3.520+003	2.936+003	4.186+003	1.189 0	1.123-004	8.904+003	0.0289	29.34	53.61*	54.96	-0 9.60 63.07 0.783 0.717
3.628+003	2.555+003	2.080+003	5.431+003	1.885 0	8.743-005	1.144+004	0.0384	49.01	51.53*	53.29	-0 12.66 62.60 0.765 0.722
2.999+003	2.328+003	5.648+003	6.956+003	2.987 0	7.035-005	1.421+004	0.0499	46.01	48.72*	50.94	-0 16.32 62.08 0.756 0.728
2.557+003	1.524+003	7.973+003	9.111+003	4.735 0	5.440-005	1.838+004	0.0666	45.79	45.95*	48.82	-0 21.02 59.91 0.808 0.754
2.340+003	1.710+003	7.391+003	8.102+003	4.735 0	6.071-005	1.647+004	0.0609	44.35	45.36*	47.95	0 20.84 64.94 0.815 0.696
1.658+003	1.370+003	9.582+003	1.012+004	7.504 0	4.932-005	2.028+004	0.0762	41.66	43.41*	46.58	-0 25.93 64.58 0.750 0.700
1.466+003	1.011+003	1.296+004	1.202+004	11.893 0	4.148-005	2.411+004	0.0956	39.12*	40.74 B	42.85	-0 32.24 64.03 0.704 0.706
1.162+003	7.815+002	1.621+004	1.473+004	18.850 0	3.379-005	2.960+004	0.1185	37.38	37.70*	42.28	-0 39.49 63.26 0.861 0.714
9.078+002	6.073+002	2.016+004	1.814+004	29.875 0	2.741-005	3.649+004	0.1505	32.80	36.22*	42.00	-0 49.17 62.02 0.788 0.729
6.910+002	4.296+002	2.571+004	2.029+004	47.348 0	2.396-005	4.173+004	0.2201	31.7*	31.0*	38.29	-0 68.62 65.10 0.880 0.694
5.541+002	3.351+002	3.712+004	2.515+004	75.042 0	1.915-005	5.222+004	0.3575	24.04	24.73*	37.22	-0 120.66 64.07 0.901 0.705
7.730+003	6.773+003	2.148+002	1.764+003	0.239 0	2.317-004	4.316+003	0.0114	61.61	62.02*	62.60	-0 3.96 66.08 0.855 0.684
4.583+003	3.138+003	1.924+003	3.105+003	0.750 0	1.449-004	6.901+003	0.0208	56.73	56.93*	57.94	-0 7.25 66.10 0.749 0.684
4.062+003	3.338+003	2.753+003	3.969+003	1.199 0	1.180-004	8.476+003	0.0273	53.68	53.98*	55.26	-0 9.49 65.92 0.792 0.686
3.407+003	2.740+003	3.843+003	5.146+003	1.885 0	9.316-005	1.073+004	0.0361	51.48	51.60*	53.26	-0 12.44 65.37 0.779 0.691
2.208+003	1.676+003	7.447+003	7.934+003	4.735 0	6.289-005	1.590+004	0.0601	43.90	44.31*	46.82	-0 20.59 65.08 0.825 0.694
1.379+004		1.000+006	7.609+001	0.006	8.636-011	1.158+010	0.0000				
1.334+004		1.000+006	1.167+002	0.009	3.673-011	2.722+010	0.0000				
1.261+004		1.000+005	1.775+002	0.014	1.586-011	6.304+010	0.0000				
1.270+004		1.000+006	2.790+002	0.022	6.424-012	1.557+011	0.0000				
1.165+004		1.000+006	4.059+002	0.035	3.036-012	3.294+011	0.0000				
1.084+004		1.000+006	5.936+002	0.055	1.396-012	7.166+011	0.0000				
9.742+003		1.000+006	8.527+002	0.087	6.865-013	1.452+012	0.0000				
8.761+003		1.000+006	1.217+003	0.139	3.374-013	2.964+012	0.0000				
8.160+003		1.000+006	1.725+003	0.220	1.586-013	6.304+012	0.0000				
6.846+003		1.000+006	2.384+003	0.348	8.797-014	1.137+013	0.0000				
5.974+003		1.000+006	3.297+003	0.552	4.599-014	2.174+013	0.0000				
2.285+003	3.719+003	7.018+003	8.235+003	4.735 0	5.995-005	1.668+004	0.0599	45.76	46.96*	49.57	-0 20.62 65.40 0.824 0.691
1.366+003	9.818+002	1.190+004	1.144+004	11.893 0	4.368-005	2.270+004	0.0098	40.32*	40.57 8	43.69	-0 31.42 66.44 0.723 0.680

4,760+003	3,987+003	7,770+002	1,191+003	0,299	0	3,842-004	2,603+003	0,0081	56,50*	56,50	56,89	-0	2,84	66,26	0,957	0,682
4,633+003	3,880+003	7,563+002	1,159+003	0,299	0	3,949+004	2,532+003	0,0079	56,50*	56,50	56,88	-0	2,78	66,59	0,888	0,679
3,382+003	2,819+003	5,531+002	0,122+002	0,299	0	5,469+004	1,829+003	0,0058	56,19*	56,19	56,46	-0	2,02	66,18	0,673	0,643
4,494+003	4,090+003	5,521+002	1,224+003	0,299	0	3,063-004	3,265+003	0,0077	65,33*	65,33	65,73	-0	2,69	66,49	0,504	0,680
4,456+003	4,069+003	5,431+002	1,215+003	0,299	0	3,064-004	3,263+003	0,0076	65,54*	65,54	65,94	-0	2,68	66,66	0,563	0,678
4,441+003	4,062+003	5,367+002	1,213+003	0,299	0	3,049+004	3,280+003	0,0076	65,75*	65,75	66,15	-0	2,66	66,47	0,638	0,680
4,246+003	3,654+003	9,993+002	1,744+003	0,473	0	2,472+004	4,045+003	0,0115	59,63*	59,63	60,20	-0	4,03	66,52	0,963	0,679
4,162+003	3,756+003	8,554+002	1,776+003	0,473	0	2,202+004	4,541+003	0,0113	63,71*	63,71	64,29	-0	3,95	66,47	0,856	0,680
3,662+003	3,193+003	1,347+003	2,396+003	0,750	0	1,783+004	5,609+003	0,0157	59,89*	59,89	60,67	-0	5,51	66,75	0,822	0,677
3,127+003	2,650+003	1,961+003	3,161+003	1,189	0	1,417+004	7,050+003	0,0211	57,17*	57,17	58,20	-0	7,39	66,37	0,735	0,681
2,647+003	2,180+003	2,806+003	4,125+003	1,885	0	1,127+004	8,870+003	0,0282	54,45*	54,45	55,78	-0	9,82	66,05	0,692	0,684
2,211+003	1,700+003	3,890+003	5,337+003	2,987	0	8,919+005	1,121+004	0,0372	52,20*	51,81	53,92	-0	12,93	66,09	0,702	0,684
1,827+003	1,422+003	5,431+003	6,735+003	4,735	0	7,256+005	1,378+004	0,0483	48,97*	48,97	51,12	-0	16,69	65,59	0,652	0,689
1,427+002	1,020+002	2,141+003	2,600+003	4,735	0	1,880+004	5,316+003	0,0192	49,72*	49,77	50,62	-0	16,52	65,27	0,658	0,277
1,468+003	1,110+003	7,209+003	8,326+003	7,504	0	5,943+005	1,683+004	0,0611	46,48*	46,48	49,12	-0	21,15	65,77	0,643	0,687
1,448+003	1,102+003	7,043+003	8,273+003	7,504	0	5,967+005	1,676+004	0,0603	46,97*	46,97	49,60	-0	20,90	65,82	0,813	0,687
1,154+003	8,520+002	9,253+003	1,013+004	11,893	0	4,914+005	2,035+004	0,0758	44,40*	44,40	47,61	-0	26,07	65,34	0,746	0,692
9,128+002	8,275+002	1,275+004	1,183+004	18,850	0	4,215+005	2,372+004	0,0960	39,11*	39,11	42,85	-0	32,64	64,55	0,695	0,700
8,903+002	8,151+002	1,234+004	1,159+004	18,850	0	4,304+005	2,323+004	0,0937	39,54*	39,54	43,22	-0	31,77	64,39	0,765	0,702
7,564+002	5,355+002	1,596+004	1,600+004	29,675	0	3,125+005	3,200+004	0,1285	39,85*	39,85	45,07	-0	42,91	63,38	0,792	0,719
5,669+002	3,613+002	2,068+004	1,710+004	27,340	0	2,871+005	3,483+004	0,1695	33,39*	33,39	39,60	-0	59,39	66,50	0,831	0,680
4,522+002	2,792+002	2,670+004	2,095+004	75,042	0	2,318+005	4,314+004	0,3109	27,06*	27,06	38,12	-0	109,12	66,64	0,832	0,678
1,773+003	1,396+003	5,163+003	6,610+003	4,732	0	7,327+005	1,365+004	0,0469	49,93*	49,93	52,05	-0	16,36	66,19	0,665	0,683
7,352+003		1,000+006	4,058+001	0,006		3,036+010	3,294+009	0,0000								
6,959+003		1,000+006	6,087+001	0,009		1,349+010	7,411+009	0,0000								
7,135+003		1,000+006	9,892+001	0,014		5,110+011	1,957+010	0,0000								
1,134+004		1,000+006	1,572+002	0,014		2,022+011	4,940+010	0,0000								
6,992+003		1,000+006	2,435+002	0,035		8,434+012	1,186+011	0,0000								
6,617+003		1,000+006	3,652+002	0,055		3,748+012	2,068+011	0,0000								
6,089+003		1,000+006	5,320+002	0,087		1,763+012	5,074+011	0,0000								
5,671+003		1,000+006	7,862+002	0,139		8,088+013	1,236+012	0,0000								
5,079+003		1,000+006	1,116+003	0,220		4,015+013	2,491+012	0,0000								
4,661+003		1,000+006	1,623+003	0,348		1,898+013	5,270+012	0,0000								
4,044+003		1,000+006	2,232+003	0,552		1,004+013	9,963+012	0,0000								
3,537+003		1,000+006	3,094+003	0,875		5,222+014	1,915+013	0,0000								
1,688+003	1,330+003	4,923+003	6,297+003	4,735	0	7,705+005	1,298+004	0,0448	49,97*	49,97	51,99	-0	15,71	66,65	0,692	0,678
3,930	2,500	1,000	5,320	0,400	16,290	207,50	1350,00	00,000								

POLYOCETADEGENE

T=140° C (AFTER 120° C)

5/16/71

3.199+003	3.071+003	1.691+002	5.789+002	0.188	0	4.649+004	2.151+003	0.0035	73.54*	73.54	73.73	-0	1.22	67.10	0.791	0.674
2.886+003	2.711+003	2.950+002	8.100+002	0.299	0	3.970+004	2.519+003	0.0049	69.73*	69.73	70.00	-0	1.75	67.05	0.777	0.674
2.642+003	2.315+003	6.022+002	1.096+003	0.473	0	3.849+004	2.598+003	0.0072	60.87*	60.87	61.23	-0	2.54	67.18	0.973	0.673
2.534+003	2.330+003	4.717+002	1.103+003	0.473	0	3.276+004	3.053+003	0.0069	66.50*	66.50	66.87	-0	2.44	67.25	0.697	0.672
2.338+003	2.122+003	7.355+002	1.592+003	0.750	0	2.390+004	4.183+003	0.0100	64.70*	64.70	65.22	-0	3.55	67.12	0.847	0.673
2.376+003	2.152+003	7.565+002	1.615+003	0.750	0	2.379+004	4.204+003	0.0102	64.38*	64.38	64.91	-0	3.60	67.01	0.938	0.674
2.059+003	1.822+003	1.141+003	2.167+003	1.189	0	1.702+004	5.256+003	0.0140	61.53*	61.53	62.24	-0	4.94	67.02	0.845	0.674
1.778+003	1.542+003	1.667+003	2.707+003	1.885	0	1.484+004	6.730+003	0.0191	59.24*	59.24	60.19	-0	6.73	66.89	0.808	0.676
1.519+003	1.282+003	2.431+003	3.831+003	2.987	0	1.181+004	8.469+003	0.0257	56.37*	56.37	57.62	-0	9.10	67.13	0.746	0.673
1.316+003	1.065+003	3.655+003	5.045+003	4.735	0	9.418+005	1.062+004	0.0351	52.45*	52.45	54.08	-0	12.33	66.62	0.736	0.678
1.280+003	1.043+003	3.509+003	4.937+003	4.735	0	9.559+005	1.046+004	0.0342	53.02*	53.02	54.62	-0	12.00	66.62	0.757	0.678
1.345+002	7.862+002	3.319+003	4.401+003	7.504	0	1.092+004	9.155+003	0.0313	51.56*	51.56	52.99	-0	10.91	66.27	0.997	0.682
1.023+003	7.935+002	7.678+003	9.438+003	11.893	0	5.187+005	1.928+004	0.0678	47.87*	47.87	50.48	-0	23.47	65.75	0.683	0.687
6.621+002	4.860+002	8.460+003	9.176+003	18.850	0	5.431+005	1.841+004	0.0706	44.86*	44.36	47.33	-0	24.07	64.70	0.800	0.698
5.722+002	4.167+002	1.172+004	1.245+004	29.875	0	4.009+005	2.494+004	0.0998	42.58*	42.58	46.75	-0	33.45	63.63	0.679	0.710
4.411+002	3.037+002	1.528+004	1.424+004	47.348	0	3.503+005	2.855+004	0.1368	37.63*	37.63	42.98	-0	48.15	66.81	0.706	0.676
2.530+002	1.521+002	1.517+004	1.142+004	75.042	0	4.208+005	2.376+004	0.1972	30.16*	30.16	36.98	-0	68.13	65.60	0.490	0.689
1.259+003	1.033+003	3.412+003	4.890+003	4.735	0	9.598+005	1.042+004	0.0337	53.52*	53.52	55.10	-0	11.76	66.27	0.772	0.682
4.595+003		1.000+006	2.536+001	0.009		7.773+010	1.287+009	0.0000								
4.639+003		1.000+006	4.058+001	0.009		3.036+010	3.294+009	0.0000								
4.025+003		1.000+006	5.580+001	0.014		1.606+010	6.227+009	0.0000								
4.386+003		1.000+006	9.638+001	0.022		5.383+011	1.858+010	0.0000								
4.224+003		1.000+006	1.471+002	0.035		2.311+011	4.328+010	0.0000								
4.044+003		1.000+006	2.232+002	0.055		1.004+011	9.963+010	0.0000								
3.943+003		1.000+006	3.449+002	0.087		4.202+012	2.380+011	0.0000								
3.769+003		1.000+006	5.225+002	0.139		1.832+012	5.460+011	0.0000								
3.463+003		1.000+006	7.809+002	0.220		8.636+013	1.158+012	0.0000								
3.059+003		1.000+006	1.065+003	0.348		4.406+013	2.269+012	0.0000								
2.757+003		1.000+006	1.522+003	0.552		2.159+013	4.632+012	0.0000								
2.494+003		1.000+006	2.181+003	0.875		1.051+013	9.515+012	0.0000								
2.195+003		1.000+006	3.044+003	1.386		5.398+014	1.853+013	0.0000								
1.260+003	1.030+003	3.433+003	4.877+003	4.735	0	9.650+005	1.036+004	0.0337	53.80*	53.30	54.87	-0	11.79	66.46	0.770	0.680
3.930	2.500	1.000	5.320	0.400	16.290	207.50	1330.00	0.000								

